FINITE ELEMENT ANALYSIS OF STRUCTURES USING A GENERAL HIGHER-ORDER PLATE AND ONE-DIMENSIONAL THEORIES FOR CLASSICAL AND COSSERAT CONTINUUM HAVING CONSTRAINED MICROROTATION

A Dissertation

by

ARCHANA ARBIND

Submitted to the Office of Graduate and Professional Studies of
Texas A&M University
in partial fulfillment of the requirements for the degree of

DOCTOR OF PHILOSOPHY

Chair of Committee,	J. N. Reddy
Committee Members,	Arun R. Srinivasa
	Anastasia Muliana
	Luciana R. Barroso
Head of Department,	Andreas A. Polycarpou

May 2017

Major Subject: Mechanical Engineering

ABSTRACT

In this study nonlinear finite element models for beams and plates considering general higher-order expansions of the displacement fields have been developed, The models account for Cosserat continuum having constrained micro-rotation. The models can be used to analyze solid continua with very small inclusions or small scale structures in which material length scales, that classical continuum mechanics fails to capture, play a role. The beam and plate models developed herein are used to study the effect of different length scale parameters and the orientation of small inclusions. Also, the classical plate theory for rotation gradient dependent potential energy (Cosserat continuum for constrained micro-rotation) is applied to model nano-indentation on a carbon nanotube (CNT)-reinforced hard coating on an elastic substrate to see the effect of CNT reinforcement, which is modeled by small material length scale parameters. A general higher-order one-dimensional theory has also been developed in cylindrical and curvilinear cylindrical coordinate systems by considering a very general displacement approximation of arbitrary cross-section of a body in polar coordinates. Based on this approximation, the governing equations of motion have been derived using the principle of virtual displacements for large deformation case. Further, a nonlinear finite element model is developed to determine nonlinear response using the theories presented. In the numerical examples, the finite element model is used to analyze shell and rod-like structures for large deformation. Also, these higher-order one-dimensional theories are very relevant for the analysis of shell and rod-like structures of Cosserat continuum for constrained micro rotation because all gradient elasticity theories require C^1 or higher-order continuity of the displacement variables, which is hard to achieve in the case of two or three dimensions, especially for non-rectangular grids. The one-dimensional theory developed herein allows continuity of any desired order of the variables by general Hermite interpolation functions in the finite element model.

DEDICATION

To my parents, sister, and brother

ACKNOWLEDGMENTS

I would like to express my sincere gratitude to my advisor Professor J. N. Reddy for his extraordinary support, guidance, and patience throughout my dissertation work. His hard work and dedication towards teaching and research have always been inspiring to me. It has been a very enriching learning experience working with him over the years during my master's and doctoral degree programs as his student, which I will surely cherish all my life. I would also like to thank Professor A. R. Srinivasa for the collaboration in this research work and serving on my dissertation advisory committee. His inputs and suggestions towards the present work have been very helpful and motivating. I also thank Drs. Barroso and Muliana for serving on my dissertation advisory committee and providing me constructive comments.

I would also like to thank all my colleagues in the Advanced Computational Mechanics Laboratory. Various discussions with them on Cosserat continuum mechanics and finite element methods and suggestions during the group meeting presentations have been very helpful. I would like to especially thank Dr. Michael Powell for helping me with the computer cluster in our Advanced Computational Mechanics Laboratory and Dr. Miguel Rivera for providing me the solution data of a shell theory example for the validation done in chapter 5 of this study.

Finally, I would like to thank my parents, sister, and brother for their love, support, and encouragement without which I would not have been able to accomplish whatever I have to this day.

CONTRIBUTORS AND FUNDING SOURCES

Contributors

This work was carried out under the supervision of a dissertation committee consisting of Professors J. N. Reddy as the advisor, and Arun R. Srinivasa and Anastasia Muliana of the Department of Mechanical Engineering and Luciana R. Barroso of the Department of Civil Engineering as the members.

All the work conducted for the dissertation was completed by the student independently. The data for validation of one of the example in Chapter 5 of this study was provided by Miguel G. Rivera.

Funding Sources

Financial support for this research was provided by Oscar S. Wyatt Endowed Chair and Aruna and J. N. Reddy Distinguished Fellowship in Computational Mechanics, both in the Department of Mechanical Engineering at Texas A&M University.

TABLE OF CONTENTS

Page

LIST OF FIGURES

LIST OF TABLES

1. INTRODUCTION

There has been surge of research in recent decades in the area of nonclassical or nonlocal continuum mechanics, in an attempt to model micro and nano sized structures, for example, nematic elastomers, fibrous composites (e.g., carbon nanotube-reinforced coating), granular solid, liquid crystal with rigid molecules, polarization inertia in ferroelectrics, intrinsic spin in ferromagnetics, to name a few. For such applications, the classical continuum mechanics fails to predict a response that correlates with the observed response. In small scale structures, the strain energy due to deformation of the material particles or microstructure, which could be a unit cell in the case of crystalline solid or stiff inclusions in fibrous or granular solid, becomes significant. In these cases, the response depends on several material length scale parameters which are very small compared to the structural dimensions. In the case of large-scale structures, when the ratio of the length scale to the structural dimensions is very small, the classical continuum model is adequate for mathematical modeling of the response. But as the structural length of the specimen becomes comparable to the characteristic length of the material, one must consider nonlocal and nonclassical continuum models.

In the nonlocal continuum models, the axiom of local action of classical mechanics is relaxed and hence the stress at a point is not only a function of the strain at that point but also of the region around that point. In some cases the nonlocality is limited and the material points of the body have orientation and move rigidly while undergoing deformation. Linear couple stress theory and Eringen's micropolar theories provide examples of this case. In general, such solids are referred to as Cosserat solids for which there could be six degrees of freedom, namely, three translations and three rotations, at each material point. Further, rotations of the material particles (or microstructures/stiff inclusions) could be considered as constraints, that is, the microrotation of the material points are same as the macrorotation at that point, and there is no "rotational mismatch energy." The additional internal rotational degrees of freedom modifies the balance of angular momentum and gives rise to couple stresses and non-symmetric stress tensor along with "surface tension" like forces in the case of solids. The existence of internal degrees of freedom could be of mechanical nature or nonmechanical nature in origin, for example, polarization

inertia in ferroelectrics and intrinsic spin in ferromagnetics. The existence of body couples (e.g., in electromagnetism: $P \times E$, where P is the dipole moment and E is the electric field) could also result in asymmetric Cauchy stress tensor. The present study deals with the nonlinear analysis of structural elements like beams and plates made of such materials and accounts for the effect of a length scale parameter on the response in case of moderate and finite rotation and strain fields.

1.1. Background

Many researchers have contributed to the development of the theory of deformable continua in the last six decades. The inception of the theories began with the seminal work of the Cosserat brothers in 1909 [1]. Under the influence of Darboux curvilinear coordinates and moving triad, Cosserats attached rigidly rotating directors to the cross-section of a rod to model the response of the rod as a one-dimensional body. In a similar manner, they attached a rigid director to the line perpendicular to the shell in the case of the two-dimensional body to model the response (which are now called Cosserat's rod and Cosserat's shell theory, respectively; see Rubin [2]). In the case of a three-dimensional body, that is, a solid continuum, Cosserat attached moving triad to each material point, which gave rise to *Cosserat's continuum* (see Maugin [3]). This way, their work includes rotational as well as translational degrees of freedom at any material point of the body, resulting in asymmetric stress tensor and the notion of couple stress in the Cosserat or oriented- or polar-continua. The idea of couple stress can also be traced back to Viogt in the 1800s.

In the decade of 1960s, Truesdell and Toupin [4] formalized Cosserat's work in the modern thermo-mechanics continuum framework, followed by Toupin [5], who attempted to find the constitutive relation for finite deformation elasticity with couple stress. Mindlin and Tiersten [6] have studied couple stress in linear elasticity for centrosymmetric (material point, the microstructure, or unit cell having center of inversion symmetry; e.g., FCC unit cell) isotropic material, which require only one length scale parameter following the constitutive relation given by Toupin. In this case, elastic strain energy is shown to be a function of symmetric part of stress tensor and the deviatoric part of couple stress. The skew symmetric part of the stress tensor and volumetric part of the couple stress are left indeterminate. Mindlin [7] also studied microstructure in elastic solid considering the unit cell of crystalline solid or grain of granular solid as rigidly rotating particle to obtain the acoustic and

optical branches of the same character as those found at long wavelengths in crystal lattice theories. In all these studies micro rotation at a point is considered to be same as the macrorotation. These theories are termed as *couple stress theories* in the literature.

Eringen and Suhubi [8, 9] introduced the nonlinear theory of a general deformable material, in which material points not only undergo rigid rotation but a general deformation, which they later termed as *micromorphic elasticity*. Their theory contains stress moments, inertial spin, and the mechanism of surface tension type behavior in solids. The concept for the conservation of microinertia was also introduced, which was missing in earlier theories. Eringen and Suhubi [8, 9] also presented the constitutive equations for what they called "simple microelastic solid," which account for material frame indifference and thermodynamic restrictions. Followed by these works, Eringen [10] considered micro-deformation of a material point as rigid rotation only, which is not constrained with macro rotation at that point, in linear elasticity framework, and termed it as the linear micropolar theory. The case of constrained micro rotation can be a special case of this when micro and macro rotation at a point are the same. Later, Eringen and co-workers have also extended the linear micropolar theory in the case of viscoelastic material [11], polar elastic dielectrics [12, 13], and ferromagnetic materials [14, 15], to name a few among a large body of work by Eringen and his colleagues. Later he summarized the kinematics, field equations, and constitutive equations for micromorphic, microstretch, and micropolar elastic solids, and all together termed as the *microcontinuum field theory* [16] for solids.

In relatively recent times, in the case of constrained micro-rotation of material points, Yang *et al.* [17], in their modified couple stress theory, proposed higher order moment balance law (i.e., balance of the couple of a couple), which suggests that the couple stress tensor should be symmetric, so that the strain energy density function should depend on the symmetric part of curvature tensor in the linear framework. Steinmann [18] studied the micropolar elastoplasticity in the case of finite deformation and finite rotation using Euler–Rodrigues formula for rotation tensor to develop generalized continuum in the nonlinear framework. More recently, Srinivasa and Reddy [19] have developed the nonlinear Cosserat/micropolar continuum formulation in the case of constrained finite rotation of material particles/microstructure. Starting from the physical reasoning, they established the energy dependence on rotation gradient through material frame indifference and presented the governing

equations and boundary conditions for the von Kármán plate and beam theories in the case of moderate rotation. The presence of surface tension like term is also shown in their work. In the case of beams and plates, they considered a general quadratic functional for the potential energy and a general shape and orientation of material particle/inclusions, that is, the material is not necessarily centrosymmetric, which allows more than one length scale parameter, depending upon the orientation of the inclusions as well as the kinematics.

In spite of seemingly fully developed theoretical framework in Cosserat continuum, challenges lie in the determination of the various length scale parameters for given material. The determination of material length scales of proposed constitutive relation requires comparison of theoretical solutions to the experimental results. Many researchers have attempted to obtain the length scale information from a comparison of experimental results and analytical solutions. Gauthier and Jahsman [20] conducted an experiment for a composite material with aluminum uniformly distributed throughout an epoxy matrix, but for their given resolution of measurement, they observed classical elastic material behavior only and hence, concluded that detection of possible micropolar phenomena will require either higher resolution static measurements or a series of dynamic tests. Askar [21] did optical (Raman or infrared) experiments on lattice of molecular crystal of KNO_3 and determined the numerical value for KNO_3 crystal considering micropolar continuum theory. Pouget and Maugin [22] studied crystals equipped with a polar group such as $NaNO_2$. Lakes [23] conducted experiments on the specimen of dense polyurethane foam and syntactic foam to determine the bending and torsional rigidity of the microstructure and found that dense polyurethane foam has small length scale effect. He obtained the value of length scale related to torsion and bending based on isotropic micropolar linear elastic constitutive relation and observed that the length scale is comparable to the dimensions (e.g., the diameter of a shaft and height of a beam) of the microstructure of the material. Lakes [24] has also reviewed the experimental work done in the Cosserat elasticity. Lam *et al.* [25] conducted bending experiment on micron sized beam using nano-indenter and observed increased beam's bending rigidity with a reduction in the beam height, which indicates the existence of the strain gradient effect in small-scale structures.

In the last decade, many papers appeared on modeling the response of structural elements like beams, plates, and shells, accounting for the length scale effects. These

include parametric studies to determine the effect on bending and vibration response. Park and Gao [26] and Ma *et al.* [27, 28] have studied the Bernoulli–Euler, Timoshenko, and Reddy–Levinson beams in the case of modified couple stress theory. Santos and Reddy [29] have studied vibrations of beams, while Reddy [30], Arbind and Reddy [31], and Arbind *et al.* [32] studied functionally graded, microstructure dependent beams considering the von Kármán nonlinearity. Gao *et al.* [33] studied plates by extending Reddy's third-order plate theory [34, 35] to account for the modified couple stress term in the strain energy function. Kim and Reddy [36, 37] obtained analytical and finite element solutions for functionally graded plates. In all these studies, constitutive relations for centrosymmetric material (see Mindlin [7]) or isotropic cosserat solid (as termed in Eringen's micropolar theory), are used and rotations of the material particles or inclusions have been considered constrained. For this reason, the curvature tensor is obtained from the deformation field of the matrix material itself. The studies show that the material length scale contributes some extra stiffness to the structure as compared to the conventional theories. Reddy and Srinivasa [38] has summarized the modified couple stress theory and the rotation gradient dependent theory and also formulated the finite element models for moderate rotation of Bernoulli–Euler and Timoshenko beam theories.

1.2. Motivation and scope for present study

The theory suggested by Srinivasa and Reddy [19, 38] have generalized the linear micropolar theory in the case of large constrained rotation and finite strain for a general class of materials, which requires more than one length scale to characterize a more general shape/structure and orientation of inclusions or material particles/microstructure. The analysis of structures like beams, plates, and shells discussed in the previous literature review are based on the constitutive relation in which material points or the small inclusions are centrosymmetric or fully isotropic. The linear modified couple stress theory has been used for mathematical modeling of the structural elements for moderate rotation case in the aforemention literature. In the present study, we wish to extend to study of the nonlinear response of beams and plates, in view of a broad class of materials with the use of the rotation gradient dependent theory, to account for finite rotations and strains. We formulate nonlinear weak form finite element model of beams with the von Kármán geometric nonlinearity using a general Taylor's series expansion of the displacement field and

then we specialize this to the case of the Bernoulli–Euler, Timoshenko, and a general third-order beam theories. Further, we also present the weak form finite element model of plates in the case of a general power series expansion for the displacement field, which later specialized to the classical, first-order, and a general third-order plate theories considering the von Kármán geometric nonlinearity. Analytical solution for simply supported beam and plate have also been obtained. The effect of the various length scales is studied. Keeping in mind the need of continuity requirement of a higher-order derivative in the case of a rotation gradient dependent theory, the mixed finite element model for the von Kármán plate is also developed. Based on a mixed finite element analysis, a rather simple model of nanoindentation on the thin CNT reinforced coating on an elastic substrate is presented, which can give some idea about material length scale parameters by comparing with the experimental results.

The strain gradient dependent theories require higher-order inter-element continuity, which is difficult to achieve for higher order approximations in two or three-dimensional cases especially in the case of non-rectangular grid in displacement finite element model. To overcome this difficulty, in our study, we have formulated a general higher order one-dimensional theory. In this theory, we approximate the displacement field of a cross-section or slice of an object which is perpendicular to the axis of the object considered by general two-dimensional basis functions; for example, polar Fourier series in the cylindrical coordinate system. Based on this approximated displacement field we develop the governing equation of motions for general one-dimensional theories in polar cylindrical and curvilinear polar cylindrical coordinate systems. The theories in cylindrical coordinate systems have been applied in the analysis of shells and rod in case of classical continuum mechanics. In the final chapter, we present the summary and conclusions along with some suggestion for future works.

1.3. Cosserat continuum theory for finite deformation and constrained micro-rotation

Consider a body $\mathcal{B}$ in which a particle X occupies a position $\mathbf{X}$ in the reference frame at time $t = 0$, and after deformation at time t it occupies position $\mathbf{x}$. Let $\mathbf{F}$ be the deformation gradient and $\mathbf{\Theta}$ be the orientation tensor of the directors attached to the material points; then the potential energy can be expressed as (see Srinivasa and

Reddy [19] for details):

$$\psi = \bar{\psi}(\mathbf{F}, \boldsymbol{\Theta}, \boldsymbol{\nabla}\boldsymbol{\Theta}) \tag{1.1}$$

where $\boldsymbol{\nabla}\boldsymbol{\Theta}$ is the gradient of the orientation tensor with respect to the reference frame. By applying the principle of invariance under superposed rigid body motion, it can be shown that the potential energy has the following dependence

$$\psi = \hat{\psi}(\mathbf{C}, \mathbf{R}^T \cdot \boldsymbol{\Theta}, \mathbf{R}^T \cdot \boldsymbol{\nabla}\boldsymbol{\Theta}) \tag{1.2}$$

where $\mathbf{C} = \mathbf{U}^2$ is the right Cauchy–Green stretch tensor and $\mathbf{R}$ is the orthogonal rotation tensor. In the case of fully constrained directors, the orientation tensor can be stipulated as the rotation tensor, and hence the potential energy functional can be expressed as[1]

$$\psi = \psi(\mathbf{U}, \mathbf{R}^T \cdot \boldsymbol{\nabla}\mathbf{R}) \tag{1.3}$$

where $\mathbf{U}$ and $\mathbf{R}$ are symmetric and proper orthogonal tensors, respectively; their variation are $\delta\mathbf{U} = \delta\mathbf{U}^T$ and $\delta\mathbf{R} = \delta\boldsymbol{\Omega} \cdot \mathbf{R}$, where $\delta\boldsymbol{\Omega}$ is skew-symmetric tensor. let us consider that the body force $\mathbf{f}$ is acting on the body which causes the displacement field $\mathbf{u}$. To obtain the equation of equilibrium, we will consider the following lagrangian:

$$\mathbb{L} = \int_{\mathcal{B}} \psi(\mathbf{U}, \mathbf{R}^T \cdot \boldsymbol{\nabla}\mathbf{R}) - tr(\mathbf{P}^T \cdot \mathbf{G}) - \mathbf{f} \cdot \mathbf{u}\, dV, \quad \text{where,} \quad \mathbf{G} = \mathbf{R} \cdot \mathbf{U} - \mathbf{F} \tag{1.4}$$

where $\mathbf{P}$ is the Lagrange multiplier and $\mathbf{G} = 0$ is the constraint condition. In the case of stable equilibrium the potential energy can be minimised with respect to the displacement field with given constrain conditions whereas in case of unstable equilibrium (e.g, bucking of beam) or neutral equilibrium of the system, the equation of equilibrium can be obtained by putting the first variation of the above lagrangian equal to zero, that is, from the stationarity condition. Hence to obtain the Euler–Lagrange equations (a general equilibrium equations) we put the stationarity condition resulting from $\delta\mathbb{L} = 0$, which can be given as following (see Appendix A

[1]The functions $\bar{\psi}, \hat{\psi}$ and ψ of the right hand side of Eqs. (1.1),(1.2) and (1.3), respectively, represent various function with different functional dependence of the same physical quantity, that is, the potential energy stored in the body during deformation denoted by ψ. We note that ψ in the RHS of Eq. (1.3) also represents the functional.

for a detail derivation):

$$\begin{aligned} \delta\mathbf{U}: &\qquad \frac{\partial\psi}{\partial\mathbf{U}} = \frac{1}{2}(\mathbf{P}^T\cdot\mathbf{R} + \mathbf{R}^T\cdot\mathbf{P}) \\ \delta\boldsymbol{\Omega}: &\qquad \mathrm{Div}(\mathbf{M}) = (\mathbf{P}\cdot\mathbf{F}^T - \mathbf{F}\cdot\mathbf{P}^T) \\ \delta\mathbf{u}: &\qquad \mathrm{Div}(\mathbf{P}) = \mathbf{f} \\ \delta\mathbf{P}: &\qquad \mathbf{G} = 0 \end{aligned} \tag{1.5}$$

where $\mathbf{P}$ is the first Piola–Kirchhoff stress tensor and $\mathbf{M}$ is the third-order couple stress tensor given by

$$M_{ijC} = -M_{jiC} := \frac{\partial\psi}{\partial\theta_{ABC}}(R_{iA}R_{jB} - R_{jA}R_{iB}), \quad \text{where } \theta_{ABC} := R_{iA}R_{iB,C} \tag{1.6}$$

and considering closed and smooth boundary surface, we have the following primary and secondary variables, either one of which may be specified at each boundary points:

$$\begin{aligned} \delta\mathbf{u}: &\qquad \mathbf{P}\cdot\mathbf{N} + (\boldsymbol{\nabla}_s\cdot\mathbf{N})\mathbf{N}\cdot\mathbf{M}^n - \mathrm{Div}_s(\mathbf{M}^n) \\ \frac{\partial\delta\mathbf{u}}{\partial n}: &\qquad \mathbf{M}^n\cdot\mathbf{N} \end{aligned} \tag{1.7}$$

where $\boldsymbol{\nabla}_s$ and Div_s are surface gradient and surface divergence operators, respectively, in the reference configuration (see [39]) and the various components of the second order tensor $\mathbf{M}^n$ can be given as:

$$M^n_{jK} = \frac{\partial R_{iB}}{\partial F_{jK}}\frac{\partial\psi}{\partial\theta_{ABC}}R_{iA}N_C \tag{1.8}$$

which is the surface tension like tensor for the solid, and $\mathbf{N}$ is the unit outward normal vector to the surface in the reference configuration, and n is the coordinate along $\mathbf{N}$.

2. ANALYSIS OF COSSERAT BEAM FOR CONSTRAINED MICRO-ROTATION [*]

The theory suggested by Srinivasa and Reddy [19, 38] is a generalization of the linear micropolar theory to the case of large constrained microrotation and finite strain for a general class of materials, which requires more than one length scale to characterize an arbitrary shape/structure. In the literature, the analysis of structures like beams, plates, and shells is based on the constitutive relation in which material points or the small inclusions are centrosymmetric or fully isotropic. And also, the linear modified couple stress theory has been used for mathematical modeling of the structural elements for moderate rotation case (see [17, 27, 28, 31, 32, 40, 36, 37]).

In this chapter, we extend the study of nonlinear response of beams, in view of a broad class of materials with the use of the rotation gradient dependent theory, to account for moderate rotations and strains. We develop a weak-form finite element model of beams with the von Kármán geometric nonlinearity. First, we formulate a general higher-order beam theory based on Taylor's series expansion of the displacement field about the centroidal axis for classical as well as microstructure dependent beams and then specialize it to the case of the Bernoulli–Euler, Timoshenko, and general third-order beam theories. Based on this, we develop a nonlinear weak-form, displacement-based, finite element model. We also present the analytical solution for simply supported linear beams to provide a benchmark for the finite element solution.

2.1. Governing equations of beam

Consider a rectangular cartesian coordinate system (x, y, z) in the reference configuration in which a beam of length L is placed along the x-axis. The y- and z-axes are along the height and width, respectively, of the beam. The beam is allowed to bend in the xz-plane due to applied loads in the xz-plane. Let A denote the cross-sectional area of the beam, which could be of any arbitrary shape and may vary along the x-axis.

[*] Reprinted with permission from "Nonlinear analysis of beams with rotation gradient dependent potential energy for constrained micro-rotation" by A. Arbind, J. N. Reddy and, A. R. Srinivasa, 2017. *European Journal of Mechanics-A/Solids*, 65, 178-194, Copyright [2017] by Elsevier.

2.1.1. Displacement field

We begin with the following displacement field (in case of general higher order beam theory; see Arbind and Reddy [32]) for a straight beam bent by forces in the xz-plane (i.e., bending about the y-axis):

$$\begin{gathered}\mathbf{u} = u_1\,\hat{\mathbf{e}}_1 + u_2\,\hat{\mathbf{e}}_2 + u_3\,\hat{\mathbf{e}}_3 \\ u_1 = \sum_{i=0}^{n} z^i \phi_x^{(i)}(x,t) = \mathbf{A}_x \mathbf{\Phi}_x, \quad u_2 = 0, \quad u_3 = \sum_{i=0}^{p} z^i \phi_z^{(i)}(x,t) = \mathbf{A}_z \mathbf{\Phi}_z\end{gathered} \tag{2.1}$$

where $\hat{\mathbf{e}}_1, \hat{\mathbf{e}}_2$ and $\hat{\mathbf{e}}_3$ are unit basis vectors along x, y and z directions respectively. Here $\phi_x^{(0)} = u$ and $\phi_z^{(0)} = w$ are midplane displacements along the x and z directions, respectively, and $\phi_x^{(i)}$ and $\phi_z^{(i)}$ have the following meaning:

$$\phi_x^{(i)} = \frac{1}{(i)!}\left(\frac{\partial^i u_1}{\partial z^i}\right)_{z=0}, \qquad \phi_z^{(i)} = \frac{1}{(i)!}\left(\frac{\partial^i u_3}{\partial z^i}\right)_{z=0} \tag{2.2}$$

and

$$\begin{aligned}\mathbf{A}_x &= \begin{bmatrix} 1 & z & z^2 & \dots & z^n \end{bmatrix}, & \mathbf{A}_z &= \begin{bmatrix} 1 & z & z^2 & \dots & z^p \end{bmatrix} \\ \mathbf{\Phi}_x &= \begin{bmatrix} \phi_x^{(0)} & \phi_x^{(1)} & \phi_x^{(2)} & \dots & \phi_x^{(n)} \end{bmatrix}^T, & \mathbf{\Phi}_z &= \begin{bmatrix} \phi_z^{(0)} & \phi_z^{(1)} & \phi_z^{(2)} & \dots & \phi_z^{(p)} \end{bmatrix}^T\end{aligned} \tag{2.3}$$

Let $\mathbf{e}$ and $\mathbf{W}$ be the symmetric[2] and skew-symmetric parts, respectively, of the displacement gradient. We will make assumptions that (1) $||\mathbf{e}||$ is of order of ϵ and (2) $||\mathbf{W}||$ is of order $\sqrt{\epsilon}$ in view of moderate rotation, where ϵ is small, and neglect all terms of order $O(\epsilon^k)$ for $k > 1$. In this case, the Green–Lagrange strain tensor and the rotation tensor can be approximated as

$$\begin{aligned}\mathbf{E} &\approx \mathbf{e} - (1/2)\mathbf{W}^2 \\ \mathbf{R} &\approx \mathbf{I} + \mathbf{W} + \frac{1}{2}\mathbf{W}^2 \\ \boldsymbol{\theta} &:= \mathbf{R}^T \cdot \boldsymbol{\nabla}\mathbf{R} \approx \boldsymbol{\nabla}\mathbf{W}\end{aligned} \tag{2.4}$$

[2]The notation $\mathbf{e}$ used for symmetric part of the displacement gradient should not be confused with the basis vectors of the coordinate system assumed.

The nonzero von Kármán nonlinear strain components associated with the displacement field (2.1) are

$$\begin{aligned}
\varepsilon_{xx} &= \frac{\partial u_1}{\partial x} + \frac{1}{2}\left(\frac{\partial \phi_z^{(0)}}{\partial x}\right)^2 = \mathbf{A}_x \frac{\partial \mathbf{\Phi}_x}{\partial x} + \frac{1}{2}\left(\frac{\partial \phi_z^{(0)}}{\partial x}\right)^2 \\
\gamma_{xz} &= \frac{\partial u_1}{\partial z} + \frac{\partial u_3}{\partial x} = \frac{\partial \mathbf{A}_x}{\partial z}\mathbf{\Phi}_x + \mathbf{A}_z \frac{\partial \mathbf{\Phi}_z}{\partial x} \\
\varepsilon_{zz} &= \frac{\partial u_3}{\partial z} = \frac{\partial \mathbf{A}_z}{\partial z}\mathbf{\Phi}_z + \frac{1}{2}\left(\phi_x^{(1)}\right)^2
\end{aligned} \tag{2.5}$$

Here we note that for $\phi_x^{(1)}$ and $\frac{\partial \phi_z^{(0)}}{\partial x}$ are of same order $\sqrt{\epsilon}$ for moderate rotation; hence, we keep those two nonlinear terms in the strain components and neglect the higher-order nonlinear terms. Then $\mathbf{W}$ and the $\boldsymbol{\theta}$ can be expressed as follows:

$$\mathbf{W} = \begin{bmatrix} 0 & 0 & \omega_y \\ 0 & 0 & 0 \\ -\omega_y & 0 & 0 \end{bmatrix}, \qquad \omega_y = \frac{1}{2}\left(\frac{\partial u_1}{\partial z} - \frac{\partial u_3}{\partial x}\right) = \frac{1}{2}\left(\frac{\partial \mathbf{A}_x}{\partial z}\mathbf{\Phi}_x - \mathbf{A}_z \frac{\partial \mathbf{\Phi}_z}{\partial x}\right)$$

$$\boldsymbol{\theta} = \theta_{\alpha\beta\gamma}\hat{\mathbf{e}}_\alpha\hat{\mathbf{e}}_\beta\hat{\mathbf{e}}_\gamma = \frac{\partial W_{\beta\gamma}}{\partial x_\alpha}\hat{\mathbf{e}}_\alpha\hat{\mathbf{e}}_\beta\hat{\mathbf{e}}_\gamma$$

and

$$\begin{aligned}
\theta_{113} = -\theta_{131} &= \frac{\partial \omega_y}{\partial x} = \frac{1}{2}\left(\frac{\partial \mathbf{A}_x}{\partial z}\frac{\partial \mathbf{\Phi}_x}{\partial x} - \mathbf{A}_z \frac{\partial^2 \mathbf{\Phi}_z}{\partial x^2}\right) \\
\theta_{313} = -\theta_{331} &= \frac{\partial \omega_y}{\partial z} = \frac{1}{2}\left(\frac{\partial^2 \mathbf{A}_x}{\partial z^2}\mathbf{\Phi}_x - \frac{\partial \mathbf{A}_z}{\partial z}\frac{\partial \mathbf{\Phi}_z}{\partial x}\right)
\end{aligned} \tag{2.6}$$

Further, the strain tensor can be expressed in vector form as

$$\boldsymbol{\varepsilon} = \begin{Bmatrix} \varepsilon_{xx} \\ \varepsilon_{zz} \\ \gamma_{xz} \end{Bmatrix} = (\mathbf{A}_1 + \frac{1}{2}\mathbf{A}_{nl_1})\mathbf{\Phi} + (\mathbf{A}_2 + \frac{1}{2}\mathbf{A}_{nl_2})\frac{d\mathbf{\Phi}}{dx} \tag{2.7}$$

The components of $\boldsymbol{\theta}$ can be written in the following vector form:

$$\boldsymbol{\chi} = \begin{Bmatrix} \theta_{113} \\ \theta_{313} \end{Bmatrix} = \begin{Bmatrix} \frac{\partial \omega_y}{\partial x} \\ \frac{\partial \omega_y}{\partial z} \end{Bmatrix} = \mathbf{B}_1\mathbf{\Phi} + \mathbf{B}_2\frac{d\mathbf{\Phi}}{dx} + \mathbf{B}_3\frac{d^2\mathbf{\Phi}}{dx^2} \tag{2.8}$$

where

$$\mathbf{A}_1 = \begin{bmatrix} \mathbf{0} & \mathbf{0} \\ \mathbf{0} & \mathbf{A}_{z,z} \\ \mathbf{A}_{x,z} & \mathbf{0} \end{bmatrix}, \quad \mathbf{A}_2 = \begin{bmatrix} \mathbf{A}_x & \mathbf{0} \\ \mathbf{0} & \mathbf{0} \\ \mathbf{0} & \mathbf{A}_z \end{bmatrix}, \quad \mathbf{A}_{nl_1} = \begin{bmatrix} \mathbf{0} & \mathbf{0} \\ \mathbf{b}_{nl} & \mathbf{0} \\ \mathbf{0} & \mathbf{0} \end{bmatrix}, \quad \mathbf{A}_{nl_2} = \begin{bmatrix} \mathbf{0} & \mathbf{a}_{nl} \\ \mathbf{0} & \mathbf{0} \\ \mathbf{0} & \mathbf{0} \end{bmatrix}$$

$$\mathbf{B}_1 = \frac{1}{2}\begin{bmatrix} \mathbf{0} & \mathbf{0} \\ \mathbf{A}_{x,zz} & \mathbf{0} \end{bmatrix}, \quad \mathbf{B}_2 = \frac{1}{2}\begin{bmatrix} \mathbf{A}_{x,z} & \mathbf{0} \\ \mathbf{0} & -\mathbf{A}_{z,z} \end{bmatrix}, \quad \mathbf{B}_3 = \frac{1}{2}\begin{bmatrix} \mathbf{0} & -\mathbf{A}_z \\ \mathbf{0} & \mathbf{0} \end{bmatrix}, \quad \mathbf{\Phi} = \begin{Bmatrix} \mathbf{\Phi}_x \\ \mathbf{\Phi}_z \end{Bmatrix} \tag{2.9}$$

The only nonzero element of $\mathbf{a}_{nl}$ is $\mathbf{a}_{nl_{11}} = \phi^{(0)}_{z,x} = w_{,x}$ and that of $\mathbf{b}_{nl}$ is $\mathbf{b}_{nl_{12}} = \phi^{(1)}_{x}$; $(\ )_{,x}$ denotes the derivative with respect to x.

2.1.2. Equations of motion

Next, we will apply the principle of virtual displacements (see Reddy [41]) to obtain the governing equations of motion for the beam when the potential energy depends on rotation gradient and strains. For the given displacement field (see Eq. (2.1)) of beam, we have three nonzero components of strain and two nonzero components of $\boldsymbol{\theta}$ tensor on which potential energy would depend. For linear hyperelastic material (see Reddy[42]), the strain energy potential can be considered as a quadratic function of the components of strain and $\boldsymbol{\theta}$:

$$U = \int_0^L \int_A \frac{1}{2}\boldsymbol{\varepsilon} \cdot \mathbf{C} \cdot \boldsymbol{\varepsilon} + \frac{1}{2}\boldsymbol{\chi} \cdot \mathbf{C}_l \cdot \boldsymbol{\chi}\, dA\, dx \tag{2.10}$$

where $\mathbf{C}$ and $\mathbf{C}_l$ are the elasticity constant and material length scale, respectively. For positive potential energy, both $\mathbf{C}$ and $\mathbf{C}_l$ should be positive-definite tensors. The nonzero components symmetric part of stress tensor and couple stress tensor can be expressed in a vector form as

$$\mathbf{S}^s = \begin{Bmatrix} S^s_{xx} \\ S^s_{zz} \\ S^s_{xz} \end{Bmatrix} = \mathbf{C} \cdot \boldsymbol{\varepsilon}, \quad \text{and } \mathbf{m} = \begin{Bmatrix} m_{113} \\ m_{313} \end{Bmatrix} = \mathbf{C}_l \cdot \boldsymbol{\chi} \tag{2.11}$$

The first variation of the strain energy potential is

$$\begin{aligned}
\delta U &= \int_0^L \int_A \delta\boldsymbol{\varepsilon}\cdot\mathbf{S}^s + \delta\boldsymbol{\chi}\cdot\mathbf{m}\,dA\,dx \\
&= \int_0^L \int_A \left((\mathbf{A}_1+\mathbf{A}_{nl_1})\delta\boldsymbol{\Phi} + (\mathbf{A}_2+\mathbf{A}_{nl_2})\frac{d\delta\boldsymbol{\Phi}}{dx}\right)\cdot\mathbf{S}^s \\
&\quad + \left(\mathbf{B}_1\delta\boldsymbol{\Phi} + \mathbf{B}_2\frac{d\delta\boldsymbol{\Phi}}{dx} + \mathbf{B}_3\frac{d^2\delta\boldsymbol{\Phi}}{dx^2}\right)\cdot\mathbf{m}\,dA\,dx \\
&= \int_0^L \delta\boldsymbol{\Phi}\cdot\left(\int_A \left((\mathbf{A}_1^T+\mathbf{A}_{nl_1}^T)\mathbf{S}^s + \mathbf{B}_1^T\mathbf{m}\right)\,dA\right) \\
&\quad + \frac{d\delta\boldsymbol{\Phi}}{dx}\cdot\left(\int_A \left((\mathbf{A}_{nl_2}^T+\mathbf{A}_2^T)\mathbf{S}^s + \mathbf{B}_2^T\mathbf{m}\right)\,dA\right) \\
&\quad + \frac{d^2\delta\boldsymbol{\Phi}}{dx^2}\cdot\left(\int_A \mathbf{B}_3^T\mathbf{m}\,dA\right)dx
\end{aligned} \tag{2.12}$$

Let us define

$$\begin{aligned}
\mathbf{M}_j &= \int_A \mathbf{A}_j^T\mathbf{S}^s\,dA \quad \text{for } j=1,2 \text{ and } \mathbf{M}_{nl_1} = \int_A \mathbf{A}_{nl_1}^T\mathbf{S}^s\,dA \\
\boldsymbol{\mathcal{M}}_j &= \int_A \mathbf{B}_j^T\mathbf{m}\,dA \quad \text{for } j=1,2,3 \text{ and } \mathbf{M}_{nl_2} = \int_A \mathbf{A}_{nl_2}^T\mathbf{S}^s\,dA
\end{aligned} \tag{2.13}$$

so that the first variation of the strain energy potential can be rewritten as

$$\begin{aligned}
\delta U = \int_0^L \Big[&\delta\boldsymbol{\Phi}\cdot(\mathbf{M}_1+\boldsymbol{\mathcal{M}}_1+\mathbf{M}_{nl_1}) + \frac{d\delta\boldsymbol{\Phi}}{dx}\cdot((\mathbf{M}_{nl_2}+\mathbf{M}_2)+\boldsymbol{\mathcal{M}}_2) \\
&+\frac{d^2\delta\boldsymbol{\Phi}}{dx^2}\cdot\boldsymbol{\mathcal{M}}_3\Big]\,dx
\end{aligned} \tag{2.14}$$

The virtual work done by external forces is given by

$$\begin{aligned}
\delta V &= -\int_0^L \Big[\int_A (f_x\delta u_1 + f_z\delta u_3)\,dA + q_x^t\delta u_1(x,\frac{h}{2}) + q_x^b\delta u_1(x,-\frac{h}{2}) \\
&\qquad + q_z^t\delta u_3(x,\frac{h}{2}) + q_z^b\delta u_3(x,-\frac{h}{2})\Big]dx \\
&= -\int_0^L \Big[\sum_{i=0}^{m} F_x^{(i)}\delta\phi_x^{(i)} + \sum_{i=0}^{m-1} F_z^{(i)}\delta\phi_z^{(i)}\Big]dx = -\int_0^L \delta\boldsymbol{\Phi}\cdot\hat{\mathbf{F}}\,dx
\end{aligned} \tag{2.15}$$

where

$$\begin{aligned}
\hat{\mathbf{F}} &= \begin{bmatrix} F_x^{(0)} & F_x^{(1)} & \cdots & F_x^{(n)} & F_z^{(0)} & F_z^{(1)} & \cdots & F_z^{(m)} \end{bmatrix}^T \\
f_x^{(i)} &= \int_A z^i f_x \, dA, \quad f_z^{(i)} = \int_A z^i f_z \, dA \\
F_\xi^{(i)} &= f_\xi^{(i)} + \left(\frac{h}{2}\right)^i \left[q_\xi^t + (-1)^i q_\xi^b\right] \quad (\xi = x, z)
\end{aligned} \tag{2.16}$$

Here f_x and f_z denote, respectively, the distributed axial and transverse loads per unit volume of the beam whereas q_x^t and q_z^t denote the distributed axial and transverse loads per unit length at the top surface and (q_x^b, q_z^b) represent the same at the bottom surface of the beam. Using the principle of virtual displacements, we obtain

$$\begin{aligned}
0 &= \delta U + \delta V \\
&= \int_0^L \Big[\delta\mathbf{\Phi} \cdot (\mathbf{M}_1 + \boldsymbol{\mathcal{M}}_1 + \mathbf{M}_{nl_1}) + \frac{d\delta\mathbf{\Phi}}{dx} \cdot ((\mathbf{M}_{nl_2} + \mathbf{M}_2) + \boldsymbol{\mathcal{M}}_2) \\
&\qquad + \frac{d^2\delta\mathbf{\Phi}}{dx^2} \cdot \boldsymbol{\mathcal{M}}_3 - \delta\mathbf{\Phi} \cdot \hat{\mathbf{F}}\Big] \, dx \\
&= \int_0^L \delta\mathbf{\Phi} \cdot \left((\mathbf{M}_1 + \boldsymbol{\mathcal{M}}_1 + \mathbf{M}_{nl_1}) - \frac{d}{dx}\left((\mathbf{M}_{nl_2} + \mathbf{M}_2) + \boldsymbol{\mathcal{M}}_2\right) + \frac{d^2\boldsymbol{\mathcal{M}}_3}{dx^2} - \hat{\mathbf{F}}\right) dx \\
&\quad + \left[\delta\mathbf{\Phi} \cdot \left((\mathbf{M}_{nl_2} + \mathbf{M}_2) + \boldsymbol{\mathcal{M}}_2 - \frac{d\boldsymbol{\mathcal{M}}_3}{dx}\right) + \frac{d\delta\mathbf{\Phi}}{dx} \cdot \boldsymbol{\mathcal{M}}_3\right]_0^L
\end{aligned} \tag{2.17}$$

Hence the equation of motion (the Euler–Lagrange equations) is

$$(\mathbf{M}_1 + \boldsymbol{\mathcal{M}}_1 + \mathbf{M}_{nl_1}) - \frac{d}{dx}\left((\mathbf{M}_{nl_2} + \mathbf{M}_2) + \boldsymbol{\mathcal{M}}_2\right) + \frac{d^2\boldsymbol{\mathcal{M}}_3}{dx^2} - \hat{\mathbf{F}} = 0 \tag{2.18}$$

and the primary and secondary variables are

$$\begin{aligned}
\delta\mathbf{\Phi} : &\quad (\mathbf{M}_{nl_2} + \mathbf{M}_2) + \boldsymbol{\mathcal{M}}_2 - \frac{d\boldsymbol{\mathcal{M}}_3}{dx} \\
\frac{d\delta\mathbf{\Phi}}{dx} : &\quad \boldsymbol{\mathcal{M}}_3.
\end{aligned} \tag{2.19}$$

In the boundary expressions, we note that the secondary variable $\boldsymbol{\mathcal{M}}_3$, which is dual to the primary variable $\frac{d\mathbf{\Phi}_x}{dx}$, is zero.

2.2. Constitutive relation

2.2.1. Homogeneous and isotropic beam

In the case of the general third-order (or possibly any higher-order beam theory), we will assume plane stress state considering the normal stress component along y-direction is very small and can be neglected. Hence the relation between symmetric part of the stress and the strain, for isotropic and linear elastic material in the case of homogeneous beam, can be expressed as

$$\begin{Bmatrix} S^s_{xx} \\ S^s_{zz} \\ S^s_{xz} \end{Bmatrix} = \frac{E}{1-\nu^2} \begin{bmatrix} 1 & \nu & 0 \\ \nu & 1 & 0 \\ 0 & 0 & \frac{(1-\nu)}{2} \end{bmatrix} \begin{Bmatrix} \varepsilon_{xx} \\ \varepsilon_{zz} \\ \gamma_{xz} \end{Bmatrix} \tag{2.20}$$

where E and ν are the modulus of elasticity and Poisson's ratio, respectively. Next, consider that the material is reinforced with very tiny chopped stiffer fibers or phases compared to the host (matrix) material, which can be considered rotating rigidly with the matrix material. The orientations of the reinforcing fibers are along the length and height of the beam (and possibly some fibers are oriented along the width of the beam also). Since we have assumed a displacement field such that there could only be rotation in xz-plane, there could be two different material length scale parameters: ℓ_1 related to the fibers oriented along the length of the beam and the other ℓ_2 related to the fibers oriented along the height of the beam. Then the relation between the couple stresses and the components of $\boldsymbol{\theta}$ can be written as

$$\begin{Bmatrix} m_{113} \\ m_{313} \end{Bmatrix} = G \begin{bmatrix} \ell_1^2 & 0 \\ 0 & \ell_2^2 \end{bmatrix} \begin{Bmatrix} \theta_{113} \\ \theta_{313} \end{Bmatrix} \tag{2.21}$$

If the rotation gradient dependent terms of the potential energy are due to micro structure of the material, then, for centro-symmetric material, we can have the length scale parameters ℓ_1 and ℓ_2 as equal (say ℓ). The material length scale parameter is the square root of the ratio of the modulus of curvature to the modulus of shear, and it is a physical a property measuring the effect of couple stress (see Mindlin [43]). This could also be the case of equally oriented stiff small inclusions or granular inclusion embedded in the comparatively soft matrix of isotropic material. Comparing with

Eq. (2.11), we have

$$\mathbf{C} = \frac{E}{1-\nu^2}\begin{bmatrix} 1 & \nu & 0 \\ \nu & 1 & 0 \\ 0 & 0 & \frac{(1-\nu)}{2} \end{bmatrix}, \quad \mathbf{C}_l = G\begin{bmatrix} \ell_1^2 & 0 \\ 0 & \ell_2^2 \end{bmatrix} \tag{2.22}$$

2.2.2. Functionally graded beam

A typical material property of a functionally graded beam through the thickness is assumed to be represented by a power-law (see Praveen and Reddy [44] and Reddy [45])

$$P(z) = [P_1 - P_2]\, f(z) + P_2, \quad f(z) = \left(\frac{1}{2} + \frac{z}{h}\right)^{\hat{n}} \tag{2.23}$$

where P_1 and P_2 are the values of a typical material property, such as the modulus, density, and conductivity, of material at the top (at $z = h/2$) and bottom (at $z = -h/2$) surface of the beam, respectively; $\hat{n}$ denotes the volume fraction exponent, called power-law index. When $\hat{n} = 0$, we obtain the single-material beam (with property P_1). In the present analysis, we will consider Poisson's ratio as a constant. Then we have

$$\mathbf{C}(z) = \frac{E(z)}{1-\nu^2}\begin{bmatrix} 1 & \nu & 0 \\ \nu & 1 & 0 \\ 0 & 0 & \frac{(1-\nu)}{2} \end{bmatrix}, \quad \mathbf{C}_l = G(z)\begin{bmatrix} \ell_1^2 & 0 \\ 0 & \ell_2^2 \end{bmatrix} \tag{2.24}$$

In the case of a rotation gradient dependent functionally graded beam, the length scale is taken as constant, which can be considered as effective value of the length scale parameter in the case of varying microstructure size (or small inclusions) through thickness.

2.2.3. Orthotropic beam

In the case of orthotropic beam, the elasticity tensor $\mathbf{C}$ for plane stress case is given by

$$\mathbf{C} = \begin{bmatrix} Q_{11} & Q_{13} & 0 \\ Q_{13} & Q_{33} & 0 \\ 0 & 0 & Q_{66} \end{bmatrix}, \quad \mathbf{C}_l = Q_{66} \begin{bmatrix} \ell_1^2 & 0 \\ 0 & \ell_2^2 \end{bmatrix} \tag{2.25}$$

where

$$\begin{aligned} Q_{11} &= \frac{E_1}{1-\nu_{13}\nu_{31}}, \quad Q_{13} = \frac{\nu_{13}E_3}{1-\nu_{13}\nu_{31}} = \frac{\nu_{31}E_1}{1-\nu_{13}\nu_{31}} \\ Q_{33} &= \frac{E_3}{1-\nu_{13}\nu_{31}}, \quad Q_{66} = G_{13} \end{aligned} \tag{2.26}$$

2.2.4. Stress resultant

For all types of beams, the generalized stress resultants can be defined as follows:

$$\begin{aligned} \mathbf{M}_i &= \left(\int_A \mathbf{A}_i^T \mathbf{C}(\mathbf{A}_1 + \tfrac{1}{2}\mathbf{A}_{nl_1})\, dA\right)\mathbf{\Phi} + \left(\int_A \tfrac{1}{2}\mathbf{A}_i^T\mathbf{C}\mathbf{A}_{nl_2} + \mathbf{A}_j^T\mathbf{C}\mathbf{A}_2\, dA\right)\frac{d\mathbf{\Phi}}{dx} \\ \mathbf{M}_{nl_1} &= \left(\int_A \mathbf{A}_{nl_1}^T \mathbf{C}(\mathbf{A}_1 + \tfrac{1}{2}\mathbf{A}_{nl_1})\, dA\right)\mathbf{\Phi} + \left(\int_A \tfrac{1}{2}\mathbf{A}_{nl_1}^T\mathbf{C}\mathbf{A}_{nl_2} + \mathbf{A}_{nl_1}^T\mathbf{C}\mathbf{A}_2\, dA\right)\frac{d\mathbf{\Phi}}{dx} \\ \mathbf{M}_{nl_2} &= \left(\int_A \mathbf{A}_{nl_2}^T \mathbf{C}(\mathbf{A}_1 + \tfrac{1}{2}\mathbf{A}_{nl_1})\, dA\right)\mathbf{\Phi} + \left(\int_A \tfrac{1}{2}\mathbf{A}_{nl_2}^T\mathbf{C}\mathbf{A}_{nl_2} + \mathbf{A}_{nl_2}^T\mathbf{C}\mathbf{A}_2\, dA\right)\frac{d\mathbf{\Phi}}{dx} \\ \boldsymbol{\mathcal{M}}_j &= \left(\int_A \mathbf{B}_j^T\mathbf{C}_l\mathbf{B}_1\, dA\right)\mathbf{\Phi} + \left(\int_A \mathbf{B}_j^T\mathbf{C}_l\mathbf{B}_2\, dA\right)\frac{d\mathbf{\Phi}}{dx} + \left(\int_A \mathbf{B}_j^T\mathbf{C}_l\mathbf{B}_3\, dA\right)\frac{d^2\mathbf{\Phi}}{dx^2} \end{aligned} \tag{2.27}$$

for $i = 1, 2$ and $j = 1, 2, 3$.

2.3. Finite element model

The domain $\bar{\Omega} = [0, L]$ is divided into a number of non-overlapping finite elements $\bar{\Omega} = \cup\bar{\Omega}^e$, a typical element being $\bar{\Omega}^e = [x_1^e, x_2^e]$. Then the weak form of the equation of motion, Eq. (2.18), over a typical element in terms of the generalized displacements

is obtained as

$$0 = \int_{x_1^e}^{x_2^e} \int_A \Bigg\{ \left[(\mathbf{A}_1 + \mathbf{A}_{nl_1})\delta\mathbf{\Phi} + (\mathbf{A}_2 + \mathbf{A}_{nl_2})\frac{d\delta\mathbf{\Phi}}{dx} \right] \cdot \mathbf{C} \Big[(\mathbf{A}_1 + \tfrac{1}{2}\mathbf{A}_{nl_1})\mathbf{\Phi} + (\mathbf{A}_2 + \tfrac{1}{2}\mathbf{A}_{nl_2})\frac{d\mathbf{\Phi}}{dx} \Big] + \left[\mathbf{B}_1\delta\mathbf{\Phi} + \mathbf{B}_2\frac{d\delta\mathbf{\Phi}}{dx} + \mathbf{B}_3\frac{d^2\delta\mathbf{\Phi}}{dx^2} \right] \cdot \mathbf{C}_l \left[\mathbf{B}_1\mathbf{\Phi} + \mathbf{B}_2\frac{d\mathbf{\Phi}}{dx} + \mathbf{B}_3\frac{d^2\mathbf{\Phi}}{dx^2} \right] dA - \delta\mathbf{\Phi} \cdot \hat{\mathbf{F}} \Bigg\} dx \tag{2.28}$$

We approximate the vector of generalized displacements as

$$\mathbf{\Phi}(x) = \mathbf{\Psi}(x)\bar{\mathbf{U}} \tag{2.29}$$

where $\mathbf{\Psi}(x)$ is the matrix of shape functions and $\bar{\mathbf{U}}$ is vector of the nodal values of the generalized displacements[3],

$$\mathbf{\Psi} = \begin{bmatrix} \psi_1^{(1)} & \dots & \psi_{\tilde{n}_1}^{(1)} & 0 & \dots & 0 & \dots & 0 & \dots & 0 \\ 0 & \dots & 0 & \psi_1^{(2)} & \dots & \psi_{\tilde{n}_2}^{(2)} & \dots & 0 & \dots & 0 \\ \vdots & \ddots & \vdots & \vdots & \ddots & \vdots & \ddots & \vdots & \ddots & \vdots \\ 0 & \dots & 0 & 0 & \dots & 0 & \dots & \psi_1^{(\bar{r})} & \dots & \psi_{\tilde{n}_{\bar{r}}}^{(\bar{r})} \end{bmatrix} \tag{2.30}$$

$$\bar{\mathbf{U}} = \begin{bmatrix} u_{1_1} & \dots & u_{1_{\tilde{n}_1}} & u_{2_1} & \dots & u_{2_{\tilde{n}_2}} & \dots & u_{\bar{r}_1} & \dots & u_{\bar{r}_{\tilde{n}_{\bar{r}}}} \end{bmatrix}^T \tag{2.31}$$

where $\tilde{n}_1, \tilde{n}_2, \dots \tilde{n}_{\bar{r}}$ are the number of nodal values for $u_1, u_2, \dots, u_{\bar{r}}$, respectively, in the considered element where $\bar{r} = n+p+2$ is the total number of degrees of freedom (dofs), and

$$\begin{aligned} u_1 &= \phi_x^{(0)}, \quad u_2 = \phi_x^{(1)}, \quad \cdots \quad u_{n+1} = \phi_x^{(n)} \\ u_{n+2} &= \phi_z^{(0)}, \quad u_{n+3} = \phi_z^{(1)}, \quad \cdots \quad u_{\bar{r}} = \phi_z^{(p)} \end{aligned} \tag{2.32}$$

We substitute the approximation for all dependent variables and $\delta\mathbf{\Phi} = \mathbf{\Psi}\tilde{\mathbf{l}}$ (where $\tilde{\mathbf{l}}$ is the column vector with all elements unity, and the number of elements are the

[3]Here distinction should be made between $\bar{\mathbf{U}}$ and $\mathbf{U}$; $\mathbf{U}$ is the right stretch tensor of chapter 1, section 1.3, whereas $\bar{\mathbf{U}}$ is vector of nodal dofs. We note that, in this work, differently superposed symbol (superposed hat or dash) have different meanings.

same as columns of $\mathbf{\Psi}$) into Eq. (2.28) to arrive at the following equation:

$$
\begin{aligned}
0 = \int_{x_1^e}^{x_2^e} \Bigg\{ \int_A \Bigg[(\mathbf{A}_1 + \mathbf{A}_{nl_1})\mathbf{\Psi} + (\mathbf{A}_2 + \mathbf{A}_{nl_2})\frac{d\mathbf{\Psi}}{dx} \Bigg] \tilde{\mathbf{l}} \cdot \mathbf{C} \Big[(\mathbf{A}_1 + \tfrac{1}{2}\mathbf{A}_{nl_1})\mathbf{\Psi} \\
+ (\mathbf{A}_2 + \tfrac{1}{2}\mathbf{A}_{nl_2})\frac{d\mathbf{\Psi}}{dx} \Big] \bar{\mathbf{U}} + \left(\mathbf{B}_1\mathbf{\Psi} + \mathbf{B}_2\frac{d\mathbf{\Psi}}{dx} + \mathbf{B}_3\frac{d^2\mathbf{\Psi}}{dx^2} \right) \tilde{\mathbf{l}} \cdot \\
\mathbf{C}_l \left(\mathbf{B}_1\mathbf{\Psi} + \mathbf{B}_2\frac{d\mathbf{\Psi}}{dx} + \mathbf{B}_3\frac{d^2\mathbf{\Psi}}{dx^2} \right) \bar{\mathbf{U}}\, dA - \mathbf{\Psi}\tilde{\mathbf{l}} \cdot \hat{\mathbf{F}} \Bigg\} dx \\
= \tilde{\mathbf{l}} \cdot \int_{x_1^e}^{x_2^e} \Bigg\{ \int_A \Bigg[(\mathbf{A}_1 + \mathbf{A}_{nl_1})\mathbf{\Psi} + (\mathbf{A}_2 + \mathbf{A}_{nl_2})\frac{d\mathbf{\Psi}}{dx} \Bigg]^T \mathbf{C} \Big[(\mathbf{A}_1 + \frac{1}{2}\mathbf{A}_{nl_1})\mathbf{\Psi} \\
+ (\mathbf{A}_2 + \frac{1}{2}\mathbf{A}_{nl_2})\frac{d\mathbf{\Psi}}{dx} \Big] \bar{\mathbf{U}} + \left(\mathbf{B}_1\mathbf{\Psi} + \mathbf{B}_2\frac{d\mathbf{\Psi}}{dx} + \mathbf{B}_3\frac{d^2\mathbf{\Psi}}{dx^2} \right)^T \\
\mathbf{C}_l \left(\mathbf{B}_1\mathbf{\Psi} + \mathbf{B}_2\frac{d\mathbf{\Psi}}{dx} + \mathbf{B}_3\frac{d^2\mathbf{\Psi}}{dx^2} \right) \bar{\mathbf{U}}\, dA - \mathbf{\Psi}^T\hat{\mathbf{F}} \Bigg\} dx
\end{aligned}
\tag{2.33}
$$

From the above equation, we obtain the following finite element equation:

$$
(\mathbf{K} + \mathbf{K}_l)\bar{\mathbf{U}} - \mathbf{f} = \mathbf{0} \tag{2.34}
$$

where $\mathbf{K}$ is the stiffness matrix related to the conventional beam and $\mathbf{K}_l$ is the stiffness matrix related to the length scale parameter of the material, which can be given as

$$
\begin{aligned}
\mathbf{K} &= \int_{x_1^e}^{x_2^e} \mathbf{\Psi}^T \left(\mathbf{H}_1\mathbf{\Psi} + \mathbf{H}_2\frac{d\mathbf{\Psi}}{dx} \right) + \frac{d\mathbf{\Psi}}{dx}^T \left(\mathbf{H}_3\mathbf{\Psi} + \mathbf{H}_4\frac{d\mathbf{\Psi}}{dx} \right) dx \\
\mathbf{K}_l &= \int_{x_1^e}^{x_2^e} \mathbf{\Psi}^T \left(\hat{\mathbf{H}}_1\mathbf{\Psi} + \hat{\mathbf{H}}_2\frac{d\mathbf{\Psi}}{dx} + \hat{\mathbf{H}}_3\frac{d^2\mathbf{\Psi}}{dx^2} \right) + \frac{d\mathbf{\Psi}}{dx}^T \left(\hat{\mathbf{H}}_4\mathbf{\Psi} + \hat{\mathbf{H}}_5\frac{d\mathbf{\Psi}}{dx} + \hat{\mathbf{H}}_6\frac{d^2\mathbf{\Psi}}{dx^2} \right) \\
&\quad + \frac{d^2\mathbf{\Psi}}{dx^2}^T \left(\hat{\mathbf{H}}_7\mathbf{\Psi} + \hat{\mathbf{H}}_8\frac{d\mathbf{\Psi}}{dx} + \hat{\mathbf{H}}_9\frac{d^2\mathbf{\Psi}}{dx^2} \right) dx \\
\mathbf{f} &= \int_{x_1^e}^{x_2^e} \mathbf{\Psi}^T\hat{\mathbf{F}}\, dx
\end{aligned}
\tag{2.35}
$$

where

$$
\begin{aligned}
&\mathbf{H}_1 = \int_A (\mathbf{A}_1 + \mathbf{A}_{nl_1})^T\mathbf{C}(\mathbf{A}_1 + \frac{1}{2}\mathbf{A}_{nl_1})\, dA, \quad \mathbf{H}_2 = \int_A (\mathbf{A}_1 + \mathbf{A}_{nl_1})^T\mathbf{C}(\mathbf{A}_2 + \frac{1}{2}\mathbf{A}_{nl_2})\, dA \\
&\mathbf{H}_3 = \int_A (\mathbf{A}_2 + \mathbf{A}_{nl_2})^T\mathbf{C}(\mathbf{A}_1 + \frac{1}{2}\mathbf{A}_{nl_1})\, dA, \quad \mathbf{H}_4 = \int_A (\mathbf{A}_{nl_2} + \mathbf{A}_2)^T\mathbf{C}(\mathbf{A}_2 + \frac{1}{2}\mathbf{A}_{nl_2})\, dA \\
&\hat{\mathbf{H}}_i = \int_A \mathbf{B}_j^T\mathbf{C}_l\mathbf{B}_k\, dA, \quad \text{where } i = 1, 2, ..., 9. \text{ and } j = \left[\frac{i}{3}\right] + 1, \quad k = (i\%3)
\end{aligned}
\tag{2.36}
$$

In the above equation, $[n]$ represents the greatest integer less than n and $(i\%3)$ is the remainder when i is divided by 3. Also we note here that matrix $\mathbf{A}_{nl_1}$ and $\mathbf{A}_{nl_2}$ depend on the displacement hence the stiffness matrix is nonlinear. We apply Newton's method (see Reddy [46]) to solve the nonlinear algebraic Eq. (2.34), which can be rewritten in the following form:

$$\mathbf{g}(\bar{\mathbf{U}}) = (\mathbf{K} + \mathbf{K}_l)\bar{\mathbf{U}} - \mathbf{f} = \mathbf{0} \tag{2.37}$$

For the guess solution $\bar{\mathbf{U}}_0$, we can write the following linear approximation of any vector-valued function,

$$\mathbf{g}(\bar{\mathbf{U}}) = \mathbf{g}(\bar{\mathbf{U}}_0) + D\mathbf{g}(\bar{\mathbf{U}}_0)(\bar{\mathbf{U}} - \bar{\mathbf{U}}_0) \tag{2.38}$$

where $D\mathbf{g}$ is (*Fréchet*) derivative of $\mathbf{g}(\bar{\mathbf{U}})$ with respect to $\bar{\mathbf{U}}$ defined at $(\bar{\mathbf{U}} = \bar{\mathbf{U}}_0)$; that is, $D\mathbf{g} = \frac{\partial \mathbf{g}}{\partial \bar{\mathbf{U}}}\big|_{(\bar{\mathbf{U}}=\bar{\mathbf{U}}_0)}$. We determine $\bar{\mathbf{U}}$ such that $\mathbf{g}(\bar{\mathbf{U}}) = 0$. Thus we have

$$D\mathbf{g}(\bar{\mathbf{U}}_0)(\bar{\mathbf{U}} - \bar{\mathbf{U}}_0) = -\mathbf{g}(\bar{\mathbf{U}}_0) \tag{2.39}$$

For $(r+1)$st iteration of Newton's method, the solution can be expressed as

$$\mathbf{T}(\bar{\mathbf{U}}_r)\delta\bar{\mathbf{U}}_{r+1} = -(\mathbf{K}(\bar{\mathbf{U}}_r) + \mathbf{K}_l(\bar{\mathbf{U}}_r))\bar{\mathbf{U}}_r + \mathbf{f}(\bar{\mathbf{U}}_r), \quad \text{and, } \bar{\mathbf{U}}_{r+1} = \bar{\mathbf{U}}_r + \delta\bar{\mathbf{U}}_{r+1} \tag{2.40}$$

where $\mathbf{T} = D\mathbf{g}$ is called the tangent matrix, which is given by

$$\begin{aligned}
\mathbf{T} &= D((\mathbf{K} + \mathbf{K}_l)\bar{\mathbf{U}} + \mathbf{f}) = (D\mathbf{K})\bar{\mathbf{U}} + \mathbf{K} + \mathbf{K}_l \\
&= \mathbf{K} + \mathbf{K}_l + \int_{x_1^e}^{x_2^e} \left[\mathbf{\Psi}^T \left(\tilde{\mathbf{H}}_1 \mathbf{\Psi} + \tilde{\mathbf{H}}_2 \frac{d\mathbf{\Psi}}{dx} \right) + \frac{d\mathbf{\Psi}}{dx}^T \left(\tilde{\mathbf{H}}_3 \mathbf{\Psi} + \tilde{\mathbf{H}}_4 \frac{d\mathbf{\Psi}}{dx} \right) \right] dx \\
&\quad + \int_{x_1^e}^{x_2^e} \left[\mathbf{\Psi}^T \mathbf{P}_{nl1} \mathbf{\Psi} + \frac{d\mathbf{\Psi}}{dx}^T \mathbf{P}_{nl2} \frac{d\mathbf{\Psi}}{dx} \right] dx
\end{aligned} \tag{2.41}$$

where

$$\begin{aligned}
\tilde{\mathbf{H}}_1 &= \frac{1}{2} \int_A (\mathbf{A}_1 + \mathbf{A}_{nl_1})^T \mathbf{C} \mathbf{A}_{nl_1} \, dA, \quad \tilde{\mathbf{H}}_2 = \frac{1}{2} \int_A (\mathbf{A}_1 + \mathbf{A}_{nl_1})^T \mathbf{C} \mathbf{A}_{nl_2} \, dA \\
\tilde{\mathbf{H}}_3 &= \frac{1}{2} \int_A (\mathbf{A}_2 + \mathbf{A}_{nl_2})^T \mathbf{C} \mathbf{A}_{nl_1} \, dA, \quad \tilde{\mathbf{H}}_4 = \frac{1}{2} \int_A (\mathbf{A}_{nl_2} + \mathbf{A}_2)^T \mathbf{C} \mathbf{A}_{nl_2} \, dA
\end{aligned} \tag{2.42}$$

and $\mathbf{P}_{nl1}$ and $\mathbf{P}_{nl2}$ are $(\bar{r} \times \bar{r})$ matrix with only nonzero element $P_{nl1_{22}} = \int_A S^s_{zz} \, dA$ and $P_{nl2_{(n+2)(n+2)}} = \int_A S^s_{xx} \, dA$. We note that the tangent matrix is symmetric.

2.4. Analytical solution

For a general higher-order beam theory, the linear governing equation is

$$(\mathbf{M}_1 + \boldsymbol{\mathcal{M}}_1) - \frac{d}{dx}(\mathbf{M}_2 + \boldsymbol{\mathcal{M}}_2) + \frac{d^2\boldsymbol{\mathcal{M}}_3}{dx^2} - \hat{\mathbf{F}} = 0 \tag{2.43}$$

where the various stress resultants from (2.27), in the linear case, can be simplified as

$$\begin{aligned} \mathbf{M}_i &= \bar{\mathbf{M}}^{(i1)}\boldsymbol{\Phi} + \bar{\mathbf{M}}^{(i2)}\frac{d\boldsymbol{\Phi}}{dx}, \quad \text{for } i = 1, 2 \\ \boldsymbol{\mathcal{M}}_j &= \bar{\boldsymbol{\mathcal{M}}}^{(j1)}\boldsymbol{\Phi} + \bar{\boldsymbol{\mathcal{M}}}^{(j2)}\frac{d\boldsymbol{\Phi}}{dx} + \bar{\boldsymbol{\mathcal{M}}}^{(j3)}\frac{d^2\boldsymbol{\Phi}}{dx^2} \quad \text{for } j = 1, 2, 3. \end{aligned} \tag{2.44}$$

where

$$\begin{aligned} \bar{\mathbf{M}}^{(jk)} &= \int_A \mathbf{A}_j^T \mathbf{C} \mathbf{A}_k \, dA, \quad \text{for } j, k = 1, 2 \\ \bar{\boldsymbol{\mathcal{M}}}^{(jk)} &= \int_A \mathbf{B}_j^T \mathbf{C}_l \mathbf{B}_k \, dA, \quad \text{for } j, k = 1, 2, 3 \end{aligned} \tag{2.45}$$

For a simply supported beam, we assume the solution in the following form:

$$\phi_x^{(i)}(x) = \sum_{r=1}^{\infty} U_r^{(i)} \cos\frac{r\pi x}{L}, \quad \psi_z^{(i)}(x) = \sum_{r=1}^{\infty} W_r^{(i)} \sin\frac{r\pi x}{L} \tag{2.46}$$

Then, the vector of unknown degrees of freedom and their derivatives can be obtained as

$$\boldsymbol{\Phi} = \sum_{r=1}^{\infty} \boldsymbol{\Phi}_r, \quad \boldsymbol{\Phi}_r = \mathbf{u}_r \begin{Bmatrix} \cos\alpha_r x \\ \sin\alpha_r x \end{Bmatrix}, \quad \frac{d^n\boldsymbol{\Phi}_r}{dx^n} = \mathbf{u}_r \boldsymbol{\alpha}_r^n \begin{Bmatrix} \cos\alpha_r x \\ \sin\alpha_r x \end{Bmatrix} \tag{2.47}$$

where $\alpha_r = \frac{r\pi}{L}$ and

$$\mathbf{u}_r = \begin{bmatrix} U_r^{(0)} & U_r^{(1)} & \cdots & U_r^{(n)} & 0 & 0 & \cdots & 0 \\ 0 & 0 & \cdots & 0 & W_r^{(0)} & W_r^{(1)} & \cdots & W_r^{(p)} \end{bmatrix}^T, \quad \boldsymbol{\alpha}_r = \begin{bmatrix} 0 & -\alpha_r \\ \alpha_r & 0 \end{bmatrix} \tag{2.48}$$

and the applied transverse force is expressed as

$$f(x) = \sum_{r=1}^{\infty} F_r \sin\alpha_r x, \quad \text{and} \quad \hat{\mathbf{F}} = \sum_{r=1}^{\infty} \mathbf{f}_r \begin{Bmatrix} \cos\alpha_r x \\ \sin\alpha_r x \end{Bmatrix} \tag{2.49}$$

where

$$\mathbf{f}_r = \begin{bmatrix} 0 & 0 & \cdots & 0 & 0 & 0 & \cdots & 0 \\ 0 & 0 & \cdots & 0 & F_{zr}^{(0)} & F_{zr}^{(1)} & \cdots & F_{zr}^{(p)} \end{bmatrix}^T, \quad \text{and} \quad F_{zr}^{(i)} = \int_A z^i F_r \, dA. \tag{2.50}$$

Substituting the force vector $\hat{\mathbf{F}}$ and dof vector $\mathbf{\Phi}$ along with its derivatives in the stress resultants and then into the equation of motion (2.43), we obtain

$$\begin{aligned} \mathbf{0} \;=\; \sum_{r=1}^{\infty} \Big[& (\bar{\mathbf{M}}^{(11)} + \bar{\boldsymbol{\mathcal{M}}}^{(11)})\mathbf{u}_r + (\bar{\mathbf{M}}^{(12)} + \bar{\boldsymbol{\mathcal{M}}}^{(12)} - \bar{\mathbf{M}}^{(21)} - \bar{\boldsymbol{\mathcal{M}}}^{(21)})\mathbf{u}_r\boldsymbol{\alpha}_r \\ & +(\bar{\boldsymbol{\mathcal{M}}}^{(13)} - \bar{\mathbf{M}}^{(22)} - \bar{\boldsymbol{\mathcal{M}}}^{(22)} + \bar{\boldsymbol{\mathcal{M}}}^{(31)})\mathbf{u}_r\boldsymbol{\alpha}_r^2 \\ & +(\bar{\boldsymbol{\mathcal{M}}}^{(32)} - \bar{\boldsymbol{\mathcal{M}}}^{(23)})\mathbf{u}_r\boldsymbol{\alpha}_r^3 + \bar{\boldsymbol{\mathcal{M}}}^{(33)}\mathbf{u}_r\boldsymbol{\alpha}_r^4 - \mathbf{f}_r \Big] \begin{Bmatrix} \cos\alpha_r x \\ \sin\alpha_r x \end{Bmatrix} \end{aligned} \tag{2.51}$$

The coefficient matrix of the vector having sine and cosine functions, in Eq. (2.51), would be equal to zero for each r in the summation due to orthogonality of sine and cosine functions. The coefficient matrix results in system of $2(n+p+2)$ linear equations and it can be shown that only half of these equations would be nonzero equations, which results in a system of $(n+p+2)$ linear equations, which can be solved for $(n+p+2)$ dof unknowns. The system of linear equations can be written as following form by simplifying the obtained set of equations from Eq. (2.51),

$$\mathbf{K}_r \mathbf{\Delta}_r = \bar{\mathbf{f}}_r \tag{2.52}$$

where

$$\begin{aligned} \mathbf{K}_r &= (\bar{\mathbf{M}}^{(11)} + \bar{\boldsymbol{\mathcal{M}}}^{(11)}) + (\bar{\mathbf{M}}^{(12)} + \bar{\boldsymbol{\mathcal{M}}}^{(12)} - \bar{\mathbf{M}}^{(21)} - \bar{\boldsymbol{\mathcal{M}}}^{(21)})\mathbf{A}_r^{(1)} \\ &\quad + (\bar{\boldsymbol{\mathcal{M}}}^{(13)} - \bar{\mathbf{M}}^{(22)} - \bar{\boldsymbol{\mathcal{M}}}^{(22)} + \bar{\boldsymbol{\mathcal{M}}}^{(31)})\mathbf{A}_r^{(2)} \\ &\quad + (\bar{\boldsymbol{\mathcal{M}}}^{(32)} - \bar{\boldsymbol{\mathcal{M}}}^{(23)})\mathbf{A}_r^{(3)} + \bar{\boldsymbol{\mathcal{M}}}^{(33)}\mathbf{A}_r^{(4)} \end{aligned} \tag{2.53}$$

$$\begin{aligned} \mathbf{\Delta}_r &= \begin{bmatrix} U_r^{(0)} & U_r^{(1)} & \cdots & U_r^{(n)} & W_r^{(0)} & W_r^{(1)} & \cdots & W_r^{(p)} \end{bmatrix}^T \\ \bar{\mathbf{f}}_r &= \begin{bmatrix} 0 & 0 & \cdots & 0 & F_{zr}^{(0)} & F_{zr}^{(1)} & \cdots & F_{zr}^{(p)} \end{bmatrix}^T \end{aligned} \tag{2.54}$$

and $\mathbf{A}_r^{(i)}$ for $i = 1, 2, 3, 4$ are $(n + p + 2) \times (n + p + 2)$ diagonal matrices with their respective diagonal vectors, $\mathbf{d}_r^{(i)}$ defined as follows:

$$\begin{aligned}
\mathbf{d}_r^{(1)} &= [\mathbf{d}_1^{(1)} \quad \mathbf{d}_2^{(1)}]^T, \quad \mathbf{d}_1^{(1)} = \alpha_{r_{12}} \mathbf{I}_n, \quad \mathbf{d}_2^{(1)} = \alpha_{r_{21}} \mathbf{I}_p \\
\mathbf{d}_r^{(2)} &= [\mathbf{d}_1^{(2)} \quad \mathbf{d}_2^{(2)}]^T, \quad \mathbf{d}_1^{(2)} = \alpha_{r_{11}}^2 \mathbf{I}_n, \quad \mathbf{d}_2^{(2)} = \alpha_{r_{22}}^2 \mathbf{I}_p \\
\mathbf{d}_r^{(3)} &= [\mathbf{d}_1^{(3)} \quad \mathbf{d}_2^{(3)}]^T, \quad \mathbf{d}_1^{(3)} = \alpha_{r_{12}}^3 \mathbf{I}_n, \quad \mathbf{d}_2^{(3)} = \alpha_{r_{21}}^3 \mathbf{I}_p \\
\mathbf{d}_r^{(4)} &= [\mathbf{d}_1^{(4)} \quad \mathbf{d}_2^{(4)}]^T, \quad \mathbf{d}_1^{(4)} = \alpha_{r_{11}}^4 \mathbf{I}_n, \quad \mathbf{d}_2^{(4)} = \alpha_{r_{22}}^4 \mathbf{I}_p
\end{aligned} \tag{2.55}$$

where $\mathbf{I}_n$ and $\mathbf{I}_p$ are matrices of size $1 \times (n + 1)$ and $1 \times (p + 1)$, respectively, with all elements as unity; $\alpha_{r_{ij}}^k$ is the $(ij)th$ element of kth power of matrix $\boldsymbol{\alpha}_r$.

2.5. Specialization to beam theories

2.5.1. The general third order beam theory

We take $n = 3$ and $p = 2$ in Eq. (2.1) and obtain the following displacement field for the general third-order beam theory for bending of beam about the y-axis,

$$\begin{aligned}
\mathbf{u} &= u_1 \, \hat{\mathbf{e}}_1 + u_2 \, \hat{\mathbf{e}}_2 + u_3 \, \hat{\mathbf{e}}_3 \quad \text{where,} \\
u_1 = u + z\phi_x^{(1)} + z^2\phi_x^{(2)} + z^3\phi_x^{(3)}, &\quad u_2 = 0, \quad u_3 = w + z\phi_z^{(1)} + z^2\phi_z^{(2)}
\end{aligned} \tag{2.56}$$

In the case of the general third-order beam theory, cross-section perpendicular to centroidal axis does not remain plane, as reflected in the displacement field; hence, two length scale parameters, namely ℓ_1 and ℓ_2, related to the inclusions oriented along x- and z-axes, would contribute in the stiffness of the beam while considering the rotation gradient dependent potential energy. Equations of motion and the corresponding finite element model can be obtained by putting $n = 3$ and $p = 2$ in the formulation presented in the above section. For the general third-order or any higher-order beam theory, plane stress condition should be assumed owing to the fact that the stress in the y-direction is very small.

2.5.2. The Timoshenko (First order) beam theory

For the Timoshenko beam theory, we take $n = 1$ and $p = 0$ in the power (Taylor) series expansion of displacement field. Equation (2.1) becomes

$$\begin{aligned} \mathbf{u} &= u_1\,\hat{\mathbf{e}}_1 + u_2\,\hat{\mathbf{e}}_2 + u_3\,\hat{\mathbf{e}}_3 \quad \text{where,} \\ u_1 &= u + z\phi_x^{(1)}, \quad u_2 = 0, \quad u_3 = w \end{aligned} \tag{2.57}$$

In the Bernoulli–Euler and the Timoshenko beam theories, the plane perpendicular to the centroidal axis remains plane after deformation and consequently the material length scale parameters related to the fibres (inclusions) oriented along the perpendicular plane do not contribute to the stiffness of the beam. Hence, only one length scale parameter related to the inclusions oriented along the length of the beam contributes to the bending stiffness of the beam for this case. In the case of the Timoshenko and Bernoulli–Euler beam theories, we neglect ε_{zz} in Eq. (2.5) as the first-order displacement fields are not equipped to deal with ε_{zz} as linear term in ε_{zz} is zero for given displacement field and only nonlinear term would be there for ε_{zz}, which is not enough to model the variation in ε_{zz} along height of the beam. The nonzero strain components for the Timoshenko beam are

$$\varepsilon_{xx} = \left[\frac{\partial u}{\partial x} + \frac{1}{2}\left(\frac{\partial w}{\partial x}\right)^2\right] + z\frac{\partial \phi_x^{(1)}}{\partial x}, \quad \gamma_{xz} = \phi_x^{(1)} + \frac{\partial w}{\partial x}. \tag{2.58}$$

The uniaxial stress–strain relations are assumed:

$$S_{xx}^s = E\varepsilon_{xx}, \quad S_{xz}^s = S_z G\gamma_{xz} \tag{2.59}$$

where S_z is the shear correction factor. Also, θ_{331} would be equal to zero. By comparing the constitutive relation given in Eq. (2.20) and (2.21), we can use the following material constant matrices in the aforemention formulation to get the finite element solution as well as the analytical solution for the linear case.

$$\mathbf{C} = \begin{bmatrix} E & 0 & 0 \\ 0 & 0 & 0 \\ 0 & 0 & S_z G \end{bmatrix}, \quad \mathbf{C}_l = G \begin{bmatrix} \ell^2 & 0 \\ 0 & 0 \end{bmatrix} \tag{2.60}$$

Also, we put $\mathbf{A}_{nl_1} = \mathbf{0}$ for the Timoshenko beam.

2.5.3. The Bernoulli–Euler beam theory

In the Bernoulli–Euler beam theory also, we take $n = 1$ and $p = 0$ but with the constrain $\phi_x^{(1)} = -\frac{dw}{dx}$ in the Eq. (2.1). Then the displacement field becomes

$$\begin{aligned} \mathbf{u} &= u_1\,\hat{\mathbf{e}}_1 + u_2\,\hat{\mathbf{e}}_2 + u_3\,\hat{\mathbf{e}}_3 \quad \text{where,} \\ u_1 &= u - z\frac{dw}{dx}, \quad u_2 = 0, \quad u_3 = w \end{aligned} \tag{2.61}$$

In this case, the plane perpendicular to the centroidal axis remain perpendicular and plane after deformation hence there is only one material length scale parameter which will contribute to the bending stiffness of the beam as in the case of the Timoshenko beam. The nonzero component of von Kármán strain and $\boldsymbol{\theta}$ from Eqs. (2.5) and (2.6) take the form

$$\begin{aligned} \varepsilon_{xx} &= \frac{du}{dx} - z\frac{d^2w}{dx^2} + \frac{1}{2}\left(\frac{dw}{dx}\right)^2 = \mathbf{A}_2\frac{d\boldsymbol{\Phi}}{dx} + \frac{1}{2}\mathbf{A}_{nl}\frac{d\boldsymbol{\Phi}}{dx} + \mathbf{A}_3\frac{d^2\boldsymbol{\Phi}}{dx^2} \\ \theta_{131} &= \frac{d^2w}{dx^2} = \mathbf{B}\frac{d^2\boldsymbol{\Phi}}{dx^2} \end{aligned} \tag{2.62}$$

where

$$\mathbf{A}_2 = [1 \quad 0], \quad \mathbf{A}_3 = [0 \quad -z], \quad \mathbf{A}_{nl} = [0 \quad \tfrac{dw}{dx}], \quad \mathbf{B} = [0 \quad 1], \quad \boldsymbol{\Phi} = [u \quad w]^T \tag{2.63}$$

Further, the constitutive relation is

$$S_{xx}^s = E\varepsilon_{xx}, \quad m_{113} = G\ell^2\theta_{131} \tag{2.64}$$

After minimizing the potential energy given in Eq. (2.10), we can have the equation of motion

$$-\frac{d}{dx}(\mathbf{M_2} + \mathbf{M}_{nl}) + \frac{d^2}{dx^2}(\mathbf{M_3} + \boldsymbol{\mathcal{M}}) - \mathbf{f} = 0 \tag{2.65}$$

The primary and secondary variables are of the form

$$\begin{aligned} \delta\boldsymbol{\Phi}: &\qquad (\mathbf{M}_{nl}+\mathbf{M}_2)-\frac{d}{dx}(\mathbf{M}_3+\boldsymbol{\mathcal{M}}) \\ \frac{d\delta\boldsymbol{\Phi}}{dx}: &\qquad \mathbf{M}_3+\boldsymbol{\mathcal{M}} \end{aligned} \tag{2.66}$$

where

$$\begin{aligned} \mathbf{M}_2 &= \int_A \mathbf{A}_2^T S_{xx}^s\, dA, \quad \mathbf{M}_3 = \int_A \mathbf{A}_3^T S_{xx}^s\, dA \\ \mathbf{M}_{nl} &= \int_A \mathbf{A}_{nl}^T S_{xx}^s\, dA, \quad \boldsymbol{\mathcal{M}} = \int_A \mathbf{B}^T m_{113}\, dA, \quad \mathbf{f} = [f_x \quad f_z]^T \end{aligned} \tag{2.67}$$

Here f_x and f_z are the axial and transverse forces per unit length of the beam. In the case of Bernoulli–Euler beam also, we note that the corresponding terms in the natural boundary term $\boldsymbol{\mathcal{M}}$ and $\mathbf{M}_3$ for $\frac{du}{dx}$ is zero; hence, $\frac{dw}{dx}$ is a primary variable. By approximating the dofs as given in Eq. (2.30), we can have the nonlinear finite element equation of the form in Eq. (2.34) and then by applying Newton's method, we will have the algebraic equation of the form in Eq. (2.39). The stiffness matrix and force vector of the finite element model are

$$\begin{aligned} \mathbf{K} &= \int_{x_a}^{x_b} \frac{d\boldsymbol{\Psi}^T}{dx}\mathbf{H}_1\frac{d\boldsymbol{\Psi}}{dx} + \frac{d\boldsymbol{\Psi}^T}{dx}\mathbf{H}_2\frac{d^2\boldsymbol{\Psi}}{dx^2} + \frac{d^2\boldsymbol{\Psi}^T}{dx^2}\mathbf{H}_3\frac{d\boldsymbol{\Psi}}{dx} + \frac{d^2\boldsymbol{\Psi}^T}{dx^2}\mathbf{H}_4\frac{d^2\boldsymbol{\Psi}}{dx^2}\, dx \\ \mathbf{K}_l &= \int_{x_a}^{x_b} \frac{d^2\boldsymbol{\Psi}^T}{dx^2}\mathbf{H}_l\frac{d^2\boldsymbol{\Psi}}{dx^2}\, dx, \quad \hat{\mathbf{F}} = \int_{x_a}^{x_b} \boldsymbol{\Psi}^T\mathbf{f}\, dx \end{aligned} \tag{2.68}$$

where

$$\begin{aligned} \mathbf{H}_1 &= \int_A (\mathbf{A}_2^T+\mathbf{A}_{nl}^T)E(\mathbf{A}_2+\frac{1}{2}\mathbf{A}_{nl})\, dA, \quad \mathbf{H}_2 = \int_A (\mathbf{A}_2^T+\mathbf{A}_{nl}^T)E\mathbf{A}_3\, dA \\ \mathbf{H}_3 &= \int_A \mathbf{A}_3^T E(\mathbf{A}_2+\frac{1}{2}\mathbf{A}_{nl})\, dA, \qquad\qquad \mathbf{H}_4 = \int_A \mathbf{A}_3^T E\mathbf{A}_3\, dA \\ \mathbf{H}_l &= \int_A \mathbf{B}^T G\ell^2\mathbf{B}\, dA \end{aligned} \tag{2.69}$$

For Newton's method, the tangent matrix can be computed as

$$\mathbf{T} = \mathbf{K}+\mathbf{K}_l+\int_{x_a}^{x_b} \frac{d\boldsymbol{\Psi}^T}{dx}(\hat{\mathbf{H}}_1+\tilde{\mathbf{H}}_1)\frac{d\boldsymbol{\Psi}}{dx} + \frac{d^2\boldsymbol{\Psi}^T}{dx^2}\hat{\mathbf{H}}_3\frac{d\boldsymbol{\Psi}}{dx}\, dx \tag{2.70}$$

where

$$\hat{\mathbf{H}}_1 = \int_A \frac{1}{2}(\mathbf{A}_2^T + \mathbf{A}_{nl}^T) E \mathbf{A}_{nl}\, dA, \quad \hat{\mathbf{H}}_3 = \int_A \frac{1}{2}\mathbf{A}_3^T E \mathbf{A}_{nl}\, dA, \quad \tilde{\mathbf{H}}_1 = \int_A \begin{bmatrix} 0 & 0 \\ 0 & S_{xx}^s \end{bmatrix} dA \tag{2.71}$$

Although the stiffness matrix is not symmetric in this case, the tangent matrix is symmetric. In the case of simply supported beam, we can obtain the analytical solution of the form given in (2.46) for the linear case. The linear governing equation is

$$-\frac{d\mathbf{M_2}}{dx} + \frac{d^2}{dx^2}(\mathbf{M_3} + \boldsymbol{\mathcal{M}}) - \mathbf{f} = 0 \tag{2.72}$$

where

$$\mathbf{M}_2 = \bar{\mathbf{M}}^{(22)}\frac{d\boldsymbol{\Phi}}{dx} + \bar{\mathbf{M}}^{(23)}\frac{d^2\boldsymbol{\Phi}}{dx^2}, \quad \mathbf{M}_3 = \bar{\mathbf{M}}^{(32)}\frac{d\boldsymbol{\Phi}}{dx} + \bar{\mathbf{M}}^{(33)}\frac{d^2\boldsymbol{\Phi}}{dx^2}, \quad \boldsymbol{\mathcal{M}} = \bar{\boldsymbol{\mathcal{M}}}\frac{d^2\boldsymbol{\Phi}}{dx^2} \tag{2.73}$$

and

$$\begin{aligned} \bar{\mathbf{M}}^{(jk)} &= \int_A E \mathbf{A}_j^T \mathbf{A}_k\, dA, \quad \text{for } j,k = 2,3 \\ \bar{\boldsymbol{\mathcal{M}}} &= \int_A G\ell^2(\mathbf{B}^T\mathbf{B})\, dA \end{aligned} \tag{2.74}$$

Following the same process as described in section 2.4, we obtained the following system of equations:

$$\mathbf{K}_r \boldsymbol{\Delta}_r = \bar{\mathbf{f}}_r \tag{2.75}$$

where

$$\begin{aligned} \mathbf{K}_r &= -\bar{\mathbf{M}}^{(22)}\boldsymbol{\alpha}_r^2 + (\bar{\mathbf{M}}^{(32)} - \bar{\mathbf{M}}^{(23)})\boldsymbol{\alpha}_r^3\hat{\mathbf{I}} + (\bar{\mathbf{M}}^{(33)} + \bar{\boldsymbol{\mathcal{M}}})\boldsymbol{\alpha}_r^4 \\ \hat{\mathbf{I}} &= \begin{bmatrix} 0 & 1 \\ 1 & 0 \end{bmatrix}, \quad \boldsymbol{\Delta}_r = \begin{bmatrix} U_r \\ W_r \end{bmatrix}, \quad \bar{\mathbf{f}}_r = \begin{bmatrix} 0 \\ F_r \end{bmatrix} \end{aligned} \tag{2.76}$$

2.6. Numerical results

For all numerical examples presented here, functionally graded as well as homogeneous beams, the following geometric and material parameters are considered:

$$E_1 = 14.4 \text{ GPa}, \quad E_2 = 1.44 \text{ GPa}, \quad \nu = 0.38,$$
$$h = 17.6 \times 10^{-6} \text{ m}, \quad b = 2h, \quad L = 20h \tag{2.77}$$

In the case of homogeneous beams the power index, $\hat{n}$, is taken as zero.

2.6.1. Analytical and linear finite element method solution for simply supported beam

For analytical and linear finite element analysis, simply supported beam under uniformly distributed load is considered. In the case of the linear FEM solution, only half of the beam is analysed due to the symmetry of the problem. The boundary conditions for various beam theories are:

$$\begin{aligned}
&\text{Eular-Bernoulli beam theory :} && \text{at } x = 0 : w = 0, \\
& && \text{at } x = \frac{L}{2} : \quad u = 0, \ \frac{dw}{dx} = 0 \\
&\text{Higher order beam theories :} && \text{at } x = 0 : \phi_z^{(i)} = 0 \text{ for } i = 0, 1, 2, ..., p, \\
& && \text{at } x = \frac{L}{2} : \phi_x^{(j)} = 0 \text{ for } j = 0, 1, 2, ..., n, \\
& && \phi_{z,x}^{(i)} = 0 \text{ for } i = 0, 1, 2, ..., p.
\end{aligned} \tag{2.78}$$

where $\phi_{z,x}^{(i)}$ represents the derivative with respect to x. For the conventional beam ($\ell = 0$), quadratic Lagrange interpolation functions (40 elements) are used for all variables for the Timoshenko and general third-order beam theory (TOBT), whereas in case of the rotation gradient-dependent beam, Hermite cubic interpolation functions are used for $\phi_z^{(i)}$, and linear Lagrange interpolation functions are used for $\phi_x^{(j)}$ for all beam theories. A mesh of 60 such elements is considered for linear FEM solutions. In the case of the analytical solution, as large a value of r (see Eq. (2.46)) is used as required to obtain error in the transverse displacement less than 10^{-8}. The analytical and linear FEM results for non-dimensional central transverse deflection ($\hat{w} = wEI/q_0L^4$)

are presented in Table 2.1 for homogeneous and functionally graded beams under uniformly distributed transverse load ($q_0 = 1$ N/m), considering conventional and rotation gradient-dependent Bernoulli–Euler (BET) and Timoshenko beam (TBT) theories. In Table 2.2, the same are tabulated for the general third-order beam theory for various combination for material length scale parameters (ℓ_1, ℓ_2) when load is applied as the traction on the top surface and also when the load is treated as the body force.

Table 2.1. Analytical and linear FEM solutions for center deflection $\hat{w} \times 10^2$ for simply supported homogeneous and FGM beam considering Bernoulli–Euler (BET) and Timoshenko (TBT) beam theories.

$\hat{n}$	ℓ/h	BET		TBT	
		Analytical	Linear FEM	Analytical	Linear FEM
0	0	1.302083	1.302083	1.310708	1.310708
	0.2	1.109182	1.109182	1.116575	1.116765
	0.4	0.767895	0.767895	0.773342	0.773315
	0.6	0.507592	0.507592	0.511753	0.511726
	0.8	0.344229	0.344229	0.347672	0.347654
	1	0.243479	0.243479	0.246514	0.246501
1	0	3.047429	3.047375	3.063111	3.063111
	0.2	2.490001	2.489963	2.502943	2.503203
	0.4	1.607746	1.607729	1.616889	1.616816
	0.6	1.010823	1.010816	1.017770	1.017714
	0.8	0.665106	0.665103	0.670920	0.670885
	1	0.461965	0.461963	0.467159	0.467136

In the tables 2.1,2.2, we observe that the results for the displacements in the case of BET, TBT, and TOBT for $\ell_1 = \ell_2$ are the same as in the case of the modified couple stress theory (see [32]), which uses only the symmetric part of the curvature tensor, which is triangular matrix for given coordinate system and displacement field of the beam theories considered. For this reason, the symmetric part of curvature tensor is the same as $\boldsymbol{\theta}$ for moderate rotation of the present study.

2.6.2. Nonlinear finite element method solution

For nonlinear response, beams with the same geometric and material parameters as given in Eq. (2.77) are considered. Following two types of boundary conditions are

Table 2.2. Analytical solution for center deflection $\hat{w} \times 10^2$ for simply supported homogeneous and functionally graded beam for general third-order beam theory.

$\hat{n}$	ℓ/h	TOBT (Load as traction at top surface)				TOBT (Load as body force)			
		$\ell_1 = \ell,\ \ell_2 = \ell$		$\ell_1 = \ell,\ \ell_2 = 0$		$\ell_1 = \ell,\ \ell_2 = \ell$		$\ell_1 = \ell,\ \ell_2 = 0$	
		Analy-tical	Linear FEM	Analy-tical	Linear FEM	Analy-tical	Linear FEM	Analy-tical	Linear FEM
0	0	1.30982	1.30981	1.30982	1.30981	1.31081	1.31081	1.31081	1.31081
	0.2	1.11547	1.11541	1.11568	1.11561	1.11631	1.11625	1.11652	1.11646
	0.4	0.77232	0.77229	0.77250	0.77247	0.77290	0.77287	0.77309	0.77306
	0.6	0.51093	0.51091	0.51102	0.51101	0.51131	0.51130	0.51141	0.51140
	0.8	0.34699	0.34699	0.34704	0.34703	0.34725	0.34725	0.34730	0.34730
	1	0.24593	0.24592	0.24595	0.24595	0.24611	0.24611	0.24614	0.24613
1	0	3.06242	3.06242	3.06242	3.06242	3.06284	3.06284	3.06284	3.06284
	0.2	2.50166	2.50153	2.50202	2.50189	2.50201	2.50188	2.50237	2.50224
	0.4	1.61551	1.61545	1.61582	1.61577	1.61574	1.61568	1.61605	1.61599
	0.6	1.01659	1.01657	1.01675	1.01673	1.01674	1.01671	1.01690	1.01688
	0.8	0.66991	0.66990	0.66999	0.66998	0.67001	0.67000	0.67008	0.67007
	1	0.46625	0.46625	0.46629	0.46629	0.46632	0.46632	0.46636	0.46636

used:

Pinned-Pinned connected beam:

$$\begin{aligned} &\text{Eular-Bernoulli beam theory :} && \text{at } x = 0 : w = 0, u = 0, \\ & && \text{at } x = L : \quad w = 0,\ u = 0 \\ &\text{Higher order beam theories :} && \text{at } x = 0 : \phi_x^{(0)} = 0,\ \phi_z^{(0)} = 0, \\ & && \text{at } x = L : \phi_x^{(0)} = 0,\ \phi_z^{(0)} = 0 \end{aligned} \tag{2.79}$$

Clamped-Clamped connected beam:

$$\begin{aligned}
&\text{Bernoulli–Euler beam theory :} && \text{at } x=0: u=0, w=0, w_{,x}=0 \\
& && \text{at } x=L: u=0, w=0, w_{,x}=0 \\
&\text{Higher order beam theories :} && \text{at } x=0: \phi_x^{(i)}=0,\ \phi_z^{(j)}=0, \phi_{z,x}^{(j)}=0 \\
& && \text{at } x=L: \phi_x^{(i)}=0,\ \phi_z^{(j)}=0,\ \phi_{z,x}^{(j)}=0 \\
& && \text{for } i=0,1,2,...,n \text{ and } j=0,1,2,...,p
\end{aligned} \tag{2.80}$$

The same kind of finite element approximations as discussed for the linear analysis are used. For a full domain, 60 quadratic lagrange elements are used for the conventional TBT and TOBT, whereas 80 elements with the Hermite cubic and linear Lagrange interpolations for $\phi_z^{(i)}$ and $\phi_x^{(j)}$, respectively, are used for BET and rotation gradient-dependent higher-order beam theories. The error tolerance used for the nonlinear analysis is 10^{-4}. The loading conditions are also assumed to be the same as in the linear analysis. In fig. 2.1, transverse deflections ($\bar{w} = q_0\hat{w} \times 10^2$) as a function of the dimensionless length (x/L) of the beam are plotted for different values of the material length scale parameters ($\ell = \ell_1 = \ell_2$) to the height (h) ratio for pinned-pinned and clamped-clamped boundary conditions for uniformly distributed load ($q_0 = 1$ N$/m$). Figure 2.2 shows the variation of maximum value of $\bar{w}$ with length scale considering the general third-order beam theory. In fig. 2.3, maximum bending moment, ($\bar{M} = ML/(E_1 bh^3/12)$) which is the secondary variable dual to $w_{,x}$ in the case of Bernoulli–Euler beam theory (see Eq. (2.66)), is plotted against material length-scale to height ratio (ℓ/h) for homogeneous and functionally graded beams for the two aforementioned boundary conditions. It is noted that the total bending moment doesn't depend on the length scale as it comes from the force equilibrium (provided that there is not much geometric nonlinearity). The bending moment has two components as given in Eq. (2.66), one depends on the length scale and another is the classical component. Their variations with the length scale parameter are also shown in the figure. Figure 2.4 shows the distribution of stress components $\bar{S}_{xx} = S_{xx}L/q_0$ along the length of the clamped beam at various heights designated by the color map for clamped beam for homogeneous microstructure dependent beam and classical functionally graded beam. Figure 2.5 shows the symmetric part of

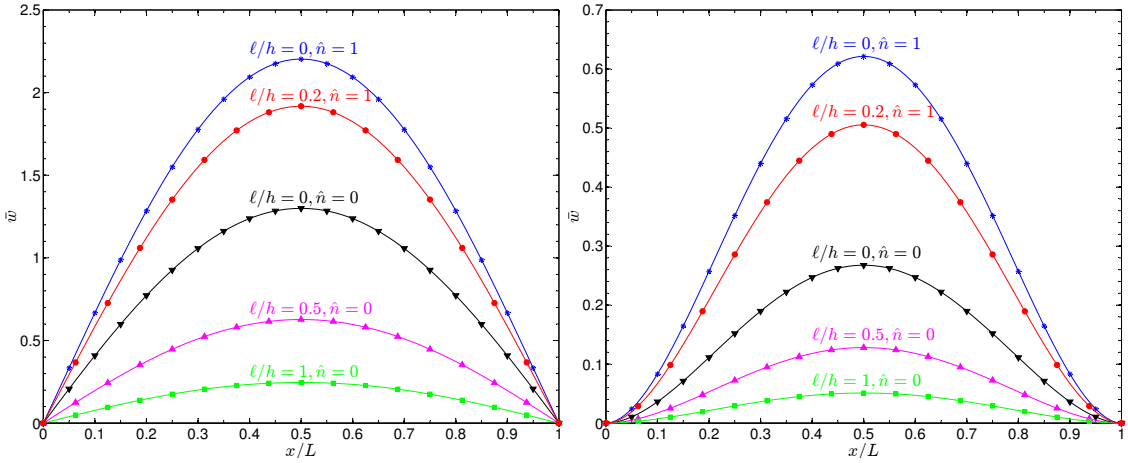

(a) Pinned-pinned connected beam (b) Clamped beam

Fig. 2.1 Transverse deflection along the length of the beam

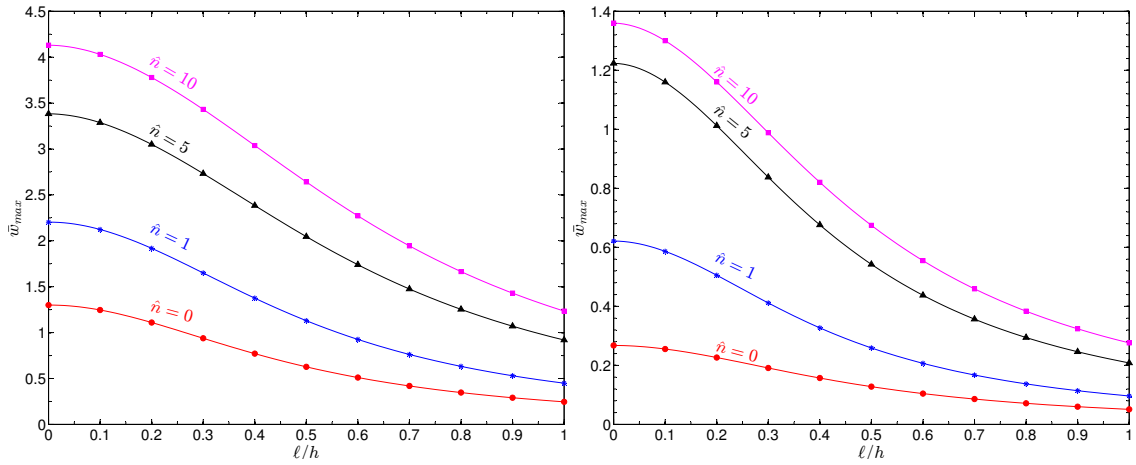

(a) Pinned-pinned connected beam (b) Clamped beam

Fig. 2.2 Variation of Maximum deflection with material length scale parameter

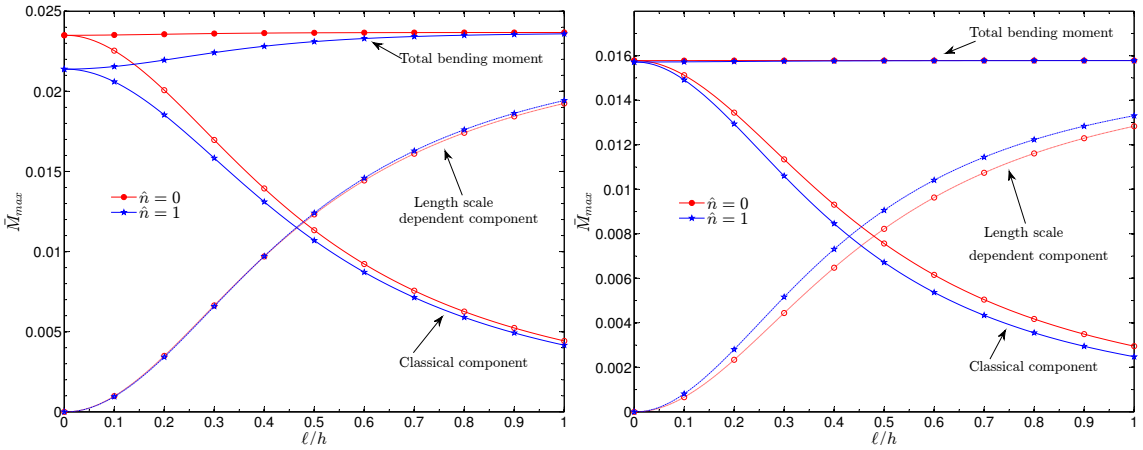

(a) Pinned-pinned connected beam (b) Clamped beam

Fig. 2.3 Variation of Maximum bending moment with material length scale parameter Using BET

shear stress, $\bar{S}^{sym}_{xz} = S^{sym}_{xz} L/q_0$, along the height at various cross-sections of the beam depicted by the color map for the same beams. We note here that the symmetric part of the shear stress is not zero at the shear-free surfaces (i.e., top and bottom surfaces) of the beam in case of microstructure dependent (i.e., $\ell \neq 0$) beam. Stresses are calculated at each element considering one Gauss-point. In this case, there would be nonzero skew-symmetric part of shear stress, which along with the symmetric part of the shear stress will result in zero shear stress at the top and bottom shear-free surfaces. The skew symmetric part of the second Piola–Kirchhoff stress tensor ($\mathbf{S}$) can be obtained by mean of angular momentum conservation equation of Eq. (1.5) as follows:

$$\mathbf{S}^a = \frac{1}{2}(\mathbf{S} - \mathbf{S}^T) = \frac{1}{2}\mathbf{F}^{-1}(\mathrm{Div}(\mathbf{M}))\mathbf{F}^{-T} \tag{2.81}$$

The variation of dimensionless symmetric and skew symmetric parts of the shear stress, S_{xz} are plotted along the length of the beam at various heights for the microstructure dependent beam in fig. 2.6. Figure 2.7 shows the variation of total shear stress along the height at various cross-section along the length for the same beam. Here the total shear stress is zero at the shear free top and bottom surfaces as expected.

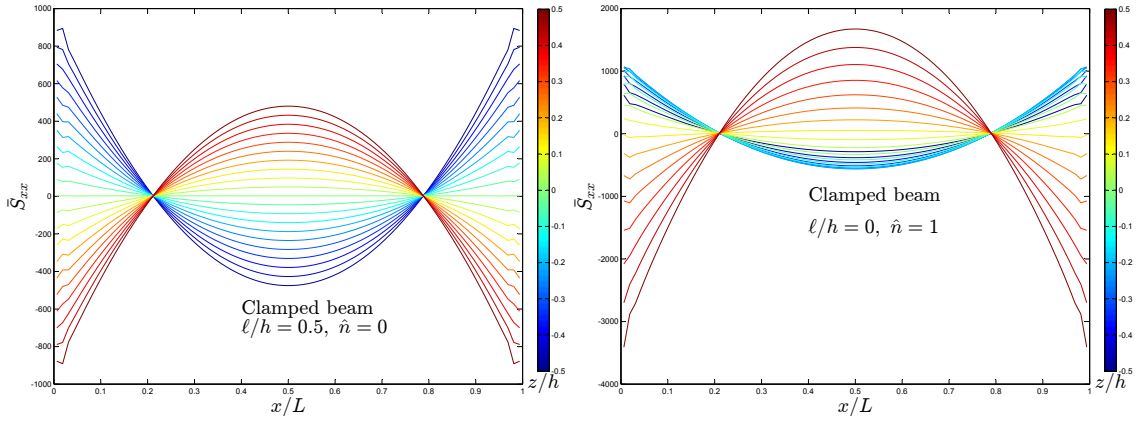

(a) Homogeneous beam with length scale (b) Functionally graded beam

Fig. 2.4 Variation of non-dimensional S_{xx} with along the length of the beam Using general third order beam theory

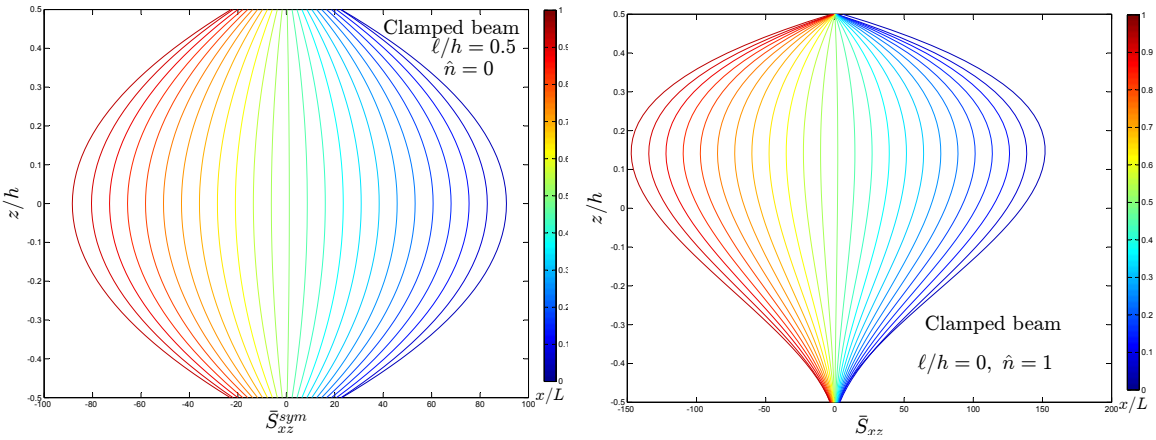

(a) Homogeneous beam with length scale (b) Functionally graded beam

Fig. 2.5 Variation of non-dimensional S_{xz} with along the length of the beam Using general third order beam theory

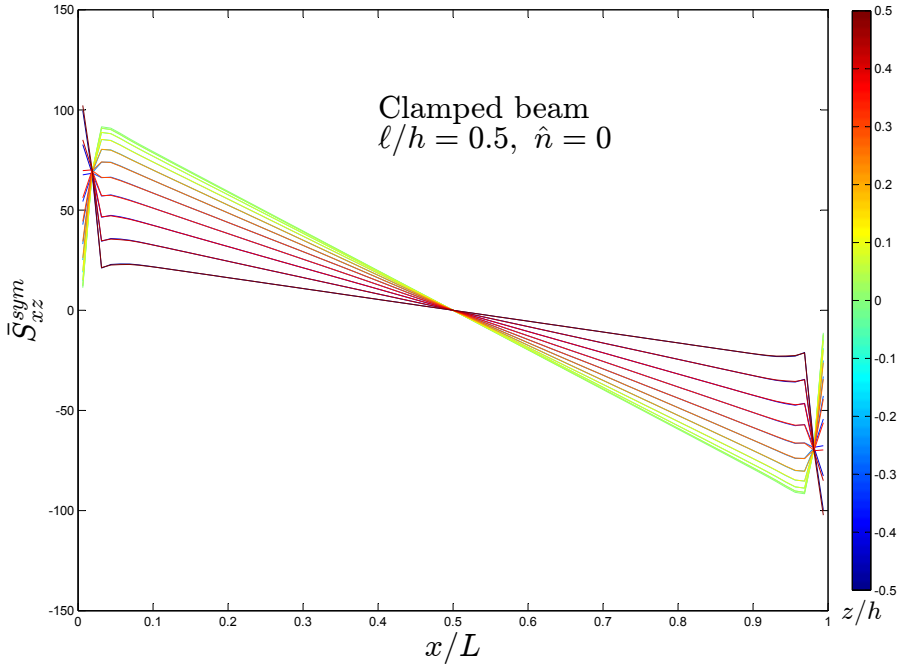

(a) symmetric part of S_{xz}

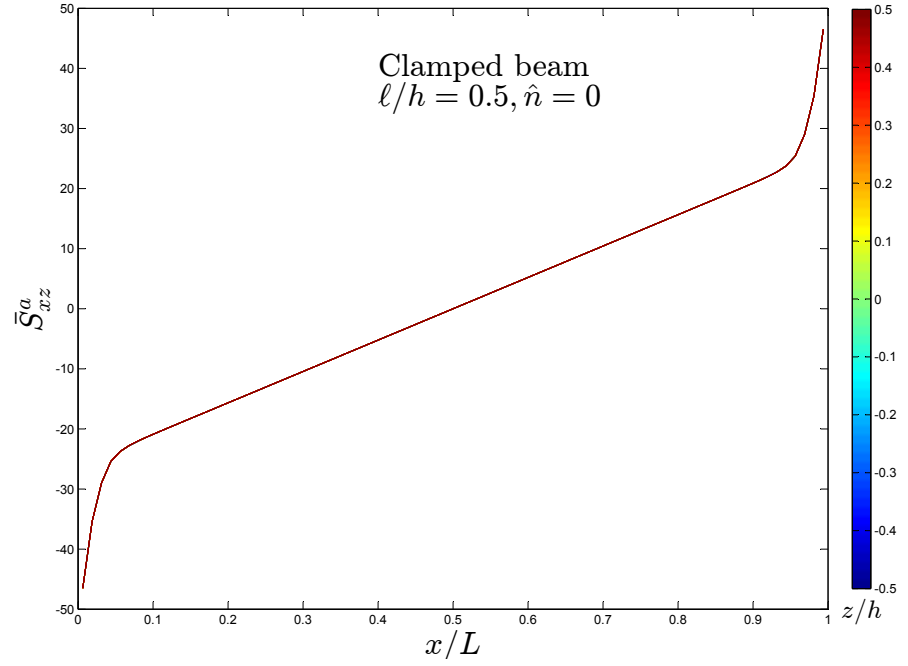

(b) skew-symmetric part of S_{xz}

Fig. 2.6 Variation of non-dimensional symmetric and skew-symmetric part of S_{xz} along the length at various height of the clamped beam using general third order beam theory

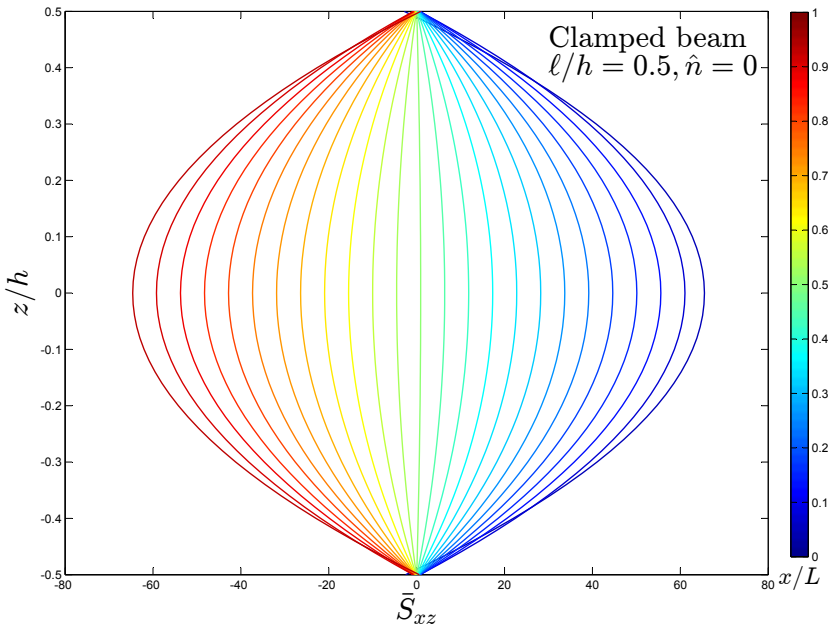

Fig. 2.7 Variation of non-dimensional total S_{xz} along the height of the beam at various cross-section along the length of the clamped beam using the general third order beam theory

2.7. Chapter summary and conclusions

In the present study, we have developed a nonlinear finite element model for moderate rotation condition (i.e., the von Kármán strains) for beams having rotation gradient-dependent potential energy. A general Taylor's series based higher-order beam theory is used for homogeneous and functionally graded beams. Specialization to a general third-order, Timoshenko, and Bernoulli–Euler beam theories are presented. Analytical solutions for the simply supported beam in the linear case are also presented. Numerical examples for various boundary conditions show the stiffening effect of the beam while considering the rotation gradient term in the potential energy functional for a given small length scale parameter of the beam. In the post-processing of the nonlinear FEM analysis, the maximum bending moment and stresses are plotted and it is shown that both classical strain energy term and the rotation gradient-dependent potential energy terms contribute to the bending moment and stresses. Also, we note that the symmetric part of shear stress (shear component of second Piola–Kirchhoff stress), which depends on the Green–Lagrange shear strain component, is not zero at the shear-free top and bottom surfaces but

the total shear stress, which includes skew-symmetric part of shear stress (which depends on rotation gradient term or curvature also) is zero at those shear-free surfaces. Hence caution should be taken while modeling the microstructure dependent beam or plate (couple stress theory, modified couple stress theory or microcontinuum theories dependent beam or plate) by the third-order beam theories, which is based on a displacement field which results in zero shear strain to have zero shear stress (*e.g.* Reddy third-order theory). In the case of microstructure dependent beam, zero shear strain does not result in zero shear stress owing to the skew-symmetric part of the stress tensor. Hence modifications would be required in such displacement field to incorporate the skew-symmetric part of shear stress in order to apply for microstructure dependent beam. A general third-order beam theory or Taylor series based higher-order beam theory should be preferred in the analysis of microstructure dependent beam.

3. ANALYSIS OF COSSERAT PLATE FOR CONSTRAINED MICRO-ROTATION

With the technological advances of manufacturing of small-scale structures of various new class of manmade or natural materials, which defy analysis using the classical continuum mechanics due to either their structural length scale or small scale material embeddings, non-classical or generalized continuum model have gained enormous attention of many researchers in recent times. Such materials include fibrous composites, carbon nanotube (CNT)-reinforced coatings (Bakshi *et. al* [47]) and composites with aligned CNT inclusions (Thostenson and Chou [48]) , granular solids, liquid crystal elastomers, polarization inertia in ferroelectrics, and intrinsic spin in ferromagnetic, and others. For such solids, Srinivasa and Reddy (see [19]) have developed a model for Cosserat continua in the case of large deformation and finite constrained micro-rotation (*i.e.* the micro-rotation is considered to be constrained with macro-rotation of the continua). They proposed that the strain energy potential should also depend on the rotation gradient along with strain in such cases of Cosserat solid. Also, their model is not limited to isotropic Cosserat solid (or centrosymmetric microstructure) and thus would be able to model the anisotropic response due ordered orientation of microstructure (see Thostenson and Chou [48]) by using appropriate constitutive relation. For example, large anisotropic deformation of liquid crystal elastomer in response to many stimuli such as light and heat (see Warner *et al.*[49, 50, 51]). Further, in their work Srinivasa and Reddy [19] have specialized their continuum model in the case of moderate rotation (von Kármán nonlinearity) in the case of the classical plate and Euler-Bernoulli beam theories. The nonlinear finite element model for the beam based on the rotation gradient dependent potential energy had been developed by Arbind, Reddy, and Srinivasa [52].

In this chapter, we develop the weak form nonlinear finite element model for bending of plates, in view of a broad class of materials with the use of the rotation gradient dependent theory (see Srinivasa and Reddy [19]), which accounts for moderate rotations and strains. Summary of this theory is discussed in Section 3.1. The formulation can be used for the analysis for a general class of material, which requires more than one length scale to characterize an arbitrary shape/structure and orientation of the material particles. First, we formulate a general higher order plate

theory based on Taylor's series expansion of the displacement field about the mid-plane displacement of the plate for conventional as well as Cosserat solid plates and then we specialize it in the case of the classical, first order, and a general third-order plate theories. Based on this, we develop nonlinear weak form finite element model. We also present the analytical solution for simply supported linear plates.

3.1. Cosserat continuum theory for finite constrained micro-rotation

Let us consider a body $\mathcal{B}$ in which particle X is at position $\mathbf{X}$ in reference frame at time, $t = 0$ and after deformation at time t it occupies position $\mathbf{x}$. Let $\mathbf{F}$ be the deformation gradient and $\boldsymbol{\Theta}$ be the orientation tensor of the directors attached to the material points; then the potential energy can be expressed as (see Srinivasa and Reddy [19] for details):

$$\psi := \hat{\psi}(\mathbf{F}, \boldsymbol{\Theta}, \boldsymbol{\nabla}\boldsymbol{\Theta}) \tag{3.1}$$

where $\boldsymbol{\nabla}\boldsymbol{\Theta}$ is the gradient of the orientation tensor with respect to the reference frame. By applying the principle of invariance under superposed rigid body motion, it can be shown that the potential energy has the following dependance in case of constrained micro-rotation:

$$\psi = \hat{\psi}(\mathbf{E}, \mathbf{R}^T \cdot \nabla\mathbf{R}) \tag{3.2}$$

where $\mathbf{E}$ is the Green–Lagrange strain tensor and $\mathbf{R}$ is the proper orthogonal rotation tensor respectively. Let $\mathbf{e}$ and $\mathbf{W}$ be the symmetric and skew symmetric part of displacement gradient. Then in view of moderate rotation, we will make a priory assumptions that (1) $||\mathbf{e}||$ is of order of ϵ, (2) $||\mathbf{W}||$ is of order $\sqrt{\epsilon}$, where ϵ is small and we neglect all the terms of order $O(\epsilon^k)$ for $k > 1$. In this case, the Green–Lagrange strain tensor and the rotation tensor (see Reddy [42]) can be approximated as

$$\begin{aligned} \mathbf{E} &\approx \mathbf{e} - (1/2)\mathbf{W}^2 \\ \mathbf{R} &\approx \mathbf{I} + \mathbf{W} + \frac{1}{2}\mathbf{W}^2 \\ \boldsymbol{\Omega} &:= \mathbf{R}^T \cdot \nabla\mathbf{R} \approx \nabla\mathbf{W} \end{aligned} \tag{3.3}$$

Hence in case of moderate rotation, the dependance of the potential energy dependence can be approximated as following:

$$\psi \approx \hat{\psi}(\mathbf{e} - (1/2)\mathbf{W}^2, \nabla\mathbf{W}) \tag{3.4}$$

Based on the above potential energy, we formulate the governing equations and its finite element model for the bending of plates.

3.2. Governing equation of plates

Consider the (x, y, z) rectangular cartesian co-ordinate system in the reference frame and a plate of arbitrary geometry and height h lies in xy-plane with the central plane of the plate coincide with xy-co-ordinate plane in its natural configuration and the height of the plate is along z-axis.

3.2.1. Displacement field

We begin with the following very general displacement field, which can later be specified as a general third-order, first-order, and classical plate theories:

$$\begin{aligned}
&\mathbf{u} = u_1\,\hat{\mathbf{e}}_1 + u_2\,\hat{\mathbf{e}}_2 + u_3\,\hat{\mathbf{e}}_3 \quad \text{where} \\
&u_1 = \sum_{i=0}^{n} z^i \phi_x^{(i)}(x,y) = \mathbf{A}_x \mathbf{\Phi}_x(x,y), \\
&u_2 = \sum_{i=0}^{m} z^i \phi_y^{(i)}(x,y) = \mathbf{A}_y \mathbf{\Phi}_y(x,y), \\
&u_3 = \sum_{i=0}^{p} z^i \phi_z^{(i)}(x,y) = \mathbf{A}_z \mathbf{\Phi}_z(x,y)
\end{aligned} \tag{3.5}$$

Where $\phi_x^{(0)} = u(x,y)$, $\phi_y^{(0)} = v(x,y)$ and $\phi_z^{(0)} = w(x,y)$ are the displacements of the mid plane at point (x,y) in x, y and z direction respectively. Various variables in the above displacement field can be expressed as follows:

$$\phi_x^{(i)} = \frac{1}{(i)!}\left(\frac{\partial^i u_1}{\partial z^i}\right)_{z=0}, \qquad \phi_y^{(i)} = \frac{1}{(i)!}\left(\frac{\partial^i u_2}{\partial z^i}\right)_{z=0}, \qquad \phi_z^{(i)} = \frac{1}{(i)!}\left(\frac{\partial^i u_3}{\partial z^i}\right)_{z=0} \tag{3.6}$$

$$\begin{aligned}
\mathbf{A}_x &= \begin{bmatrix} 1 & z & z^2 & \dots & z^n \end{bmatrix}, \quad \mathbf{\Phi}_x = \begin{bmatrix} \phi_x^{(0)} & \phi_x^{(1)} & \phi_x^{(2)} & \dots & \phi_x^{(n)} \end{bmatrix}^T \\
\mathbf{A}_y &= \begin{bmatrix} 1 & z & z^2 & \dots & z^m \end{bmatrix}, \quad \mathbf{\Phi}_y = \begin{bmatrix} \phi_y^{(0)} & \phi_y^{(1)} & \phi_y^{(2)} & \dots & \phi_y^{(m)} \end{bmatrix}^T \\
\mathbf{A}_z &= \begin{bmatrix} 1 & z & z^2 & \dots & z^p \end{bmatrix}, \quad \mathbf{\Phi}_z = \begin{bmatrix} \phi_z^{(0)} & \phi_z^{(1)} & \phi_z^{(2)} & \dots & \phi_z^{(p)} \end{bmatrix}^T
\end{aligned} \tag{3.7}$$

In the case of moderate rotation plates, using Eq. (3.3), we have following approximated strain components:

$$
\begin{aligned}
\varepsilon_{xx} &= u_{1,x} + (1/2)\left(\phi^{(0)}_{z,x}\right)^2 = \mathbf{A}_x\mathbf{\Phi}_{x,x} + (1/2)\left(\phi^{(0)}_{z,x}\right)^2 \\
\varepsilon_{yy} &= u_{2,y} + (1/2)\left(\phi^{(0)}_{z,y}\right)^2 = \mathbf{A}_y\mathbf{\Phi}_{y,y} + (1/2)\left(\phi^{(0)}_{z,y}\right)^2 \\
\varepsilon_{zz} &= u_{3,z} + (1/2)\left(\phi^{(1)}_{x}\right)^2 + (1/2)\left(\phi^{(1)}_{y}\right)^2 = \mathbf{A}_{z,z}\mathbf{\Phi}_z + (1/2)\left(\phi^{(1)}_{x}\right)^2 + (1/2)\left(\phi^{(1)}_{y}\right)^2 \\
\gamma_{yz} &= u_{2,z} + u_{3,y} = \mathbf{A}_{y,z}\mathbf{\Phi}_y + \mathbf{A}_z\mathbf{\Phi}_{z,y} \\
\gamma_{zx} &= u_{1,z} + u_{3,x} = \mathbf{A}_{x,z}\mathbf{\Phi}_x + \mathbf{A}_z\mathbf{\Phi}_{z,x} \\
\gamma_{xy} &= u_{1,y} + u_{2,x} = \mathbf{A}_x\mathbf{\Phi}_{x,y} + \mathbf{A}_y\mathbf{\Phi}_{y,x} + \phi^{(0)}_{z,x}\phi^{(0)}_{z,y}
\end{aligned}
\tag{3.8}
$$

In the above expression of strain components, $(u_{3,x})^2$, $(u_{3,y})^2$, $u_{3,x}u_{3,y}$, $(u_{1,z})^2$ and $(u_{2,z})^2$ are approximated as $\left(\phi^{(0)}_{z,x}\right)^2$, $\left(\phi^{(0)}_{z,x}\right)^2$, $\phi^{(0)}_{z,x}\phi^{(0)}_{z,y}$, $(\phi^{(1)}_{x})^2$ and $\left(\phi^{(1)}_{y}\right)^2$ respectively owing to the fact that the square of higher order term in the displacement field are small and thus neglected. Further, in the vector form the strain tensor can be rewritten as,

$$
\boldsymbol{\varepsilon} \;=\; (\mathbf{A}_1 + \frac{1}{2}\mathbf{A}_{nl})\mathbf{\Phi} + \mathbf{A}_{2_x}\mathbf{\Phi}_{,x} + \mathbf{A}_{2_y}\mathbf{\Phi}_{,y} + \frac{1}{2}\mathbf{A}_{nl_x}\mathbf{\Phi}_{,x} + \frac{1}{2}\mathbf{A}_{nl_y}\mathbf{\Phi}_{,y} \tag{3.9}
$$

where

$$
\begin{aligned}
\boldsymbol{\varepsilon} &= \begin{bmatrix} \varepsilon_{xx} & \varepsilon_{yy} & \varepsilon_{zz} & \gamma_{yz} & \gamma_{zx} & \gamma_{xy} \end{bmatrix}^T, \quad \mathbf{\Phi} = \begin{bmatrix} \mathbf{\Phi}_x^T & \mathbf{\Phi}_y^T & \mathbf{\Phi}_z^T \end{bmatrix}^T \\
\mathbf{A}_1 &= \begin{bmatrix} \mathbf{0} & \mathbf{0} & \mathbf{0} \\ \mathbf{0} & \mathbf{0} & \mathbf{0} \\ \mathbf{0} & \mathbf{0} & \mathbf{A}_{z,z} \\ \mathbf{0} & \mathbf{A}_{y,z} & \mathbf{0} \\ \mathbf{A}_{x,z} & \mathbf{0} & \mathbf{0} \\ \mathbf{0} & \mathbf{0} & \mathbf{0} \end{bmatrix}, \quad \mathbf{A}_{2_x} = \begin{bmatrix} \mathbf{A}_x & \mathbf{0} & \mathbf{0} \\ \mathbf{0} & \mathbf{0} & \mathbf{0} \\ \mathbf{0} & \mathbf{0} & \mathbf{0} \\ \mathbf{0} & \mathbf{0} & \mathbf{0} \\ \mathbf{0} & \mathbf{0} & \mathbf{A}_z \\ \mathbf{0} & \mathbf{A}_y & \mathbf{0} \end{bmatrix}, \quad \mathbf{A}_{2_y} = \begin{bmatrix} \mathbf{0} & \mathbf{0} & \mathbf{0} \\ \mathbf{0} & \mathbf{A}_y & \mathbf{0} \\ \mathbf{0} & \mathbf{0} & \mathbf{0} \\ \mathbf{0} & \mathbf{0} & \mathbf{A}_z \\ \mathbf{0} & \mathbf{0} & \mathbf{0} \\ \mathbf{A}_x & \mathbf{0} & \mathbf{0} \end{bmatrix} \\
\mathbf{A}_{nl} &= \begin{bmatrix} \mathbf{0} & \mathbf{0} & \mathbf{0} \\ \mathbf{0} & \mathbf{0} & \mathbf{0} \\ \mathbf{a}_{nl} & \mathbf{b}_{nl} & \mathbf{0} \\ \mathbf{0} & \mathbf{0} & \mathbf{0} \\ \mathbf{0} & \mathbf{0} & \mathbf{0} \\ \mathbf{0} & \mathbf{0} & \mathbf{0} \end{bmatrix}, \quad \mathbf{A}_{nl_x} = \begin{bmatrix} \mathbf{0} & \mathbf{0} & \mathbf{a}_{nl_x} \\ \mathbf{0} & \mathbf{0} & \mathbf{0} \\ \mathbf{0} & \mathbf{0} & \mathbf{0} \\ \mathbf{0} & \mathbf{0} & \mathbf{0} \\ \mathbf{0} & \mathbf{0} & \mathbf{0} \\ \mathbf{0} & \mathbf{0} & \mathbf{a}_{nl_y} \end{bmatrix}, \quad \mathbf{A}_{nl_y} = \begin{bmatrix} \mathbf{0} & \mathbf{0} & \mathbf{0} \\ \mathbf{0} & \mathbf{0} & \mathbf{a}_{nl_y} \\ \mathbf{0} & \mathbf{0} & \mathbf{0} \\ \mathbf{0} & \mathbf{0} & \mathbf{0} \\ \mathbf{0} & \mathbf{0} & \mathbf{0} \\ \mathbf{0} & \mathbf{0} & \mathbf{a}_{nl_x} \end{bmatrix}
\end{aligned}
\tag{3.10}
$$

In the above expression, $\mathbf{a}_{nl_x}$ and $\mathbf{a}_{nl_y}$ are $(1 \times p)$ matrices with only nonzero components $\mathbf{a}_{nl_{x11}} = \phi^{(0)}_{z,x}$ and $\mathbf{a}_{nl_{y11}} = \phi^{(0)}_{z,y}$ respectively. $\mathbf{a}_{nl}$ and $\mathbf{b}_{nl}$ are $(1 \times n)$ and $(1 \times m)$ matrices respectively with only nonzero element $\mathbf{a}_{nl_{12}} = \phi^{(1)}_x$ and $\mathbf{b}_{nl_{12}} = \phi^{(1)}_y$. And $(\ )_{,x}$ represent the derivative with respect to x and so on; $\mathbf{W}$ and the $\mathbf{\Omega}$ are defined as

$$\begin{aligned}
\mathbf{W} &= \begin{bmatrix} 0 & -\omega_z & \omega_y \\ \omega_z & 0 & -\omega_x \\ -\omega_y & \omega_x & 0 \end{bmatrix}, \qquad \begin{aligned} \omega_x &= (1/2)\,(u_{3,y} - u_{2,z}) = (1/2)\,(\mathbf{A}_z\mathbf{\Phi}_{z,y} - \mathbf{A}_{y,z}\mathbf{\Phi}_y) \\ \omega_y &= (1/2)\,(u_{1,z} - u_{3,x}) = (1/2)\,(\mathbf{A}_{x,z}\mathbf{\Phi}_x - \mathbf{A}_z\mathbf{\Phi}_{z,x}) \\ \omega_z &= (1/2)\,(u_{2,x} - u_{1,y}) = (1/2)\,(\mathbf{A}_y\mathbf{\Phi}_{y,x} - \mathbf{A}_x\mathbf{\Phi}_{x,y}) \end{aligned} \\
\mathbf{\Omega} &= \Omega_{\alpha\beta\gamma}\hat{\mathbf{e}}_\alpha\hat{\mathbf{e}}_\beta\hat{\mathbf{e}}_\gamma = \frac{\partial W_{\beta\gamma}}{\partial x_\alpha}\hat{\mathbf{e}}_\alpha\hat{\mathbf{e}}_\beta\hat{\mathbf{e}}_\gamma
\end{aligned} \tag{3.11}$$

The unique component of $\mathbf{\Omega}$ are

$$\begin{aligned}
&2\omega_{x,x} = \mathbf{A}_z\mathbf{\Phi}_{z,xy} - \mathbf{A}_{y,z}\mathbf{\Phi}_{y,x}, \quad 2\omega_{x,y} = \mathbf{A}_z\mathbf{\Phi}_{z,yy} - \mathbf{A}_{y,z}\mathbf{\Phi}_{y,y} \\
&2\omega_{x,z} = \mathbf{A}_{z,z}\mathbf{\Phi}_{z,y} - \mathbf{A}_{y,zz}\mathbf{\Phi}_y, \quad 2\omega_{y,x} = \mathbf{A}_{x,z}\mathbf{\Phi}_{x,x} - \mathbf{A}_z\mathbf{\Phi}_{z,xx} \\
&2\omega_{y,y} = \mathbf{A}_{x,z}\mathbf{\Phi}_{x,y} - \mathbf{A}_z\mathbf{\Phi}_{z,xy}, \quad 2\omega_{y,z} = \mathbf{A}_{x,zz}\mathbf{\Phi}_x - \mathbf{A}_{z,z}\mathbf{\Phi}_{z,x} \\
&2\omega_{z,x} = \mathbf{A}_y\mathbf{\Phi}_{y,xx} - \mathbf{A}_x\mathbf{\Phi}_{x,xy}, \quad 2\omega_{z,y} = \mathbf{A}_y\mathbf{\Phi}_{y,xy} - \mathbf{A}_x\mathbf{\Phi}_{x,yy} \\
&2\omega_{z,z} = \mathbf{A}_{y,z}\mathbf{\Phi}_{y,x} - \mathbf{A}_{x,z}\mathbf{\Phi}_{x,y}.
\end{aligned} \tag{3.12}$$

Let us write the components of $\mathbf{\Omega}$ in the following vector form:

$$\begin{aligned}
\boldsymbol{\chi} &= \begin{bmatrix} 2\omega_{x,x} & 2\omega_{x,y} & 2\omega_{x,z} & 2\omega_{y,x} & 2\omega_{y,y} & 2\omega_{y,z} & 2\omega_{z,x} & 2\omega_{z,y} & 2\omega_{z,z} \end{bmatrix}^T \\
&= \mathbf{B}_1\mathbf{\Phi} + \mathbf{B}_{2_x}\mathbf{\Phi}_{,x} + \mathbf{B}_{2_y}\mathbf{\Phi}_{,y} + \mathbf{B}_{3_x}\mathbf{\Phi}_{,xx} + \mathbf{B}_{3_{xy}}\mathbf{\Phi}_{,xy} + \mathbf{B}_{3_y}\mathbf{\Phi}_{,yy}
\end{aligned} \tag{3.13}$$

where

$$\mathbf{B}_1 = \begin{bmatrix} \mathbf{0} & \mathbf{0} & \mathbf{0} \\ \mathbf{0} & \mathbf{0} & \mathbf{0} \\ \mathbf{0} & -\mathbf{A}_{y,zz} & \mathbf{0} \\ \mathbf{0} & \mathbf{0} & \mathbf{0} \\ \mathbf{0} & \mathbf{0} & \mathbf{0} \\ \mathbf{A}_{x,zz} & \mathbf{0} & \mathbf{0} \\ \mathbf{0} & \mathbf{0} & \mathbf{0} \\ \mathbf{0} & \mathbf{0} & \mathbf{0} \\ \mathbf{0} & \mathbf{0} & \mathbf{0} \end{bmatrix}, \ \mathbf{B}_{2_x} = \begin{bmatrix} \mathbf{0} & -\mathbf{A}_{y,z} & \mathbf{0} \\ \mathbf{0} & \mathbf{0} & \mathbf{0} \\ \mathbf{0} & \mathbf{0} & \mathbf{0} \\ \mathbf{A}_{x,z} & \mathbf{0} & \mathbf{0} \\ \mathbf{0} & \mathbf{0} & -\mathbf{A}_{z,z} \\ \mathbf{0} & \mathbf{0} & \mathbf{0} \\ \mathbf{0} & \mathbf{0} & \mathbf{0} \\ \mathbf{0} & \mathbf{0} & \mathbf{0} \\ \mathbf{0} & \mathbf{A}_{y,z} & \mathbf{0} \end{bmatrix}, \ \mathbf{B}_{2_y} = \begin{bmatrix} \mathbf{0} & \mathbf{0} & \mathbf{0} \\ \mathbf{0} & -\mathbf{A}_{y,z} & \mathbf{0} \\ \mathbf{0} & \mathbf{0} & \mathbf{A}_{z,z} \\ \mathbf{0} & \mathbf{0} & \mathbf{0} \\ \mathbf{A}_{x,z} & \mathbf{0} & \mathbf{0} \\ \mathbf{0} & \mathbf{0} & \mathbf{0} \\ \mathbf{0} & \mathbf{0} & \mathbf{0} \\ \mathbf{0} & \mathbf{0} & \mathbf{0} \\ -\mathbf{A}_{x,z} & \mathbf{0} & \mathbf{0} \end{bmatrix}$$

$$\mathbf{B}_{3_x} = \begin{bmatrix} \mathbf{0} & \mathbf{0} & \mathbf{0} \\ \mathbf{0} & \mathbf{0} & \mathbf{0} \\ \mathbf{0} & \mathbf{0} & \mathbf{0} \\ \mathbf{0} & \mathbf{0} & -\mathbf{A}_z \\ \mathbf{0} & \mathbf{0} & \mathbf{0} \\ \mathbf{0} & \mathbf{0} & \mathbf{0} \\ \mathbf{0} & \mathbf{A}_y & \mathbf{0} \\ \mathbf{0} & \mathbf{0} & \mathbf{0} \\ \mathbf{0} & \mathbf{0} & \mathbf{0} \end{bmatrix}, \ \mathbf{B}_{3_{xy}} = \begin{bmatrix} \mathbf{0} & \mathbf{0} & \mathbf{A}_z \\ \mathbf{0} & \mathbf{0} & \mathbf{0} \\ \mathbf{0} & \mathbf{0} & \mathbf{0} \\ \mathbf{0} & \mathbf{0} & \mathbf{0} \\ \mathbf{0} & \mathbf{0} & -\mathbf{A}_z \\ \mathbf{0} & \mathbf{0} & \mathbf{0} \\ -\mathbf{A}_x & \mathbf{0} & \mathbf{0} \\ \mathbf{0} & \mathbf{A}_y & \mathbf{0} \\ \mathbf{0} & \mathbf{0} & \mathbf{0} \end{bmatrix}, \ \mathbf{B}_{3_y} = \begin{bmatrix} \mathbf{0} & \mathbf{0} & \mathbf{0} \\ \mathbf{0} & \mathbf{0} & \mathbf{A}_z \\ \mathbf{0} & \mathbf{0} & \mathbf{0} \\ \mathbf{0} & \mathbf{0} & \mathbf{0} \\ \mathbf{0} & \mathbf{0} & \mathbf{0} \\ \mathbf{0} & \mathbf{0} & \mathbf{0} \\ \mathbf{0} & \mathbf{0} & \mathbf{0} \\ -\mathbf{A}_x & \mathbf{0} & \mathbf{0} \\ \mathbf{0} & \mathbf{0} & \mathbf{0} \end{bmatrix}. \tag{3.14}$$

Let us consider the strain energy due to strain and rotation gradient as follows:

$$U = \int_A \int_{-h/2}^{h/2} \frac{1}{2}\boldsymbol{\varepsilon} \cdot \mathbf{C} \cdot \boldsymbol{\varepsilon} + \frac{1}{2}\boldsymbol{\chi} \cdot \mathbf{C}_l \cdot \boldsymbol{\chi} \, dz \, dxdy \tag{3.15}$$

where $\mathbf{C}$ and $\mathbf{C}_l$ are the material constant of elasticity and material constant with material length scale. For a positive potential energy, both $\mathbf{C}$ and $\mathbf{C}_l$ should be positive-definite tensor. The symmetric part of stress and couple stress can be given as

$$\mathbf{S}^s = \mathbf{C} \cdot \boldsymbol{\varepsilon}, \quad \text{and} \quad \mathbf{m} = \mathbf{C}_l \cdot \boldsymbol{\chi} \tag{3.16}$$

The first variation of the strain energy is

$$\begin{aligned}
\delta U &= \int_A \int_{-h/2}^{h/2} \delta\boldsymbol{\varepsilon} \cdot \mathbf{S}^s + \delta\boldsymbol{\chi} \cdot \mathbf{m} \, dz \, dxdy \\
&= \int_A \int_{-h/2}^{h/2} \big((\mathbf{A}_1 + \mathbf{A}_{nl})\delta\boldsymbol{\Phi} + \mathbf{A}_{2_x}\delta\boldsymbol{\Phi}_{,x} + \mathbf{A}_{2_y}\delta\boldsymbol{\Phi}_{,y} + \mathbf{A}_{nl_x}\delta\boldsymbol{\Phi}_{,x} + \mathbf{A}_{nl_y}\delta\boldsymbol{\Phi}_{,y}\big) \cdot \mathbf{S}^s \\
&\qquad + \big(\mathbf{B}_1\delta\boldsymbol{\Phi} + \mathbf{B}_{2_x}\delta\boldsymbol{\Phi}_{,x} + \mathbf{B}_{2_y}\delta\boldsymbol{\Phi}_{,y} + \mathbf{B}_{3_x}\delta\boldsymbol{\Phi}_{,xx} \\
&\qquad + \mathbf{B}_{3_{xy}}\delta\boldsymbol{\Phi}_{,xy} + \mathbf{B}_{3_y}\delta\boldsymbol{\Phi}_{,yy}\big) \cdot \mathbf{m} \, dz \, dx \, dy \\
&= \int_A \Big[\delta\boldsymbol{\Phi} \cdot \left(\int_{-h/2}^{h/2} \left(\mathbf{A}_1^T\mathbf{S}^s + \mathbf{B}_1^T\mathbf{m}\right) \, dz\right) \\
&\quad + \delta\boldsymbol{\Phi}_{,x} \cdot \left(\int_{-h/2}^{h/2} \left((\mathbf{A}_{nl_x}^T + \mathbf{A}_{2_x}^T)\mathbf{S}^s + \mathbf{B}_{2_x}^T\mathbf{m}\right) \, dz\right) \\
&\quad + \delta\boldsymbol{\Phi}_{,y} \cdot \left(\int_{-h/2}^{h/2} \left((\mathbf{A}_{nl_y}^T + \mathbf{A}_{2_y}^T)\mathbf{S}^s + \mathbf{B}_{2_y}^T\mathbf{m}\right) \, dz\right) + \delta\boldsymbol{\Phi}_{,xx} \cdot \left(\int_{-h/2}^{h/2} \mathbf{B}_{3_x}^T\mathbf{m} \, dz\right) \\
&\quad + \delta\boldsymbol{\Phi}_{,xy} \cdot \left(\int_{-h/2}^{h/2} \mathbf{B}_{3_{xy}}^T\mathbf{m} \, dz\right) + \delta\boldsymbol{\Phi}_{,yy} \cdot \left(\int_{-h/2}^{h/2} \mathbf{B}_{3_y}^T\mathbf{m} \, dz\right)\Big] \, dx \, dy
\end{aligned} \tag{3.17}$$

Let us define the following generalized stress and couple stress resultants,

$$\begin{aligned}
\mathbf{M}_1 &= \int_{-h/2}^{h/2} \mathbf{A}_1^T \mathbf{S}^s \, dz, \quad \mathbf{M}_{2_j} = \int_{-h/2}^{h/2} \mathbf{A}_{2_j}^T \mathbf{S}^s \, dz, \quad \text{for } j = x, y \\
\mathbf{M}_{nl} &= \int_{-h/2}^{h/2} \mathbf{A}_{nl}^T \mathbf{S}^s \, dz, \quad \mathbf{M}_{nl_j} = \int_{-h/2}^{h/2} \mathbf{A}_{nl_j}^T \mathbf{S}^s \, dz \quad \text{for } j = x, y \\
\boldsymbol{\mathcal{M}}_1 &= \int_{-h/2}^{h/2} \mathbf{B}_1^T \mathbf{m} \, dz, \quad \boldsymbol{\mathcal{M}}_{2_j} = \int_{-h/2}^{h/2} \mathbf{B}_{2_j}^T \mathbf{m} \, dz \quad \text{for } j = x, y \\
\boldsymbol{\mathcal{M}}_{3_{xx}} &= \int_{-h/2}^{h/2} \mathbf{B}_{3_{xx}}^T \mathbf{m} \, dz, \quad \boldsymbol{\mathcal{M}}_{3_{xy}} = \frac{1}{2} \int_{-h/2}^{h/2} \mathbf{B}_{3_{xy}}^T \mathbf{m} \, dz, \quad \boldsymbol{\mathcal{M}}_{3_{yy}} = \int_{-h/2}^{h/2} \mathbf{B}_{3_{yy}}^T \mathbf{m} \, dz
\end{aligned} \tag{3.18}$$

Then the variation in strain energy can be rewritten as

$$\begin{aligned}
\delta U \;=\; \int_A \Big[& \delta\boldsymbol{\Phi} \cdot (\mathbf{M}_1 + \mathbf{M}_{nl} + \boldsymbol{\mathcal{M}}_1) + \delta\boldsymbol{\Phi}_{,x} \cdot (\mathbf{M}_{nl_x} + \mathbf{M}_{2_x} + \boldsymbol{\mathcal{M}}_{2_x}) \\
& + \delta\boldsymbol{\Phi}_{,y} \cdot \left(\mathbf{M}_{nl_y} + \mathbf{M}_{2_y} + \boldsymbol{\mathcal{M}}_{2_y}\right) + \delta\boldsymbol{\Phi}_{,xx} \cdot \boldsymbol{\mathcal{M}}_{3_x} \\
& + 2\delta\boldsymbol{\Phi}_{,xy} \cdot \boldsymbol{\mathcal{M}}_{3_{xy}} + \delta\boldsymbol{\Phi}_{,yy} \cdot \boldsymbol{\mathcal{M}}_{3_y} \Big] \, dx \, dy
\end{aligned} \tag{3.19}$$

and virtual work done by external forces is

$$\begin{aligned}
\delta V \;=\; & -\int_A \Big[\int_{-h/2}^{h/2} (f_x \delta u_1 + f_y \delta u_2 + f_z \delta u_3) \, dz + q_x^t \delta u_1(x, y, \frac{h}{2}) + q_x^b \delta u_1(x, y, -\frac{h}{2}) \\
& + q_y^t \delta u_2(x, y, \frac{h}{2}) + q_y^b \delta u_2(x, y, -\frac{h}{2}) + q_z^t \delta u_3(x, y, \frac{h}{2}) + q_z^b \delta u_3(x, y, -\frac{h}{2}) \Big] \, dx \, dy \\
& = -\int_A \delta\boldsymbol{\Phi} \cdot \hat{\mathbf{F}} \, dx \, dy
\end{aligned} \tag{3.20}$$

where

$$\begin{aligned}
\hat{\mathbf{F}} &= \begin{bmatrix} \mathbf{F}_x & \mathbf{F}_y & \mathbf{F}_z \end{bmatrix}^T \\
\mathbf{F}_x &= \int_{-h/2}^{h/2} f_x \mathbf{A}_x(z) \, dz + q_x^t \mathbf{A}_x(h/2) + q_x^b \mathbf{A}_x(-h/2) \\
\mathbf{F}_y &= \int_{-h/2}^{h/2} f_y \mathbf{A}_y(z) \, dz + q_y^t \mathbf{A}_y(h/2) + q_y^b \mathbf{A}_y(-h/2) \\
\mathbf{F}_z &= \int_{-h/2}^{h/2} f_z \mathbf{A}_z(z) \, dz + q_z^t \mathbf{A}_z(h/2) + q_z^b \mathbf{A}_z(-h/2)
\end{aligned} \tag{3.21}$$

where f_x, f_y and f_z are the body forces acting per unit volume of the plate in x, y and z directions, respectively; q_x^t and q_x^b are forces acting on the top and bottom surfaces,

respectively, of the plate per unit area in the x direction. Similarly, q_y^t and q_y^b are forces acting on the top and bottom surfaces of the plate per unit area in y direction and q_z^t and q_z^b are forces per unit area at top and bottom surfaces, respectively, of the plate in the z direction. Further, from the principle of virtual displacement (see Reddy [41]), we have the following:

$$\begin{aligned}
0 &= \delta U + \delta V \\
&= \int_A \Big[\delta\boldsymbol{\Phi}\cdot(\mathbf{M}_1+\mathbf{M}_{nl}+\boldsymbol{\mathcal{M}}_1-\mathbf{F}) + \delta\boldsymbol{\Phi}_{,x}\cdot(\mathbf{M}_{nl_x}+\mathbf{M}_{2_x}+\boldsymbol{\mathcal{M}}_{2_x}) \\
&\qquad +\delta\boldsymbol{\Phi}_{,y}\cdot\left(\mathbf{M}_{nl_y}+\mathbf{M}_{2_y}+\boldsymbol{\mathcal{M}}_{2_y}\right) + \delta\boldsymbol{\Phi}_{,xx}\cdot\boldsymbol{\mathcal{M}}_{3_x} \\
&\qquad +2\delta\boldsymbol{\Phi}_{,xy}\cdot\boldsymbol{\mathcal{M}}_{3_{xy}} + \delta\boldsymbol{\Phi}_{,yy}\cdot\boldsymbol{\mathcal{M}}_{3_y}\Big]\,dx\,dy \\
&= \int_A \delta\boldsymbol{\Phi}\cdot\Big[(\mathbf{M}_1+\mathbf{M}_{nl}+\boldsymbol{\mathcal{M}}_1-\mathbf{F}) - (\mathbf{M}_{nl_x}+\mathbf{M}_{2_x}+\boldsymbol{\mathcal{M}}_{2_x})_{,x} \\
&\qquad -\left(\mathbf{M}_{nl_y}+\mathbf{M}_{2_y}+\boldsymbol{\mathcal{M}}_{2_y}\right)_{,y} + \boldsymbol{\mathcal{M}}_{3_x,xx} + 2\boldsymbol{\mathcal{M}}_{3_{xy},xy} + \boldsymbol{\mathcal{M}}_{3_y,yy}\Big]\,dx\,dy \\
&\qquad + \oint_\Gamma \delta\boldsymbol{\Phi}\cdot\left[\left(\mathbf{M}_{nl_x}+\mathbf{M}_{2_x}+\boldsymbol{\mathcal{M}}_{2_x}-\boldsymbol{\mathcal{M}}_{3_x,x}-\boldsymbol{\mathcal{M}}_{3_{xy},y}\right)n_x\right. \\
&\qquad\quad \left.+\left(\mathbf{M}_{nl_y}+\mathbf{M}_{2_y}+\boldsymbol{\mathcal{M}}_{2_y}-\boldsymbol{\mathcal{M}}_{3_y,y}-\boldsymbol{\mathcal{M}}_{3_{xy},x}\right)n_y\right] \\
&\qquad\quad +\delta\boldsymbol{\Phi}_{,x}\cdot(\boldsymbol{\mathcal{M}}_{3_x}n_x+\boldsymbol{\mathcal{M}}_{3_{xy}}n_y) + \delta\boldsymbol{\Phi}_{,y}\cdot(\boldsymbol{\mathcal{M}}_{3_y}n_y+\boldsymbol{\mathcal{M}}_{3_{xy}}n_x)\,ds
\end{aligned} \tag{3.22}$$

Along the boundary of the plate, we can write the derivative of the displacement variable in terms of the normal and tangential derivatives as follows:

$$\boldsymbol{\Phi}_{,x} = \boldsymbol{\Phi}_{,n}n_x - \boldsymbol{\Phi}_{,s}n_y, \quad \boldsymbol{\Phi}_{,y} = \boldsymbol{\Phi}_{,n}n_y + \boldsymbol{\Phi}_{,s}n_x, \tag{3.23}$$

where n and s are co-ordinate along the outward normal and tangential direction at the boundary curve of the plate. n_x and n_y are the component of outward unit normal along $x-$ and $y-$ axes respectively. Then the part of the boundary integral can be rewritten as:

$$\begin{aligned}
&\oint_\Gamma [\delta\boldsymbol{\Phi}_{,x}\cdot(\boldsymbol{\mathcal{M}}_{3_x}n_x+\boldsymbol{\mathcal{M}}_{3_{xy}}n_y) + \delta\boldsymbol{\Phi}_{,y}\cdot(\boldsymbol{\mathcal{M}}_{3_y}n_y+\boldsymbol{\mathcal{M}}_{3_{xy}}n_x)]\,ds \\
&= \oint_\Gamma \delta\boldsymbol{\Phi}_{,n}\cdot(\boldsymbol{\mathcal{M}}_{3_x}n_x^2 + 2\boldsymbol{\mathcal{M}}_{3_{xy}}n_xn_y + \boldsymbol{\mathcal{M}}_{3_y}n_y^2) \\
&\qquad +\delta\boldsymbol{\Phi}_{,s}\cdot((\boldsymbol{\mathcal{M}}_{3_y}-\boldsymbol{\mathcal{M}}_{3_x})n_xn_y + \boldsymbol{\mathcal{M}}_{3_{xy}}(n_x^2-n_y^2))\,ds
\end{aligned} \tag{3.24}$$

Further, for a smooth boundary, the boundary term in Eq. (3.22) can be modified as follows:

$$\begin{aligned} 0 \;=\; & \int_A \delta\boldsymbol{\Phi}\cdot\Big[\,(\mathbf{M}_1+\mathbf{M}_{nl}+\boldsymbol{\mathcal{M}}_1-\mathbf{F})-(\mathbf{M}_{nl_x}+\mathbf{M}_{2_x}+\boldsymbol{\mathcal{M}}_{2_x})_{,x} \\ & \qquad -\left(\mathbf{M}_{nl_y}+\mathbf{M}_{2_y}+\boldsymbol{\mathcal{M}}_{2_y}\right)_{,y}+\boldsymbol{\mathcal{M}}_{3_x,xx}+2\boldsymbol{\mathcal{M}}_{3_{xy},xy}+\boldsymbol{\mathcal{M}}_{3_y,yy}\Big]\,dx\,dy \\ & +\oint_\Gamma\Big[\delta\boldsymbol{\Phi}\cdot[\left(\mathbf{M}_{nl_x}+\mathbf{M}_{2_x}+\boldsymbol{\mathcal{M}}_{2_x}-\boldsymbol{\mathcal{M}}_{3_x,x}-\boldsymbol{\mathcal{M}}_{3_{xy},y}\right)n_x \\ & \qquad +\left(\mathbf{M}_{nl_y}+\mathbf{M}_{2_y}+\boldsymbol{\mathcal{M}}_{2_y}-\boldsymbol{\mathcal{M}}_{3_y,y}-\boldsymbol{\mathcal{M}}_{3_{xy},x}\right)n_y \\ & \qquad -((\boldsymbol{\mathcal{M}}_{3_y}-\boldsymbol{\mathcal{M}}_{3_x})n_xn_y+\boldsymbol{\mathcal{M}}_{3_{xy}}(n_x^2-n_y^2))_{,s}] \\ & \qquad +\delta\boldsymbol{\Phi}_{,n}\cdot(\boldsymbol{\mathcal{M}}_{3_x}n_x^2+2\boldsymbol{\mathcal{M}}_{3_{xy}}n_xn_y+\boldsymbol{\mathcal{M}}_{3_y}n_y^2)\Big]\,ds \end{aligned} \tag{3.25}$$

Then the Euler–Lagrange equations of the plate are

$$\begin{aligned} \hat{\mathbf{F}} \;=\; & (\mathbf{M}_1+\mathbf{M}_{nl}+\boldsymbol{\mathcal{M}}_1)-(\mathbf{M}_{nl_x}+\mathbf{M}_{2_x}+\boldsymbol{\mathcal{M}}_{2_x})_{,x}-\left(\mathbf{M}_{nl_y}+\mathbf{M}_{2_y}+\boldsymbol{\mathcal{M}}_{2_y}\right)_{,y} \\ & +\boldsymbol{\mathcal{M}}_{3_x,xx}+2\boldsymbol{\mathcal{M}}_{3_{xy},xy}+\boldsymbol{\mathcal{M}}_{3_y,yy} \end{aligned} \tag{3.26}$$

and the primary and secondary variables are

$$\begin{aligned} \boldsymbol{\Phi} \quad &: \quad \mathbf{P} \\ \boldsymbol{\Phi}_{,n} \quad &: \quad (\boldsymbol{\mathcal{M}}_{3_x}n_x^2+2\boldsymbol{\mathcal{M}}_{3_{xy}}n_xn_y+\boldsymbol{\mathcal{M}}_{3_y}n_y^2) \end{aligned} \tag{3.27}$$

where

$$\begin{aligned} \mathbf{P} \;=\; & [\left(\mathbf{M}_{nl_x}+\mathbf{M}_{2_x}+\boldsymbol{\mathcal{M}}_{2_x}-\boldsymbol{\mathcal{M}}_{3_x,x}-\boldsymbol{\mathcal{M}}_{3_{xy},y}\right)n_x \\ & \qquad +\left(\mathbf{M}_{nl_y}+\mathbf{M}_{2_y}+\boldsymbol{\mathcal{M}}_{2_y}-\boldsymbol{\mathcal{M}}_{3_y,y}-\boldsymbol{\mathcal{M}}_{3_{xy},x}\right)n_y \\ & \qquad -((\boldsymbol{\mathcal{M}}_{3_y}-\boldsymbol{\mathcal{M}}_{3_x})n_xn_y+\boldsymbol{\mathcal{M}}_{3_{xy}}(n_x^2-n_y^2))_{,s}] \end{aligned} \tag{3.28}$$

3.3. Constitutive relation

The relation between the symmetric part of stress and strain for the isotropic and homogeneous material can be given as

$$\mathbf{S}^s=\mathbf{C}\boldsymbol{\varepsilon} \tag{3.29}$$

where

$$\begin{aligned}
\mathbf{C} &= \frac{E(1-\nu)}{(1+\nu)(1-2\nu)}\begin{bmatrix} 1 & \frac{\nu}{1-\nu} & \frac{\nu}{1-\nu} & 0 & 0 & 0 \\ \frac{\nu}{1-\nu} & 1 & \frac{\nu}{1-\nu} & 0 & 0 & 0 \\ \frac{\nu}{1-\nu} & \frac{\nu}{1-\nu} & 1 & 0 & 0 & 0 \\ 0 & 0 & 0 & \frac{1-2\nu}{2(1-\nu)} & 0 & 0 \\ 0 & 0 & 0 & 0 & \frac{1-2\nu}{2(1-\nu)} & 0 \\ 0 & 0 & 0 & 0 & 0 & \frac{1-2\nu}{2(1-\nu)} \end{bmatrix} \\
\boldsymbol{\varepsilon} &= \begin{bmatrix} \varepsilon_{xx} & \varepsilon_{yy} & \varepsilon_{zz} & \gamma_{yz} & \gamma_{zx} & \gamma_{xy} \end{bmatrix}^T \\
\mathbf{S}^s &= \begin{bmatrix} S^s_{xx} & S^s_{yy} & S^s_{zz} & S^s_{yz} & S^s_{zx} & S^s_{xy} \end{bmatrix}^T
\end{aligned} \tag{3.30}$$

where E and ν are the modulus of elasticity and Poisson's ratio, respectively. Further, the relation between $\boldsymbol{\chi}$ and its energy conjugate, namely, the couple stress $\mathbf{m}$, can be given as

$$\mathbf{m} = \mathbf{C}_l \boldsymbol{\chi}. \tag{3.31}$$

The long ordered orientation of small inclusions in the matrix of isotropic materials could bring anisotropic effect in the overall response of the material, for example, as in the case of liquid crystal elastomers. In this study, we will consider the material constant $\mathbf{C}_l$ as diagonal tensor with the diagonal elements given by

$$\mathbf{C}_{l_{ii}} = G\ell_i^2 \tag{3.32}$$

where G is the shear modulus and ℓ_i are the material length scale related to the corresponding rotation gradient component.

The present formulation of the bending of plates will also be valid for the spatial variation of material properties, for example, if the small inclusions are embedded in functionally graded plate or varying orientation of the microstructure or embedding. In the numerical example, we have considered a power law functionally graded plate with small embedding for which the constitutive relation can be assumed as the power law variation of the material properties through its thickness,

$$P(z) = [P_1 - P_2]\, f(z) + P_2, \quad f(z) = \left(\frac{1}{2} + \frac{z}{h}\right)^{\hat{n}} \tag{3.33}$$

where P_1 and P_2 are the values of a typical material property, such as the modulus, density, and conductivity, of material at the top (at $z = h/2$) and bottom (at $z = -h/2$) surface of the plate respectively; $\hat{n}$ denotes the volume fraction exponent, called power-law index. When $\hat{n} = 0$, we obtain the single-material plate (with property P_1). Poisson's ratio is considered as a constant. We have the material constants $\mathbf{C}$ and $\mathbf{C}_l$ of same form as in Eqs. (3.30) and (3.32) with the modulus of elasticity and shear modulus varying according to Eq. (3.33) along the thickness of the plate; the material length scale is taken as constant in the numerical examples of the present study. The material length scale can also vary spatially, for example, in the case of functionally graded material with varying microstructure (see [53]) or in case of spatial variation of orientation of mesogen in liquid crystal elastomer (*e.g.* spiral orientation of mesogenic molecules in Cholesteric liquid crystal elastomers; see [49]).

3.4. Finite element model

We discretize the computational domain into non-overlapping sub-domain (elements), Ω^e. The weak form of the governing equations (3.26) for an element can be given as follows:

$$
\begin{aligned}
0 = \int_{\Omega^e} \Big[& \delta\boldsymbol{\Phi} \cdot \left(\mathbf{H}_1^0\boldsymbol{\Phi} + \mathbf{H}_{2_x}^0\boldsymbol{\Phi}_{,x} + \mathbf{H}_{2_y}^0\boldsymbol{\Phi}_{,y} + \frac{1}{2}\mathbf{H}_{nl}^0\boldsymbol{\Phi} + \frac{1}{2}\mathbf{H}_{nl_x}^0\boldsymbol{\Phi}_{,x} + \frac{1}{2}\mathbf{H}_{nl_y}^0\boldsymbol{\Phi}_{,y} \right) \\
& + \delta\boldsymbol{\Phi} \cdot \left(\mathbf{H}_1\boldsymbol{\Phi} + \mathbf{H}_{2_x}\boldsymbol{\Phi}_{,x} + \mathbf{H}_{2_y}\boldsymbol{\Phi}_{,y} + \frac{1}{2}\mathbf{H}_{nl}\boldsymbol{\Phi} + \frac{1}{2}\mathbf{H}_{nl_x}\boldsymbol{\Phi}_{,x} + \frac{1}{2}\mathbf{H}_{nl_y}\boldsymbol{\Phi}_{,y} \right) \\
& + \delta\boldsymbol{\Phi}_{,x} \cdot \left(\mathbf{H}_1^1\boldsymbol{\Phi} + \mathbf{H}_{2_x}^1\boldsymbol{\Phi}_{,x} + \mathbf{H}_{2_y}^1\boldsymbol{\Phi}_{,y} + \frac{1}{2}\mathbf{H}_{nl}^1\boldsymbol{\Phi} + \frac{1}{2}\mathbf{H}_{nl_x}^1\boldsymbol{\Phi}_{,x} + \frac{1}{2}\mathbf{H}_{nl_y}^1\boldsymbol{\Phi}_{,y} \right) \\
& + \delta\boldsymbol{\Phi}_{,y} \cdot \left(\mathbf{H}_1^2\boldsymbol{\Phi} + \mathbf{H}_{2_x}^2\boldsymbol{\Phi}_{,x} + \mathbf{H}_{2_y}^2\boldsymbol{\Phi}_{,y} + \frac{1}{2}\mathbf{H}_{nl}^2\boldsymbol{\Phi} + \frac{1}{2}\mathbf{H}_{nl_x}^2\boldsymbol{\Phi}_{,x} + \frac{1}{2}\mathbf{H}_{nl_y}^2\boldsymbol{\Phi}_{,y} \right) \\
& + \delta\boldsymbol{\Phi} \cdot \left(\mathbf{N}_1\boldsymbol{\Phi} + \mathbf{N}_{2_x}\boldsymbol{\Phi}_{,x} + \mathbf{N}_{2_y}\boldsymbol{\Phi}_{,y} + \mathbf{N}_{3_{xx}}\boldsymbol{\Phi}_{,xx} + \mathbf{N}_{3_{xy}}\boldsymbol{\Phi}_{,xy} + \mathbf{N}_{3_{yy}}\boldsymbol{\Phi}_{,yy} \right) \\
& + \delta\boldsymbol{\Phi}_{,x} \cdot \left(\mathbf{N}_1^1\boldsymbol{\Phi} + \mathbf{N}_{2_x}^1\boldsymbol{\Phi}_{,x} + \mathbf{N}_{2_y}^1\boldsymbol{\Phi}_{,y} + \mathbf{N}_{3_{xx}}^1\boldsymbol{\Phi}_{,xx} + \mathbf{N}_{3_{xy}}^1\boldsymbol{\Phi}_{,xy} + \mathbf{N}_{3_{yy}}^1\boldsymbol{\Phi}_{,yy} \right) \\
& + \delta\boldsymbol{\Phi}_{,y} \cdot \left(\mathbf{N}_1^2\boldsymbol{\Phi} + \mathbf{N}_{2_x}^2\boldsymbol{\Phi}_{,x} + \mathbf{N}_{2_y}^2\boldsymbol{\Phi}_{,y} + \mathbf{N}_{3_{xx}}^2\boldsymbol{\Phi}_{,xx} + \mathbf{N}_{3_{xy}}^2\boldsymbol{\Phi}_{,xy} + \mathbf{N}_{3_{yy}}^2\boldsymbol{\Phi}_{,yy} \right) \\
& + \delta\boldsymbol{\Phi}_{,xx} \cdot \left(\mathbf{N}_1^3\boldsymbol{\Phi} + \mathbf{N}_{2_x}^3\boldsymbol{\Phi}_{,x} + \mathbf{N}_{2_y}^3\boldsymbol{\Phi}_{,y} + \mathbf{N}_{3_{xx}}^3\boldsymbol{\Phi}_{,xx} + \mathbf{N}_{3_{xy}}^3\boldsymbol{\Phi}_{,xy} + \mathbf{N}_{3_{yy}}^3\boldsymbol{\Phi}_{,yy} \right) \\
& + \delta\boldsymbol{\Phi}_{,xy} \cdot \left(\mathbf{N}_1^4\boldsymbol{\Phi} + \mathbf{N}_{2_x}^4\boldsymbol{\Phi}_{,x} + \mathbf{N}_{2_y}^4\boldsymbol{\Phi}_{,y} + \mathbf{N}_{3_{xx}}^4\boldsymbol{\Phi}_{,xx} + \mathbf{N}_{3_{xy}}^4\boldsymbol{\Phi}_{,xy} + \mathbf{N}_{3_{yy}}^4\boldsymbol{\Phi}_{,yy} \right) \\
& + \delta\boldsymbol{\Phi}_{,yy} \cdot \left(\mathbf{N}_1^5\boldsymbol{\Phi} + \mathbf{N}_{2_x}^5\boldsymbol{\Phi}_{,x} + \mathbf{N}_{2_y}^5\boldsymbol{\Phi}_{,y} + \mathbf{N}_{3_{xx}}^5\boldsymbol{\Phi}_{,xx} + \mathbf{N}_{3_{xy}}^5\boldsymbol{\Phi}_{,xy} + \mathbf{N}_{3_{yy}}^5\boldsymbol{\Phi}_{,yy} \right) \\
& - \delta\boldsymbol{\Phi} \cdot \hat{\mathbf{F}} \Big] \, dxdy
\end{aligned}
\tag{3.34}
$$

where

$$\mathbf{H}_j^0 = \int_{-h/2}^{h/2} \mathbf{A}_1^T \mathbf{C} \mathbf{A}_j \, dz, \quad \mathbf{H}_j = \int_{-h/2}^{h/2} \mathbf{A}_{nl}^T \mathbf{C} \mathbf{A}_j \, dz$$
$$\mathbf{H}_j^1 = \int_{-h/2}^{h/2} (\mathbf{A}_{nl_x}^T + \mathbf{A}_{2_x}^T) \mathbf{C} \mathbf{A}_j \, dz, \quad \mathbf{H}_j^2 = \int_{-h/2}^{h/2} (\mathbf{A}_{nl_y}^T + \mathbf{A}_{2_y}^T) \mathbf{C} \mathbf{A}_j \, dz$$
$$\text{where, } j = 1, 2_x, 2_y, nl, nl_x, nl_y$$
$$\mathbf{N}_i = \int_{-h/2}^{h/2} \mathbf{B}_1^T \mathbf{C}_l \mathbf{B}_i \, dz, \quad \mathbf{N}_i^1 = \int_{-h/2}^{h/2} \mathbf{B}_{2_x}^T \mathbf{C}_l \mathbf{B}_i \, dz, \mathbf{N}_i^2 = \int_{-h/2}^{h/2} \mathbf{B}_{2_y}^T \mathbf{C}_l \mathbf{B}_i \, dz$$
$$\mathbf{N}_i^3 = \int_{-h/2}^{h/2} \mathbf{B}_{3_{xx}}^T \mathbf{C}_l \mathbf{B}_i \, dz, \quad \mathbf{N}_i^4 = \int_{-h/2}^{h/2} \mathbf{B}_{3_{xy}}^T \mathbf{C}_l \mathbf{B}_i \, dz, \quad \mathbf{N}_i^5 = \int_{-h/2}^{h/2} \mathbf{B}_{3_{yy}}^T \mathbf{C}_l \mathbf{B}_i \, dz,$$
$$\text{where, } j = 1, 2_x, 2_y, 3_{xx}, 3_{xy}, 3_{yy}. \tag{3.35}$$

We approximate the vector of generalized displacements as

$$\mathbf{\Phi}(x) = \mathbf{\Psi}(x)\mathbf{U} \tag{3.36}$$

where $\mathbf{\Psi}(x, y)$ is the matrix of shape functions and $\bar{\mathbf{U}}$ is vector of the nodal values[1] of the generalized displacements,

$$\mathbf{\Psi} = \begin{bmatrix} \psi_1^{(1)} & \dots & \psi_{\tilde{n}_1}^{(1)} & 0 & \dots & 0 & \dots & 0 & \dots & 0 \\ 0 & \dots & 0 & \psi_1^{(2)} & \dots & \psi_{\tilde{n}_2}^{(2)} & \dots & 0 & \dots & 0 \\ \vdots & \ddots & \vdots & \vdots & \ddots & \vdots & \ddots & \vdots & \ddots & \vdots \\ 0 & \dots & 0 & 0 & \dots & 0 & \dots & \psi_1^{(\bar{r})} & \dots & \psi_{\tilde{n}_{\bar{r}}}^{(\bar{r})} \end{bmatrix} \tag{3.37}$$

$$\mathbf{U} = \begin{bmatrix} u_{1_1} & \dots & u_{1_{\tilde{n}_1}} & u_{2_1} & \dots & u_{2_{\tilde{n}_2}} & \dots & u_{r_1} & \dots & u_{r_{\tilde{n}_r}} \end{bmatrix}^T \tag{3.38}$$

where $\tilde{n}_1, \tilde{n}_2, \cdots \tilde{n}_{\bar{r}}$ are the number of nodal values for $u_1, u_2, \cdots, u_{\bar{r}}$ respectively in the considered element. $\bar{r} = (n+m+p+3)$ is the total number of degrees of freedom

[1] $\mathbf{U}$ in this chapter represent the vector of the nodal values and should not be confused with the right stretch tensor of chapter 1.

(dofs), and

$$\begin{aligned}
u_1 &= \phi_x^{(0)}, \quad u_2 = \phi_x^{(1)}, \quad \cdots \quad u_{n+1} = \phi_x^{(n)} \\
u_{n+2} &= \phi_y^{(0)}, \quad u_{n+3} = \phi_y^{(1)}, \quad \cdots \quad u_{n+m+2} = \phi_y^{(m)} \\
u_{n+m+3} &= \phi_z^{(0)}, \quad u_{n+m+4} = \phi_z^{(1)}, \quad \cdots \quad u_{\bar{r}} = \phi_z^{(p)}.
\end{aligned} \tag{3.39}$$

We substitute the approximation of dofs and $\delta\mathbf{\Phi} = \mathbf{\Psi}\tilde{\mathbf{l}}$ (where $\tilde{\mathbf{l}}$ is vector with each element is unity and same size as $\mathbf{\Phi}$) into Eq. (3.34) to arrive at the following finite element equation:

$$(\mathbf{K} + \mathbf{K}_l)\mathbf{U} - \mathbf{f} = \mathbf{0} \tag{3.40}$$

where $\mathbf{K}$ is the stiffness matrix related to the conventional plate and $\mathbf{K}_l$ is the stiffness matrix related to the length scale parameters of the material, and are given as:

$$\begin{aligned}
\mathbf{K} &= \int_{\Omega^e} \Big[\mathbf{\Psi}^T \left(\mathbf{H}_1^0 \mathbf{\Psi} + \mathbf{H}_{2_x}^0 \mathbf{\Psi}_{,x} + \mathbf{H}_{2_y}^0 \mathbf{\Psi}_{,y} + \frac{1}{2}\mathbf{H}_{nl}^0 \mathbf{\Psi} + \frac{1}{2}\mathbf{H}_{nl_x}^0 \mathbf{\Psi}_{,x} + \frac{1}{2}\mathbf{H}_{nl_y}^0 \mathbf{\Psi}_{,y} \right) \\
&\quad + \mathbf{\Psi}^T \left(\mathbf{H}_1 \mathbf{\Psi} + \mathbf{H}_{2_x} \mathbf{\Psi}_{,x} + \mathbf{H}_{2_y} \mathbf{\Psi}_{,y} + \frac{1}{2}\mathbf{H}_{nl} \mathbf{\Psi} + \frac{1}{2}\mathbf{H}_{nl_x} \mathbf{\Psi}_{,x} + \frac{1}{2}\mathbf{H}_{nl_y} \mathbf{\Psi}_{,y} \right) \\
&\quad + \mathbf{\Psi}_{,x}^T \left(\mathbf{H}_1^1 \mathbf{\Psi} + \mathbf{H}_{2_x}^1 \mathbf{\Psi}_{,x} + \mathbf{H}_{2_y}^1 \mathbf{\Psi}_{,y} + \frac{1}{2}\mathbf{H}_{nl}^1 \mathbf{\Psi} + \frac{1}{2}\mathbf{H}_{nl_x}^1 \mathbf{\Psi}_{,x} + \frac{1}{2}\mathbf{H}_{nl_y}^1 \mathbf{\Psi}_{,y} \right) \\
&\quad + \mathbf{\Psi}_{,y}^T \left(\mathbf{H}_1^2 \mathbf{\Psi} + \mathbf{H}_{2_x}^2 \mathbf{\Psi}_{,x} + \mathbf{H}_{2_y}^2 \mathbf{\Psi}_{,y} + \frac{1}{2}\mathbf{H}_{nl}^2 \mathbf{\Psi} + \frac{1}{2}\mathbf{H}_{nl_x}^2 \mathbf{\Psi}_{,x} + \frac{1}{2}\mathbf{H}_{nl_y}^2 \mathbf{\Psi}_{,y} \right) \Big] \, dxdy \\
\mathbf{K}_l &= \int_{\Omega^e} \Big[\mathbf{\Psi}^T \left(\mathbf{N}_1 \mathbf{\Psi} + \mathbf{N}_{2_x} \mathbf{\Psi}_{,x} + \mathbf{N}_{2_y} \mathbf{\Psi}_{,y} + \mathbf{N}_{3_{xx}} \mathbf{\Psi}_{,xx} + \mathbf{N}_{3_{xy}} \mathbf{\Psi}_{,xy} + \mathbf{N}_{3_{yy}} \mathbf{\Psi}_{,yy} \right) \\
&\quad + \mathbf{\Psi}_{,x}^T \left(\mathbf{N}_1^1 \mathbf{\Psi} + \mathbf{N}_{2_x}^1 \mathbf{\Psi}_{,x} + \mathbf{N}_{2_y}^1 \mathbf{\Psi}_{,y} + \mathbf{N}_{3_{xx}}^1 \mathbf{\Psi}_{,xx} + \mathbf{N}_{3_{xy}}^1 \mathbf{\Psi}_{,xy} + \mathbf{N}_{3_{yy}}^1 \mathbf{\Psi}_{,yy} \right) \\
&\quad + \mathbf{\Psi}_{,y}^T \left(\mathbf{N}_1^2 \mathbf{\Psi} + \mathbf{N}_{2_x}^2 \mathbf{\Psi}_{,x} + \mathbf{N}_{2_y}^2 \mathbf{\Psi}_{,y} + \mathbf{N}_{3_{xx}}^2 \mathbf{\Psi}_{,xx} + \mathbf{N}_{3_{xy}}^2 \mathbf{\Psi}_{,xy} + \mathbf{N}_{3_{yy}}^2 \mathbf{\Psi}_{,yy} \right) \\
&\quad + \mathbf{\Psi}_{,xx}^T \left(\mathbf{N}_1^3 \mathbf{\Psi} + \mathbf{N}_{2_x}^3 \mathbf{\Psi}_{,x} + \mathbf{N}_{2_y}^3 \mathbf{\Psi}_{,y} + \mathbf{N}_{3_{xx}}^3 \mathbf{\Psi}_{,xx} + \mathbf{N}_{3_{xy}}^3 \mathbf{\Psi}_{,xy} + \mathbf{N}_{3_{yy}}^3 \mathbf{\Psi}_{,yy} \right) \\
&\quad + \mathbf{\Psi}_{,xy}^T \left(\mathbf{N}_1^4 \mathbf{\Psi} + \mathbf{N}_{2_x}^4 \mathbf{\Psi}_{,x} + \mathbf{N}_{2_y}^4 \mathbf{\Psi}_{,y} + \mathbf{N}_{3_{xx}}^4 \mathbf{\Psi}_{,xx} + \mathbf{N}_{3_{xy}}^4 \mathbf{\Psi}_{,xy} + \mathbf{N}_{3_{yy}}^4 \mathbf{\Psi}_{,yy} \right) \\
&\quad + \mathbf{\Psi}_{,yy}^T \left(\mathbf{N}_1^5 \mathbf{\Psi} + \mathbf{N}_{2_x}^5 \mathbf{\Psi}_{,x} + \mathbf{N}_{2_y}^5 \mathbf{\Psi}_{,y} + \mathbf{N}_{3_{xx}}^5 \mathbf{\Psi}_{,xx} + \mathbf{N}_{3_{xy}}^5 \mathbf{\Psi}_{,xy} + \mathbf{N}_{3_{yy}}^5 \mathbf{\Psi}_{,yy} \right) \Big] \, dxdy \\
\mathbf{f} &= \int_{\Omega^e} \mathbf{\Psi}^T \hat{\mathbf{F}} \, dxdy
\end{aligned} \tag{3.41}$$

Also we note here that stiffness matrix is not symmetric and depends on the displacement hence is nonlinear. We will apply Newton's method to solve the nonlinear

algebraic Eq. (3.40), which can be rewritten in the following form:

$$\mathbf{g}(\mathbf{U}) = (\mathbf{K} + \mathbf{K}_l)\mathbf{U} - \mathbf{f} = \mathbf{0} \tag{3.42}$$

For the guess solution $\mathbf{U}_0$, we can write the following linear approximation of any vector-valued function,

$$\mathbf{g}(\mathbf{U}) = \mathbf{g}(\mathbf{U}_0) + D\mathbf{g}(\mathbf{U}_0)(\mathbf{U} - \mathbf{U}_0) \tag{3.43}$$

where $D\mathbf{g}$ is (*Fréchet*) derivative of $\mathbf{g}(\mathbf{U})$with respect to $\mathbf{U}$ defined at $(\mathbf{U} = \mathbf{U}_0)$ i.e. $D\mathbf{g} = \frac{\partial \mathbf{g}}{\partial \mathbf{U}}\big|_{(\mathbf{U}=\mathbf{U}_0)}$. We need to obtain $\mathbf{U}$ such that $\mathbf{g}(\mathbf{U}) = 0$. Thus we have

$$D\mathbf{g}(\mathbf{U}_0)(\mathbf{U} - \mathbf{U}_0) = -\mathbf{g}(\mathbf{U}_0) \tag{3.44}$$

For $(r+1)$st iteration of Newton's method, the solution can be expressed as

$$\mathbf{T}(\mathbf{U}_r)\delta\mathbf{U}_{r+1} = -(\mathbf{K}(\mathbf{U}_r) + \mathbf{K}_l(\mathbf{U}_r))\mathbf{U}_r + \mathbf{f}(\mathbf{U}_r), \text{ and, } \mathbf{U}_{r+1} = \mathbf{U}_r + \delta\mathbf{U}_{r+1} \tag{3.45}$$

where $\mathbf{T} = D\mathbf{g}$ is called the tangent matrix, which is given as following:

$$\begin{aligned}
\mathbf{T} &= D((\mathbf{K} + \mathbf{K}_l)\mathbf{U} + \mathbf{f}) = (D\mathbf{K})\mathbf{U} + \mathbf{K} + \mathbf{K}_l \\
&= \mathbf{K} + \mathbf{K}_l + \int_{\Omega^e} \Big[\frac{1}{2}\Big(\mathbf{\Psi}^T\left(\mathbf{H}^0_{nl}\mathbf{\Psi} + \mathbf{H}^0_{nl_x}\mathbf{\Psi}_{,x} + \mathbf{H}^0_{nl_y}\mathbf{\Psi}_{,y}\right) \\
&\quad + \mathbf{\Psi}^T\left(\mathbf{H}_{nl}\mathbf{\Psi} + \mathbf{H}_{nl_x}\mathbf{\Psi}_{,x} + \mathbf{H}_{nl_y}\mathbf{\Psi}_{,y}\right) + \mathbf{\Psi}^T_{,x}\left(\mathbf{H}^1_{nl}\mathbf{\Psi} + \mathbf{H}^1_{nl_x}\mathbf{\Psi}_{,x} + \mathbf{H}^1_{nl_y}\mathbf{\Psi}_{,y}\right) \\
&\quad + \mathbf{\Psi}^T_{,y}\left(\mathbf{H}^2_{nl}\mathbf{\Psi} + \mathbf{H}^2_{nl_x}\mathbf{\Psi}_{,x} + \mathbf{H}^2_{nl_y}\mathbf{\Psi}_{,y}\right)\Big) + \mathbf{\Psi}^T\mathbf{P}_{nl}\mathbf{\Psi} + \mathbf{\Psi}^T_{,x}\mathbf{P}^x_{nl}\mathbf{\Psi}_{,x} \\
&\quad + \mathbf{\Psi}^T_{,y}\mathbf{P}^y_{nl}\mathbf{\Psi}_{,y} + \mathbf{\Psi}^T_{,x}\mathbf{P}^{xy}_{nl}\mathbf{\Psi}_{,y} + + \mathbf{\Psi}^T_{,y}\mathbf{P}^{xy}_{nl}\mathbf{\Psi}_{,x}\Big]\, dxdy
\end{aligned} \tag{3.46}$$

where $\mathbf{P}_{nl}$, $\mathbf{P}^x_{nl}$, $\mathbf{P}^y_{nl}$ and $\mathbf{P}^{xy}_{nl}$ are $(\bar{r}\times\bar{r})$ matrices with only following nonzero element,

$$\begin{aligned}
P_{nl_{22}} &= \int_{-h/2}^{h/2} S^s_{zz}\, dz, \quad P_{nl_{(n+3)(n+3)}} = \int_{-h/2}^{h/2} S^s_{zz}\, dz \\
P^x_{nl_{(n+m+3)(n+m+3)}} &= \int_{-h/2}^{h/2} S^s_{xx}\, dz \\
P^y_{nl_{(n+m+3)(n+m+3)}} &= \int_{-h/2}^{h/2} S^s_{yy}\, dz \\
P^{xy}_{nl_{(n+m+3)(n+m+3)}} &= \int_{-h/2}^{h/2} S^s_{xy}\, dz,
\end{aligned} \tag{3.47}$$

Here we note that the tangent matrix is symmetric.

3.5. Analytical solution for simply supported linear plate

let us consider a rectangular plate with dimension $(a \times b)$ and height h with simply supported boundary condition. The governing equation of the plate in linear case can be given as following:

$$\begin{aligned}\hat{\mathbf{F}} &= (\mathbf{M}_1 + \boldsymbol{\mathcal{M}}_1) - (\mathbf{M}_{2_x} + \boldsymbol{\mathcal{M}}_{2_x})_{,x} - \left(\mathbf{M}_{2_y} + \boldsymbol{\mathcal{M}}_{2_y}\right)_{,y} \\ &\quad + \boldsymbol{\mathcal{M}}_{3_x,xx} + \boldsymbol{\mathcal{M}}_{3_{xy},xy} + \boldsymbol{\mathcal{M}}_{3_y,yy}\end{aligned} \tag{3.48}$$

where

$$\mathbf{M}_\xi = \bar{\mathbf{M}}_{\xi 1}\boldsymbol{\Phi} + \bar{\mathbf{M}}_{\xi 2_x}\boldsymbol{\Phi}_{,x} + \bar{\mathbf{M}}_{\xi 2_y}\boldsymbol{\Phi}_{,y} \quad \text{for } \xi = 1, 2_x, 2_y$$

$$\boldsymbol{\mathcal{M}}_\eta = \bar{\boldsymbol{\mathcal{M}}}_{\eta 1}\boldsymbol{\Phi} + \bar{\boldsymbol{\mathcal{M}}}_{\eta 2_x}\boldsymbol{\Phi}_{,x} + \bar{\boldsymbol{\mathcal{M}}}_{\eta 2_y}\boldsymbol{\Phi}_{,y} + \bar{\boldsymbol{\mathcal{M}}}_{\eta 3_x}\boldsymbol{\Phi}_{,xx} + \bar{\boldsymbol{\mathcal{M}}}_{\eta 3_{xy}}\boldsymbol{\Phi}_{,xy} + \bar{\boldsymbol{\mathcal{M}}}_{\eta 3_y}\boldsymbol{\Phi}_{,yy}$$

$$\text{for } \eta = 1, 2_x, 2_y, 3_x, 3_{xy}, 3_y \tag{3.49}$$

and

$$\begin{aligned}\bar{\mathbf{M}}_{\xi\gamma} &= \int_{-h/2}^{h/2} \mathbf{A}_\xi^T \mathbf{C} \mathbf{A}_\gamma \, dz \quad \text{for } \xi, \gamma = 1, 2_x, 2_y \\ \bar{\boldsymbol{\mathcal{M}}}_{\eta\delta} &= \int_{-h/2}^{h/2} \mathbf{B}_\eta^T \mathbf{C}_l \mathbf{B}_\delta \, dz \quad \text{for } \eta, \delta = 1, 2_x, 2_y, 3_x, 3_{xy}, 3_y\end{aligned} \tag{3.50}$$

The above generalized stress resultant at any point (x, y) can be function of spatial co-ordinate x or y for varying material properties (*e.g.* varying material length scale parameter) or possibly varying height of the plate. let us assume the solution for the generalized displacement in the following form, which satisfies the simply supported boundary condition:

$$\begin{aligned}\phi_x^{(i)}(x) &= \sum_{\alpha=1}^{\infty}\sum_{\beta=1}^{\infty} U_{\alpha\beta}^{(i)} \cos\left(\frac{\alpha\pi x}{a}\right) \sin\left(\frac{\beta\pi y}{b}\right) \\ \phi_y^{(i)}(x) &= \sum_{\alpha=1}^{\infty}\sum_{\beta=1}^{\infty} V_{\alpha\beta}^{(i)} \sin\left(\frac{\alpha\pi x}{a}\right) \cos\left(\frac{\beta\pi y}{b}\right) \\ \phi_z^{(i)}(x) &= \sum_{\alpha=1}^{\infty}\sum_{\beta=1}^{\infty} W_{\alpha\beta}^{(i)} \sin\left(\frac{\alpha\pi x}{a}\right) \sin\left(\frac{\beta\pi y}{b}\right)\end{aligned} \tag{3.51}$$

and also, the transverse force per unit area of the plate can be written as:

$$\begin{aligned} q &= \sum_{\alpha=1}^{\infty}\sum_{\beta=1}^{\infty} q_{\alpha\beta}\sin\left(\frac{\alpha\pi x}{a}\right)\sin\left(\frac{\beta\pi y}{b}\right), \quad \text{where} \\ q_{\alpha\beta} &= \frac{4}{ab}\int_0^a\int_0^b q\sin\left(\frac{\alpha\pi x}{a}\right)\sin\left(\frac{\beta\pi y}{b}\right)dxdy \end{aligned} \tag{3.52}$$

In vector form, we can write the generalized displacement vectors as following:

$$\begin{aligned} \mathbf{\Phi}_x^{\alpha\beta} &= \mathbf{U}_{\alpha\beta}\cos(\alpha\pi x/a)\sin(\beta\pi y/b) \\ \mathbf{\Phi}_y^{\alpha\beta} &= \mathbf{V}_{\alpha\beta}\sin(\alpha\pi x/a)\cos(\beta\pi y/b) \\ \mathbf{\Phi}_z^{\alpha\beta} &= \mathbf{W}_{\alpha\beta}\sin(\alpha\pi x/a)\sin(\beta\pi y/b) \\ \hat{\mathbf{F}}_z^{\alpha\beta} &= \mathbf{q}_{\alpha\beta}\sin(\alpha\pi x/a)\sin(\beta\pi y/b) \end{aligned} \tag{3.53}$$

The linear governing Eq.(3.48) can be rewritten in terms of displacement vector as following:

$$\begin{aligned} \hat{\mathbf{F}} &= \hat{\mathbf{M}}_1\mathbf{\Phi} + \hat{\mathbf{M}}_{2_x}\mathbf{\Phi}_{,x} + \hat{\mathbf{M}}_{2_y}\mathbf{\Phi}_{,y} + \hat{\mathbf{M}}_{3_x}\mathbf{\Phi}_{,xx} + \hat{\mathbf{M}}_{3_{xy}}\mathbf{\Phi}_{,xy} + \hat{\mathbf{M}}_{3_y}\mathbf{\Phi}_{,yy} \\ &\quad + \hat{\mathbf{M}}_{4_1}\mathbf{\Phi}_{,xxx} + \hat{\mathbf{M}}_{4_2}\mathbf{\Phi}_{,xxy} + \hat{\mathbf{M}}_{4_3}\mathbf{\Phi}_{,xyy} + \hat{\mathbf{M}}_{4_4}\mathbf{\Phi}_{,yyy} \\ &\quad + \hat{\mathbf{M}}_{5_1}\mathbf{\Phi}_{,xxxx} + \hat{\mathbf{M}}_{5_2}\mathbf{\Phi}_{,xxxy} + \hat{\mathbf{M}}_{5_3}\mathbf{\Phi}_{,xxyy} + \hat{\mathbf{M}}_{5_4}\mathbf{\Phi}_{,xyyy} + \hat{\mathbf{M}}_{5_5}\mathbf{\Phi}_{,yyyy} \end{aligned} \tag{3.54}$$

where

$$\begin{aligned} \hat{\mathbf{M}}_1 &= \bar{\mathbf{M}}_{11} + \bar{\boldsymbol{\mathcal{M}}}_{11} - \bar{\mathbf{M}}_{2_x1,x} - \bar{\mathbf{M}}_{2_y1,y} - \bar{\boldsymbol{\mathcal{M}}}_{2_x1,x} \\ &\quad - \bar{\boldsymbol{\mathcal{M}}}_{2_y1,y} + \bar{\boldsymbol{\mathcal{M}}}_{3_x1,xx} + \bar{\boldsymbol{\mathcal{M}}}_{3_{xy}1,xy} + \bar{\boldsymbol{\mathcal{M}}}_{3_y1,yy} \\ \hat{\mathbf{M}}_{2_x} &= \bar{\mathbf{M}}_{12_x} - \bar{\mathbf{M}}_{2_x1} - \bar{\mathbf{M}}_{2_x2_x,x} - \bar{\mathbf{M}}_{2_y2_x,y} \\ &\quad - \bar{\boldsymbol{\mathcal{M}}}_{2_x2_x,x} - \bar{\boldsymbol{\mathcal{M}}}_{2_y2_x,y} + \bar{\boldsymbol{\mathcal{M}}}_{3_x2_x,xx} + \bar{\boldsymbol{\mathcal{M}}}_{3_{xy}2_x,xy} + \bar{\boldsymbol{\mathcal{M}}}_{3_y2_x,yy} \\ \hat{\mathbf{M}}_{2_y} &= \bar{\mathbf{M}}_{12_y} - \bar{\mathbf{M}}_{2_y1} + \bar{\boldsymbol{\mathcal{M}}}_{12_y} - \bar{\boldsymbol{\mathcal{M}}}_{2_y1} - \bar{\mathbf{M}}_{2_x2_y,x} - \bar{\mathbf{M}}_{2_y2_y,y} \\ &\quad - \bar{\boldsymbol{\mathcal{M}}}_{2_x2_y,x} - \bar{\boldsymbol{\mathcal{M}}}_{2_y2_y,y} + \bar{\boldsymbol{\mathcal{M}}}_{3_x2_y,xx} + \bar{\boldsymbol{\mathcal{M}}}_{3_{xy}2_y,xy} + \bar{\boldsymbol{\mathcal{M}}}_{3_y2_y,yy} \\ \hat{\mathbf{M}}_{3_x} &= -\bar{\mathbf{M}}_{2_x2_x} - \bar{\boldsymbol{\mathcal{M}}}_{2_x2_x} + \bar{\boldsymbol{\mathcal{M}}}_{13_x} + \bar{\boldsymbol{\mathcal{M}}}_{3_x1} - \bar{\boldsymbol{\mathcal{M}}}_{2_x3_x,x} - \bar{\boldsymbol{\mathcal{M}}}_{2_y3_x,y} \\ &\quad + \bar{\boldsymbol{\mathcal{M}}}_{3_x3_x,xx} + \bar{\boldsymbol{\mathcal{M}}}_{3_{xy}3_x,xy} + \bar{\boldsymbol{\mathcal{M}}}_{3_y3_x,yy} \\ \hat{\mathbf{M}}_{3_{xy}} &= -\bar{\mathbf{M}}_{2_x2_y} - \bar{\mathbf{M}}_{2_y2_x} - \bar{\boldsymbol{\mathcal{M}}}_{2_x2_y} - \bar{\boldsymbol{\mathcal{M}}}_{2_y2_x} + \bar{\boldsymbol{\mathcal{M}}}_{13_{xy}} + \bar{\boldsymbol{\mathcal{M}}}_{3_{xy}1} \\ &\quad - \bar{\boldsymbol{\mathcal{M}}}_{2_x3_{xy},x} - \bar{\boldsymbol{\mathcal{M}}}_{2_y3_{xy},y} + \bar{\boldsymbol{\mathcal{M}}}_{3_x3_{xy},xx} + \bar{\boldsymbol{\mathcal{M}}}_{3_{xy}3_{xy},xy} + \bar{\boldsymbol{\mathcal{M}}}_{3_y3_{xy},yy} \\ \hat{\mathbf{M}}_{3_y} &= -\bar{\mathbf{M}}_{2_y2_y} + \bar{\boldsymbol{\mathcal{M}}}_{13_y} + \bar{\boldsymbol{\mathcal{M}}}_{3_y1} - \bar{\boldsymbol{\mathcal{M}}}_{2_y2_y} - \bar{\boldsymbol{\mathcal{M}}}_{2_x3_y,x} \\ &\quad - \bar{\boldsymbol{\mathcal{M}}}_{2_y3_y,y} + \bar{\boldsymbol{\mathcal{M}}}_{3_x3_y,xx} + \bar{\boldsymbol{\mathcal{M}}}_{3_{xy}3_y,xy} + \bar{\boldsymbol{\mathcal{M}}}_{3_y3_y,yy} \\ \hat{\mathbf{M}}_{4_1} &= \bar{\boldsymbol{\mathcal{M}}}_{3_x2_x} - \bar{\boldsymbol{\mathcal{M}}}_{2_x3_x} \\ \hat{\mathbf{M}}_{4_2} &= \bar{\boldsymbol{\mathcal{M}}}_{3_x2_y} + \bar{\boldsymbol{\mathcal{M}}}_{3_{xy}2_x} - \bar{\boldsymbol{\mathcal{M}}}_{2_x3_{xy}} - \bar{\boldsymbol{\mathcal{M}}}_{2_y3_x} \end{aligned}$$

$$
\begin{aligned}
\hat{\mathbf{M}}_{4_3} &= \bar{\boldsymbol{\mathcal{M}}}_{3_{xy}2_y} + \bar{\boldsymbol{\mathcal{M}}}_{3_y2_x} - \bar{\boldsymbol{\mathcal{M}}}_{2_x3_y} - \bar{\boldsymbol{\mathcal{M}}}_{2_y3_{xy}} \\
\hat{\mathbf{M}}_{4_4} &= \bar{\boldsymbol{\mathcal{M}}}_{3_y2_y} - \bar{\boldsymbol{\mathcal{M}}}_{2_y3_y} \\
\hat{\mathbf{M}}_{5_1} &= \bar{\boldsymbol{\mathcal{M}}}_{3_x3_x} \\
\hat{\mathbf{M}}_{5_2} &= \bar{\boldsymbol{\mathcal{M}}}_{3_x3_{xy}} + \bar{\boldsymbol{\mathcal{M}}}_{3_{xy}3_x} \\
\hat{\mathbf{M}}_{5_3} &= \bar{\boldsymbol{\mathcal{M}}}_{3_x3_y} + \bar{\boldsymbol{\mathcal{M}}}_{3_{xy}3_{xy}} + \bar{\boldsymbol{\mathcal{M}}}_{3_y3_x} \\
\hat{\mathbf{M}}_{5_4} &= \bar{\boldsymbol{\mathcal{M}}}_{3_{xy}3_y} + \bar{\boldsymbol{\mathcal{M}}}_{3_y3_{xy}} \\
\hat{\mathbf{M}}_{5_5} &= \bar{\boldsymbol{\mathcal{M}}}_{3_y3_y}
\end{aligned} \tag{3.55}
$$

Now we substitute the assumed solution for generalized displacement (3.53) to obtain the following algebraic equation for $(\alpha\beta)$th coefficient of the solution as following:

$$
\begin{bmatrix}
\mathbf{K}^{11}_{\alpha\beta} & \mathbf{K}^{12}_{\alpha\beta} & \mathbf{K}^{13}_{\alpha\beta} \\
\mathbf{K}^{21}_{\alpha\beta} & \mathbf{K}^{22}_{\alpha\beta} & \mathbf{K}^{23}_{\alpha\beta} \\
\mathbf{K}^{31}_{\alpha\beta} & \mathbf{K}^{32}_{\alpha\beta} & \mathbf{K}^{33}_{\alpha\beta}
\end{bmatrix}
\begin{Bmatrix}
\mathbf{U}^{\alpha\beta} \\ \mathbf{V}^{\alpha\beta} \\ \mathbf{W}^{\alpha\beta}
\end{Bmatrix}
=
\begin{Bmatrix}
\mathbf{0} \\ \mathbf{0} \\ \mathbf{q}^{\alpha\beta}_z
\end{Bmatrix} \tag{3.56}
$$

where

$$
\begin{aligned}
\mathbf{K}^{11}_{\alpha\beta} &= \hat{\mathbf{M}}^{11}_1 - (\alpha\pi/a)^2\hat{\mathbf{M}}^{11}_{3_x} - (\beta\pi/b)^2\hat{\mathbf{M}}^{11}_{3_y} \\
&\quad +(\alpha\pi/a)^4\hat{\mathbf{M}}^{11}_{5_1} + (\alpha\pi/a)^2(\beta\pi/b)^2\hat{\mathbf{M}}^{11}_{5_3} + (\beta\pi/b)^4\hat{\mathbf{M}}^{11}_{5_5} \\
\mathbf{K}^{12}_{\alpha\beta} &= -(\alpha\pi/a)(\beta\pi/b)\hat{\mathbf{M}}^{12}_{3_{xy}} + (\alpha\pi/a)^3(\beta\pi/b)\hat{\mathbf{M}}^{12}_{5_2} + (\alpha\pi/a)(\beta\pi/b)^3\hat{\mathbf{M}}^{12}_{5_4} \\
\mathbf{K}^{13}_{\alpha\beta} &= (\alpha\pi/a)\hat{\mathbf{M}}^{13}_{2_x} - (\alpha\pi/a)^3\hat{\mathbf{M}}^{13}_{4_1} - (\alpha\pi/a)(\beta\pi/b)^2\hat{\mathbf{M}}^{13}_{4_3} \\
\mathbf{K}^{21}_{\alpha\beta} &= -(\alpha\pi/a)(\beta\pi/b)\hat{\mathbf{M}}^{21}_{3_{xy}} + (\alpha\pi/a)^3(\beta\pi/b)\hat{\mathbf{M}}^{21}_{5_2} + (\alpha\pi/a)(\beta\pi/b)^3\hat{\mathbf{M}}^{21}_{5_4} \\
\mathbf{K}^{22}_{\alpha\beta} &= \hat{\mathbf{M}}^{22}_1 - (\alpha\pi/a)^2\hat{\mathbf{M}}^{22}_{3_x} - (\beta\pi/b)^2\hat{\mathbf{M}}^{22}_{3_y} \\
&\quad +(\alpha\pi/a)^4\hat{\mathbf{M}}^{22}_{5_1} + (\alpha\pi/a)^2(\beta\pi/b)^2\hat{\mathbf{M}}^{22}_{5_3} + (\beta\pi/b)^4\hat{\mathbf{M}}^{22}_{5_5} \\
\mathbf{K}^{23}_{\alpha\beta} &= (\beta\pi/b)\hat{\mathbf{M}}^{23}_{2_y} - (\alpha\pi/a)^2(\beta\pi/b)\hat{\mathbf{M}}^{23}_{4_2} - (\beta\pi/b)^3\hat{\mathbf{M}}^{23}_{4_4} \\
\mathbf{K}^{31}_{\alpha\beta} &= -(\alpha\pi/a)\hat{\mathbf{M}}^{31}_{2_x} + (\alpha\pi/a)^3\hat{\mathbf{M}}^{31}_{4_1} + (\alpha\pi/a)(\beta\pi/b)^2\hat{\mathbf{M}}^{31}_{4_3} \\
\mathbf{K}^{32}_{\alpha\beta} &= -(\beta\pi/b)\hat{\mathbf{M}}^{32}_{2_y} + (\alpha\pi/a)^2(\beta\pi/b)\hat{\mathbf{M}}^{32}_{4_2} + (\beta\pi/b)^3\hat{\mathbf{M}}^{32}_{4_4} \\
\mathbf{K}^{33}_{\alpha\beta} &= \hat{\mathbf{M}}^{33}_1 - (\alpha\pi/a)^2\hat{\mathbf{M}}^{33}_{3_x} - (\beta\pi/b)^2\hat{\mathbf{M}}^{33}_{3_y} \\
&\quad +(\alpha\pi/a)^4\hat{\mathbf{M}}^{33}_{5_1} + (\alpha\pi/a)^2(\beta\pi/b)^2\hat{\mathbf{M}}^{33}_{5_3} + (\beta\pi/b)^4\hat{\mathbf{M}}^{33}_{5_5}
\end{aligned} \tag{3.57}
$$

The superscripts of the stress resultant coefficients (see Eq. (3.55)) in the above expression represent the same block matrices as of $\mathbf{K}_{\alpha\beta}$ in Eq. (3.56).

3.6. Specialization to plate theories

3.6.1. The general third order plate theory

For general third order plate, we take $n = 3,\ m = 3$ and $p = 2$ in the above formulation. The displacement field for a general third order plate theory can be specialised as following:

$$\begin{aligned} \mathbf{u} &= u_1\,\hat{\mathbf{e}}_1 + u_2\,\hat{\mathbf{e}}_2 + u_3\,\hat{\mathbf{e}}_3 \quad \text{where,} \\ u_1 &= u + z\phi_x^{(1)} + z^2\phi_x^{(2)} + z^3\phi_x^{(3)}, \\ u_2 &= v + z\phi_y^{(1)} + z^2\phi_y^{(2)} + z^3\phi_y^{(3)}, \\ u_3 &= w + z\phi_z^{(1)} + z^2\phi_z^{(2)} \end{aligned} \tag{3.58}$$

In the case of the general third-order plate theory, straight lines perpendicular to mid plane do not remain straight after deformation as reflected in the displacement field; hence, there is a possibility of nonzero length scale parameters for all possible rotations related to the small inclusions oriented along the x, y or z directions. Hence, these would contribute to the stiffness of the plate while considering the rotation gradient dependent potential energy along with conventional strain energy. The governing equation and the corresponding finite element model can be obtained by putting $n = 3,\ m = 3$ and $p = 2$ in the formulation presented in above sections.

3.6.2. The first order plate theory

For the first-order plate theory, we take $n = 1,\ m = 1$, and $p = 0$ in the displacement field, Eq. (3.5). In the case of the first-order plate theory, straight lines perpendicular to midplane remain straight after deformation as reflected in the specialized displacement field:

$$\begin{aligned} &\mathbf{u} = u_1\,\hat{\mathbf{e}}_1 + u_2\,\hat{\mathbf{e}}_2 + u_3\,\hat{\mathbf{e}}_3 \quad \text{where} \\ &u_1 = u + z\phi_x^{(1)} = \mathbf{A}_x\mathbf{\Phi}_x, \quad u_2 = v + z\phi_y^{(1)} = \mathbf{A}_y\mathbf{\Phi}_y, \quad u_3 = w = \mathbf{A}_z\mathbf{\Phi}_z \end{aligned} \tag{3.59}$$

where

$$\begin{aligned}
\mathbf{A}_x &= \begin{bmatrix} 1 & z \end{bmatrix}, \quad \mathbf{\Phi}_x = \begin{bmatrix} u & \phi_x^{(1)} \end{bmatrix}^T \\
\mathbf{A}_y &= \begin{bmatrix} 1 & z \end{bmatrix}, \quad \mathbf{\Phi}_y = \begin{bmatrix} v & \phi_y^{(1)} \end{bmatrix}^T \\
\mathbf{A}_z &= \begin{bmatrix} 1 \end{bmatrix}, \qquad \mathbf{\Phi}_z = \begin{bmatrix} w \end{bmatrix}
\end{aligned} \tag{3.60}$$

In the case of moderate rotation, the nonzero components of the von Kármán strain tensor are:

$$\begin{aligned}
\varepsilon_{xx} &= u_{1,x} + (1/2)\left(w_{,x}\right)^2 = \mathbf{A}_x \mathbf{\Phi}_{x,x} + (1/2)\left(w_{,x}\right)^2 \\
\varepsilon_{yy} &= u_{2,y} + (1/2)\left(w_{,y}\right)^2 = \mathbf{A}_y \mathbf{\Phi}_{y,y} + (1/2)\left(w_{,y}\right)^2 \\
\gamma_{yz} &= u_{2,z} + u_{3,y} = \mathbf{A}_{y,z} \mathbf{\Phi}_y + \mathbf{A}_z \mathbf{\Phi}_{z,y} \\
\gamma_{zx} &= u_{1,z} + u_{3,x} = \mathbf{A}_{x,z} \mathbf{\Phi}_x + \mathbf{A}_z \mathbf{\Phi}_{z,x} \\
\gamma_{xy} &= u_{1,y} + u_{2,x} = \mathbf{A}_x \mathbf{\Phi}_{x,y} + \mathbf{A}_y \mathbf{\Phi}_{y,x} + w_{,x} w_{,y}
\end{aligned} \tag{3.61}$$

These strain components can be written in vector form as

$$\boldsymbol{\varepsilon} = \mathbf{A}_1 \mathbf{\Phi} + \mathbf{A}_{2_x} \mathbf{\Phi}_{,x} + \mathbf{A}_{2_y} \mathbf{\Phi}_{,y} + \frac{1}{2} \mathbf{A}_{nl_x} \mathbf{\Phi}_{,x} + \frac{1}{2} \mathbf{A}_{nl_y} \mathbf{\Phi}_{,y} \tag{3.62}$$

where

$$\boldsymbol{\varepsilon} = \begin{bmatrix} \varepsilon_{xx} & \varepsilon_{yy} & \gamma_{yz} & \gamma_{zx} & \gamma_{xy} \end{bmatrix}^T, \quad \mathbf{\Phi} = \begin{bmatrix} \mathbf{\Phi}_x^T & \mathbf{\Phi}_y^T & \mathbf{\Phi}_z^T \end{bmatrix}^T$$

$$\mathbf{A}_1 = \begin{bmatrix} \mathbf{0} & \mathbf{0} & \mathbf{0} \\ \mathbf{0} & \mathbf{0} & \mathbf{0} \\ \mathbf{0} & \mathbf{A}_{y,z} & \mathbf{0} \\ \mathbf{A}_{x,z} & \mathbf{0} & \mathbf{0} \\ \mathbf{0} & \mathbf{0} & \mathbf{0} \end{bmatrix}, \quad \mathbf{A}_{2_x} = \begin{bmatrix} \mathbf{A}_x & \mathbf{0} & \mathbf{0} \\ \mathbf{0} & \mathbf{0} & \mathbf{0} \\ \mathbf{0} & \mathbf{0} & \mathbf{0} \\ \mathbf{0} & \mathbf{0} & \mathbf{A}_z \\ \mathbf{0} & \mathbf{A}_y & \mathbf{0} \end{bmatrix}, \quad \mathbf{A}_{2_y} = \begin{bmatrix} \mathbf{0} & \mathbf{0} & \mathbf{0} \\ \mathbf{0} & \mathbf{A}_y & \mathbf{0} \\ \mathbf{0} & \mathbf{0} & \mathbf{A}_z \\ \mathbf{0} & \mathbf{0} & \mathbf{0} \\ \mathbf{A}_x & \mathbf{0} & \mathbf{0} \end{bmatrix}$$

$$\mathbf{A}_{nl_x} = \begin{bmatrix} \mathbf{0} & \mathbf{0} & \mathbf{a}_{nl_x} \\ \mathbf{0} & \mathbf{0} & \mathbf{0} \\ \mathbf{0} & \mathbf{0} & \mathbf{0} \\ \mathbf{0} & \mathbf{0} & \mathbf{0} \\ \mathbf{0} & \mathbf{0} & \mathbf{a}_{nl_y} \end{bmatrix}, \quad \mathbf{A}_{nl_y} = \begin{bmatrix} \mathbf{0} & \mathbf{0} & \mathbf{0} \\ \mathbf{0} & \mathbf{0} & \mathbf{a}_{nl_y} \\ \mathbf{0} & \mathbf{0} & \mathbf{0} \\ \mathbf{0} & \mathbf{0} & \mathbf{0} \\ \mathbf{0} & \mathbf{0} & \mathbf{a}_{nl_x} \end{bmatrix} \tag{3.63}$$

$\mathbf{W}$ and the $\mathbf{\Omega}$ (see Eq. (3.3) for definition) can be given as following:

$$\begin{aligned} \mathbf{W} &= \begin{bmatrix} 0 & -\omega_z & \omega_y \\ \omega_z & 0 & -\omega_x \\ -\omega_y & \omega_x & 0 \end{bmatrix}, \quad \begin{aligned} \omega_x &= (1/2)\left(u_{3,y} - u_{2,z}\right) = (1/2)\left(\mathbf{A}_z\mathbf{\Phi}_{z,y} - \mathbf{A}_{y,z}\mathbf{\Phi}_y\right) \\ \omega_y &= (1/2)\left(u_{1,z} - u_{3,x}\right) = (1/2)\left(\mathbf{A}_{x,z}\mathbf{\Phi}_x - \mathbf{A}_z\mathbf{\Phi}_{z,x}\right) \\ \omega_z &= (1/2)\left(u_{2,x} - u_{1,y}\right) = (1/2)\left(\mathbf{A}_y\mathbf{\Phi}_{y,x} - \mathbf{A}_x\mathbf{\Phi}_{x,y}\right) \end{aligned} \\ \mathbf{\Omega} &= \Omega_{\alpha\beta\gamma}\hat{\mathbf{e}}_\alpha\hat{\mathbf{e}}_\beta\hat{\mathbf{e}}_\gamma = \frac{\partial W_{\beta\gamma}}{\partial x_\alpha}\hat{\mathbf{e}}_\alpha\hat{\mathbf{e}}_\beta\hat{\mathbf{e}}_\gamma \end{aligned} \tag{3.64}$$

The unique nonzero components of $\mathbf{\Omega}$ are

$$\begin{aligned} 2\omega_{x,x} &= \mathbf{A}_z\mathbf{\Phi}_{z,xy} - \mathbf{A}_{y,z}\mathbf{\Phi}_{y,x}, \quad 2\omega_{x,y} = \mathbf{A}_z\mathbf{\Phi}_{z,yy} - \mathbf{A}_{y,z}\mathbf{\Phi}_{y,y} \\ 2\omega_{y,x} &= \mathbf{A}_{x,z}\mathbf{\Phi}_{x,x} - \mathbf{A}_z\mathbf{\Phi}_{z,xx}, \quad 2\omega_{y,y} = \mathbf{A}_{x,z}\mathbf{\Phi}_{x,y} - \mathbf{A}_z\mathbf{\Phi}_{z,xy} \\ 2\omega_{z,x} &= \mathbf{A}_y\mathbf{\Phi}_{y,xx} - \mathbf{A}_x\mathbf{\Phi}_{x,xy}, \quad 2\omega_{z,y} = \mathbf{A}_y\mathbf{\Phi}_{y,xy} - \mathbf{A}_x\mathbf{\Phi}_{x,yy} \\ 2\omega_{z,z} &= \mathbf{A}_{y,z}\mathbf{\Phi}_{y,x} - \mathbf{A}_{x,z}\mathbf{\Phi}_{x,y} \end{aligned} \tag{3.65}$$

Now let us also write the nonzero components of $\mathbf{\Omega}$ as following vector:

$$\begin{aligned} \boldsymbol{\chi} &= \begin{bmatrix} 2\omega_{x,x} & 2\omega_{x,y} & 2\omega_{y,x} & 2\omega_{y,y} & 2\omega_{z,x} & 2\omega_{z,y} & 2\omega_{z,z} \end{bmatrix}^T \\ &= \mathbf{B}_{2_x}\mathbf{\Phi}_{,x} + \mathbf{B}_{2_y}\mathbf{\Phi}_{,y} + \mathbf{B}_{3_x}\mathbf{\Phi}_{,xx} + \mathbf{B}_{3_{xy}}\mathbf{\Phi}_{,xy} + \mathbf{B}_{3_y}\mathbf{\Phi}_{,yy} \end{aligned} \tag{3.66}$$

where

$$\mathbf{B}_{2_x} = \begin{bmatrix} \mathbf{0} & -\mathbf{A}_{y,z} & \mathbf{0} \\ \mathbf{0} & \mathbf{0} & \mathbf{0} \\ \mathbf{A}_{x,z} & \mathbf{0} & \mathbf{0} \\ \mathbf{0} & \mathbf{0} & \mathbf{0} \\ \mathbf{0} & \mathbf{0} & \mathbf{0} \\ \mathbf{0} & \mathbf{0} & \mathbf{0} \\ \mathbf{0} & \mathbf{A}_{y,z} & \mathbf{0} \end{bmatrix}, \; \mathbf{B}_{2_y} = \begin{bmatrix} \mathbf{0} & \mathbf{0} & \mathbf{0} \\ \mathbf{0} & -\mathbf{A}_{y,z} & \mathbf{0} \\ \mathbf{0} & \mathbf{0} & \mathbf{0} \\ \mathbf{A}_{x,z} & \mathbf{0} & \mathbf{0} \\ \mathbf{0} & \mathbf{0} & \mathbf{0} \\ \mathbf{0} & \mathbf{0} & \mathbf{0} \\ -\mathbf{A}_{x,z} & \mathbf{0} & \mathbf{0} \end{bmatrix}$$

$$\mathbf{B}_{3_x} = \begin{bmatrix} \mathbf{0} & \mathbf{0} & \mathbf{0} \\ \mathbf{0} & \mathbf{0} & \mathbf{0} \\ \mathbf{0} & \mathbf{0} & -\mathbf{A}_z \\ \mathbf{0} & \mathbf{0} & \mathbf{0} \\ \mathbf{0} & \mathbf{A}_y & \mathbf{0} \\ \mathbf{0} & \mathbf{0} & \mathbf{0} \\ \mathbf{0} & \mathbf{0} & \mathbf{0} \end{bmatrix}, \ \mathbf{B}_{3_{xy}} = \begin{bmatrix} \mathbf{0} & \mathbf{0} & \mathbf{A}_z \\ \mathbf{0} & \mathbf{0} & \mathbf{0} \\ \mathbf{0} & \mathbf{0} & \mathbf{0} \\ \mathbf{0} & \mathbf{0} & -\mathbf{A}_z \\ -\mathbf{A}_x & \mathbf{0} & \mathbf{0} \\ \mathbf{0} & \mathbf{A}_y & \mathbf{0} \\ \mathbf{0} & \mathbf{0} & \mathbf{0} \end{bmatrix}, \ \mathbf{B}_{3_y} = \begin{bmatrix} \mathbf{0} & \mathbf{0} & \mathbf{0} \\ \mathbf{0} & \mathbf{0} & \mathbf{A}_z \\ \mathbf{0} & \mathbf{0} & \mathbf{0} \\ \mathbf{0} & \mathbf{0} & \mathbf{0} \\ \mathbf{0} & \mathbf{0} & \mathbf{0} \\ -\mathbf{A}_x & \mathbf{0} & \mathbf{0} \\ \mathbf{0} & \mathbf{0} & \mathbf{0} \end{bmatrix} \tag{3.67}$$

The relation between the symmetric part of stress and strain tensors for the isotropic material can be written as,

$$\mathbf{S}^s = \mathbf{C}\boldsymbol{\varepsilon} \tag{3.68}$$

where

$$\begin{aligned} \mathbf{C} &= \frac{E(z)(1-\nu)}{(1+\nu)(1-2\nu)} \begin{bmatrix} 1 & \frac{\nu}{1-\nu} & 0 & 0 & 0 \\ \frac{\nu}{1-\nu} & 1 & 0 & 0 & 0 \\ 0 & 0 & K_s\frac{1-2\nu}{2(1-\nu)} & 0 & 0 \\ 0 & 0 & 0 & K_s\frac{1-2\nu}{2(1-\nu)} & 0 \\ 0 & 0 & 0 & 0 & \frac{1-2\nu}{2(1-\nu)} \end{bmatrix} \\ \boldsymbol{\varepsilon} &= \begin{bmatrix} \varepsilon_{xx} & \varepsilon_{yy} & \gamma_{yz} & \gamma_{zx} & \gamma_{xy} \end{bmatrix}^T \\ \mathbf{S}^s &= \begin{bmatrix} S^s_{xx} & S^s_{yy} & S^s_{yz} & S^s_{zx} & S^s_{xy} \end{bmatrix}^T \end{aligned} \tag{3.69}$$

and K_s is the shear correction factor. Further, the relation between $\boldsymbol{\chi}$ and its energy conjugate, $\mathbf{m}$ (couple stress), can be given as:

$$\mathbf{m} = \mathbf{C}_l\boldsymbol{\chi}. \tag{3.70}$$

In this study, we will consider the material constant $\mathbf{C}_l$ as diagonal matrix and the components can be given as,

$$\mathbf{C}_{l_{ii}} = G(z)\ell_i^2, \qquad \text{(no sum on repeated index)}. \tag{3.71}$$

With the above definition of strain and rotation gradient term along with the constitutive relation, the governing equation, boundary variables are the same as Eq. (3.26)

and (3.27), respectively, with $\boldsymbol{\mathcal{M}}_1 = 0$ and $\hat{\mathbf{F}}$ defined as:

$$\hat{\mathbf{F}} = \begin{bmatrix} f_u & 0 & f_v & 0 & f_w \end{bmatrix}^T \tag{3.72}$$

where f_u, f_v, and f_w are the forces acting per unit area of the plate in x, y, and z directions, respectively. The nonlinear finite element formulation also would have same form as described in section 3.4 with $\mathbf{A}_{nl} = \mathbf{0}$ and consequently $\mathbf{P}_{nl} = \mathbf{0}$ in the definition of tangent matrix. The linear analytical solution described in section 3.5 can also be specialized for the first-order plate theory by taking $\mathbf{B}_1 = \mathbf{0}$.

3.6.3. The classical plate theory

3.6.3.1. The governing equation

For the classical plate theory, we take $n = 1,\ m = 1$ and $p = 0$ in the displacement field of Eq. (3.5) but with the constraint, $\phi_x^{(1)} = -w_{,x}$ and $\phi_y^{(1)} = -w_{,y}$. Hence the displacement field becomes

$$\mathbf{u} = (u(x,y) - zw_{,x})\,\hat{\mathbf{e}}_1 + (v(x,y) - zw_{,y})\,\hat{\mathbf{e}}_2 + w(x,y)\,\hat{\mathbf{e}}_3. \tag{3.73}$$

The nonzero components of von Kármán strain can be given as following:

$$\begin{aligned} \varepsilon_{xx} &= u_{,x} - zw_{,xx} + (1/2)\,(w_{,x})^2 \\ \varepsilon_{yy} &= v_{,y} - zw_{,yy} + (1/2)\,(w_{,y})^2 \\ \gamma_{xy} &= (u_{,y} + v_{,x}) - 2zw_{,xy} + w_{,x}w_{,y} \end{aligned} \tag{3.74}$$

Let $\boldsymbol{\Phi} = [u \quad v \quad w]^T$ and $\boldsymbol{\varepsilon} = [\varepsilon_{xx} \quad \varepsilon_{yy} \quad \gamma_{xy}]^T$. Then Eq. (3.74) can be rewritten as following:

$$\begin{aligned} \boldsymbol{\varepsilon} = {} & (\mathbf{A}_{2_x} + (1/2)\mathbf{A}_{nl_x})\boldsymbol{\Phi}_{,x} + (\mathbf{A}_{2_y} + (1/2)\mathbf{A}_{nl_y})\boldsymbol{\Phi}_{,y} \\ & + \mathbf{A}_{3_x}\boldsymbol{\Phi}_{,xx} + 2\mathbf{A}_{3_{xy}}\boldsymbol{\Phi}_{,xy} + \mathbf{A}_{3_y}\boldsymbol{\Phi}_{,yy} \end{aligned} \tag{3.75}$$

where

$$\mathbf{A}_{2_x} = \begin{bmatrix} 1 & 0 & 0 \\ 0 & 0 & 0 \\ 0 & 1 & 0 \end{bmatrix},\ \mathbf{A}_{2_y} = \begin{bmatrix} 0 & 0 & 0 \\ 0 & 1 & 0 \\ 1 & 0 & 0 \end{bmatrix},\ \mathbf{A}_{nl_x} = \begin{bmatrix} 0 & 0 & w_{,x} \\ 0 & 0 & 0 \\ 0 & 0 & w_{,y} \end{bmatrix},\ \mathbf{A}_{nl_y} = \begin{bmatrix} 0 & 0 & 0 \\ 0 & 0 & w_{,y} \\ 0 & 0 & w_{,x} \end{bmatrix}$$

$$\mathbf{A}_{3_x} = \begin{bmatrix} 0 & 0 & -z \\ 0 & 0 & 0 \\ 0 & 0 & 0 \end{bmatrix}, \quad \mathbf{A}_{3_{xy}} = \begin{bmatrix} 0 & 0 & 0 \\ 0 & 0 & 0 \\ 0 & 0 & -z \end{bmatrix}, \quad \mathbf{A}_{3_y} = \begin{bmatrix} 0 & 0 & 0 \\ 0 & 0 & -z \\ 0 & 0 & 0 \end{bmatrix}, \tag{3.76}$$

$\mathbf{W}$ and the $\mathbf{\Omega}$ can be given as following,

$$\begin{aligned} \mathbf{W} &= \begin{bmatrix} 0 & -\omega_z & \omega_y \\ \omega_z & 0 & -\omega_x \\ -\omega_y & \omega_x & 0 \end{bmatrix}, \qquad \begin{aligned} \omega_x &= (1/2)\left(u_{3,y} - u_{2,z}\right) = w_{,y} \\ \omega_y &= (1/2)\left(u_{1,z} - u_{3,x}\right) = -w_{,x} \\ \omega_z &= (1/2)\left(u_{2,x} - u_{1,y}\right) = (1/2)(v_{,x} - u_{,y}) \end{aligned} \\ \mathbf{\Omega} &= \Omega_{\alpha\beta\gamma}\hat{\mathbf{e}}_\alpha\hat{\mathbf{e}}_\beta\hat{\mathbf{e}}_\gamma = \frac{\partial W_{\beta\gamma}}{\partial x_\alpha}\hat{\mathbf{e}}_\alpha\hat{\mathbf{e}}_\beta\hat{\mathbf{e}}_\gamma \end{aligned} \tag{3.77}$$

The unique nonzero components of $\mathbf{\Omega}$ are

$$\begin{aligned} &2\omega_{x,x} = 2w_{,xy}, && 2\omega_{x,y} = 2w_{,yy} \\ &2\omega_{y,x} = -2w_{,xx}, && 2\omega_{y,y} = -2w_{,xy} \\ &2\omega_{z,x} = v_{,xx} - u_{,xy}, && 2\omega_{z,y} = v_{,xy} - u_{,yy} \end{aligned} \tag{3.78}$$

which can also be arranged in vector form as following:

$$\begin{aligned} \boldsymbol{\chi} &= \begin{bmatrix} 2\omega_{x,x} & 2\omega_{x,y} & 2\omega_{y,x} & 2\omega_{y,y} & 2\omega_{z,x} & 2\omega_{z,y} \end{bmatrix}^T \\ &= \mathbf{B}_{3_x}\mathbf{\Phi}_{,xx} + 2\mathbf{B}_{3_{xy}}\mathbf{\Phi}_{,xy} + \mathbf{B}_{3_y}\mathbf{\Phi}_{,yy} \end{aligned} \tag{3.79}$$

where

$$\mathbf{B}_{3_x} = \begin{bmatrix} 0 & 0 & 0 \\ 0 & 0 & 0 \\ 0 & 0 & -2 \\ 0 & 0 & 0 \\ 0 & 1 & 0 \\ 0 & 0 & 0 \end{bmatrix}, \quad \mathbf{B}_{3_{xy}} = \begin{bmatrix} 0 & 0 & 1 \\ 0 & 0 & 0 \\ 0 & 0 & 0 \\ 0 & 0 & -1 \\ -0.5 & 0 & 0 \\ 0 & 0.5 & 0 \end{bmatrix}, \quad \mathbf{B}_{3_y} = \begin{bmatrix} 0 & 0 & 0 \\ 0 & 0 & 2 \\ 0 & 0 & 0 \\ 0 & 0 & 0 \\ 0 & 0 & 0 \\ -1 & 0 & 0 \end{bmatrix}. \tag{3.80}$$

We will apply the plane stress condition because the stresses in the z-direction are very small. Hence, the constitutive relation between symmetric part of the stress

and the strain are

$$\mathbf{S}^s = \mathbf{C}\boldsymbol{\varepsilon} \tag{3.81}$$

where

$$\mathbf{C} = \frac{E(z)}{1-\nu^2}\begin{bmatrix} 1 & \nu & 0 \\ \nu & 1 & 0 \\ 0 & 0 & \frac{(1-\nu)}{2} \end{bmatrix}, \quad \mathbf{S}^s = \begin{Bmatrix} S^s_{xx} \\ S^s_{yy} \\ S^s_{xy} \end{Bmatrix} \tag{3.82}$$

The relation between $\boldsymbol{\chi}$ and its energy conjugate $\mathbf{m}$ (couple stress) is considered same as Eqs. (3.70) and (3.71). In the case of CPT and FOPT, the material length scale parameters (ℓ_{11} and ℓ_{44}) which correspond to $\omega_{x,x}$ and $\omega_{y,y}$ are related to the twist of the embedded inclusions oriented along the x and y directions, respectively. Similarly, ℓ_{22} and ℓ_{33}, which correspond to $\omega_{x,y}$ and $\omega_{y,x}$, are related to out of plane curvature of embedded inclusions oriented along x and y directions, respectively. The parameters ℓ_{55} and ℓ_{66} corresponds to in-plane curvature of the inclusions or microstructures. We obtain the equation of equilibrium from the principle of virtual displacement as

$$\begin{aligned} \hat{\mathbf{F}} = & -\left(\mathbf{M}_{nl_x} + \mathbf{M}_{2_x}\right)_{,x} - \left(\mathbf{M}_{nl_y} + \mathbf{M}_{2_y}\right)_{,y} \\ & + (\mathbf{M}_{3_x} + \boldsymbol{\mathcal{M}}_{3_x})_{,xx} + 2(\mathbf{M}_{3_{xy}} + \boldsymbol{\mathcal{M}}_{3_{xy}})_{,xy} + (\mathbf{M}_{3_{yy}} + \boldsymbol{\mathcal{M}}_{3_{yy}})_{,yy} \end{aligned} \tag{3.83}$$

where

$$\begin{aligned} &\mathbf{M}_{2_j} = \int_{-h/2}^{h/2} \mathbf{A}_{2_j}^T \mathbf{S}^s \, dz, \quad \mathbf{M}_{nl_j} = \int_{-h/2}^{h/2} \mathbf{A}_{nl_j}^T \mathbf{S}^s \, dz \, dz \quad \text{for } j = x, y \\ &\mathbf{M}_{3_{xx}} = \int_{-h/2}^{h/2} \mathbf{A}_{3_x}^T \mathbf{S}^s \, dz, \quad \mathbf{M}_{3_{xy}} = \int_{-h/2}^{h/2} \mathbf{A}_{3_{xy}}^T \mathbf{S}^s \, dz, \quad \mathbf{M}_{3_{yy}} = \int_{-h/2}^{h/2} \mathbf{A}_{3_y}^T \mathbf{S}^s \, dz \\ &\boldsymbol{\mathcal{M}}_{3_{xx}} = \int_{-h/2}^{h/2} \mathbf{B}_{3_x}^T \mathbf{m} \, dz, \quad \boldsymbol{\mathcal{M}}_{3_{xy}} = \int_{-h/2}^{h/2} \mathbf{B}_{3_{xy}}^T \mathbf{m} \, dz, \quad \boldsymbol{\mathcal{M}}_{3_{yy}} = \int_{-h/2}^{h/2} \mathbf{B}_{3_y}^T \mathbf{m} \, dz \\ &\hat{\mathbf{F}} = [f_x \quad f_y \quad f_z]^T \end{aligned} \tag{3.84}$$

where f_x, f_y, and f_z are the forces per unit area of the plate in the x, y, and z directions, respectively. The boundary conditions are:

$$\begin{aligned} \mathbf{\Phi} &: \mathbf{P} \\ \mathbf{\Phi}_{,n} &: ((\boldsymbol{\mathcal{M}}_{3_x} + \mathbf{M}_{3_x})n_x^2 + 2(\boldsymbol{\mathcal{M}}_{3_{xy}} + \mathbf{M}_{3_{xy}})n_x n_y + (\boldsymbol{\mathcal{M}}_{3_y} + \mathbf{M}_{3_y})n_y^2) \end{aligned} \tag{3.85}$$

where

$$\begin{aligned} \mathbf{P} = & \left(\mathbf{M}_{nl_x} + \mathbf{M}_{2_x} - (\boldsymbol{\mathcal{M}}_{3_x} + \mathbf{M}_{3_x})_{,x} - (\boldsymbol{\mathcal{M}}_{3_{xy}} + \mathbf{M}_{3_{xy}})_{,y}\right) n_x \\ & + \left(\mathbf{M}_{nl_y} + \mathbf{M}_{2_y} - (\boldsymbol{\mathcal{M}}_{3_y} + \mathbf{M}_{3_y})_{,y} - (\boldsymbol{\mathcal{M}}_{3_{xy}} + \mathbf{M}_{3_{xy}})_{,x}\right) n_y \\ & -((\boldsymbol{\mathcal{M}}_{3_y} + \mathbf{M}_{3_y} - \boldsymbol{\mathcal{M}}_{3_x} - \mathbf{M}_{3_x})n_x n_y + (\boldsymbol{\mathcal{M}}_{3_{xy}} + \mathbf{M}_{3_{xy}})(n_x^2 - n_y^2))_{,s}] \end{aligned} \tag{3.86}$$

3.6.3.2. Finite element model

We approximate the displacement field given in Eqs. (3.36), (3.37),(3.38) to obtain the nonlinear finite element equation as in Eq. (3.40), with the following definitions of stiffness matrix and force vector:

$$\begin{aligned} \mathbf{K} = & \int_{\Omega^e} \Big[\mathbf{\Psi}_{,x}^T \Big(\mathbf{H}_{2_x}^1 \mathbf{\Psi}_{,x} + \mathbf{H}_{2_y}^1 \mathbf{\Psi}_{,y} + \frac{1}{2}\mathbf{H}_{nl_x}^1 \mathbf{\Psi}_{,x} + \frac{1}{2}\mathbf{H}_{nl_y}^1 \mathbf{\Psi}_{,y} \\ & \qquad + \mathbf{H}_{3_x}^1 \mathbf{\Psi}_{,xx} + 2\mathbf{H}_{3_{xy}}^1 \mathbf{\Psi}_{,xy} + \mathbf{H}_{3_y}^1 \mathbf{\Psi}_{,yy} \Big) \\ & + \mathbf{\Psi}_{,y}^T \Big(\mathbf{H}_{2_x}^2 \mathbf{\Psi}_{,x} + \mathbf{H}_{2_y}^2 \mathbf{\Psi}_{,y} + \frac{1}{2}\mathbf{H}_{nl_x}^2 \mathbf{\Psi}_{,x} + \frac{1}{2}\mathbf{H}_{nl_y}^2 \mathbf{\Psi}_{,y} \\ & \qquad + \mathbf{H}_{3_x}^2 \mathbf{\Psi}_{,xx} + 2\mathbf{H}_{3_{xy}}^2 \mathbf{\Psi}_{,xy} + \mathbf{H}_{3_y}^2 \mathbf{\Psi}_{,yy} \Big) \\ & + \mathbf{\Psi}_{,xx}^T \Big(\mathbf{G}_{2_x}^1 \mathbf{\Psi}_{,x} + \mathbf{G}_{2_y}^1 \mathbf{\Psi}_{,y} + \frac{1}{2}\mathbf{G}_{nl_x}^1 \mathbf{\Psi}_{,x} + \frac{1}{2}\mathbf{G}_{nl_y}^1 \mathbf{\Psi}_{,y} \\ & \qquad + \mathbf{G}_{3_x}^1 \mathbf{\Psi}_{,xx} + 2\mathbf{G}_{3_{xy}}^1 \mathbf{\Psi}_{,xy} + \mathbf{G}_{3_y}^1 \mathbf{\Psi}_{,yy} \Big) \\ & + 2\mathbf{\Psi}_{,xy}^T \Big(\mathbf{G}_{2_x}^2 \mathbf{\Psi}_{,x} + \mathbf{G}_{2_y}^2 \mathbf{\Psi}_{,y} + \frac{1}{2}\mathbf{G}_{nl_x}^2 \mathbf{\Psi}_{,x} + \frac{1}{2}\mathbf{G}_{nl_y}^2 \mathbf{\Psi}_{,y} \\ & \qquad + \mathbf{G}_{3_x}^2 \mathbf{\Psi}_{,xx} + 2\mathbf{G}_{3_{xy}}^2 \mathbf{\Psi}_{,xy} + \mathbf{G}_{3_y}^2 \mathbf{\Psi}_{,yy} \Big) \\ & + \mathbf{\Psi}_{,yy}^T \Big(\mathbf{G}_{2_x}^3 \mathbf{\Psi}_{,x} + \mathbf{G}_{2_y}^3 \mathbf{\Psi}_{,y} + \frac{1}{2}\mathbf{G}_{nl_x}^3 \mathbf{\Psi}_{,x} + \frac{1}{2}\mathbf{G}_{nl_y}^3 \mathbf{\Psi}_{,y} \\ & \qquad + \mathbf{G}_{3_x}^3 \mathbf{\Psi}_{,xx} + 2\mathbf{G}_{3_{xy}}^3 \mathbf{\Psi}_{,xy} + \mathbf{G}_{3_y}^3 \mathbf{\Psi}_{,yy} \Big) \Big] \, dx \, dy \\ \mathbf{K}_l = & \int_{\Omega^e} \Big[\mathbf{\Psi}_{,xx}^T \Big(\mathbf{N}_{3_x}^1 \mathbf{\Psi}_{,xx} + 2\mathbf{N}_{3_{xy}}^1 \mathbf{\Psi}_{,xy} + \mathbf{N}_{3_y}^1 \mathbf{\Psi}_{,yy} \Big) \\ & + \mathbf{\Psi}_{,xy}^T \Big(2\mathbf{N}_{3_x}^2 \mathbf{\Psi}_{,xx} + 4\mathbf{N}_{3_{xy}}^2 \mathbf{\Psi}_{,xy} + 2\mathbf{N}_{3_y}^2 \mathbf{\Psi}_{,yy} \Big) \end{aligned}$$

$$+\boldsymbol{\Psi}_{,yy}^T\Big(\mathbf{N}_{3_x}^3\boldsymbol{\Psi}_{,xx}+2\mathbf{N}_{3_{xy}}^3\boldsymbol{\Psi}_{,xy}+\mathbf{N}_{3_y}^3\boldsymbol{\Psi}_{,yy}\Big)\Big]\,dx\,dy$$

$$\mathbf{f} = \int_{\Omega^e}\boldsymbol{\Psi}^T\hat{\mathbf{F}}\,dx\,dy \tag{3.87}$$

where

$$\mathbf{H}_j^1=\int_{-h/2}^{h/2}(\mathbf{A}_{nl_x}^T+\mathbf{A}_{2_x}^T)\mathbf{C}\mathbf{A}_j\,dz$$

$$\mathbf{H}_j^2=\int_{-h/2}^{h/2}(\mathbf{A}_{nl_y}^T+\mathbf{A}_{2_y}^T)\mathbf{C}\mathbf{A}_j\,dz,\quad \text{where } j=2_x,2_y,nl_x,nl_y,3_x,3_{xy},3_y$$

$$\mathbf{G}_i^1=\int_{-h/2}^{h/2}\mathbf{A}_{3_x}^T\mathbf{C}\mathbf{A}_i\,dz,\quad \mathbf{G}_i^2=\int_{-h/2}^{h/2}\mathbf{A}_{3_{xy}}^T\mathbf{C}\mathbf{A}_i\,dz,\quad \mathbf{G}_i^3=\int_{-h/2}^{h/2}\mathbf{A}_{3_y}^T\mathbf{C}\mathbf{A}_i\,dz,$$
$$\text{where } j=2_x,2_y,nl_x,nl_y,3_x,3_{xy},3_y.$$

$$\mathbf{N}_i^1=\int_{-h/2}^{h/2}\mathbf{B}_{3_x}^T\mathbf{C}_l\mathbf{B}_i\,dz,\quad \mathbf{N}_i^2=\int_{-h/2}^{h/2}\mathbf{B}_{3_{xy}}^T\mathbf{C}_l\mathbf{B}_i\,dz,\quad \mathbf{N}_i^3=\int_{-h/2}^{h/2}\mathbf{B}_{3_y}^T\mathbf{C}_l\mathbf{B}_i\,dz,$$
$$\text{where } j=3_x,3_{xy},3_y. \tag{3.88}$$

The nonlinear finite element equation can be solved by Newton's method, with the tangent matrix given by

$$\begin{aligned}\mathbf{T} = \mathbf{K}+\mathbf{K}_l+\int_{\Omega^e}\Big[\frac{1}{2}\Big(&\boldsymbol{\Psi}_{,x}^T\left(\mathbf{H}_{nl_x}^1\boldsymbol{\Psi}_{,x}+\mathbf{H}_{nl_y}^1\boldsymbol{\Psi}_{,y}\right)+\boldsymbol{\Psi}_{,y}^T\left(\mathbf{H}_{nl_x}^2\boldsymbol{\Psi}_{,x}+\mathbf{H}_{nl_y}^2\boldsymbol{\Psi}_{,y}\right)\\
&+\boldsymbol{\Psi}_{,xx}^T\left(\mathbf{G}_{nl_x}^1\boldsymbol{\Psi}_{,x}+\mathbf{G}_{nl_y}^1\boldsymbol{\Psi}_{,y}\right)+2\boldsymbol{\Psi}_{,xy}^T\left(\mathbf{G}_{nl_x}^2\boldsymbol{\Psi}_{,x}+\mathbf{G}_{nl_y}^2\boldsymbol{\Psi}_{,y}\right)\\
&+\boldsymbol{\Psi}_{,yy}^T\left(\mathbf{G}_{nl_x}^3\boldsymbol{\Psi}_{,x}+\mathbf{G}_{nl_y}^3\boldsymbol{\Psi}_{,y}\right)\Big)+\boldsymbol{\Psi}_{,x}^T\mathbf{P}_{nl}^x\boldsymbol{\Psi}_{,x}\\
&+\boldsymbol{\Psi}_{,y}^T\mathbf{P}_{nl}^y\boldsymbol{\Psi}_{,y}+\boldsymbol{\Psi}_{,x}^T\mathbf{P}_{nl}^{xy}\boldsymbol{\Psi}_{,y}+\boldsymbol{\Psi}_{,y}^T\mathbf{P}_{nl}^{xy}\boldsymbol{\Psi}_{,x}\Big]\,dx\,dy\end{aligned} \tag{3.89}$$

where $\mathbf{P}_{nl}^x$, $\mathbf{P}_{nl}^y$ and $\mathbf{P}_{nl}^{xy}$ are (3×3) matrices with following only nonzero element,

$$P_{nl_{33}}^x=\int_{-h/2}^{h/2}S_{xx}^s\,dz,\quad P_{nl_{33}}^y=\int_{-h/2}^{h/2}S_{yy}^s\,dz,\quad P_{nl_{33}}^{xy}=\int_{-h/2}^{h/2}S_{xy}^s\,dz \tag{3.90}$$

In case of classical plate theory also, we note that the tangent matrix is symmetric.

3.6.3.3. Analytical solution for simply supported linear plate

The nonlinear governing equation for classical plate theory can be linearized as follows:

$$\begin{aligned}\hat{\mathbf{F}} = &-\mathbf{M}_{2_x,x}-\mathbf{M}_{2_y,y}+(\mathbf{M}_{3_x}+\boldsymbol{\mathcal{M}}_{3_x})_{,xx}\\
&+2(\mathbf{M}_{3_{xy}}+\boldsymbol{\mathcal{M}}_{3_{xy}})_{,xy}+(\mathbf{M}_{3_y}+\boldsymbol{\mathcal{M}}_{3_y})_{,yy}\end{aligned} \tag{3.91}$$

where

$$\begin{aligned}
\mathbf{M}_{\xi} &= \bar{\mathbf{M}}_{\xi 2_x}\mathbf{\Phi}_{,x} + \bar{\mathbf{M}}_{\xi 2_y}\mathbf{\Phi}_{,y} + \bar{\mathbf{M}}_{\xi 3_x}\mathbf{\Phi}_{,xx} + 2\bar{\mathbf{M}}_{\xi 3_{xy}}\mathbf{\Phi}_{,xy} + \bar{\mathbf{M}}_{\xi 3_y}\mathbf{\Phi}_{,yy} \\
&\qquad\qquad \text{for } \xi = 2_x, 2_y, 3_x, 3_{xy}, 3_y \\
\boldsymbol{\mathcal{M}}_{\eta} &= \bar{\boldsymbol{\mathcal{M}}}_{\eta 3_x}\mathbf{\Phi}_{,xx} + 2\bar{\boldsymbol{\mathcal{M}}}_{\eta 3_{xy}}\mathbf{\Phi}_{,xy} + \bar{\boldsymbol{\mathcal{M}}}_{\eta 3_y}\mathbf{\Phi}_{,yy} \quad \text{for } \eta = 3_x, 3_{xy}, 3_y
\end{aligned} \tag{3.92}$$

and

$$\begin{aligned}
\bar{\mathbf{M}}_{\xi\gamma} &= \int_{-h/2}^{h/2} \mathbf{A}_{\xi}^{T}\mathbf{C}\mathbf{A}_{\gamma}\, dz, \quad \text{for } \xi, \gamma = 2_x, 2_y, 3_x, 3_{xy}, 3_y \\
\bar{\boldsymbol{\mathcal{M}}}_{\eta\delta} &= \int_{-h/2}^{h/2} \mathbf{B}_{\eta}^{T}\mathbf{C}_{l}\mathbf{B}_{\delta}\, dz, \quad \text{for } \eta, \delta = 3_x, 3_{xy}, 3_y
\end{aligned} \tag{3.93}$$

Further the linear equation can be expressed in terms of displacement variables as follows:

$$\begin{aligned}
\hat{\mathbf{F}} &= \hat{\mathbf{M}}_{2_x}\mathbf{\Phi}_{,x} + \hat{\mathbf{M}}_{2_y}\mathbf{\Phi}_{,y} + \hat{\mathbf{M}}_{3_x}\mathbf{\Phi}_{,xx} + \hat{\mathbf{M}}_{3_{xy}}\mathbf{\Phi}_{,xy} + \hat{\mathbf{M}}_{3_y}\mathbf{\Phi}_{,yy} \\
&\quad + \hat{\mathbf{M}}_{4_1}\mathbf{\Phi}_{,xxx} + \hat{\mathbf{M}}_{4_2}\mathbf{\Phi}_{,xxy} + \hat{\mathbf{M}}_{4_3}\mathbf{\Phi}_{,xyy} + \hat{\mathbf{M}}_{4_4}\mathbf{\Phi}_{,yyy} \\
&\quad + \hat{\mathbf{M}}_{5_1}\mathbf{\Phi}_{,xxxx} + \hat{\mathbf{M}}_{5_2}\mathbf{\Phi}_{,xxxy} + \hat{\mathbf{M}}_{5_3}\mathbf{\Phi}_{,xxyy} + \hat{\mathbf{M}}_{5_4}\mathbf{\Phi}_{,xyyy} + \hat{\mathbf{M}}_{5_5}\mathbf{\Phi}_{,yyyy}
\end{aligned} \tag{3.94}$$

where

$$\begin{aligned}
\hat{\mathbf{M}}_{2_x} &= -\bar{\mathbf{M}}_{2_x2_x,x} - \bar{\mathbf{M}}_{2_y2_x,y} + \bar{\mathbf{M}}_{3_x2_x,xx} + 2\bar{\mathbf{M}}_{3_{xy}2_x,xy} + \bar{\mathbf{M}}_{3_y2_x,yy} \\
\hat{\mathbf{M}}_{2_y} &= -\bar{\mathbf{M}}_{2_x2_y,x} - \bar{\mathbf{M}}_{2_y2_y,y} + \bar{\mathbf{M}}_{3_x2_y,xx} + 2\bar{\mathbf{M}}_{3_{xy}2_y,xy} + \bar{\mathbf{M}}_{3_y2_y,yy} \\
\hat{\mathbf{M}}_{3_x} &= -\bar{\mathbf{M}}_{2_x2_x} - \bar{\mathbf{M}}_{2_x3_x,x} - \bar{\mathbf{M}}_{2_y3_x,y} + \bar{\mathbf{M}}_{3_x3_x,xx} + \bar{\boldsymbol{\mathcal{M}}}_{3_x3_x,xx} \\
&\quad + 2\bar{\mathbf{M}}_{3_{xy}3_x,xy} + 2\bar{\boldsymbol{\mathcal{M}}}_{3_{xy}3_x,xy} + \bar{\mathbf{M}}_{3_y3_x,yy} + \bar{\boldsymbol{\mathcal{M}}}_{3_y3_x,yy} \\
\hat{\mathbf{M}}_{3_{xy}} &= -\bar{\mathbf{M}}_{2_x2_y} - \bar{\mathbf{M}}_{2_y2_x} - 2\bar{\mathbf{M}}_{2_x3_{xy},x} - 2\bar{\mathbf{M}}_{2_y3_{xy},y} + 2\bar{\mathbf{M}}_{3_x3_{xy},xx} + 2\bar{\boldsymbol{\mathcal{M}}}_{3_x3_{xy},xx} \\
&\quad + 4\bar{\mathbf{M}}_{3_{xy}3_{xy},xy} + 4\bar{\boldsymbol{\mathcal{M}}}_{3_{xy}3_{xy},xy} + 2\bar{\mathbf{M}}_{3_y3_{xy},yy} + 2\bar{\boldsymbol{\mathcal{M}}}_{3_y3_{xy},yy} \\
\hat{\mathbf{M}}_{3_y} &= -\bar{\mathbf{M}}_{2_y2_y} - \bar{\mathbf{M}}_{2_x3_y,x} - \bar{\mathbf{M}}_{2_y3_y,y} + \bar{\mathbf{M}}_{3_x3_y,xx} + \bar{\boldsymbol{\mathcal{M}}}_{3_x3_y,xx} \\
&\quad + 2\bar{\mathbf{M}}_{3_{xy}3_y,xy} + 2\bar{\boldsymbol{\mathcal{M}}}_{3_{xy}3_y,xy} + \bar{\mathbf{M}}_{3_y3_y,yy} + \bar{\boldsymbol{\mathcal{M}}}_{3_y3_y,yy} \\
\hat{\mathbf{M}}_{4_1} &= -\bar{\mathbf{M}}_{2_x3_x} + \bar{\mathbf{M}}_{3_x2_x} \\
\hat{\mathbf{M}}_{4_2} &= -2\bar{\mathbf{M}}_{2_x3_{xy}} - \bar{\mathbf{M}}_{2_y3_x} + \bar{\mathbf{M}}_{3_x2_y} + 2\bar{\mathbf{M}}_{3_{xy}2_x} \\
\hat{\mathbf{M}}_{4_3} &= -\bar{\mathbf{M}}_{2_x3_y} - 2\bar{\mathbf{M}}_{2_y3_{xy}} + 2\bar{\mathbf{M}}_{3_{xy}2_y} + \bar{\mathbf{M}}_{3_y2_x} \\
\hat{\mathbf{M}}_{4_4} &= -\bar{\mathbf{M}}_{2_y3_y} + \bar{\mathbf{M}}_{3_y2_y} \\
\hat{\mathbf{M}}_{5_1} &= \bar{\mathbf{M}}_{3_x3_x} + \bar{\boldsymbol{\mathcal{M}}}_{3_x3_x} \\
\hat{\mathbf{M}}_{5_2} &= 2\bar{\mathbf{M}}_{3_x3_{xy}} + 2\bar{\boldsymbol{\mathcal{M}}}_{3_x3_{xy}} + 2\bar{\mathbf{M}}_{3_{xy}3_x} + 2\bar{\boldsymbol{\mathcal{M}}}_{3_{xy}3_x} \\
\hat{\mathbf{M}}_{5_3} &= \bar{\mathbf{M}}_{3_x3_y} + \bar{\boldsymbol{\mathcal{M}}}_{3_x3_y} + 4\bar{\mathbf{M}}_{3_{xy}3_{xy}} + 4\bar{\boldsymbol{\mathcal{M}}}_{3_{xy}3_{xy}} + \bar{\mathbf{M}}_{3_y3_x} + \bar{\boldsymbol{\mathcal{M}}}_{3_y3_x}
\end{aligned}$$

$$\begin{aligned}\hat{\mathbf{M}}_{5_4} &= 2\bar{\mathbf{M}}_{3_{xy}3_y} + 2\bar{\boldsymbol{\mathcal{M}}}_{3_{xy}3_y} + 2\bar{\mathbf{M}}_{3_y3_{xy}} + 2\bar{\boldsymbol{\mathcal{M}}}_{3_y3_{xy}} \\ \hat{\mathbf{M}}_{5_5} &= \bar{\mathbf{M}}_{3_y3_y} + \bar{\boldsymbol{\mathcal{M}}}_{3_y3_y} \end{aligned} \tag{3.95}$$

In this case also, the generalized stress resultants can be function of point coordinates (x, y). The solution of the form Eq. (3.51) can be assumed for simply supported boundary condition, and each $(\alpha\beta)$th coefficient of the assumed displacement variables function can be obtained by solving the system of equations which is given by Eq. (3.56) with the coefficient matrix $\mathbf{K}$ defined as in Eq. (3.57) with $\hat{\mathbf{M}}_1$ equal to zero.

3.7. Numerical examples

For the numerical examples, we consider the plates with microstructure embedded in functionally graded or homogeneous matrix of material with following geometric and material parameters:

$$\begin{aligned} &E_1 = 14.4 \text{ GPa}, \quad E_2 = 1.44 \text{ GPa}, \quad \nu = 0.38, \\ &h = 10 \times 10^{-6} \text{ m}, \quad a = b = 20h \end{aligned} \tag{3.96}$$

where a and b are the length and width of the plate and h is the height of plate. In the case of the plate with homogeneous matrix material, the power index $\hat{n}$ is taken as zero and the modulus of elasticity becomes E_1.

3.7.1. Analytical and finite element method solution for simply supported linear plate

For analytical and linear finite element method (FEM) solutions, simply supported isotropic Cosserat solid plate under uniformly distributed load is considered. The boundary conditions for various plate theories for simply supported plate are following:

$$\begin{aligned} \text{The classical plate theory}: \quad \text{at } x = 0, a: \quad & u_{,x} = u_{,xy} = v = v_{,y} = w = w_{,y} = 0 \\ \text{at } y = 0, b: \quad & u = u_{,x} = v_{,y} = v_{,xy} = w = w_{,x} = 0 \end{aligned} \tag{3.97}$$

$$
\begin{aligned}
\text{Higher order plate theories}: \quad \text{at } x=0,a: \quad & \phi^{(i)}_{x,x}=\phi^{(i)}_{x,xy}=0 \quad \text{for } i=0,...,n \\
& \phi^{(i)}_{y}=\phi^{(i)}_{y,y}=0 \quad \text{for } i=0,...,m \\
& \phi^{(i)}_{z}=\phi^{(i)}_{z,y}=0 \quad \text{for } i=0,...,p \\
\text{at } y=0,b: \quad & \phi^{(i)}_{x}=\phi^{(i)}_{x,x}=0 \quad \text{for } i=0,...,n \\
& \phi^{(i)}_{y,y}=\phi^{(i)}_{y,xy}=0 \quad \text{for } i=0,...,m \\
& \phi^{(i)}_{z}=\phi^{(i)}_{z,x}=0 \quad \text{for } i=0,...,p
\end{aligned}
\tag{3.98}
$$

The maximum value of non-dimensional transverse central deflections ($\hat{w}=\frac{wEh^3}{q_0(ab)^2}$) are presented in Tables 3.1, 3.2, and 3.3 (comparing the analytical and linear FE solutions) for homogeneous and functionally graded plates with embedded inclusions (microstructure) for the classical, first-order, and general third-order plate theories, respectively. Different combinations of the material length scale parameters have been used in such a way that the deflections remain the same in the x and y directions, that is, same material length scale parameter corresponds to out of plane, in-plane curvatures, and twist of the inclusion oriented along the x, y, and z axes are used. For analytical solution, the maximum values of α and β (see Eq. (3.51)) are taken as 100 and for linear FEM solution, 16×16 mesh is used for the full plate. In the finite element analysis, conforming rectangular elements, which can be obtained by tensor product of hermite cubic function for one dimension are used. In case of classical and first-order plate theories, three groups of nonzero material length scale parameters have been considered: (1) correspond to the out of plane curvature of embedded inclusions oriented along x and y direction, (2) correspond to in plane and out of plane curvatures of microstructure at the same time, and (3) accounts for out of plane curvature and twist of directors together. Here we note that the material length scales correspond to in-plane curvature of microstructure have negligible effect on the bending of the plate. In the case of a general third-order plate theory, the material scales corresponding to six curvatures and three twists come into play. The material length scales for in plane curvature of directors of microstructure are taken as zero, as it have been shown, in the case of classical and first-order plate theories, to have negligible effect on the bending response. In this case four groups of length scale are considered, which correspond to: (1) out of plane curvature of directors

oriented along x and y directions, (2) out of plane curvature of directors oriented along x and y directions along with curvature of director oriented along z direction, (3) out of plane curvature and twist of directors oriented along x and y directions and (4) all possible curvature and twist of directors oriented along the x-, y-, and z-axes, except the inplane curvature of directors oriented along the x and y directions. Here, we note that the central deflection results for the first and second group of material length scales do not differ much. In the case of the thin plate limit, this difference would be negligible, whereas for thick plates they will show some difference due to the curvature of directors of inclusions oriented along the z direction. In all cases the stiffening effect due the consideration of microstructure is evident. The analytical and linear FEM solutions are in good agreement. Also, we will see in the nonlinear FEM solution presented in the forthcoming section that different length scale parameters for inclusions oriented along x and y directions would bring anisotropic effect in the deflection.

Table 3.1. Analytical and linear FEM solutions for center deflection $\hat{w} \times 10^2$ for simply supported homogeneous and FGM beam for the classical plate theory.

$\hat{n}$	ℓ/h	Classical plate theory					
		(1) $\ell_2 = \ell_3 = \ell$		(2) $\ell_2 = \ell_3 = \ell$ $\ell_5 = \ell_6 = \ell$		(3) $\ell_2 = \ell_3 = \ell$ $\ell_1 = \ell_4 = \ell$	
		Analytical	Linear FEM	Analytical	Linear FEM	Analytical	Linear FEM
0	0.0	4.1699	4.1709	4.1699	4.1709	4.1699	4.1709
	0.2	3.2238	3.2245	3.2238	3.2245	2.6141	2.6147
	0.4	1.9160	1.9164	1.9160	1.9164	1.2334	1.2337
	0.6	1.1426	1.1429	1.1426	1.1429	0.6560	0.6561
	0.8	0.7300	0.7302	0.7300	0.7302	0.3963	0.3964
	1.0	0.4985	0.4986	0.4985	0.4986	0.2626	0.2627
1	0.0	9.7594	9.7578	9.7594	9.7617	9.7594	9.7578
	0.2	7.0827	7.0844	7.0827	7.0844	5.5258	5.5271
	0.4	3.8808	3.8817	3.8808	3.8817	2.4011	2.4016
	0.6	2.2124	2.2130	2.2124	2.2130	1.2361	1.2364
	0.8	1.3811	1.3814	1.3811	1.3814	0.7361	0.7363
	1.0	0.9312	0.9314	0.9312	0.9314	0.4842	0.4844

3.7.2. Nonlinear finite element method solution

For nonlinear solution, plates with the same geometric and material parameters as given in Eq. (3.96) are considered. The general third order plate theory has been used

Table 3.2. Analytical and linear FEM solutions for center deflection $\hat{w} \times 10^2$ for simply supported homogeneous and FGM beam for the first order plate theory.

$\hat{n}$	ℓ/h	First order plate theory					
		(1) $\ell_2 = \ell_3 = \ell$		(2) $\ell_2 = \ell_3 = \ell$ $\ell_5 = \ell_6 = \ell$		(3) $\ell_2 = \ell_3 = \ell$ $\ell_1 = \ell_4 = \ell$	
		Analytical	Linear FEM	Analytical	Linear FEM	Analytical	Linear FEM
0	0.0	4.2309	4.2334	4.2309	4.2334	4.2309	4.2323
	0.2	3.2722	3.2729	3.2722	3.2727	2.6544	2.6550
	0.4	1.9488	1.9493	1.9488	1.9490	1.2590	1.2592
	0.6	1.1675	1.1678	1.1675	1.1676	0.6764	0.6765
	0.8	0.7511	0.7512	0.7511	0.7511	0.4145	0.4146
	1.0	0.5176	0.5177	0.5176	0.5176	0.2798	0.2798
1	0.0	9.8703	9.8813	9.8703	9.8813	9.8703	9.8735
	0.2	7.1661	7.1678	7.1661	7.1674	5.5937	5.5950
	0.4	3.9355	3.9364	3.9355	3.9359	2.4440	2.4446
	0.6	2.2543	2.2549	2.2543	2.2545	1.2712	1.2715
	0.8	1.4171	1.4175	1.4171	1.4173	0.7681	0.7682
	1.0	0.9643	0.9645	0.9643	0.9643	0.5147	0.5148

to analyse the plate in this section. Uniformly distributed load of $q_0 = 1\text{MN/m}^2$ is applied at the top surface of the plate to do the nonlinear analysis with the following two types of boundary conditions:

Simply supported (pinned edges) plate:

$$\begin{aligned} &\text{Classical plate theory :} && \text{at } x = \pm\frac{a}{2}, \text{ and } y = \pm\frac{b}{2} : u = v = w = 0 \\ &\text{Higher order plate theories :} && \text{at } x = \pm\frac{a}{2}, \text{ and } y = \pm\frac{b}{2} : \phi_x^{(0)} = \phi_y^{(0)} = \phi_z^{(0)} = 0 \end{aligned} \tag{3.99}$$

Table 3.3. Analytical and linear FEM solutions for center deflection $\hat{w} \times 10^2$ for simply supported homogeneous and FGM beam for the general third order plate theory.

$\hat{n}$	ℓ/h	Third order plate theory							
		(1) $\ell_2 = \ell_4 = \ell$		(2) $\ell_2 = \ell_4 = \ell$ $\ell_3 = \ell_6 = \ell$		(3) $\ell_2 = \ell_4 = \ell$ $\ell_1 = \ell_5 = \ell$		(4) $\ell_2 = \ell_4 = \ell$ $\ell_3 = \ell_6 = \ell$ $\ell_1 = \ell_5 = \ell_9 = \ell$	
		Analytical	Linear FEM	Analytical	Linear FEM	Analytical	Linear FEM	Analytical	Linear FEM
0	0.0	4.2222	4.2232	4.2222	4.2232	4.2222	4.2232	4.2222	4.2232
	0.2	3.2641	3.2649	3.2625	3.2632	2.6471	2.6477	2.6460	2.6466
	0.4	1.9424	1.9429	1.9417	1.9421	1.2538	1.2541	1.2535	1.2538
	0.6	1.1625	1.1628	1.1622	1.1625	0.6724	0.6725	0.6723	0.6724
	0.8	0.7469	0.7471	0.7468	0.7469	0.4111	0.4112	0.4110	0.4111
	1.0	0.5139	0.5140	0.5138	0.5140	0.2766	0.2767	0.2766	0.2767
1	0.0	9.8635	9.8657	9.8635	9.8657	9.8635	9.8657	9.8635	9.8657
	0.2	7.1579	7.1595	7.1540	7.1557	5.5854	5.5867	5.5831	5.5844
	0.4	3.9275	3.9284	3.9256	3.9266	2.4370	2.4375	2.4363	2.4369
	0.6	2.2474	2.2479	2.2467	2.2472	1.2652	1.2655	1.2650	1.2653
	0.8	1.4110	1.4113	1.4107	1.4110	0.7626	0.7627	0.7625	0.7627
	1.0	0.9586	0.9588	0.9584	0.9587	0.5095	0.5096	0.5095	0.5096

Plate with clamped edges:

Classical plate theory : at $x = -\frac{a}{2}, \frac{a}{2}$, and $y = -\frac{b}{2}, \frac{b}{2}$:

$$u = v = w = 0, \quad w_{,x} = w_{,y} = w_{,xy} = 0 \tag{3.100}$$

Higher order plate theories : at $x = -\frac{a}{2}, \frac{a}{2}$, and $y = -\frac{b}{2}, \frac{b}{2}$:

$$\phi_x^{(0)} = \phi_y^{(0)} = \phi_z^{(0)} = 0, \quad \phi_x^{(1)} = \phi_y^{(1)} = \phi_{z,x}^{(0)} = \phi_{z,y}^{(0)} = 0$$

For nonlinear analysis, similar type of meshes and elements, as described in section 3.7.1 for linear analysis, are used. Newton's method is employed to obtain converged solutions. The error tolerance used for the nonlinear analysis is 10^{-4}. Two types of microstructure dependent plates are used along with the conventional plate; that is, when the small inclusions are oriented along x and y directions and material length scale corresponds to out of plane curvature of the director are used, $\ell_4 \neq 0$.

Figure 3.1 shows the transverse displacement ($\bar{w} = q_0\hat{w} \times 10^2$) of the conventional plate, plates with the inclusion oriented along the x and y directions for the simply supported boundary condition. The material length scale corresponds to the out of plane curvature of the inclusions. The anisotropic effect is evident in the microstructure dependent plate due to the ordered orientation of the small inclusions embedded in isotropic matrix of material. The stiffening effect due to the microstructure is

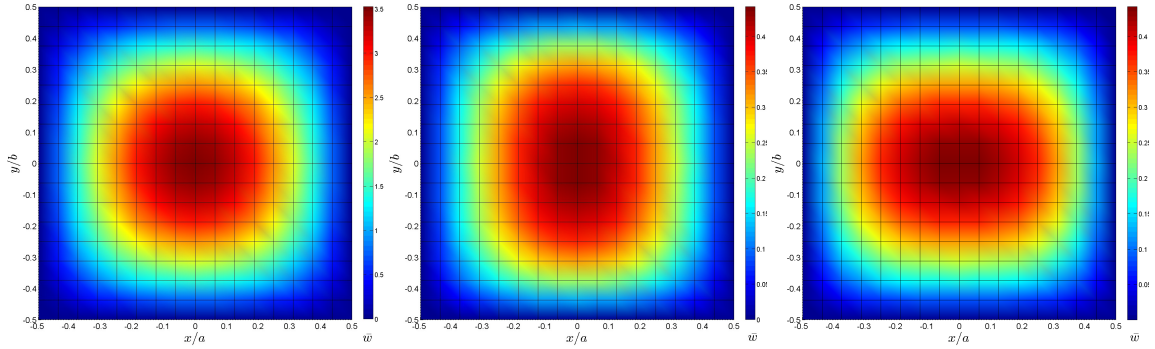

(a) $\ell_i = 0$ (b) $\ell_4 = 1.5h$ (c) $\ell_2 = 1.5h$

Fig. 3.1 Transverse deflection $\bar{w}$ (a) of conventional plate (b) of plate with inclusions oriented along $x-$direction (c) of plate with inclusions oriented along $y-$direction for simply supported boundary condition using general third order plate theory.

shown in fig. 3.2 for simply supported and clamped plates, considering homogeneous and functionally graded plates with microstructure, employing the general third-order plate theory. The maximum transverse deflection, $\bar{w}_{max}$, is plotted against the material length scale considering equal length scales related to curvature and twist of inclusions in all directions, except the same related to the in-plane curvature of inclusions is taken as zero because it is shown to have negligible effect on the bending response. Further, the components of the stress tensor, which includes both symmetric and skew symmetric part of the stress tensor are plotted for simply supported plate. The skew symmetric part of stress tensor can be obtain by mean of the angular conservation equation as following:

$$\mathbf{S}^a = \frac{1}{2}(\mathbf{S} - \mathbf{S}^T) = \frac{1}{2}\mathbf{F}^{-1}(\mathrm{Div}(\mathbf{M}))\mathbf{F}^{-T} \tag{3.101}$$

where $\mathbf{M}$ is the third order couple stress tensor defined for the finite rotation case (see [19]) and $\mathbf{F}$ is the deformation gradient. The divergence is calculated with

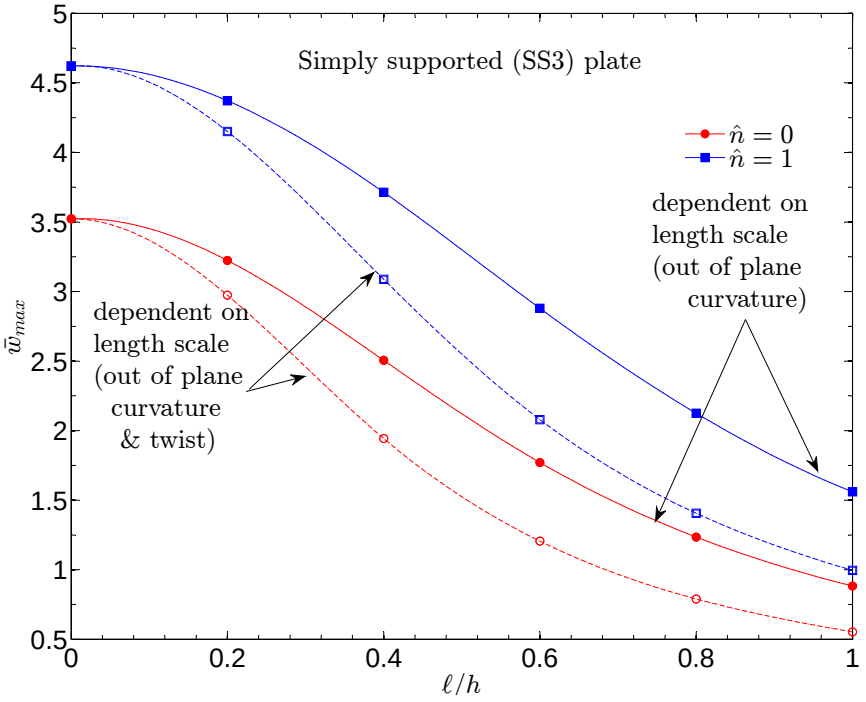

(a) Simply supported plate

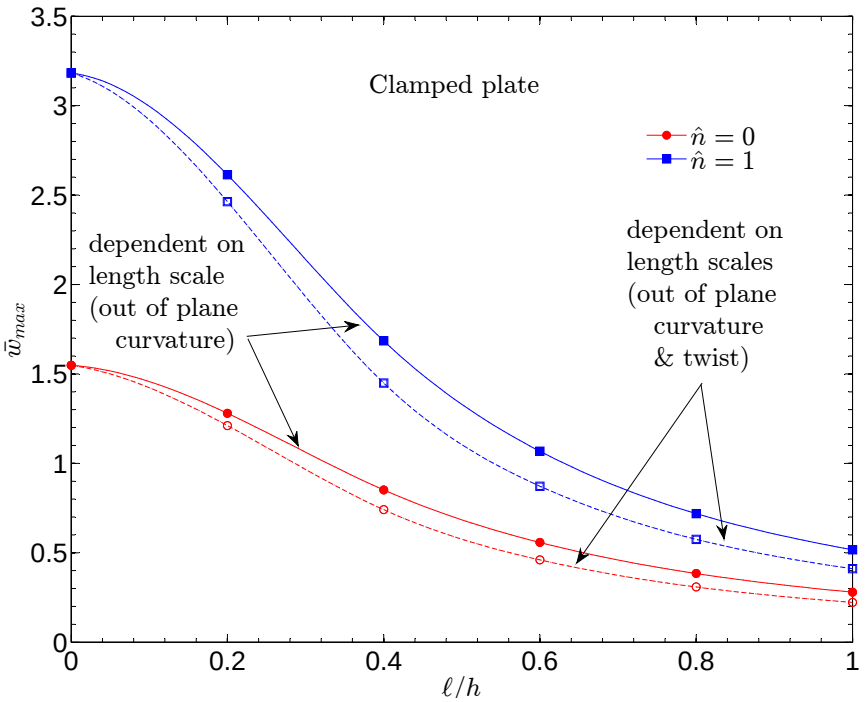

(b) Clamped plate

Fig. 3.2 Variation of maximum transverse deflection $\bar{w}_{max}$ with material length scale

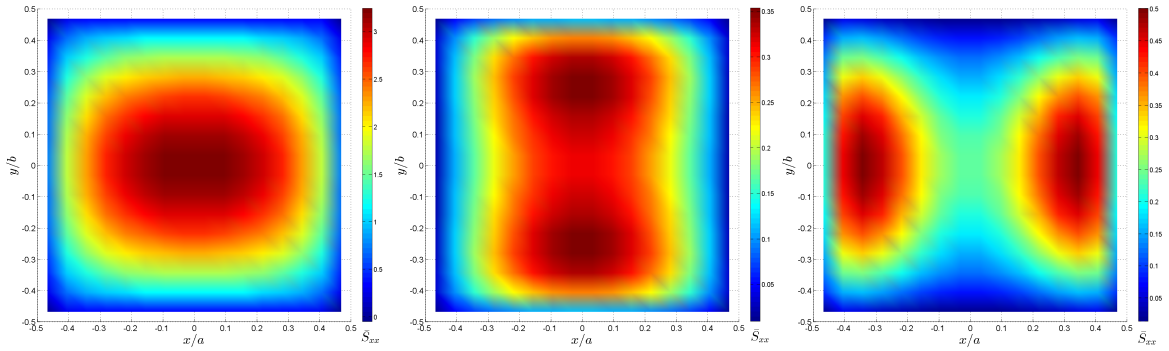

(a) $\bar{S}_{xx}$ for $\ell_i = 0$ (b) $\bar{S}_{xx}$ for $\ell_4 = 1.5h$ (c) $\bar{S}_{xx}$ for $\ell_2 = 1.5h$

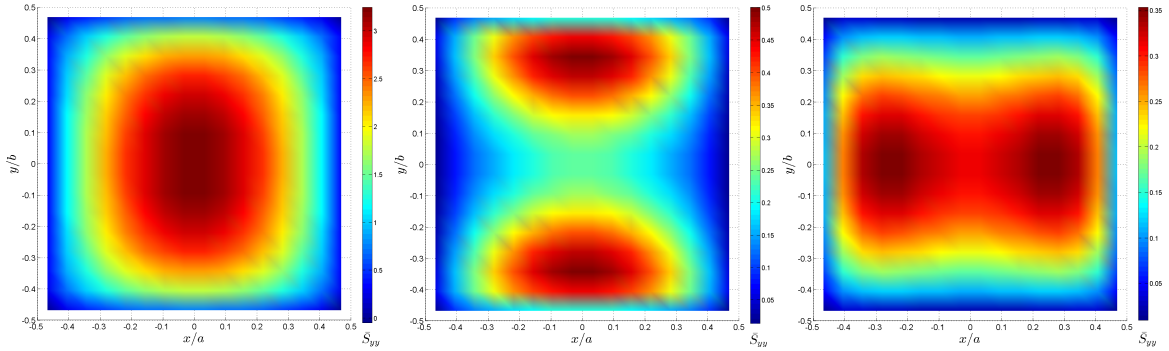

(d) $\bar{S}_{yy}$ for $\ell_i = 0$ (e) $\bar{S}_{yy}$ for $\ell_4 = 1.5h$ (f) $\bar{S}_{yy}$ for $\ell_2 = 1.5h$

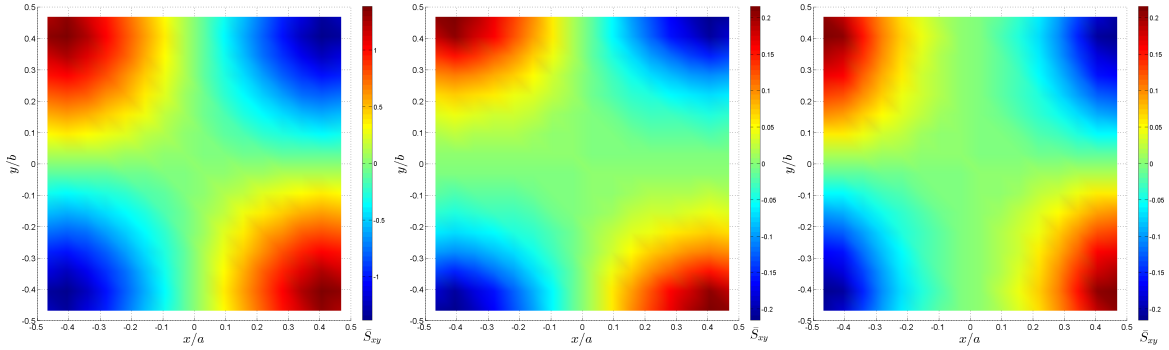

(g) $\bar{S}_{xy}$ for $\ell_i = 0$ (h) $\bar{S}_{xy}$ for $\ell_4 = 1.5h$ (i) $\bar{S}_{xy}$ for $\ell_2 = 1.5h$

Fig. 3.3 Distribution of the stress components $\bar{S}_{xx}$, $\bar{S}_{yy}$ and $\bar{S}_{xy}$ at the top surface of plate for conventional and microstructure dependent simply supported plate under uniformly distributed load considering general third order plate theory.

respect to the reference frame. For a detailed derivation of the skew symmetric part of the stress tensor in th e case of the general third (or higher) order plate theory, see appendix B. The stress components are computed at one Gauss point for each finite elements. Figure 3.3 shows the distribution of the stress components $\bar{S}_{xx}, \bar{S}_{yy}$ and $\bar{S}_{xy}$ of the total stress at the top surface of simply supported conventional and microstructure dependent plate where $\bar{\mathbf{S}} = (a^2/Eh^2)\mathbf{S}$. The stress component $\bar{S}^{skew}_{xy}$ is found to be not very significant in the plate bending as shown in fig. 3.4 and hence the component $\bar{S}_{yx}$ would have almost similar distribution as $\bar{S}_{xy}$. Figure 3.5 shows the distribution of the transverse shear components of the stress tensor namely $\bar{S}_{xz}$ and $\bar{S}_{yz}$ (which gives the shear force on integrating through cross-section) at the mid surface of the plate. In all these plots the direction effect on the distribution of stress components due to the specific orientation of the small inclusions are evident. Further, the distribution of $\bar{S}_{zz}$, $\bar{S}_{zx}$ and $\bar{S}_{zy}$ with respect to the height of the plate is plotted in fig. 3.6 and fig. 3.7, respectively, at $x = -a/32$ and various y (depicted by the color code) considering the microstructure oriented along $x-$direction considering the length scale corresponding to out of plane curvature of director. Here we note that the component $\bar{S}_{zz}$ away from the plate boundary at the top surface is same as the uniformly distributed load applied on the plate, as expected. Also the shear components ($\bar{S}_{zx}$ and $\bar{S}_{zy}$) are zero at the shear free top and bottom surfaces of the plate, as expected.

3.8. Chapter summary and conclusion

In the present study, we have developed a nonlinear finite element model for moderate rotation condition (i.e., von Kármán strains) for plates having rotation gradient dependent strain energy potential. A general Taylor's series based higher-order plate theory is used in the case of homogeneous or spatially varying material properties. Specialization to a general third-order, first-order, and the classical plate theories is also presented. Analytical solutions for simply supported linear plates are presented. The stiffening effect of the plate while considering the rotation gradient term in potential energy is shown in the numerical examples considered. Also, the anisotropic response is observed due to the ordered orientation of the small inclusions embedded in the plate, which is modeled through the rotation gradient dependent term in the potential energy. In the post-processing of the nonlinear FEM analysis, distribution of various stress components, which includes both symmetric and skew-symmetric

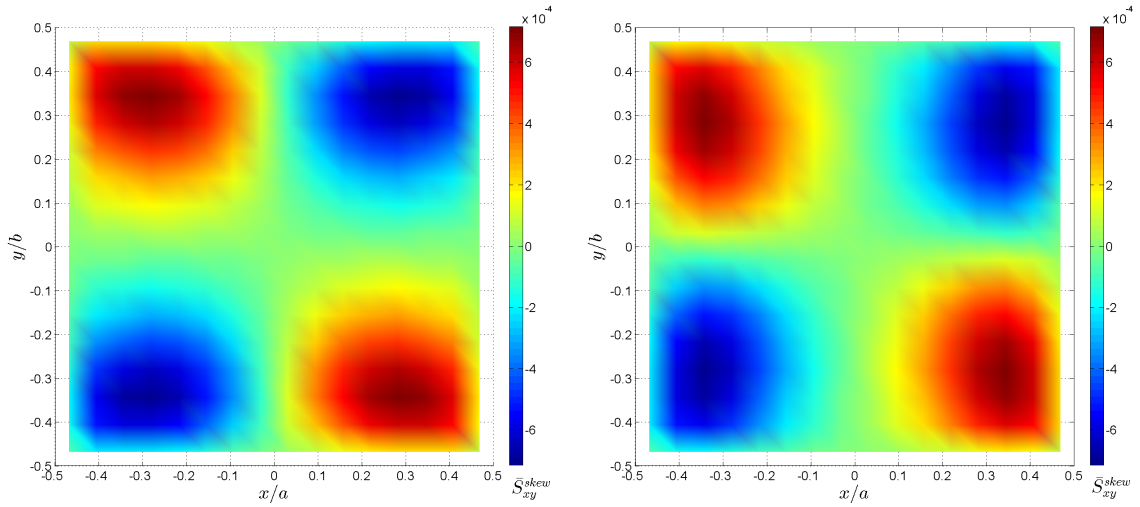

(a) $\bar{S}_{xy}^{skew}$ for $\ell_4 = 1.5h$ (b) $\bar{S}_{xy}^{skew}$ for $\ell_2 = 1.5h$

Fig. 3.4 Distribution of the stress components $\bar{S}_{xy}^{skew}$ at the top surface of microstructure dependent simply supported plate under uniformly distributed load considering general third order plate theory.

parts in the case of microstructure dependent plate, are plotted. The thickness profile of shear stress components showed zero in-plane shear at the shear-free top and bottom surfaces, as expected. Also, the normal stress at the top surface is found to be same as the applied uniformly distributed load and zero at the bottom surface, as one would expect. As a concluding remark, we want to highlight the possibility of anisotropic response, along with the stiffening effect, due to the ordered orientation of microstructure considering different material length scales corresponding to the curvatures and twists in different directions as opposed to the centrosymmetric microstructure considered in all the previous studies in the literature.

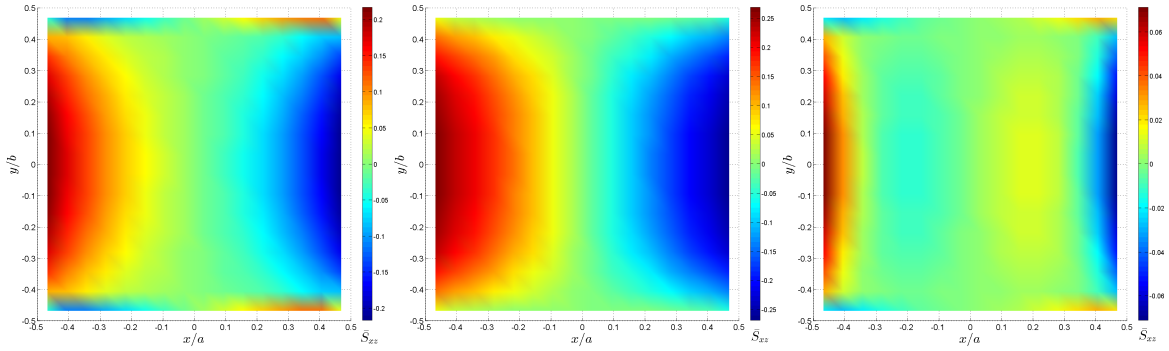

(a) $\bar{S}_{xz}$ for $\ell_i = 0$ (b) $\bar{S}_{xz}$ for $\ell_4 = 1.5h$ (c) $\bar{S}_{xz}$ for $\ell_2 = 1.5h$

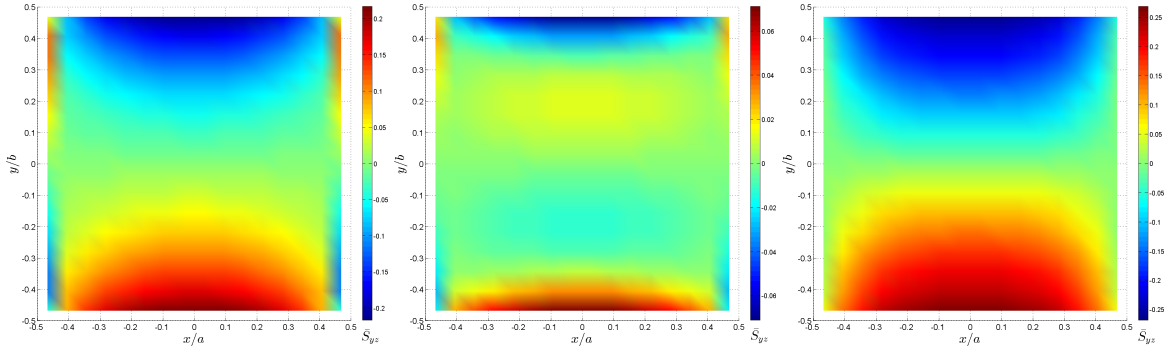

(d) $\bar{S}_{yz}$ for $\ell_i = 0$ (e) $\bar{S}_{yz}$ for $\ell_4 = 1.5h$ (f) $\bar{S}_{yz}$ for $\ell_2 = 1.5h$

Fig. 3.5 Distribution of the transverse shear stresses, $\bar{S}_{xz}$ and $\bar{S}_{yz}$ at the mid surface of conventional and microstructure dependent simply supported plate under uniformly distributed load considering general third order plate theory.

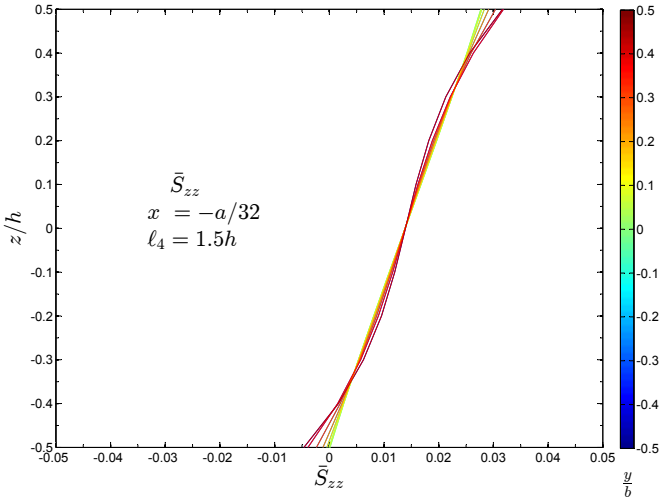

Fig. 3.6 Variation of non-dimensional stress component $\bar{S}_{zz}$ through the height of the microstructure dependent simply supported plate with the inclusions oriented along $x-$axis considering general third order plate theory.

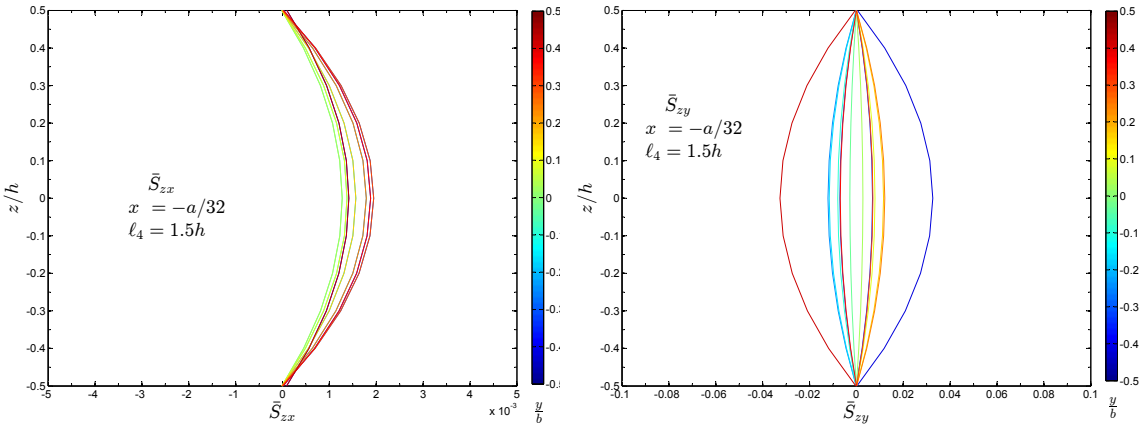

(a) $\bar{S}_{zx}$ for $\ell_4 = 1.5h$ (b) $\bar{S}_{zy}$ for $\ell_4 = 1.5h$

Fig. 3.7 Variation of non-dimensional shear stress components $\bar{S}_{zx}$ and $\bar{S}_{zy}$ through the height of the microstructure dependent simply supported plate with the inclusions oriented along $x-$axis considering general third order plate theory.

4. MODELLING OF THIN CARBON NANOTUBE REINFORCED HARD COATING ON ELASTIC SUBSTRATE

In this chapter, we discuss one of the possible applications of the Cosserat continuum theory with constrained micro-rotation. Composites with very small inclusions, for example, carbon nanotube (CNT)-reinforced composites can be thought of as a Cosserat solid where the small constituents (CNT strands) rotate with its matrix and there is no rotational mismatch or gap created during the deformation. In this chapter, we model indentation of a thin hard CNT reinforced coating on an elastic substrate by the rotation gradient dependent theory of Srinivasa and Reddy [19]. We use the classical plate theory for the rotation gradient dependent theory developed in chapter 3 to model deformation of the hard coatings due to an indentation in a circular computational domain with the indentation at the center. Circular computational domain requires non-rectangular finite element mesh in the finite element grid for which a C^1 continuous approximation function is hard to achieve. Hence, we employ a mixed finite element model to obtained the solution. A schematic diagram of the nano-indentation is shown in fig. 4.1. To model the contact between the substrate and the coating, we assume a smooth Hertzian contact between them. The effect of CNT-reinforcement is modeled by various length scale parameters. It is assumed that the CNT strands are distributed uniformly and are randomly oriented. Hence, all the length scale related to various curvatures (see Chapter 3) are taken as equal and the length scale related to twist is taken as zero.

4.1. Mixed finite element model for microstructure dependent plate on elastic substrate

4.1.1. Governing equations of motion

Consider the (x, y, z) rectangular cartesian coordinate system in the reference frame and a plate of arbitrary geometry and height h lies in xy-plane with the central plane of the plate coincide with xy-coordinate plane in its natural configuration and the height of the plate is along z-axis. The displacement field for the classical plate

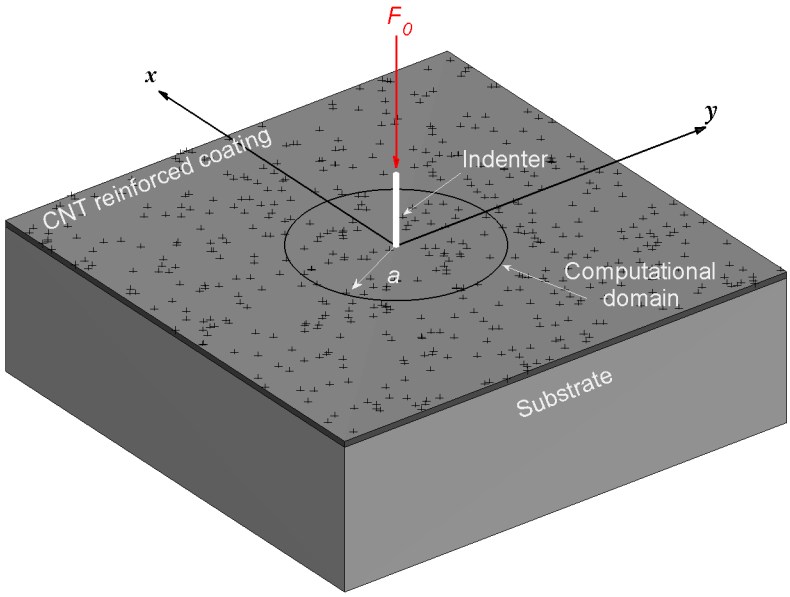

Fig. 4.1 Schematic diagram for the indentation on a CNT-reinforced hard coating on elastic substrate.

theory is given by

$$\mathbf{u} = (u(x,y) - zw_{,x})\,\hat{\mathbf{e}}_1 + (v(x,y) - zw_{,y})\,\hat{\mathbf{e}}_2 + w(x,y)\,\hat{\mathbf{e}}_3. \tag{4.1}$$

where $u(x,y)$, $v(x,y)$, and $w(x,y)$ are the displacements of the central plane of the plate along the x, y, and z directions, respectively. The governing equations of motion of the classical plate theory on elastic foundation, considering the rotation gradient dependant strain energy for moderate constrained micro-rotation (see Arbind *et al.* [57] or chapter 3), are

$$\begin{aligned}\hat{\mathbf{F}} \;=\; & -\left(\mathbf{P}_{nl_x} + \mathbf{P}_{2_x}\right)_{,x} - \left(\mathbf{P}_{nl_y} + \mathbf{P}_{2_y}\right)_{,y} \\ & + (\mathbf{M}_{3_x} + \boldsymbol{\mathcal{M}}_{3_x})_{,xx} + 2(\mathbf{M}_{3_{xy}} + \boldsymbol{\mathcal{M}}_{3_{xy}})_{,xy} + (\mathbf{M}_{3_{yy}} + \boldsymbol{\mathcal{M}}_{3_{yy}})_{,yy} + \mathbf{k}\boldsymbol{\Phi}\end{aligned} \tag{4.2}$$

where $\boldsymbol{\Phi} = [u \;\; v \;\; w]^T$. And $\mathbf{k}$ is (3×3) matrix with only nonzero element $\mathbf{k}_{33} = k$, where k is the contact stiffness between the coating and the elastic substrate. The

generalized forces in Eq. (4.2) are defined as follows:

$$\begin{aligned}
&\mathbf{P}_{2_j} = \int_{-h/2}^{h/2} \mathbf{A}_{2_j}^T \mathbf{S}^s \, dz, \quad \mathbf{P}_{nl_j} = \int_{-h/2}^{h/2} \mathbf{A}_{nl_j}^T \mathbf{S}^s \, dz \, dz \quad \text{for } j = x, y \\
&\mathbf{M}_{3_{xx}} = \int_{-h/2}^{h/2} \mathbf{A}_{3_x}^T \mathbf{S}^s \, dz, \quad \mathbf{M}_{3_{xy}} = \int_{-h/2}^{h/2} \mathbf{A}_{3_{xy}}^T \mathbf{S}^s \, dz, \quad \mathbf{M}_{3_{yy}} = \int_{-h/2}^{h/2} \mathbf{A}_{3_y}^T \mathbf{S}^s \, dz \\
&\boldsymbol{\mathcal{M}}_{3_{xx}} = \int_{-h/2}^{h/2} \mathbf{B}_{3_x}^T \mathbf{m} \, dz, \quad \boldsymbol{\mathcal{M}}_{3_{xy}} = \int_{-h/2}^{h/2} \mathbf{B}_{3_{xy}}^T \mathbf{m} \, dz, \quad \boldsymbol{\mathcal{M}}_{3_{yy}} = \int_{-h/2}^{h/2} \mathbf{B}_{3_y}^T \mathbf{m} \, dz
\end{aligned} \tag{4.3}$$

Here $\mathbf{S}^s = \mathbf{C} \cdot \boldsymbol{\varepsilon}$ is the symmetric part of the second Piola–Kirchhoff stress components and $\boldsymbol{\varepsilon} = [\varepsilon_{xx} \ \varepsilon_{yy} \ \gamma_{xy}]^T$ are Green–Lagrange strain tensor components approximated for moderate rotation case (see [57]); $\mathbf{m} = \mathbf{C}_l \boldsymbol{\chi}$ are components of couple stress tensor; $\boldsymbol{\chi} = [2\omega_{x,x} \, 2\omega_{x,y} \, 2\omega_{y,x} \, 2\omega_{y,y} \, 2\omega_{z,x} \, 2\omega_{z,y}]^T$ are various curvatures and twists of the microstructure oriented along x and y directions (see chapter 3 or [57] for details); $\mathbf{C}$ and $\mathbf{C}_l$ are matrix of material properties which, and for homogeneous isotropic material with microstructures embedding, are given as

$$\mathbf{C} = \frac{E}{1-\nu^2} \begin{bmatrix} 1 & \nu & 0 \\ \nu & 1 & 0 \\ 0 & 0 & \frac{(1-\nu)}{2} \end{bmatrix}, \quad \mathbf{C}_{l_{ii}} = G\ell_i^2, \quad \text{(no sum on } i\text{) and } i = 1, 2, ..6 \tag{4.4}$$

where E, G, and ν are modulus of elasticity, shear modulus, and Poisson's ratio, respectively, and ℓ_i are various material length scale parameters. In the case of CPT, the material length scale parameters ℓ_1 and ℓ_4 which correspond to $\omega_{x,x}$ and $\omega_{y,y}$ are related to twist of the embedded inclusions oriented along the x and y directions, respectively, and ℓ_2 and ℓ_3 corresponding to $\omega_{x,y}$ and $\omega_{y,x}$ are related to the out of plane curvature of embedded inclusions oriented along the x and y directions, respectively. These length scales parameters contribute to the bending moments of the plate. The parameters ℓ_5 and ℓ_6 corresponds to the inplane curvature of the inclusions or microstructures, and they contribute to the drilling type moment (see

[19]). Also, we have

$$\mathbf{A}_{2_x} = \begin{bmatrix} 1 & 0 & 0 \\ 0 & 0 & 0 \\ 0 & 1 & 0 \end{bmatrix}, \quad \mathbf{A}_{2_y} = \begin{bmatrix} 0 & 0 & 0 \\ 0 & 1 & 0 \\ 1 & 0 & 0 \end{bmatrix}, \quad \mathbf{A}_{nl_x} = \begin{bmatrix} 0 & 0 & w_{,x} \\ 0 & 0 & 0 \\ 0 & 0 & w_{,y} \end{bmatrix}, \quad \mathbf{A}_{nl_y} = \begin{bmatrix} 0 & 0 & 0 \\ 0 & 0 & w_{,y} \\ 0 & 0 & w_{,x} \end{bmatrix}$$

$$\mathbf{A}_{3_x} = \begin{bmatrix} 0 & 0 & -z \\ 0 & 0 & 0 \\ 0 & 0 & 0 \end{bmatrix}, \quad \mathbf{A}_{3_{xy}} = \begin{bmatrix} 0 & 0 & 0 \\ 0 & 0 & 0 \\ 0 & 0 & -z \end{bmatrix}, \quad \mathbf{A}_{3_y} = \begin{bmatrix} 0 & 0 & 0 \\ 0 & 0 & -z \\ 0 & 0 & 0 \end{bmatrix}, \tag{4.5}$$

and

$$\mathbf{B}_{3_x} = \begin{bmatrix} 0 & 0 & 0 \\ 0 & 0 & 0 \\ 0 & 0 & -2 \\ 0 & 0 & 0 \\ 0 & 1 & 0 \\ 0 & 0 & 0 \end{bmatrix}, \quad \mathbf{B}_{3_{xy}} = \begin{bmatrix} 0 & 0 & 1 \\ 0 & 0 & 0 \\ 0 & 0 & 0 \\ 0 & 0 & -1 \\ -0.5 & 0 & 0 \\ 0 & 0.5 & 0 \end{bmatrix}, \quad \mathbf{B}_{3_y} = \begin{bmatrix} 0 & 0 & 0 \\ 0 & 0 & 2 \\ 0 & 0 & 0 \\ 0 & 0 & 0 \\ 0 & 0 & 0 \\ -1 & 0 & 0 \end{bmatrix}. \tag{4.6}$$

The force vector is defined as:

$$\hat{\mathbf{F}} = [f_x \quad f_y \quad f_z]^T \tag{4.7}$$

where f_x, f_y, and f_z are the forces per unit area of the plate in the x, y, and z directions, respectively. The force resultants used in Eq. (4.2) are known in terms of the generalized displacements as follows:

$$\begin{aligned} \mathbf{P}_{nl_x} + \mathbf{P}_{2_x} &= \int_{-h/2}^{h/2} (\mathbf{A}_{2_x}^T + \mathbf{A}_{nl_x}^T)\mathbf{C}\left((\mathbf{A}_{2_x} + (1/2)\mathbf{A}_{nl_x})\mathbf{\Phi}_{,x}\right. \\ &\qquad \left. +(\mathbf{A}_{2_y} + (1/2)\mathbf{A}_{nl_y})\mathbf{\Phi}_{,y}\right)\, dz \\ \mathbf{P}_{nl_y} + \mathbf{P}_{2_y} &= \int_{-h/2}^{h/2} (\mathbf{A}_{2_y}^T + \mathbf{A}_{nl_y}^T)\mathbf{C}\left((\mathbf{A}_{2_x} + (1/2)\mathbf{A}_{nl_x})\mathbf{\Phi}_{,x}\right. \\ &\qquad \left. +(\mathbf{A}_{2_y} + (1/2)\mathbf{A}_{nl_y})\mathbf{\Phi}_{,y}\right)\, dz \end{aligned} \tag{4.8}$$

and, similarly, various moments are given as

$$\begin{aligned}
\mathbf{M}^1 &= \mathbf{M}_{3_x} + \boldsymbol{\mathcal{M}}_{3_x} = \left\{ \begin{array}{c} 0 \\ M_1 \\ M_{11} \end{array} \right\} \\
\mathbf{M}^2 &= \mathbf{M}_{3_{xy}} + \boldsymbol{\mathcal{M}}_{3_{xy}} = \frac{1}{2} \left\{ \begin{array}{c} -M_1 \\ M_2 \\ M_{12} \end{array} \right\} \\
\mathbf{M}^3 &= \mathbf{M}_{3_y} + \boldsymbol{\mathcal{M}}_{3_y} = \left\{ \begin{array}{c} -M_2 \\ 0 \\ M_{22} \end{array} \right\}
\end{aligned} \tag{4.9}$$

where

$$\begin{aligned}
M_{11} &= (4hG\ell_3^2 + D_1)w_{,xx} + D_2 w_{,yy} \\
M_{12} &= (4hG(\ell_1^2 + \ell_4^2) + 2D_3)w_{,xy} \\
M_{22} &= D_2 w_{,xx} + (4hG\ell_2^2 + D_1)w_{,yy} \\
M_1 &= hG\ell_5^2 \left(v_{,xx} - u_{,xy}\right) \\
M_2 &= hG\ell_6^2 \left(v_{,xy} - u_{,yy}\right)
\end{aligned} \tag{4.10}$$

and

$$D_1 = \frac{Eh^3}{12(1-\nu^2)}, \quad D_2 = \frac{\nu Eh^3}{12(1-\nu^2)}, \quad D_3 = \frac{Eh^3}{12(1+\nu)} \tag{4.11}$$

Then the governing equation is

$$\hat{\mathbf{F}} = -\left(\mathbf{P}_{nl_x} + \mathbf{P}_{2_x}\right)_{,x} - \left(\mathbf{P}_{nl_y} + \mathbf{P}_{2_y}\right)_{,y} + \hat{\mathbf{M}}^1_{,xx} + 2\hat{\mathbf{M}}^2_{,xy} + \hat{\mathbf{M}}^3_{,yy} + \mathbf{k}\boldsymbol{\Phi} \tag{4.12}$$

and Eqs. (4.10) can be rewritten as following:

$$\begin{aligned}
0 &= -\Delta\, w_{,xx} + D_{11}M_{11} + D_{12}M_{12} + D_{13}M_{22} \\
0 &= -\Delta\, w_{,xy} + D_{21}M_{11} + D_{22}M_{12} + D_{23}M_{22} \\
0 &= -\Delta\, w_{,yy} + D_{31}M_{11} + D_{32}M_{12} + D_{33}M_{22} \\
0 &= -hG\ell_5^2 \left(v_{,xx} - u_{,xy}\right) + M_1 \\
0 &= -hG\ell_6^2 \left(v_{,xy} - u_{,yy}\right) + M_2
\end{aligned} \tag{4.13}$$

where D_{ij} are various components of matrix $\mathbf{D}$ defined as

$$\mathbf{D} = \begin{bmatrix} \frac{D_1+4hG\ell_2^2}{D_2} & 0 & -1 \\ 0 & \frac{\Delta}{2D_3+4hG(\ell_1^2+\ell_4^2)} & 0 \\ -1 & 0 & \frac{D_1+4hG\ell_3^2}{D_2} \end{bmatrix} \tag{4.14}$$

with

$$\Delta = \frac{(4hG\ell_3^2 + D_1)(4hG\ell_2^2 + D_1)}{D_2} - D_2 \tag{4.15}$$

We consider the governing equation (4.2) along with various moments equations (4.13) to obtain the solution by the mixed finite element model, treating displacements and moments as unknown variables (see Reddy [41]).

4.1.2. Weak form of governing equations

The weak form of the governing equation (4.2) is

$$\begin{aligned} \int_\Omega \delta\mathbf{\Phi}\cdot\hat{\mathbf{F}}\,dx\,dy &= \int_\Omega \Big[\delta\mathbf{\Phi}_{,x}\cdot\left(\mathbf{H}^1_{2_x}\mathbf{\Psi}_{,x} + \mathbf{H}^1_{2_y}\mathbf{\Phi}_{,y} + \frac{1}{2}\mathbf{H}^1_{nl_x}\mathbf{\Phi}_{,x} + \frac{1}{2}\mathbf{H}^1_{nl_y}\mathbf{\Phi}_{,y}\right) \\ &\quad +\delta\mathbf{\Phi}_{,y}\cdot\left(\mathbf{H}^2_{2_x}\mathbf{\Phi}_{,x} + \mathbf{H}^2_{2_y}\mathbf{\Phi}_{,y} + \frac{1}{2}\mathbf{H}^2_{nl_x}\mathbf{\Phi}_{,x} + \frac{1}{2}\mathbf{H}^2_{nl_y}\mathbf{\Phi}_{,y}\right) \\ &\quad +\delta\mathbf{\Phi}_{,x}\cdot(-\mathbf{M}^1_{,x} - \mathbf{M}^2_{,y}) + \delta\mathbf{\Phi}_{,y}(-\mathbf{M}^2_{,x} - \mathbf{M}^3_{,y}) + \delta\mathbf{\Phi}\cdot\mathbf{k}\mathbf{\Phi}\Big]\,dx\,dy \\ &\quad -\oint_{\partial\Omega}\delta\mathbf{\Phi}[(\mathbf{P}_{nl_x} + \mathbf{P}_{2_x} - \mathbf{M}^1_{,x} - \mathbf{M}^2_{,y})n_x + (\mathbf{P}_{nl_y} + \mathbf{P}_{2_y} - \mathbf{M}^2_{,x} - \mathbf{M}^3_{,y})n_y]\,ds \end{aligned} \tag{4.16}$$

where

$$\begin{aligned} \mathbf{H}^1_j &= \int_{-h/2}^{h/2}(\mathbf{A}^T_{nl_x} + \mathbf{A}^T_{2_x})\mathbf{C}\mathbf{A}_j\,dz \\ \mathbf{H}^2_j &= \int_{-h/2}^{h/2}(\mathbf{A}^T_{nl_y} + \mathbf{A}^T_{2_y})\mathbf{C}\mathbf{A}_j\,dz, \quad \text{where } j = 2_x, 2_y, nl_x, nl_y \end{aligned} \tag{4.17}$$

and the weak forms of Eqs. (4.13) are

$$\begin{aligned} 0 &= \int_\Omega \Big[\Delta\ \delta M_{11,x}w_{,x} + D_{11}\delta M_{11}M_{11} + D_{12}\delta M_{11}M_{12} + D_{13}\delta M_{11}M_{22}\Big]\,dx\,dy \\ &\quad -\oint_{\partial\Omega}\Delta\delta M_{11}w_{,x}n_x ds \end{aligned}$$

$$
\begin{aligned}
0 &= \int_\Omega \Big[\frac{\Delta}{2}\left(\delta M_{12,x} w_{,y} + \delta M_{12,y} w_{,x}\right) + D_{21}\delta M_{12} M_{11} + D_{22}\delta M_{12} M_{12} \\
&\quad + D_{23}\delta M_{12} M_{22}\Big]\, dx\, dy - \oint_{\partial\Omega} \frac{\Delta}{2}\delta M_{12}(w_{,y} n_x + w_{,x} n_y) ds \\
0 &= \int_\Omega \Big[\Delta\ \delta M_{22,y} w_{,y} + D_{31}\delta M_{22} M_{11} + D_{32}\delta M_{22} M_{12} + D_{33}\delta M_{22} M_{22}\Big]\, dx\, dy \\
&\quad - \oint_{\partial\Omega} \Delta \delta M_{22} w_{,y} n_y ds \\
0 &= \int_\Omega \Big[\frac{hG\ell_5^2}{2}\left(-\delta M_{1,x} u_{,y} - \delta M_{1,y} u_{,x} + 2\delta M_{1,x} v_{,x}\right) + \delta M_1 M_1\Big]\, dx\, dy \\
&\quad - \oint_{\partial\Omega} \delta M_1((v_x - u_y) n_x - u_{,x} n_y)\, ds \\
0 &= \int_\Omega \Big[\frac{hG\ell_6^2}{2}\left(-2\delta M_{2,y} u_{,y} + \delta M_{2,y} v_{,x} + \delta M_{2,x} v_{,y}\right) + \delta M_2 M_2\Big]\, dx\, dy \\
&\quad - \oint_{\partial\Omega} \delta M_2((v_x - u_y) n_y + v_{,y} n_x)\, ds
\end{aligned}
\tag{4.18}
$$

Let us write the augmented vector of unknown variables as

$$
\begin{aligned}
\mathbf{\Phi}^a &= [u \quad v \quad w \quad M_{11} \quad M_{12} \quad M_{22} \quad M_1 \quad M_2]^T \\
\hat{\mathbf{F}}^a &= [f_x \quad f_y \quad f_z \quad 0 \quad 0 \quad 0 \quad 0 \quad 0]^T
\end{aligned}
\tag{4.19}
$$

We can write the above weak form in the following vector form:

$$
\begin{aligned}
\int_\Omega \delta\mathbf{\Phi}^a \cdot \hat{\mathbf{F}}^a\, dx\, dy = \int_\Omega \Big[&\delta\mathbf{\Phi}^a \cdot (\mathbf{B}\mathbf{\Phi}^a) + \delta\mathbf{\Phi}^a_{,x} \cdot (\mathbf{B}_{xx}\mathbf{\Phi}^a_{,x} + \mathbf{B}_{xy}\mathbf{\Phi}^a_{,y}) \\
&+ \delta\mathbf{\Phi}^a_{,y} \cdot (\mathbf{B}_{yx}\mathbf{\Phi}^a_{,x} + \mathbf{B}_{yy}\mathbf{\Phi}^a_{,y}) + \delta\mathbf{\Phi}^a_{,x} \cdot \left(\frac{1}{2}\hat{\mathbf{H}}^1_{nl_x}\mathbf{\Phi}^a_{,x} + \frac{1}{2}\hat{\mathbf{H}}^1_{nl_y}\mathbf{\Phi}^a_{,y}\right) \\
&+ \delta\mathbf{\Phi}^a_{,y} \cdot \left(\frac{1}{2}\hat{\mathbf{H}}^2_{nl_x}\mathbf{\Phi}^a_{,x} + \frac{1}{2}\hat{\mathbf{H}}^2_{nl_y}\mathbf{\Phi}^a_{,y}\right)\Big]\, dx\, dy - \oint_{\partial\Omega} \delta\mathbf{\Phi}^a \cdot \mathbf{V}\, ds
\end{aligned}
\tag{4.20}
$$

where

$$
\begin{aligned}
&\mathbf{B} = \begin{bmatrix} \mathbf{k} & \mathbf{0} \\ \mathbf{0} & \tilde{\mathbf{D}} \end{bmatrix}, \quad \mathbf{B}_{xx} = \begin{bmatrix} \mathbf{H}^1_{2x} & \mathbf{G}_{xx} \\ \mathbf{N}_{xx} & \mathbf{0} \end{bmatrix}, \quad \mathbf{B}_{xy} = \begin{bmatrix} \mathbf{H}^1_{2y} & \mathbf{G}_{xy} \\ \mathbf{N}_{xy} & \mathbf{0} \end{bmatrix}, \\
&\mathbf{B}_{yx} = \begin{bmatrix} \mathbf{H}^2_{2x} & \mathbf{G}_{yx} \\ \mathbf{N}_{yx} & \mathbf{0} \end{bmatrix}, \quad \mathbf{B}_{yy} = \begin{bmatrix} \mathbf{H}^2_{2y} & \mathbf{G}_{yy} \\ \mathbf{N}_{yy} & \mathbf{0} \end{bmatrix}, \quad \tilde{\mathbf{D}} = \begin{bmatrix} \mathbf{D} & \mathbf{0} \\ \mathbf{0} & \mathbf{I} \end{bmatrix}
\end{aligned}
\tag{4.21}
$$

$$\hat{\mathbf{H}}^1_{nl_x} = \begin{bmatrix} \mathbf{H}^1_{nl_x} & \mathbf{0} \\ \mathbf{0} & \mathbf{0} \end{bmatrix},\ \hat{\mathbf{H}}^1_{nl_y} = \begin{bmatrix} \mathbf{H}^1_{nl_y} & \mathbf{0} \\ \mathbf{0} & \mathbf{0} \end{bmatrix},\ \hat{\mathbf{H}}^2_{nl_x} = \begin{bmatrix} \mathbf{H}^2_{nl_x} & \mathbf{0} \\ \mathbf{0} & \mathbf{0} \end{bmatrix},\ \hat{\mathbf{H}}^2_{nl_y} = \begin{bmatrix} \mathbf{H}^2_{nl_y} & \mathbf{0} \\ \mathbf{0} & \mathbf{0} \end{bmatrix} \tag{4.22}$$

$$\mathbf{G}_{xx} = \begin{bmatrix} 0 & 0 & 0 & 0 & 0 \\ 0 & 0 & 0 & -1 & 0 \\ -1 & 0 & 0 & 0 & 0 \end{bmatrix}, \quad \mathbf{G}_{yy} = \begin{bmatrix} 0 & 0 & 0 & 0 & 1 \\ 0 & 0 & 0 & 0 & 0 \\ 0 & 0 & -1 & 0 & 0 \end{bmatrix}$$
$$\mathbf{G}_{xy} = \mathbf{G}_{yx} = \begin{bmatrix} 0 & 0 & 0 & 0.5 & 0 \\ 0 & 0 & 0 & 0 & -0.5 \\ 0 & -0.5 & 0 & 0 & 0 \end{bmatrix} \tag{4.23}$$

$$\mathbf{N}_{xx} = \begin{bmatrix} 0 & 0 & \Delta \\ 0 & 0 & 0 \\ 0 & 0 & 0 \\ 0 & hG\ell_5^2 & 0 \\ 0 & 0 & 0 \end{bmatrix}, \quad \mathbf{N}_{yy} = \begin{bmatrix} 0 & 0 & 0 \\ 0 & 0 & 0 \\ 0 & 0 & \Delta \\ 0 & 0 & 0 \\ -hG\ell_6^2 & 0 & 0 \end{bmatrix},$$
$$\mathbf{N}_{xy} = \mathbf{N}_{yx} = \begin{bmatrix} 0 & 0 & 0 \\ 0 & 0 & \frac{\Delta}{2} \\ 0 & 0 & 0 \\ -\frac{hG\ell_5^2}{2} & 0 & 0 \\ 0 & \frac{hG\ell_6^2}{2} & 0 \end{bmatrix} \tag{4.24}$$

and the boundary term $\mathbf{V}$ is:

$$\mathbf{V} = \left\{ \begin{array}{c} (\mathbf{P}_{nl_x} + \mathbf{P}_{2_x} - \mathbf{M}^1_{,x} - \mathbf{M}^2_{,y})n_x + (\mathbf{P}_{nl_y} + \mathbf{P}_{2_y} - \mathbf{M}^2_{,x} - \mathbf{M}^3_{,y})n_y \\ \Delta w_{,x} n_x \\ \frac{\Delta}{2}(w_{,y} n_x + w_{,x} n_y) \\ \Delta w_{,y} n_y \\ (-u_y + v_x)n_x - u_{,x} n_y \\ (-u_y + v_x)n_y + v_{,y} n_x \end{array} \right\} \tag{4.25}$$

4.1.3. Finite element model

We discretize the computational domain into a set of non-overlapping subdomains (elements), Ω^e and approximate the vector of unknown variables as

$$\mathbf{\Phi}^a(x) = \mathbf{\Psi}(x)\mathbf{U} \tag{4.26}$$

where $\mathbf{\Psi}(x, y)$ is the matrix of approximation (or interpolation) functions and $\mathbf{U}$ is vector of the nodal values of $\mathbf{\Phi}^a$,

$$\mathbf{\Psi} = \left[\begin{array}{ccccccccccc} \psi_1^{(1)} & \dots & \psi_{n_1}^{(1)} & 0 & \dots & 0 & \dots & 0 & \dots & 0 \\ 0 & \dots & 0 & \psi_1^{(2)} & \dots & \psi_{n_2}^{(2)} & \dots & 0 & \dots & 0 \\ \vdots & \ddots & \vdots & \vdots & \ddots & \vdots & \ddots & \vdots & \ddots & \vdots \\ 0 & \dots & 0 & 0 & \dots & 0 & \dots & \psi_1^{(8)} & \dots & \psi_{n_8}^{(8)} \end{array} \right] \tag{4.27}$$

$$\mathbf{U} = \left[\begin{array}{ccccccccc} u_{1_1} & \dots & u_{1_{\tilde{n}_1}} & u_{2_1} & \dots & u_{2_{n_2}} & \dots & u_{8_1} & \dots & u_{8_{n_8}} \end{array} \right]^T \tag{4.28}$$

Here $n_1, n_2, \cdots n_8$ are the number of nodal values of $u_1, u_2, \dots, u_8$, respectively, in the element, and

$$u_1 = u, \quad u_2 = v, \quad u_3 = w, \quad u_4 = M_{11}, \quad u_5 = M_{12}, \quad u_6 = M_{22}, \quad u_7 = M_1, \quad u_8 = M_2. \tag{4.29}$$

We substitute the approximations of the degrees of freedom (dofs) and $\delta\mathbf{\Phi}^a = \mathbf{\Psi}\mathbf{l}$ (where $\mathbf{l}$ is vector with each element as unity and of the same size as $\mathbf{\Phi}^a$) into

Eq. (4.20) and arrive at the following finite element equations:

$$\mathbf{KU} - \mathbf{f} = \mathbf{0} \tag{4.30}$$

where $\mathbf{K}$ is the stiffness matrix, which is given as follows:

$$\begin{aligned}
\mathbf{K} &= \int_\Omega^e \Big[\mathbf{\Psi}^T \mathbf{B} \mathbf{\Psi} + \mathbf{\Psi}_{,x}^T (\mathbf{B}_{xx} \mathbf{\Psi}_{,x} + \mathbf{B}_{xy} \mathbf{\Psi}_{,y}) + \mathbf{\Psi}_{,y}^T (\mathbf{B}_{yx} \mathbf{\Psi}_{,x} + \mathbf{B}_{yy} \mathbf{\Psi}_{,y}) \\
&\quad + \mathbf{\Psi}_{,x}^T \left(\frac{1}{2} \hat{\mathbf{H}}_{nl_x}^1 \mathbf{\Psi}_{,x} + \frac{1}{2} \hat{\mathbf{H}}_{nl_y}^1 \mathbf{\Psi}_{,y} \right) + \mathbf{\Psi}_{,y}^T \left(\frac{1}{2} \hat{\mathbf{H}}_{nl_x}^2 \mathbf{\Psi}_{,x} + \frac{1}{2} \hat{\mathbf{H}}_{nl_y}^2 \mathbf{\Psi}_{,y} \right) \Big] \, dx \, dy \\
\mathbf{f} &= \int_\Omega^e \mathbf{\Psi}^T \hat{\mathbf{F}}^a \, dx \, dy
\end{aligned} \tag{4.31}$$

Here we note that stiffness matrix is not symmetric and depends on the displacement (i.e., nonlinear). We will apply Newton's method to solve the nonlinear algebraic equations in Eq. (4.30). For $(j+1)$st iteration of Newton's method, the solution can be expressed as

$$\mathbf{T}(\mathbf{U}_j) \delta \mathbf{U}_{j+1} = -\mathbf{K}(\mathbf{U}_j) \mathbf{U}_j + \mathbf{f}(\mathbf{U}_j), \quad \text{and } \mathbf{U}_{j+1} = \mathbf{U}_j + \delta \mathbf{U}_{j+1} \tag{4.32}$$

where $\mathbf{T}$ is the tangent matrix,

$$\begin{aligned}
\mathbf{T} &= \mathbf{K} + \int_{\Omega^e} \Big[\frac{1}{2} \Big(\mathbf{\Psi}_{,x}^T \left(\mathbf{H}_{nl_x}^1 \mathbf{\Psi}_{,x} + \mathbf{H}_{nl_y}^1 \mathbf{\Psi}_{,y} \right) + \mathbf{\Psi}_{,y}^T \left(\mathbf{H}_{nl_x}^2 \mathbf{\Psi}_{,x} + \mathbf{H}_{nl_y}^2 \mathbf{\Psi}_{,y} \right) \\
&\quad + \mathbf{\Psi}_{,x}^T \mathbf{P}_{nl}^x \mathbf{\Psi}_{,x} + \mathbf{\Psi}_{,y}^T \mathbf{P}_{nl}^y \mathbf{\Psi}_{,y} + \mathbf{\Psi}_{,x}^T \mathbf{P}_{nl}^{xy} \mathbf{\Psi}_{,y} + \mathbf{\Psi}_{,y}^T \mathbf{P}_{nl}^{xy} \mathbf{\Psi}_{,x} \Big] \, dx \, dy
\end{aligned} \tag{4.33}$$

and $\mathbf{P}_{nl}^x$, $\mathbf{P}_{nl}^y$ and $\mathbf{P}_{nl}^{xy}$ are (8×8) matrices with following nonzero coefficients,

$$P_{nl_{33}}^x = \int_{-h/2}^{h/2} S_{xx}^s \, dz, \quad P_{nl_{33}}^y = \int_{-h/2}^{h/2} S_{yy}^s \, dz, \quad P_{nl_{33}}^{xy} = \int_{-h/2}^{h/2} S_{xy}^s \, dz \tag{4.34}$$

We note here that the tangent matrix is symmetric.

4.1.4. Contact stiffness of the elastic substrate

To model the nano indentation of hard coating on an elastic substrate, we model the coating as a classical plate resting on an elastic substrate. A flat circular punch of very small radius is applied at the center of computational domain of the coating by a rigid indenter. As the plate bends due to the applied load at the center, the flat surface of the coating becomes curved and can be approximated as a part of a sphere of large radius. This curved surface can be modeled as the contact region between

the rigid sphere (as hard coating) on the elastic half space. But we do not know the radius of the sphere or the contact radius in advance. Therefore, we guess an initial area of influence in the numerical calculations and then increase the area to obtain a convergent indentation depth for contact area iteratively. The Hertzian pressure distribution (see [54]) for this case is given by

$$\hat{p}(r) = p_0 \left(1 - \frac{r^2}{a^2}\right)^{\frac{1}{2}} \tag{4.35}$$

where $\hat{p}(r)$ is the pressure distribution at a distance r from the center of the contact circle and p_0 is the limiting pressure at the center. The transverse displacement of the substrate at any distance r from the centre in the contact circle can be expressed as (see [54]):

$$\hat{u}_z(r) \;=\; \frac{\pi p_0}{4E^* a}\left(2a^2 - r^2\right) \tag{4.36}$$

Then the contact stiffness can be computed as

$$k_0 = \frac{\hat{p}(r)}{\hat{u}_z} \tag{4.37}$$

Here the contact between the coating and the substrate has been considered as very smooth and frictionless. No surface roughness has been taken into account, which could result in an elevated contact stiffness (see Polycarpou [55]) and hence this approximation would result in lesser indentation depth as compared to an experimental value; nevertheless, we can study the effect of the length scale parameter on indentation. The model can be improved by taking roughness and friction into account.

4.2. Numerical study

Let us consider CNT-reinforced coating with matrix material as aluminium on an aluminum substrate. The material properties of the coating and substrate and the height of the coating are taken as follows:

$$E = 69 \text{ GPa}, \quad \nu = 0.34, \quad h = 20 \ \mu\text{m} \tag{4.38}$$

For the finite element analysis of the indentation on such coatings, we approximate the unknown variables of the mixed formulation discussed in the preceding section

using linear Lagrange interpolation functions. The computational domain is considered as an annular plate with inner radius the same as the radius of the indenter's tip. In the present numerical examples, we consider indenter of radius 10^{-6} m (1 micron). The outer radius of the computational domain is same as the contact radius between the coating and the substrate, which we do not know in advance. The mesh used for the finite element analysis is shown in fig. 4.2; 30 quadrilateral elements are used on each concentric circle, and the size of the element is such that radial length of the element is the same as the length of the side, which is near the center. This way the mesh density and the total number of elements are governed by the outer radius of the domain and the number of element in each concentric circle (let us call this number n_c). The CNT reinforcement is modeled by the material length scale. Since the CNT strands are randomly oriented, we take all the length scale related to the various curvatures as equal, that is, $\ell_2 = \ell_3 = \ell_5 = \ell_6 = \ell$. The material length scale related to the twist are taken as zero owing to the fact that the diameter of the CNT strands are small compared to their length, and hence it resists the bending prominently than twisting. The boundary conditions at the outer circumference of the computational domain are taken as free. Table 4.1 shows the indentation depth on the coating for different mesh densities (governed by n_c); the indentation force is equal to 10 mN and $\ell/h = 0.5$. It can be observed that the indentation depth converged for denser mesh densities. For further study, we take $n_c = 30$ and the radius

Table 4.1. Indentation depth for various grid density and computational domain for indenting force, $F_0 = 10$ mN

R_{outer} (μm)	w_{max} (nm) $n_c = 10$	w_{max} (nm) $n_c = 15$	w_{max} (nm) $n_c = 20$	w_{max} (nm) $n_c = 25$	w_{max} (nm) $n_c = 30$
50	0.1928	0.1973	0.1988	0.1995	0.1999
100	0.1919	0.1969	0.1986	0.1994	0.1998
150	0.1919	0.1968	0.1986	0.1994	0.1998
200	0.1919	0.1968	0.1986	0.1994	0.1998

of computational domain as 200 μm. Figure 4.3 shows a plot of indentation for various values of the material length scale. We observe that as the material length scale

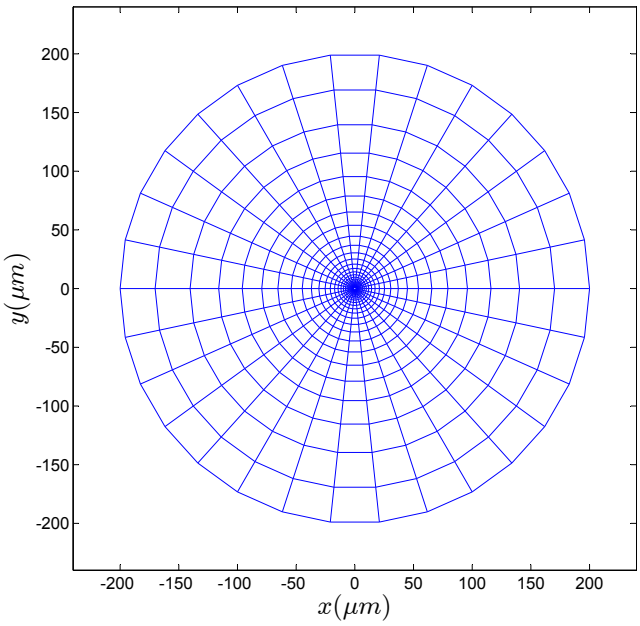

Fig. 4.2 The grid for the computational domain for FE analysis.

increases the indentation depth decreases, and the indentation gets little bit more spread over the area. As the larger value of the material length scale characterized by denser CNT reinforcement, one can expect such behavior because the coating becomes harder in such cases. Figure 4.4 shows the variation of the indentation depth with respect to the indentation force for various values of the material length scale and the same with respect to the material length scale for different values of the indentation force.

4.3. Chapter summary and conclusions

In this chapter, we have applied the rotation gradient dependent theory to analyze nanoindentation of CNT-reinforced hard coatings on elastic substrates. Since such gradient dependent theory requires C^1 continuity of the displacement variables, which is difficult to achieve in the case of a general quadrilateral element, a mixed finite element formulation that requires C^0 continuity of displacements and moments is developed. The contact stiffness is obtained assuming smooth contact between the coating and the substrate. We observe a stiffer response in the case of larger values

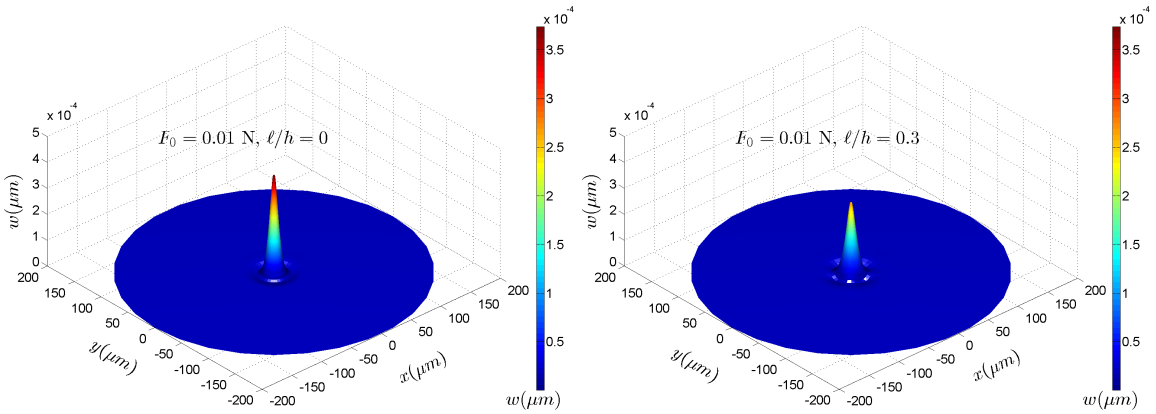

(a) $\ell/h = 0$ (b) $\ell/h = 0.3$

(c) $\ell/h = 0.5$ (d) $\ell/h = 1$

Fig. 4.3 Indentation on the CNT reinforced coating on elastic substrate considering different material length scale.

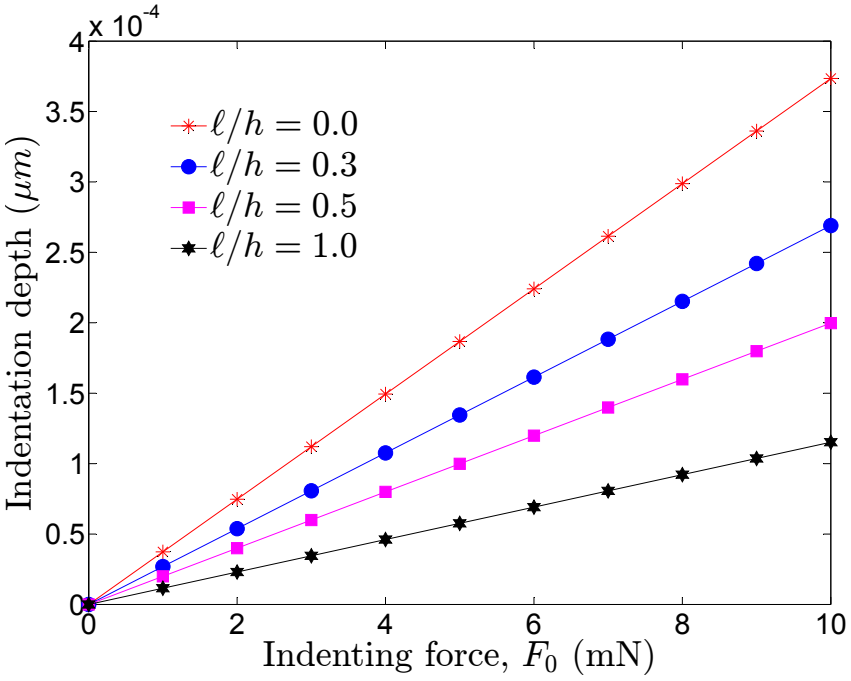

(a) Indentation depth Vs load applied

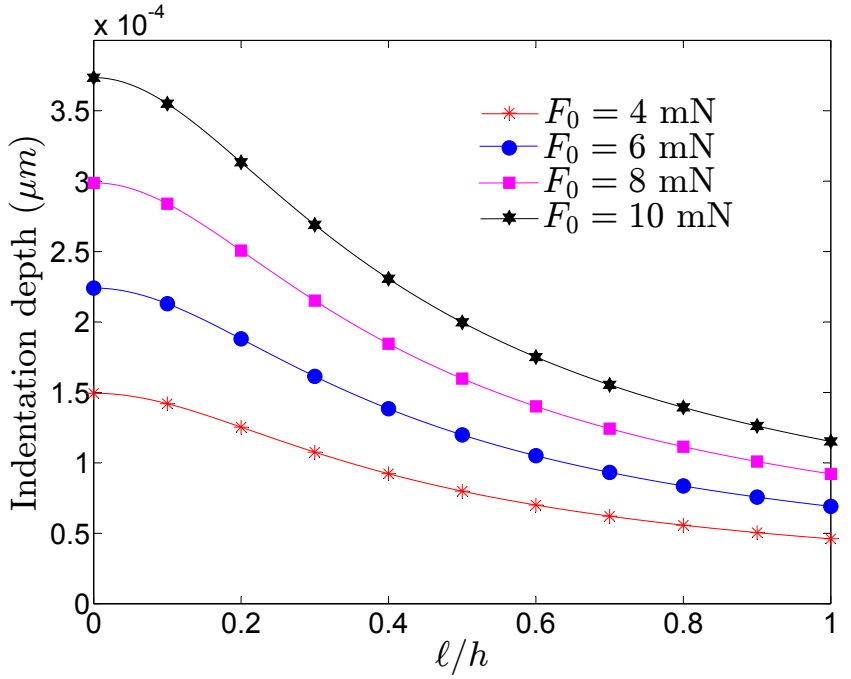

(b) Indentation depth Vs ℓ/h

Fig. 4.4 Variation of indentation depth Vs indenting force applied and the material length scale ratio, ℓ/h

of the material length scale parameter. In the present model of contact between coating and substrate, no friction or roughness of the surfaces has been taken into consideration; this omission may result in elevated values of the contact stiffness and hence a stiffer response. To obtain a more realistic model, both the surface roughness and the friction should be considered.

5. A GENERAL HIGHER-ORDER THEORY FOR ONE-DIMENSIONAL ANALYSIS

5.1. Introduction

In this chapter, we develop a general higher-order theory to analyze three-dimensional body by one-dimensional model. All solid bodies are three-dimensional and can be analyzed by 3-D elasticity to obtain their response due to various stimuli. The reduction of dimensionality is very common in solid mechanics. For example, various beam theories convert the 3-D problem into 1-D problem by approximating the kinematics of deformation of the beam cross-section. Similarly, various plate and shell theories (see Reddy [56]) convert the 3-D problem into 2-D problem by approximating the deformation of lines perpendicular to the mid-surface of the plate or shell. The approximation of the deformation of cross-section in the case of beam theories is such that it can be said to be a good approximation if the width and height are less compared to the length of the body; similar is the case of plate and shell theories when the thickness is very small compared to the inplane dimensions. In the present study, we generalize the assumed approximation of the displacement field of the cross-section or slices of the solid body by considering general basis functions in the polar coordinate system in the plane of the cross-section, for example, by the Fourier series in polar coordinate or other similar series of polynomial basis functions. In such approximations of the displacement field, the coefficients of various basis functions have attenuating values for higher-order basis functions. Hence truncated Fourier series or other appropriate polynomial series would be good enough for approximating the displacement field of the cross-section of a body. Based on such prior general displacement approximation, we use the principle of virtual displacement to obtain the governing differential equation of a three-dimensional body, with the coefficients of the basis functions used in approximation as unknowns in the case of large deformation.

The present formulation of converting three-dimensional problem to one-dimensional problem and developing its finite element model have not been reported in present solid mechanics literature. Solid mechanics problems of three- or two-dimensional bodies can be analyzed by three- or two-dimensional finite element models, but

one-dimensional analysis of such problem certainly reduces the computational effort. One-dimensional finite element model allows higher-order continuity (i.e., $C^n,\ n > 0$ continuity) or any order with any number of nodes with the general Hermite interpolation functions, which is not possible in the case of two- or three-dimensional problems. Problems with higher-order continuity requirement of the unknown variables arises very often in Cosserat continuum and other nonlocal continuum theories; for example, rotation gradient dependent theory for Cosserat continua (see Srinivasa and Reddy [19] and Arbind, Reddy and Srinivasa [52, 57]) require C^1 continuity of the dependent variables in the case of beam, plate, and shell structures. Other higher-order strain gradient-dependent theories (see Khodabakhshi and Reddy [58]) require C^2 or higher-order continuity of unknown variables. In such cases, reduction of 2-D or 3-D problem to 1-D analysis would be very useful as far as finite element modeling is concerned.

For the present higher-order theory, a nonlinear finite element model is also developed. This model can be used to analyze various shell structures (e.g., cylindrical with constant or varying radius or structures with solid arbitrary cross-sections). Other applications could be to model straight ducts or beams with arbitrary cross sections under a system of body or traction forces in three dimensions. The existing 2-D or 3-D beam theories would not be able to model such a phenomenon.

5.2. The governing equation of motion

Let us consider a cylindrical coordinate system (x, r, θ) in the reference frame of the solid body, whose axis coincide with the x-axis. The polar coordinate (r, θ) define the cross-section of the body, whose normal is along the x-axis. The solid body is acted upon a system of body and traction forces which tend to deform the body. The displacement field at a point in the assumed coordinate system is given by

$$\mathbf{u} = u_x\hat{\mathbf{e}}_x + u_r\hat{\mathbf{e}}_r + u_\theta\hat{\mathbf{e}}_\theta \tag{5.1}$$

where $\hat{\mathbf{e}}_x,\ \hat{\mathbf{e}}_r$, and $\hat{\mathbf{e}}_\theta$ are orthonormal basis vectors. In full generality, we approximate the components of displacement field of the cross-section of the body as follows:

$$u_x = \phi_x^{(0)}(x) + \sum_{j=1}^{n_\theta}\sum_{i=0}^{n_r} f_i(r)(\sin(j\theta)\phi_x^{(k_1)}(x) + \cos(j\theta)\phi_x^{(k_2)}(x)) = \mathbf{A}_x\mathbf{\Phi}_x$$

$$u_r = \phi_r^{(0)}(x) + \sum_{j=1}^{m_\theta}\sum_{i=0}^{m_r} f_i(r)(\sin(j\theta)\phi_r^{(k_1)}(x) + \cos(j\theta)\phi_r^{(k_2)}(x)) = \mathbf{A}_r\mathbf{\Phi}_r$$
$$u_\theta = \phi_\theta^{(0)}(x) + \sum_{j=1}^{p_\theta}\sum_{i=0}^{p_r} f_i(r)(\sin(j\theta)\phi_\theta^{(k_1)}(x) + \cos(j\theta)\phi_\theta^{(k_2)}(x)) = \mathbf{A}_\theta\mathbf{\Phi}_\theta \quad (5.2)$$

where

$$\begin{aligned}
\mathbf{A}_x &= [\mathbf{a}_x \quad (\cos\theta)\mathbf{a}_x \quad (\sin\theta)\mathbf{a}_x \quad (\cos 2\theta)\mathbf{a}_x \quad (\sin 2\theta)\mathbf{a}_x \quad \dots \quad (\cos n_\theta\theta)\mathbf{a}_x \quad (\sin n_\theta\theta)\mathbf{a}_x] \\
\mathbf{A}_r &= [\mathbf{a}_r \quad (\cos\theta)\mathbf{a}_r \quad (\sin\theta)\mathbf{a}_r \quad (\cos 2\theta)\mathbf{a}_r \quad (\sin 2\theta)\mathbf{a}_r \quad \dots \quad (\cos m_\theta\theta)\mathbf{a}_r \quad (\sin m_\theta\theta)\mathbf{a}_r] \\
\mathbf{A}_\theta &= [\mathbf{a}_\theta \quad (\cos\theta)\mathbf{a}_\theta \quad (\sin\theta)\mathbf{a}_\theta \quad (\cos 2\theta)\mathbf{a}_\theta \quad (\sin 2\theta)\mathbf{a}_\theta \quad \dots \quad (\cos p_\theta\theta)\mathbf{a}_\theta \quad (\sin p_\theta\theta)\mathbf{a}_\theta]
\end{aligned} \quad (5.3)$$

where

$$\begin{aligned}
\mathbf{a}_x &= [1 \quad f_1(r) \quad f_2(r) \quad \dots \quad f_{n_r}(r)] \\
\mathbf{a}_r &= [1 \quad f_1(r) \quad f_2(r) \quad \dots \quad f_{m_r}(r)] \\
\mathbf{a}_\theta &= [1 \quad f_1(r) \quad f_2(r) \quad \dots \quad f_{p_r}(r)]
\end{aligned} \quad (5.4)$$

and

$$\begin{aligned}
\mathbf{\Phi}_x &= [\phi_x^{(0)} \quad \phi_x^{(1)} \quad \phi_x^{(2)} \quad \dots \quad \phi_x^{(\tilde{n})}]^T, \quad \tilde{n} = (1+n_r)(1+2n_\theta) \\
\mathbf{\Phi}_r &= [\phi_r^{(0)} \quad \phi_r^{(1)} \quad \phi_r^{(2)} \quad \dots \quad \phi_r^{(\tilde{m})}]^T, \quad \tilde{m} = (1+m_r)(1+2m_\theta) \\
\mathbf{\Phi}_\theta &= [\phi_\theta^{(0)} \quad \phi_\theta^{(1)} \quad \phi_\theta^{(2)} \quad \dots \quad \phi_\theta^{(\tilde{p})}]^T, \quad \tilde{p} = (1+p_r)(1+2p_\theta)
\end{aligned} \quad (5.5)$$

where $f_i(r)$ are basis functions of r, which could a polynomial of the type $f_i(r) = r^i$ or linear combination of Bessel functions of the first and second kinds. If we consider linear combination of Bessel functions of the first and second kinds for $f_i(r)$, the approximations of displacement components become the Fourier series in the polar coordinate system; $\phi_x^{(0)} = u$, $\phi_r^{(0)} = v$, and $\phi_\theta^{(0)} = w$ are the displacements of the centroid of the cross-section along the unit basis vectors of the assumed coordinate system, namely, $\hat{\mathbf{e}}_x, \hat{\mathbf{e}}_r$, and $\hat{\mathbf{e}}_\theta$, respectively. The displacement vector at a point can

be written as:

$$\mathbf{u} = \mathbf{A}\mathbf{\Phi}, \quad \text{where } \mathbf{A} = \begin{bmatrix} \mathbf{A}_x & \mathbf{0} & \mathbf{0} \\ \mathbf{0} & \mathbf{A}_r & \mathbf{0} \\ \mathbf{0} & \mathbf{0} & \mathbf{A}_\theta \end{bmatrix}, \quad \mathbf{\Phi} = \begin{Bmatrix} \mathbf{\Phi}_x \\ \mathbf{\Phi}_r \\ \mathbf{\Phi}_\theta \end{Bmatrix}, \quad \mathbf{u} = \begin{Bmatrix} u_x \\ u_r \\ u_\theta \end{Bmatrix} \tag{5.6}$$

Based on the above displacement field, the components of Green–Lagrange strain tensor in the assumed cylindrical coordinate system can be given as follows:

$$\begin{aligned}
E_{xx} &= \mathbf{A}_x\mathbf{\Phi}_{x,x} + (1/2)((\mathbf{A}_x\mathbf{\Phi}_{x,x})^2 + (\mathbf{A}_\theta\mathbf{\Phi}_{\theta,x})^2 + (\mathbf{A}_r\mathbf{\Phi}_{r,x})^2) \\
E_{rr} &= \mathbf{A}_{r,r}\mathbf{\Phi}_r + (1/2)\left((\mathbf{A}_{r,r}\mathbf{\Phi}_r)^2 + (\mathbf{A}_{\theta,r}\mathbf{\Phi}_\theta)^2 + (\mathbf{A}_{x,r}\mathbf{\Phi}_x)^2\right) \\
E_{\theta\theta} &= (1/r)(\mathbf{A}_r\mathbf{\Phi}_r + \mathbf{A}_{\theta,\theta}\mathbf{\Phi}_\theta) + (1/2r^2)((\mathbf{A}_{r,\theta}\mathbf{\Phi}_r - \mathbf{A}_\theta\mathbf{\Phi}_\theta)^2 \\
&\quad +(\mathbf{A}_r\mathbf{\Phi}_r + \mathbf{A}_{\theta,\theta}\mathbf{\Phi}_\theta)^2 + (\mathbf{A}_{x,\theta}\mathbf{\Phi}_x)^2) \\
2E_{r\theta} &= (1/r)\mathbf{A}_{r,\theta}\mathbf{\Phi}_r + \mathbf{A}_{\theta,r}\mathbf{\Phi}_\theta - (1/r)\mathbf{A}_\theta\mathbf{\Phi}_\theta + (1/r)((\mathbf{A}_{r,r}\mathbf{\Phi}_r)(\mathbf{A}_{r,\theta}\mathbf{\Phi}_r - \mathbf{A}_\theta\mathbf{\Phi}_\theta) \\
&\quad +(\mathbf{A}_{\theta,r}\mathbf{\Phi}_\theta)(\mathbf{A}_r\mathbf{\Phi}_r + \mathbf{A}_{\theta,\theta}\mathbf{\Phi}_\theta) + (\mathbf{A}_{x,r}\mathbf{\Phi}_x)(\mathbf{A}_{x,\theta}\mathbf{\Phi}_x)) \\
2E_{rx} &= \mathbf{A}_r\mathbf{\Phi}_{r,x} + \mathbf{A}_{x,r}\mathbf{\Phi}_x + (\mathbf{A}_{r,r}\mathbf{\Phi}_r)(\mathbf{A}_r\mathbf{\Phi}_{r,x}) + (\mathbf{A}_{\theta,r}\mathbf{\Phi}_\theta)(\mathbf{A}_\theta\mathbf{\Phi}_{\theta,x}) \\
&\quad +(\mathbf{A}_{x,r}\mathbf{\Phi}_x)(\mathbf{A}_x\mathbf{\Phi}_{x,x}) \\
2E_{\theta x} &= \mathbf{A}_\theta\mathbf{\Phi}_{\theta,x} + (1/r)\mathbf{A}_{x,\theta}\mathbf{\Phi}_x + (1/r)((\mathbf{A}_{r,\theta}\mathbf{\Phi}_r - \mathbf{A}_\theta\mathbf{\Phi}_\theta)(\mathbf{A}_r\mathbf{\Phi}_{r,x}) \\
&\quad +(\mathbf{A}_{\theta,\theta}\mathbf{\Phi}_\theta + \mathbf{A}_r\mathbf{\Phi}_r)(\mathbf{A}_\theta\mathbf{\Phi}_{\theta,x}) + (\mathbf{A}_{x,\theta}\mathbf{\Phi}_x)(\mathbf{A}_x\mathbf{\Phi}_{x,x}))
\end{aligned} \tag{5.7}$$

where $(\ )_{,x}$ represent the derivative with respect to x and so on. The Green-Lagrange strain tensor can be rewritten in vector form as:

$$\mathbf{E} = (\mathbf{A}_1 + \frac{1}{2}\mathbf{A}_{nl})\mathbf{\Phi} + (\mathbf{A}_2 + \frac{1}{2}\mathbf{A}_{nl_x})\frac{d\mathbf{\Phi}}{dx} \tag{5.8}$$

where

$$\mathbf{E} = \begin{bmatrix} E_{xx} & E_{rr} & E_{\theta\theta} & 2E_{r\theta} & 2E_{rx} & 2E_{\theta x} \end{bmatrix}^T, \quad \mathbf{\Phi} = \begin{bmatrix} \mathbf{\Phi}_x^T & \mathbf{\Phi}_r^T & \mathbf{\Phi}_\theta^T \end{bmatrix}^T$$

$$\mathbf{A}_1 = \begin{bmatrix} \mathbf{0} & \mathbf{0} & \mathbf{0} \\ \mathbf{0} & \mathbf{A}_{r,r} & \mathbf{0} \\ \mathbf{0} & (1/r)\mathbf{A}_r & (1/r)\mathbf{A}_{\theta,\theta} \\ \mathbf{0} & (1/r)\mathbf{A}_{r,\theta} & \mathbf{A}_{\theta,r} - (1/r)\mathbf{A}_\theta \\ \mathbf{A}_{x,r} & \mathbf{0} & \mathbf{0} \\ (1/r)\mathbf{A}_{x,\theta} & \mathbf{0} & \mathbf{0} \end{bmatrix}, \quad \mathbf{A}_2 = \begin{bmatrix} \mathbf{A}_x & \mathbf{0} & \mathbf{0} \\ \mathbf{0} & \mathbf{0} & \mathbf{0} \\ \mathbf{0} & \mathbf{0} & \mathbf{0} \\ \mathbf{0} & \mathbf{0} & \mathbf{0} \\ \mathbf{0} & \mathbf{A}_r & \mathbf{0} \\ \mathbf{0} & \mathbf{0} & \mathbf{A}_\theta \end{bmatrix}$$

$$
\mathbf{A}_{nl} = \begin{bmatrix}
\mathbf{0} & \mathbf{0} & \mathbf{0} \\
u_{x,r}\mathbf{A}_{x,r} & u_{r,r}\mathbf{A}_{r,r} & u_{\theta,r}\mathbf{A}_{\theta,r} \\
\frac{u_{x,\theta}}{r^2}\mathbf{A}_{x,\theta} & \frac{1}{r^2}\Big\{(u_{r,\theta}-u_\theta)\mathbf{A}_{r,\theta} \\ \quad +(u_r+u_{\theta,\theta})\mathbf{A}_r\Big\} & \frac{1}{r^2}\Big\{(u_\theta-u_{r,\theta})\mathbf{A}_\theta \\ \quad +(u_r+u_{\theta,\theta})\mathbf{A}_{\theta,\theta}\Big\} \\
\frac{1}{r}\Big\{u_{x,r}\mathbf{A}_{x,\theta} & \frac{1}{r}\Big\{(u_{r,\theta}-u_\theta)\mathbf{A}_{r,r} & \frac{1}{r}\Big\{(u_r+u_{\theta,\theta})\mathbf{A}_{\theta,r} \\ \quad +u_{x,\theta}\mathbf{A}_{x,r}\Big\} & \quad +u_{r,r}\mathbf{A}_{r,\theta}+u_{\theta,r}\mathbf{A}_r\Big\} & \quad +u_{\theta,r}\mathbf{A}_{\theta,\theta}-u_{r,r}\mathbf{A}_\theta\Big\} \\
u_{x,x}\mathbf{A}_{x,r} & u_{r,x}\mathbf{A}_{r,r} & u_{\theta,x}\mathbf{A}_{\theta,r} \\
\frac{u_{x,x}}{r}\mathbf{A}_{x,\theta} & \frac{1}{r}\Big\{u_{r,x}\mathbf{A}_{r,\theta}+u_{\theta,x}\mathbf{A}_r\Big\} & \frac{1}{r}\Big\{u_{\theta,x}\mathbf{A}_{\theta,\theta}-u_{r,x}\mathbf{A}_\theta\Big\}
\end{bmatrix}
$$

$$
\mathbf{A}_{nl_x} = \begin{bmatrix}
u_{x,x}\mathbf{A}_x & u_{r,x}\mathbf{A}_r & u_{\theta,x}\mathbf{A}_\theta \\
\mathbf{0} & \mathbf{0} & \mathbf{0} \\
\mathbf{0} & \mathbf{0} & \mathbf{0} \\
\mathbf{0} & \mathbf{0} & \mathbf{0} \\
u_{x,r}\mathbf{A}_x & u_{r,r}\mathbf{A}_r & u_{\theta,r}\mathbf{A}_\theta \\
\frac{1}{r}u_{x,\theta}\mathbf{A}_x & \frac{1}{r}(u_{r,\theta}-u_\theta)\mathbf{A}_r & \frac{1}{r}(u_{\theta,\theta}+u_r)\mathbf{A}_\theta
\end{bmatrix} \tag{5.9}
$$

Now, let us consider the following potential energy due to strain,

$$
\mathcal{U} = \int_0^L \int_A \frac{1}{2}\mathbf{E}\cdot\mathbf{C}_e\cdot\mathbf{E}\, dA\, dx \tag{5.10}
$$

Where L is the length of the body along the x-axis, A is the cross-sectional area and $\mathbf{C}_e$ is the material constant of elasticity. And the energy conjugate stress tensor of the Green-Lagrange strain tensor i.e. the second Piola stress tensor can be obtained as following vector form:

$$
\mathbf{S} = \mathbf{C}_e\cdot\mathbf{E} \tag{5.11}
$$

Further the first variation in potential energy can be given as:

$$
\delta\mathcal{U} = \int_0^L \int_A \delta\mathbf{E}\cdot\mathbf{S}\, dA\, dx
$$

$$= \int_0^L \delta\mathbf{\Phi} \cdot (\mathbf{M}_1 + \mathbf{M}_{nl}) + \frac{d\delta\mathbf{\Phi}}{dx} \cdot (\mathbf{M}_{nl_x} + \mathbf{M}_2)\, dx \tag{5.12}$$

where

$$\begin{aligned} \mathbf{M}_j &= \int_A \mathbf{A}_j^T \mathbf{S}\, dA \quad \text{for } j = 1, 2 \\ \mathbf{M}_{nl} &= \int_A \mathbf{A}_{nl}^T \mathbf{S}\, dA, \quad \mathbf{M}_{nl_x} = \int_A \mathbf{A}_{nl_x}^T \mathbf{S}\, dA \end{aligned} \tag{5.13}$$

Now let us consider that $\mathbf{f}_b$ is the body force applied on per unit deformed volume and $\mathbf{q}_i$ are traction force applied on the ith boundary surfaces (inner and outer surfaces in case of hollow structures) of the body in the deformed (current) configuration, then the virtual work done by the applied forces in the course of virtual displacement $\delta\mathbf{u}$ in the deformed configuration can be given as following:

$$\delta\mathcal{V} = -\left(\int_v \mathbf{f}_b \cdot \delta\mathbf{u}\, dv + \int_{\bar{\mathcal{S}}_i} \mathbf{q}_i \cdot \delta\mathbf{u}\, d\bar{\mathcal{S}}_i \right) \tag{5.14}$$

where dv and $d\bar{\mathcal{S}}_i$ are the infinitesimal volume and area element in the deformed configuration. The corresponding volume and area element dV and $d\mathcal{S}_i$ in the reference configuration can be given as following:

$$dv = \det(\mathbf{F})\, dV, \quad d\bar{\mathcal{S}}_i\mathbf{n} = \det(\mathbf{F})\, \mathbf{F}^{-T} \cdot (d\mathcal{S}_i\mathbf{N}) \tag{5.15}$$

where $\mathbf{F}$ is the deformation gradient and $\mathbf{n}$ and $\mathbf{N}$ are the outward unit normal vector to the area element in deformed and the reference configuration respectively (see Appendix C for the expression of $\mathbf{N}$ for an arbitrary surface in assumed cylindrical coordinate system in reference configuration). The magnitude of area element and the normal vector can be transformed back to the reference frame as following:

$$d\bar{\mathcal{S}}_i = \det(\mathbf{F}) \sqrt{(\mathbf{C}^{-1} \cdot \mathbf{N}) \cdot \mathbf{N}}\, d\mathcal{S}_i, \quad \mathbf{n} = \frac{\mathbf{F}^{-T} \cdot \mathbf{N}}{\sqrt{(\mathbf{C}^{-1} \cdot \mathbf{N}) \cdot \mathbf{N}}} \tag{5.16}$$

where $\mathbf{C} = \mathbf{F}^T \cdot \mathbf{F}$ is the right Cauchy–Green deformation tensor. Using eqs. (5.14), (5.15) and (5.16), the virtual work done by the external forces can be rewritten as following:

$$\delta\mathcal{V} = -\int_V (\det(\mathbf{F})\mathbf{f}_b) \cdot \delta\mathbf{u}\, dV - \int_{\mathcal{S}_i} \left(\det(\mathbf{F}) \sqrt{(\mathbf{C}^{-1} \cdot \mathbf{N}) \cdot \mathbf{N}} \right) \mathbf{q}_i \cdot \delta\mathbf{u}\, d\mathcal{S}_i$$

$$
\begin{aligned}
&= -\int_0^L \Big[\int_A (\det(\mathbf{F})\mathbf{f}_b) \cdot \delta\mathbf{u}\, dA + \int_0^{2\pi} \Big(\det(\mathbf{F}) \sqrt{(\mathbf{C}^{-1}\cdot\mathbf{N})\cdot\mathbf{N}} \Big) \mathbf{q}_i \cdot \delta\mathbf{u} \sqrt{G_i}\, d\theta \Big] dx \\
&= -\int_0^L \delta\mathbf{\Phi} \cdot \hat{\mathbf{f}}\, dx
\end{aligned} \tag{5.17}
$$

where $\hat{\mathbf{f}}$ is defined as follows (given $\mathbf{f}_b = f_{b_x}\hat{\mathbf{e}}_x + f_{b_r}\hat{\mathbf{e}}_r + f_{b_\theta}\hat{\mathbf{e}}_\theta$ and $\mathbf{q}_i = q_{x_i}\hat{\mathbf{e}}_x + q_{r_i}\hat{\mathbf{e}}_r + q_{\theta_i}\hat{\mathbf{e}}_\theta$):

$$
\begin{aligned}
\hat{\mathbf{f}} &= \begin{bmatrix} \hat{\mathbf{f}}_x & \hat{\mathbf{f}}_r & \hat{\mathbf{f}}_\theta \end{bmatrix}^T, \\
\hat{\mathbf{f}}_x &= \int_A \det(\mathbf{F}) f_{b_x} \mathbf{A}_x^T\, dA + \int_0^{2\pi} \sqrt{G_i} \left(\det(\mathbf{F}) \sqrt{(\mathbf{C}^{-1}\cdot\mathbf{N})\cdot\mathbf{N}} \right) q_{x_i} \mathbf{A}_x^T\, d\theta \\
\hat{\mathbf{f}}_r &= \int_A \det(\mathbf{F}) f_{b_r} \mathbf{A}_r^T\, dA + \int_0^{2\pi} \sqrt{G_i} \left(\det(\mathbf{F}) \sqrt{(\mathbf{C}^{-1}\cdot\mathbf{N})\cdot\mathbf{N}} \right) q_{r_i} \mathbf{A}_r^T\, d\theta \\
\hat{\mathbf{f}}_\theta &= \int_A \det(\mathbf{F}) f_{b_\theta} \mathbf{A}_\theta^T\, dA + \int_0^{2\pi} \sqrt{G_i} \left(\det(\mathbf{F}) \sqrt{(\mathbf{C}^{-1}\cdot\mathbf{N})\cdot\mathbf{N}} \right) q_{\theta_i} \mathbf{A}_\theta^T\, d\theta
\end{aligned} \tag{5.18}
$$

and G_i is the determinant of covariant matric tensor for surface coordinate (x, θ) for the ith boundary surface of the body which is defined by $r_i(x, \theta)$ in the reference frame (see Appendix C for details). For an arbitrary boundary surface, G_i can be given as following:

$$
G_i = \left(\frac{\partial r_i(x,\theta)}{\partial \theta} \right)^2 + (r_i(x,\theta))^2 + \left(r_i(x,\theta) \frac{\partial r_i(x,\theta)}{\partial x} \right)^2 \tag{5.19}
$$

If the body force is given as force per unit mass then it can be expressed as $\mathbf{f}_b = \rho\mathbf{f}_m = (\rho_0/\det(\mathbf{F}))\mathbf{f}_m$. Here ρ and ρ_0 are the mass density of the body in the deformed and reference configuration respectively. A very common example of distributed traction force at the boundary surface is pressure force which can be given as $\mathbf{q}_i = P_{0_i}\mathbf{n} = (P_{0_i}/\sqrt{(\mathbf{C}^{-1}\cdot\mathbf{N})\cdot\mathbf{N}})\mathbf{F}^{-T}\cdot\mathbf{N}$, where P_{0_i} is the magnitude of the pressure. The point load at any point can be considered as dirac delta function in two dimensions for the surface traction force and but it should be noted that constant point force means the volume under such dirac-delta function should be taken as constant and it would not depend on the deformation. Further, from the principle of virtual displacement (see Reddy [41]), we can write the following:

$$
0 = \delta\mathcal{U} + \delta\mathcal{V}
$$

$$= \int_0^L \delta\mathbf{\Phi} \cdot \left((\mathbf{M}_1 + \mathbf{M}_{nl}) - \frac{d}{dx}(\mathbf{M}_2 + \mathbf{M}_{nl_x}) - \hat{\mathbf{f}} \right) dx + [\delta\mathbf{\Phi} \cdot (\mathbf{M}_2 + \mathbf{M}_{nl_x})]_0^L \tag{5.20}$$

From the above equation, we arrive at the following Euler-Lagrange equation (the equation of motion):

$$(\mathbf{M}_1 + \mathbf{M}_{nl}) - \frac{d}{dx}(\mathbf{M}_2 + \mathbf{M}_{nl_x}) - \hat{\mathbf{f}} = 0 \tag{5.21}$$

and the essential and natural boundary variables are

$$\delta\mathbf{\Phi}: \qquad \mathbf{M}_2 + \mathbf{M}_{nl_x} \tag{5.22}$$

The equation of motion (Eq. (5.21)) can be solved for the unknown displacement variables by various numerical methods like finite element method or finite difference method. In the following sections we have developed a nonlinear finite element model to obtain the solution of the governing equation.

5.3. Constitutive relation

In this study, we will consider isotropic and homogeneous material with the linear relation between second Piola stress tensor and Green-Lagrange strain tensor:

$$\mathbf{S} = \mathbf{C}_e \cdot \mathbf{E} \tag{5.23}$$

where

$$\begin{aligned}
\mathbf{C}_e &= \frac{E(1-\nu)}{(1+\nu)(1-2\nu)} \begin{bmatrix} 1 & \frac{\nu}{1-\nu} & \frac{\nu}{1-\nu} & 0 & 0 & 0 \\ \frac{\nu}{1-\nu} & 1 & \frac{\nu}{1-\nu} & 0 & 0 & 0 \\ \frac{\nu}{1-\nu} & \frac{\nu}{1-\nu} & 1 & 0 & 0 & 0 \\ 0 & 0 & 0 & \frac{1-2\nu}{2(1-\nu)} & 0 & 0 \\ 0 & 0 & 0 & 0 & \frac{1-2\nu}{2(1-\nu)} & 0 \\ 0 & 0 & 0 & 0 & 0 & \frac{1-2\nu}{2(1-\nu)} \end{bmatrix} \\
\mathbf{E} &= \begin{bmatrix} E_{xx} & E_{rr} & E_{\theta\theta} & 2E_{r\theta} & 2E_{rx} & 2E_{\theta x} \end{bmatrix}^T \\
\mathbf{S} &= \begin{bmatrix} S_{xx} & S_{rr} & S_{\theta\theta} & S_{r\theta} & S_{rx} & S_{\theta x} \end{bmatrix}^T
\end{aligned} \tag{5.24}$$

where E and ν are the modulus of elasticity and Poisson's ratio respectively.

5.4. Weak form finite element model

In order to develop a weak form finite element model for the above formulation, we divide the computational domain $[0, L]$ into non-overlapping finite elements, $\Omega^e = [x_1^e, x_2^e]$. Further we write the weak form the governing equation of motion Eq. (5.21) in terms of displacement variables as following:

$$\begin{aligned} 0 \;=\; \int_{x_1^e}^{x_2^e} \int_A \Big[\bigg((\mathbf{A}_1 + \mathbf{A}_{nl}) \delta\mathbf{\Phi} + (\mathbf{A}_2 + \mathbf{A}_{nl_x}) \frac{d\delta\mathbf{\Phi}}{dx} \bigg) \cdot \mathbf{C}_e \bigg((\mathbf{A}_1 + \frac{1}{2}\mathbf{A}_{nl}) \mathbf{\Phi} \\ + (\mathbf{A}_2 + \frac{1}{2}\mathbf{A}_{nl_x}) \frac{d\mathbf{\Phi}}{dx} \bigg) - \delta\mathbf{\Phi} \cdot \hat{\mathbf{f}} \Big] \, dA \, dx \end{aligned} \tag{5.25}$$

We approximate the degrees of freedom vector as:

$$\mathbf{\Phi}(x) = \mathbf{\Psi}(x)\mathbf{U} \tag{5.26}$$

where $\mathbf{\Psi}(x)$ is matrix of shape functions which are function of x and $\mathbf{U}$ is vector of displacement variables at nodal points which is defined as following:

$$\mathbf{\Psi} \;=\; \begin{bmatrix} \psi_1^{(1)} & \dots & \psi_{\tilde{n}_1}^{(1)} & 0 & \dots & 0 & \dots & 0 & \dots & 0 \\ 0 & \dots & 0 & \psi_1^{(2)} & \dots & \psi_{\tilde{n}_2}^{(2)} & \dots & 0 & \dots & 0 \\ \vdots & \ddots & \vdots & \vdots & \ddots & \vdots & \ddots & \vdots & \ddots & \vdots \\ 0 & \dots & 0 & 0 & \dots & 0 & \dots & \psi_1^{(n)} & \dots & \psi_{\tilde{n}_p}^{(n)} \end{bmatrix} \tag{5.27}$$

$$\mathbf{U} \;=\; \begin{bmatrix} u_{1_1} & \dots & u_{1_{\tilde{n}_1}} & u_{2_1} & \dots & u_{2_{\tilde{n}_2}} & \dots & u_{n_1} & \dots & u_{n_{\tilde{n}_n}} \end{bmatrix}^T \tag{5.28}$$

where $\tilde{n}_1, \tilde{n}_2, \cdots \tilde{n}_n$ are the number of nodal values for $u_1, u_2, \cdots, u_n$ respectively in the considered element. n is the total number of Dofs. And

$$\begin{aligned} u_1 &= \phi_x^{(0)}, \quad u_2 = \phi_x^{(1)}, \quad \cdots \quad u_{(\tilde{n})} = \phi_x^{(\tilde{n})} \\ u_{\tilde{n}+1} &= \phi_r^{(0)}, \quad u_{\tilde{n}+2} = \phi_r^{(1)}, \quad \cdots \quad u_{\tilde{n}+\tilde{m}} = \phi_r^{(\tilde{m})} \\ u_{\tilde{n}+\tilde{m}+1} &= \phi_\theta^{(0)}, \quad u_{\tilde{n}+\tilde{m}+2} = \phi_\theta^{(1)}, \quad \cdots \quad u_{\tilde{n}+\tilde{m}+\tilde{p}} = \phi_\theta^{(\tilde{p})}. \end{aligned} \tag{5.29}$$

We substitute the approximation of dofs and $\delta\mathbf{\Phi} = \mathbf{\Psi}\tilde{\mathbf{l}}$ (where $\tilde{\mathbf{l}}$ is the column vector with all element unity and as many elements as the columns of $\mathbf{\Psi}$) into the weak

form Eq. (5.25) to arrive at the following finite element equation:

$$\mathbf{KU} - \mathbf{f} = \mathbf{0} \tag{5.30}$$

where $\mathbf{K}$ and $\mathbf{f}$ are the stiffness matrix and force vector respectively, which are given as follows:

$$\begin{aligned} \mathbf{K} &= \int_{x_1^e}^{x_2^e} \mathbf{\Psi}^T \left(\mathbf{H}_1 \mathbf{\Psi} + \mathbf{H}_2 \frac{d\mathbf{\Psi}}{dx} \right) + \frac{d\mathbf{\Psi}}{dx}^T \left(\mathbf{H}_3 \mathbf{\Psi} + \mathbf{H}_4 \frac{d\mathbf{\Psi}}{dx} \right) dx \\ \mathbf{f} &= \int_{x_1^e}^{x_2^e} \mathbf{\Psi}^T \hat{\mathbf{f}} \, dx \end{aligned} \tag{5.31}$$

where

$$\begin{aligned} \mathbf{H}_1 = \int_A (\mathbf{A}_1 + \mathbf{A}_{nl})^T \mathbf{C}_e (\mathbf{A}_1 + \frac{1}{2}\mathbf{A}_{nl}) \, dA, \;\; \mathbf{H}_2 = \int_A (\mathbf{A}_1 + \mathbf{A}_{nl})^T \mathbf{C}_e (\mathbf{A}_2 + \frac{1}{2}\mathbf{A}_{nl_x}) \, dA \\ \mathbf{H}_3 = \int_A (\mathbf{A}_2 + \mathbf{A}_{nl_x})^T \mathbf{C}_e (\mathbf{A}_1 + \frac{1}{2}\mathbf{A}_{nl}) \, dA, \;\; \mathbf{H}_4 = \int_A (\mathbf{A}_{nl_x} + \mathbf{A}_2)^T \mathbf{C}_e (\mathbf{A}_2 + \frac{1}{2}\mathbf{A}_{nl_x}) \, dA \end{aligned} \tag{5.32}$$

We note here that matrices $\mathbf{A}_{nl}$ and $\mathbf{A}_{nl_x}$ depend on the displacement variables hence the stiffness matrix is nonlinear and also not symmetric. The nonlinear finite element equation can be solved by direct (Picard) method or Newton's method (see Reddy [46]). For the $(t+1)$th iteration of Newton's method, the solution can be expressed as:

$$\mathbf{T}(\mathbf{U}_t)\delta\mathbf{U}_{t+1} = -(\mathbf{K}(\mathbf{U}_t))\mathbf{U}_t - \mathbf{f}(\mathbf{U}_t), \quad \text{and, } \mathbf{U}_{t+1} = \mathbf{U}_t + \delta\mathbf{U}_{t+1} \tag{5.33}$$

where $\mathbf{T}$ is the tangent matrix, which is given by

$$\begin{aligned} \mathbf{T} &= D(\mathbf{KU} - \mathbf{f}) = (D\mathbf{K})\mathbf{U} + \mathbf{K} - D\mathbf{f} \\ &= \mathbf{K} + \int_{x_1^e}^{x_2^e} \mathbf{\Psi}^T \left(\tilde{\mathbf{H}}_1 \mathbf{\Psi} + \tilde{\mathbf{H}}_2 \frac{d\mathbf{\Psi}}{dx} \right) + \frac{d\mathbf{\Psi}}{dx}^T \left(\tilde{\mathbf{H}}_3 \mathbf{\Psi} + \tilde{\mathbf{H}}_4 \frac{d\mathbf{\Psi}}{dx} \right) dx \\ &\quad + \int_{x_1^e}^{x_2^e} \mathbf{\Psi}^T \left(\tilde{\mathbf{P}}_1 \mathbf{\Psi} + \tilde{\mathbf{P}}_2 \frac{d\mathbf{\Psi}}{dx} \right) + \frac{d\mathbf{\Psi}}{dx}^T \left(\tilde{\mathbf{P}}_3 \mathbf{\Psi} + \tilde{\mathbf{P}}_4 \frac{d\mathbf{\Psi}}{dx} \right) dx - \int_{x_1^e}^{x_2^e} \mathbf{\Psi}^T \tilde{\mathbf{P}}_f \mathbf{\Psi} \, dx \end{aligned} \tag{5.34}$$

where $D(\mathbf{K})$ represent the derivative of $\mathbf{K}$ with respect to $\mathbf{U}$ and

$$\tilde{\mathbf{H}}_1 = \frac{1}{2} \int_A (\mathbf{A}_1 + \mathbf{A}_{nl})^T \mathbf{C}_e \mathbf{A}_{nl} \, dA, \quad \tilde{\mathbf{H}}_2 = \frac{1}{2} \int_A (\mathbf{A}_1 + \mathbf{A}_{nl})^T \mathbf{C}_e \mathbf{A}_{nl_x} \, dA$$

$$\tilde{\mathbf{H}}_3 = \frac{1}{2}\int_A (\mathbf{A}_2 + \mathbf{A}_{nl_x})^T \mathbf{C}_e \mathbf{A}_{nl}\, dA, \quad \tilde{\mathbf{H}}_4 = \frac{1}{2}\int_A (\mathbf{A}_2 + \mathbf{A}_{nl_x})^T \mathbf{C}_e \mathbf{A}_{nl_x}\, dA \tag{5.35}$$

and

$$\tilde{\mathbf{P}}_1 = \int_A \begin{bmatrix} \mathbf{P}_1^{11} & \mathbf{0} & \mathbf{0} \\ \mathbf{0} & \mathbf{P}_1^{22} & \mathbf{P}_1^{23} \\ \mathbf{0} & \mathbf{P}_1^{32} & \mathbf{P}_1^{33} \end{bmatrix} dA, \quad \tilde{\mathbf{P}}_2 = \int_A \begin{bmatrix} \mathbf{P}_2^{11} & \mathbf{0} & \mathbf{0} \\ \mathbf{0} & \mathbf{P}_2^{22} & \mathbf{P}_2^{23} \\ \mathbf{0} & \mathbf{P}_2^{32} & \mathbf{P}_2^{33} \end{bmatrix} dA$$

$$\tilde{\mathbf{P}}_3 = \int_A \begin{bmatrix} \mathbf{P}_3^{11} & \mathbf{0} & \mathbf{0} \\ \mathbf{0} & \mathbf{P}_3^{22} & \mathbf{P}_3^{23} \\ \mathbf{0} & \mathbf{P}_3^{32} & \mathbf{P}_3^{33} \end{bmatrix} dA, \quad \tilde{\mathbf{P}}_4 = \int_A \begin{bmatrix} \mathbf{P}_4^{11} & \mathbf{0} & \mathbf{0} \\ \mathbf{0} & \mathbf{P}_4^{22} & \mathbf{0} \\ \mathbf{0} & \mathbf{0} & \mathbf{P}_4^{33} \end{bmatrix} dA \tag{5.36}$$

The block components of matrix $\tilde{\mathbf{P}}_i$ for $i = 1, 2, 3, 4$ are given as following:

$$\begin{aligned}
\mathbf{P}_1^{11} &= S_{rr}\mathbf{A}_{x,r}^T\mathbf{A}_{x,r} + \frac{1}{r^2}S_{\theta\theta}\mathbf{A}_{x,\theta}^T\mathbf{A}_{x,\theta} + \frac{1}{r}S_{r\theta}(\mathbf{A}_{x,\theta}^T\mathbf{A}_{x,r} + \mathbf{A}_{x,r}^T\mathbf{A}_{x,\theta}) \\
\mathbf{P}_1^{22} &= S_{rr}\mathbf{A}_{r,r}^T\mathbf{A}_{r,r} + \frac{1}{r^2}S_{\theta\theta}(\mathbf{A}_{r,\theta}^T\mathbf{A}_{r,\theta} + \mathbf{A}_r^T\mathbf{A}_r) + \frac{1}{r}S_{r\theta}(\mathbf{A}_{r,r}^T\mathbf{A}_{r,\theta} + \mathbf{A}_{r,\theta}^T\mathbf{A}_{r,r}) \\
\mathbf{P}_1^{23} &= \frac{1}{r^2}S_{\theta\theta}(-\mathbf{A}_{r,\theta}^T\mathbf{A}_\theta + \mathbf{A}_r^T\mathbf{A}_{\theta,\theta}) + \frac{1}{r}S_{r\theta}(-\mathbf{A}_{r,r}^T\mathbf{A}_\theta + \mathbf{A}_r^T\mathbf{A}_{\theta,r}) \\
\mathbf{P}_1^{32} &= \frac{1}{r^2}S_{\theta\theta}(-\mathbf{A}_\theta^T\mathbf{A}_{r,\theta} + \mathbf{A}_{\theta,\theta}^T\mathbf{A}_r) + \frac{1}{r}S_{r\theta}(\mathbf{A}_{\theta,r}^T\mathbf{A}_r - \mathbf{A}_\theta^T\mathbf{A}_{r,r}) \\
\mathbf{P}_1^{33} &= S_{rr}\mathbf{A}_{\theta,r}^T\mathbf{A}_{\theta,r} + \frac{1}{r^2}S_{\theta\theta}(\mathbf{A}_\theta^T\mathbf{A}_\theta + \mathbf{A}_{\theta,\theta}^T\mathbf{A}_{\theta,\theta}) + \frac{1}{r}S_{r\theta}(\mathbf{A}_{\theta,r}^T\mathbf{A}_{\theta,\theta} + \mathbf{A}_{\theta,\theta}^T\mathbf{A}_{\theta,r}) \\
\mathbf{P}_2^{11} &= S_{rx}\mathbf{A}_{x,r}^T\mathbf{A}_x + \frac{1}{r}S_{\theta x}\mathbf{A}_{x,\theta}^T\mathbf{A}_x \\
\mathbf{P}_2^{22} &= S_{rx}\mathbf{A}_{r,r}^T\mathbf{A}_r + \frac{1}{r}S_{\theta x}\mathbf{A}_{r,\theta}^T\mathbf{A}_r \\
\mathbf{P}_2^{23} &= \frac{1}{r}S_{\theta x}\mathbf{A}_r^T\mathbf{A}_\theta \\
\mathbf{P}_2^{32} &= -\frac{1}{r}S_{\theta x}\mathbf{A}_\theta^T\mathbf{A}_r \\
\mathbf{P}_2^{33} &= S_{rx}\mathbf{A}_{\theta,r}^T\mathbf{A}_\theta + \frac{1}{r}S_{\theta x}\mathbf{A}_{\theta,\theta}^T\mathbf{A}_\theta \\
\mathbf{P}_3^{11} &= S_{rx}\mathbf{A}_x^T\mathbf{A}_{x,r} + \frac{1}{r}S_{\theta x}\mathbf{A}_x^T\mathbf{A}_{x,\theta} \\
\mathbf{P}_3^{22} &= S_{rx}\mathbf{A}_r^T\mathbf{A}_{r,r} + \frac{1}{r}S_{\theta x}\mathbf{A}_r^T\mathbf{A}_{r,\theta} \\
\mathbf{P}_3^{23} &= -\frac{1}{r}S_{\theta x}\mathbf{A}_r^T\mathbf{A}_\theta \\
\mathbf{P}_3^{32} &= \frac{1}{r}S_{\theta x}\mathbf{A}_\theta^T\mathbf{A}_r
\end{aligned}$$

$$
\begin{aligned}
\mathbf{P}_3^{33} &= S_{rx}\mathbf{A}_\theta^T\mathbf{A}_{\theta,r} + \frac{1}{r}S_{\theta x}\mathbf{A}_\theta^T\mathbf{A}_{\theta,\theta} \\
\mathbf{P}_4^{11} &= S_{xx}\mathbf{A}_x^T\mathbf{A}_x \\
\mathbf{P}_4^{22} &= S_{xx}\mathbf{A}_r^T\mathbf{A}_r \\
\mathbf{P}_4^{33} &= S_{xx}\mathbf{A}_\theta^T\mathbf{A}_\theta
\end{aligned} \tag{5.37}
$$

And $\tilde{\mathbf{P}}_f$ is the matrix related to nonlinear force term in the tangent matrix. If the body force is given as force per unit mass then the body force can be given as $\mathbf{f}_b = \rho\mathbf{f}_m = (\rho_0/\det(\mathbf{F}))\mathbf{f}_m$.

$$
\begin{aligned}
\hat{\mathbf{f}} &= \begin{bmatrix} \hat{\mathbf{f}}_x & \hat{\mathbf{f}}_r & \hat{\mathbf{f}}_\theta \end{bmatrix}^T, \\
\hat{\mathbf{f}}_x &= \int_A \rho_0 f_{m_x}\mathbf{A}_x^T\, dA + \int_0^{2\pi} \sqrt{G_i}\, q_{x_i}\, \zeta \mathbf{A}_x^T\, d\theta \\
\hat{\mathbf{f}}_r &= \int_A \rho_0 f_{m_r}\mathbf{A}_r^T\, dA + \int_0^{2\pi} \sqrt{G_i}\, q_{r_i}\, \zeta \mathbf{A}_r^T\, d\theta \\
\hat{\mathbf{f}}_\theta &= \int_A \rho_0 f_{m_\theta}\mathbf{A}_\theta^T\, dA + \int_0^{2\pi} \sqrt{G_i}\, q_{\theta_i}\, \zeta \mathbf{A}_\theta^T\, d\theta
\end{aligned} \tag{5.38}
$$

where $\zeta = \left(\det(\mathbf{F})\sqrt{(\mathbf{C}^{-1}\cdot\mathbf{N})\cdot\mathbf{N}}\right)$. If the force (per unit area) vector $\mathbf{q}_i$ does not depends on deformed configuration (*i.e.* the magnitude and direction of $\mathbf{q}_i$ is independent of deformed configuration) then the matrix $\tilde{\mathbf{P}}_f$ used in tangent matrix can be given as following:

$$
\tilde{\mathbf{P}}_f = \int_0^{2\pi} \sqrt{G_i} \begin{bmatrix}
q_{x_i}\frac{\partial\zeta}{\partial u_x}\mathbf{A}_x^T\mathbf{A}_x & q_{x_i}\frac{\partial\zeta}{\partial u_r}\mathbf{A}_x^T\mathbf{A}_r & q_{x_i}\frac{\partial\zeta}{\partial u_\theta}\mathbf{A}_x^T\mathbf{A}_\theta \\
q_{r_i}\frac{\partial\zeta}{\partial u_x}\mathbf{A}_r^T\mathbf{A}_x & q_{r_i}\frac{\partial\zeta}{\partial u_r}\mathbf{A}_r^T\mathbf{A}_r & q_{r_i}\frac{\partial\zeta}{\partial u_\theta}\mathbf{A}_r^T\mathbf{A}_\theta \\
q_{\theta_i}\frac{\partial\zeta}{\partial u_x}\mathbf{A}_\theta^T\mathbf{A}_x & q_{\theta_i}\frac{\partial\zeta}{\partial u_r}\mathbf{A}_\theta^T\mathbf{A}_r & q_{\theta_i}\frac{\partial\zeta}{\partial u_\theta}\mathbf{A}_\theta^T\mathbf{A}_\theta
\end{bmatrix} d\theta \tag{5.39}
$$

The constant point force with fixed direction, $\mathbf{q}_i$ can be expressed as dirac-delta function in two dimensions. But in this case, we note that constant point force means the volume under the two dimensional dirac-delta function should be taken as constant and it would not depend on the deformation. And further, the derivative $\frac{\partial\zeta}{\partial\alpha}$ in Eq. (5.39) for $\alpha = u_x, u_r, u_\theta$ can be given as following:

$$
\frac{\partial\zeta}{\partial\alpha} = \frac{\partial\det(\mathbf{F})}{\partial\alpha}\sqrt{(\mathbf{C}^{-1}\cdot\mathbf{N})\cdot\mathbf{N}}) - \frac{\det(\mathbf{F})}{2\sqrt{(\mathbf{C}^{-1}\cdot\mathbf{N})\cdot\mathbf{N}}}\left((\mathbf{C}^{-1}\cdot\frac{\partial\mathbf{C}}{\partial\alpha}\cdot\mathbf{C}^{-1})\cdot\mathbf{N}\right)\cdot\mathbf{N} \tag{5.40}
$$

where

$$\frac{\partial \det(\mathbf{F})}{\partial \alpha} = \text{cofactor}(F_{ij}) \frac{\partial F_{ij}}{\partial \alpha}, \quad \frac{\partial \mathbf{C}}{\partial \alpha} = \frac{\partial \mathbf{F}^T}{\partial \alpha} \cdot \mathbf{F} + \mathbf{F}^T \cdot \frac{\partial \mathbf{F}}{\partial \alpha} \tag{5.41}$$

and F_{ij} are the components of $\mathbf{F}$ in the assumed coordinate system, and sum on repeated indices is implied.

Another very common example of the distributed traction force at the boundary surface is the pressure, which can be given as $\mathbf{q}_i = P_{0_i}\mathbf{n} = (P_{0_i}/\sqrt{(\mathbf{C}^{-1}\cdot\mathbf{N})\cdot\mathbf{N}})\mathbf{F}^{-T}\cdot\mathbf{N}$, where P_{0_i} is the magnitude of the pressure. If we use two-dimensional Dirac delta function for P_0 such that the volume under the Dirac delta function (of x and θ) remains constant, we obtain a constant follower force, which acts always along the normal direction to the surface at the point of application. In such cases we have,

$$\hat{\mathbf{f}}_x = \int_0^{2\pi} \sqrt{G_i}\, P_{0_i}\, \zeta_x \mathbf{A}_x^T \, d\theta, \;\; \hat{\mathbf{f}}_r = \int_0^{2\pi} \sqrt{G_i}\, P_{0_i}\, \zeta_r \mathbf{A}_r^T \, d\theta, \;\; \hat{\mathbf{f}}_\theta = \int_0^{2\pi} \sqrt{G_i}\, P_{0_i}\, \zeta_\theta \mathbf{A}_\theta^T \, d\theta \tag{5.42}$$

where $\boldsymbol{\zeta} = \det(\mathbf{F})\,\mathbf{F}^{-T}\cdot\mathbf{N} = \zeta_x\hat{\mathbf{e}}_x + \zeta_r\hat{\mathbf{e}}_r + \zeta_\theta\hat{\mathbf{e}}_\theta$. Then the the matrix $\tilde{\mathbf{P}}_f$ can be given as following:

$$\tilde{\mathbf{P}}_f = \int_0^{2\pi} \sqrt{G_i}\, P_{0_i} \begin{bmatrix} \frac{\partial \zeta_x}{\partial u_x}\mathbf{A}_x^T\mathbf{A}_x & \frac{\partial \zeta_x}{\partial u_r}\mathbf{A}_x^T\mathbf{A}_r & \frac{\partial \zeta_x}{\partial u_\theta}\mathbf{A}_x^T\mathbf{A}_\theta \\ \frac{\partial \zeta_r}{\partial u_x}\mathbf{A}_r^T\mathbf{A}_x & \frac{\partial \zeta_r}{\partial u_r}\mathbf{A}_r^T\mathbf{A}_r & \frac{\partial \zeta_r}{\partial u_\theta}\mathbf{A}_r^T\mathbf{A}_\theta \\ \frac{\partial \zeta_\theta}{\partial u_x}\mathbf{A}_\theta^T\mathbf{A}_x & \frac{\partial \zeta_\theta}{\partial u_r}\mathbf{A}_\theta^T\mathbf{A}_r & \frac{\partial \zeta_\theta}{\partial u_\theta}\mathbf{A}_\theta^T\mathbf{A}_\theta \end{bmatrix} d\theta \tag{5.43}$$

where the derivative $\frac{\partial \boldsymbol{\zeta}}{\partial \alpha}$ for $\alpha = u_x, u_r, u_\theta$ can be given as following:

$$\begin{aligned} \frac{\partial \boldsymbol{\zeta}}{\partial \alpha} &= \frac{\partial \zeta_x}{\partial \alpha}\hat{\mathbf{e}}_x + \frac{\partial \zeta_r}{\partial \alpha}\hat{\mathbf{e}}_r + \frac{\partial \zeta_\theta}{\partial \alpha}\hat{\mathbf{e}}_\theta \\ &= \frac{\partial \det(\mathbf{F})}{\partial \alpha}\mathbf{F}^{-T}\cdot\mathbf{N} - \det(\mathbf{F})\left(\mathbf{F}^{-T}\cdot\frac{\partial \mathbf{F}^T}{\partial \alpha}\cdot\mathbf{F}^{-T}\right)\cdot\mathbf{N} \end{aligned} \tag{5.44}$$

We note that the tangent matrix is not symmetric due to $D\mathbf{f}$ in Eq. (5.34) but the part of the tangent matrix coming from the derivative of $\mathbf{KU}$ is symmetric. To keep the symmetry, the tangent matrix can be approximated by dropping $D\mathbf{f}$ terms from the expression. This may make the convergence slower.

5.5. Numerical examples

In this section, we employ the formulation developed herein to analyse cylindrical shell structures under internal pressure and constant point forces.

5.5.1. Cylindrical shell with fixed edges subjected to internal pressure

Let us consider a hollow cylinder under constant internal pressure, with the following geometrical properties:

$$L = 20 \text{ m}, \qquad r_1 = 5 \text{ m}, \qquad r_2 = 5.01 \text{ m} \tag{5.45}$$

where L is the length of the cylinder and r_1 and r_2 are the inner and outer radii of the cylinder (see fig. 5.1). The material properties of the cylinder are taken as

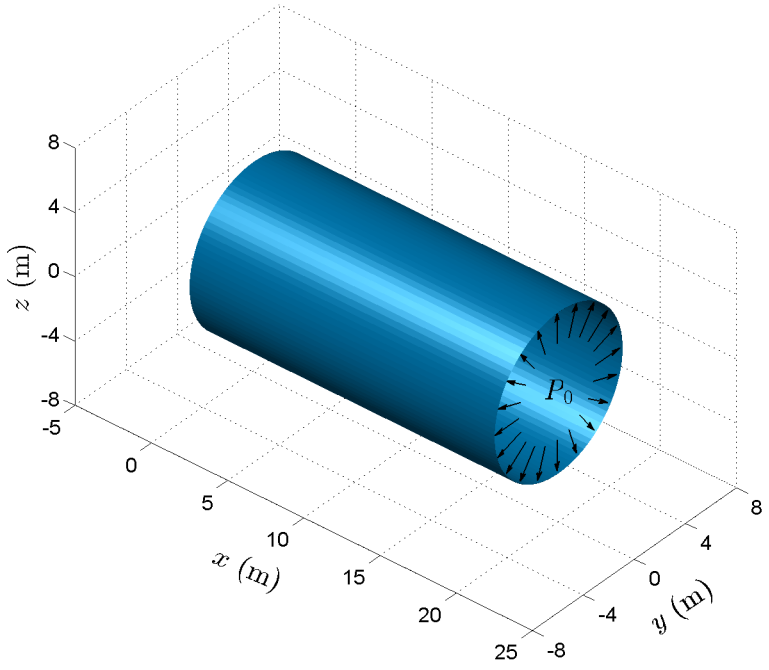

Fig. 5.1 Original shape of the cylindrical shell.

follows:

$$E = 0.7 \times 10^9 \text{ N/ m}^2, \quad \nu = 0.3 \tag{5.46}$$

This problem is one of the cases considered in the work of Rivera and Reddy [59] using a 7-parameter shell theory; they have only considered non-displacement dependent

internal pressure, that is, the pressure force is taken as radially distributed force and have been calculated over the internal surface area of the cylinder in the reference frame for all subsequent load steps. In the present study, we consider the nonlinearity of pressure force due to the change in the inner surface area of the cylinder and the normal direction at any point of the inner surface during the deformation. We also consider the non-displacement dependent pressure to compare our results from the 7-parameter shell theory of Rivera and Reddy [59].

5.5.1.1. Linear analysis

The linear response for the maximum radial displacement of the cylindrical shell, with both ends fixed, is presented in Table 5.1 for different orders of approximation (n_r, n_θ), (m_r, m_θ) and (p_r, p_θ) of the three different components of the displacement vector, using $f_i(r) = r^i$ and $f_i(r) = J_i(r)$ as the radial basis functions in Eq. (5.2), where $J_i(r)$ is the Bessel function of the first kind. The internal pressure, P_0, is taken as 0.4 MPa in the linear analysis. All the unknown displacements (i.e., the degrees of freedom) are approximated by either linear or quadratic Lagrange interpolation functions. As can be seen from Table 5.1, the response for the maximum radial displacement agrees with each other for the power of r or Bessel functions as radial basis functions in Eq. (5.2). Further, we notice that the radial displacements are not affected by the values of n_θ, m_θ, and p_θ, which is expected because the problem has a radial symmetry and hence the displacement vector should not depend on θ. We also note that approximation up to the second order of radial basis functions is good enough for the thickness of considered cylindrical shell. Also, Since the problem has the radial symmetry, u_θ will always be zero; hence we can remove the terms that contain u_θ from the analysis to reduce the size of the problem. So, if we take $n_r, m_r = 2$ and $u_\theta = 0$ for this problem, there will be only six degrees of freedom at each cross-section of the cylindrical shell; hence the size of the system of algebraic equation can be reduced drastically as compared to shell theory for the radially symmetric problems.

5.5.1.2. Nonlinear solution

Deformed shape of the same cylindrical shell which is described by Eqs. (5.45) and (5.46) has been shown in figs. 5.2(a) and (b) for internal pressures, $P_0 = 0.6, 1$ MPa, respectively. For the nonlinear finite element analysis, twenty linear Lagrange inter-

Table 5.1. Linear FEM solutions for maximum radial displacement of a cylindrical shell under internal pressure, $P_0 = 0.04$ MPa with fixed end boundary condition.

order of approximation of u_x, u_r and u_θ			Magnitude of displacement (in m) at $(x, r, \theta) = (10 \text{ m}, r_2, \pi/2)$.					
			linear element			Quadratic element		
n_r, n_θ	m_r, m_θ	p_r, p_θ	no. of elements	$f_i(r) = r^i$ disp.	$f_i(r) = J_i(r)$ disp.	no. of elements	$f_i(r) = r^i$ disp.	$f_i(r) = J_i(r)$ disp.
1,0	1,0	1,0	20	0.13138	0.13135	10	0.13033	0.13030
			40	0.13121	0.13117	20	0.13086	0.13083
			60	0.13101	0.13097	30	0.13062	0.13059
			80	0.13090	0.13086	40	0.13052	0.13048
2,0	2,0	2,0	20	0.13138	0.13138	10	0.13033	0.13033
			40	0.13121	0.13121	20	0.13086	0.13086
			60	0.13101	0.13101	30	0.13062	0.13062
			80	0.13090	0.13090	40	0.13051	0.13051
3,0	3,0	3,0	20	0.13138	0.13138	10	0.13033	0.13033
			40	0.13121	0.13121	20	0.13086	0.13086
			60	0.13101	0.13101	30	0.13062	0.13062
			80	0.13091	0.13090	40	0.13051	0.13051
1,1	1,1	1,1	20	0.13138	0.13135	10	0.13033	0.13030
			40	0.13121	0.13117	20	0.13086	0.13083
			60	0.13101	0.13097	30	0.13062	0.13059
			80	0.13090	0.13086	40	0.13052	0.13048
1,2	1,2	1,2	20	0.13138	0.13135	10	0.13033	0.13030
			40	0.13121	0.13117	20	0.13086	0.13083
			60	0.13101	0.13097	30	0.13062	0.13059
			80	0.13090	0.13086	40	0.13052	0.13048
1,3	1,3	1,3	20	0.13138	0.13135	10	0.13033	0.13030
			40	0.13121	0.13117	20	0.13086	0.13083
			60	0.13101	0.13097	30	0.13062	0.13059
			80	0.13090	0.13086	40	0.13052	0.13048

polation functions have been used for approximating all degrees of freedom.The orders of the approximation for the displacement components are taken as $n_r = m_r = 2$, and $n_\theta = m_\theta = 0$ (with $u_\theta = 0$). Newton's method has been employed to solve the nonlinear finite element equations with error tolerance of 10^{-3}. In Table 5.2, maxi-

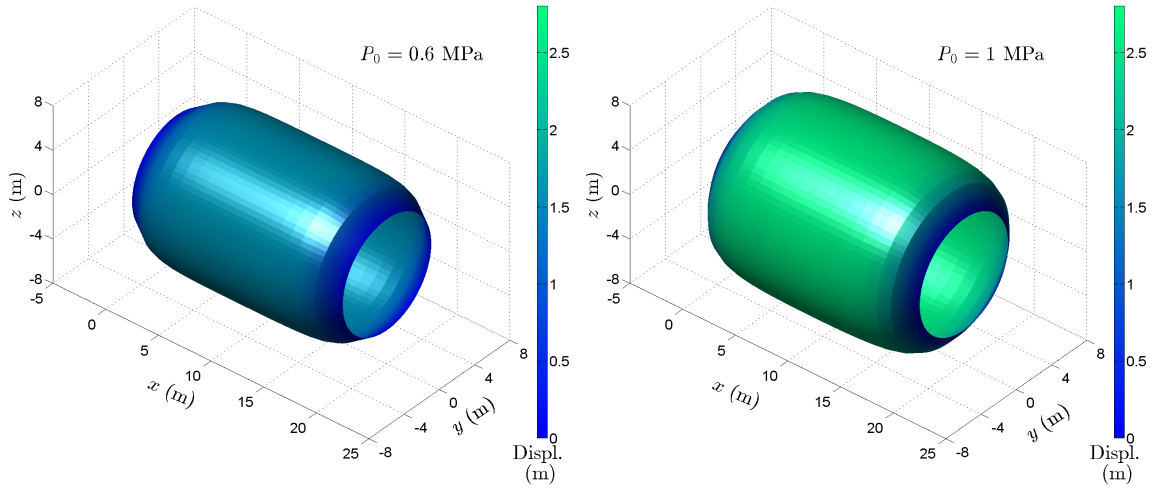

(a) $P_0 = 0.6$ MPa (b) $P_0 = 1$ MPa

Fig. 5.2 Deformed shape of cylindrical shell under internal pressure.

mum radial displacements of the cylindrical shell are presented for various values of the internal pressure for non-displacement dependent as well as fully nonlinear cases. Twenty linear Lagrange elements are used in the nonlinear finite element analysis. To solve the nonlinear equations, the Direct (Picard) method is used with the error tolerance of 10^{-2}. The maximum radial displacements from the 7-parameter shell theory[1] (see Rivera and Reddy [59]) are also tabulated for comparison. Also, fig. 5.3 shows the variation of the maximum radial displacements with respect to the magnitudes of internal pressure (for both non-displacement dependent and fully nonlinear internal pressure) from the one-dimensional theory presented in this study and those of Rivera and Reddy [59]. The response from two studies agrees with each other for the non-displacement dependent internal pressure. But for fully nonlinear pressure, when the pressure increases, difference between responses from the two different analyses (non-displacement dependent and nonlinear pressure) differ, which is justi-

[1]The solution data for 7-parameter shell theory, using finite element method, is provided by Dr. Miguel G. Rivera.

fied because, in the case of nonlinear pressure, the change in inner boundary surface area (and its normal direction) of the cylindrical shell is taken into consideration and hence the pressure force increases with deformation and hence the deflection increases in comparison to the same from non-displacement dependent pressure.

Table 5.2. Comparison of maximum radial displacement of cylindrical shell by one dimensional (1-D) theory and 7-parameter shell theory by nonlinear analysis.

Internal pressure (MPa)	Max. radial displacement (in m)		
	7-parameter shell theory (see [59])	1-D theory (non-disp. dependent pressure)	1-D theory (Fully nonlinear pressure)
0.12	0.3497	0.3515	0.3748
0.24	0.6427	0.6456	0.7244
0.36	0.8984	0.9003	1.0547
0.48	1.1274	1.1308	1.3741
0.60	1.3359	1.3395	1.6831
0.72	1.5280	1.5315	1.9897
0.84	1.7068	1.7105	2.2956
0.96	1.8744	1.8783	2.5976

5.5.2. Pinched cylindrical shell with fixed edges

For the second example, we consider a cylindrical shell of the following geometric and material properties:

$$L = 4 \text{ in}, \qquad r_1 = 0.5 \text{ in}, \qquad r_2 = 0.51 \text{ in} \tag{5.47}$$

$$E = 10 \times 10^6 \text{ psi}, \qquad \nu = 0.3, \tag{5.48}$$

Both ends of the cylinder are completely fixed. Two pinching point forces are applied at the middle point of the cylinder at $\theta = 0$ and $\theta = \pi$ towards the central axis of the cylinder, as shown in fig. 5.4.

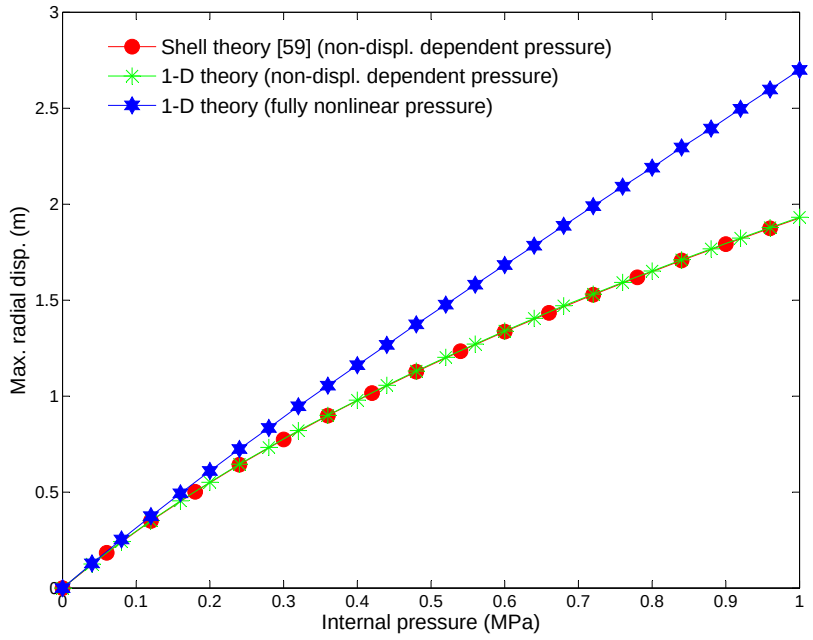

Fig. 5.3 Comparison of maximum radial displacement of cylindrical shell by present one-dimensional theory and 7-parameter shell theory.

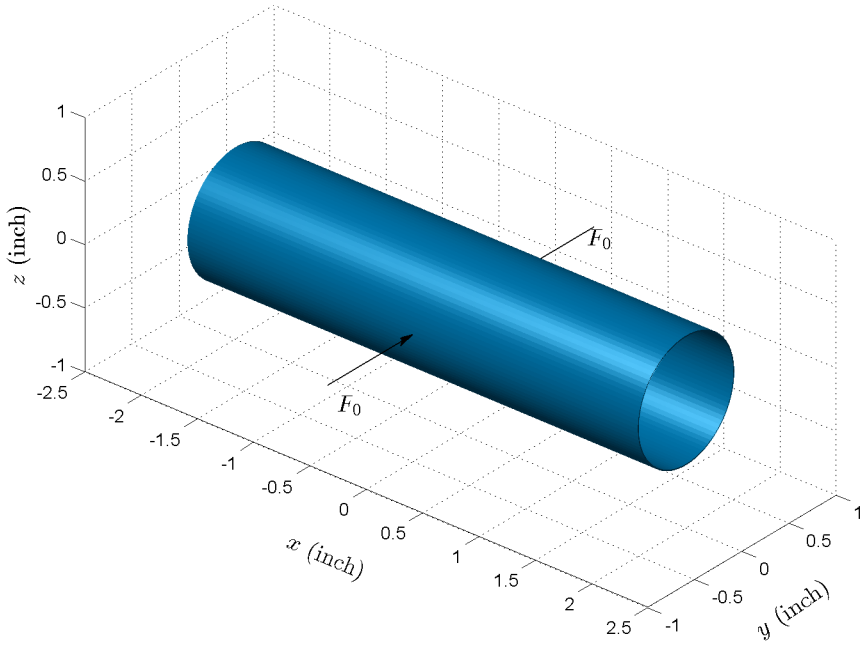

Fig. 5.4 Original shape of cylindrical shell with applied point force.

5.5.2.1. Linear analysis

The radial displacements at the point of pinching are tabulated in Table 5.3 for various order of approximation of the displacements, considering the polynomial and Bessel function of the first kind as radial basis function. The value of each point force is taken as 0.2 kip. The displacement variables or the coefficients are approximated by of linear and quadratic Lagrange elements. Here we observe that approximation order up to two for all approximation orders $n_r, m_r, p_r, n_\theta, m_\theta$, and p_θ give convergent response for both the radial basis functions used.

Table 5.3. Linear FEM solutions for maximum displacement of a cylindrical shell considering various order of approximation of displacement in case of point pinching forces with fixed end boundary condition.

order of approximation of u_s, u_r and u_θ			Magnitude of displacement (in m) at $(x, r, \theta) = (0, r_2, 0)$.					
			linear element			Quadratic element		
n_r, n_θ	m_r, m_θ	p_r, p_θ	no. of elements	$f_i(r) = r^i$ Disp.	$f_i(r) = J_i(r)$ Disp.	no. of elements	$f_i(r) = r^i$ Disp.	$f_i(r) = J_i(r)$ Disp.
1,2	1,2	1,2	20	0.06200	0.06212	10	0.06971	0.06986
			40	0.06941	0.06956	20	0.07276	0.07292
			60	0.07178	0.07194	30	0.07456	0.07473
			80	0.07308	0.07324	40	0.07571	0.07587
			100	0.07394	0.07411	50	0.07641	0.07658
1,3	1,3	1,3	20	0.06200	0.06212	10	0.06971	0.06986
			40	0.06941	0.06956	20	0.07276	0.07292
			60	0.07178	0.07194	30	0.07456	0.07473
			80	0.07308	0.07324	40	0.07571	0.07587
			100	0.07394	0.07411	50	0.07641	0.07658
2,2	2,2	2,2	20	0.06268	0.06268	10	0.07057	0.07057
			40	0.07025	0.07025	20	0.07368	0.07368
			60	0.07267	0.07267	30	0.07555	0.07555
			80	0.07400	0.07400	40	0.07677	0.07677
			100	0.07489	0.07489	50	0.07755	0.07755
2,3	2,3	2,3	20	0.06268	0.06268	10	0.07057	0.07057
			40	0.07025	0.07025	20	0.07368	0.07368
			60	0.07267	0.07267	30	0.07555	0.07555
			80	0.07400	0.07400	40	0.07677	0.07677
			100	0.07489	0.07489	50	0.07755	0.07755
3,3	3,3	3,3	20	0.06268	0.06268	10	0.07057	0.07057
			40	0.07025	0.07025	20	0.07368	0.07368
			60	0.07267	0.07267	30	0.07555	0.07555
			80	0.07400	0.07400	40	0.07677	0.07677
			100	0.07489	0.07489	50	0.07755	0.07755

5.5.2.2. Nonlinear solution

For the nonlinear analysis, Newton's method is employed with the error tolerance equal to 10^{-3}. Forty linear Lagrange elements have been used and all approximation orders, $n_r, m_r, p_r, n_\theta, m_\theta$, and p_θ, are taken as 2. The deformed shape for two different loads, $F_0 = 1$ and 2 kip, are shown in figs. 5.5(a) and 5.5(b), respectively. Figure 5.6 shows the distribution of various components of the second Piola–Kirchhoff stress tensor on the deformed configuration through the colormap.

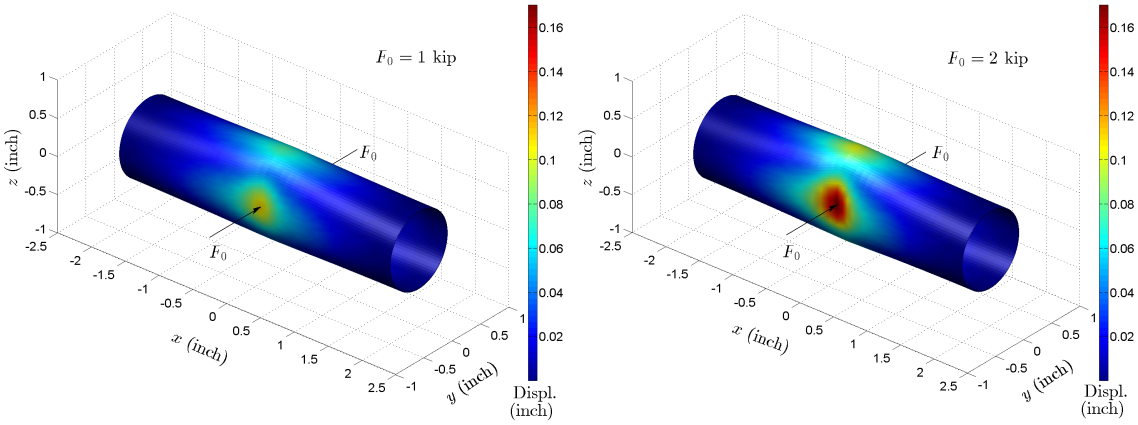

(a) $F_0 = 1$ kip (b) $F_0 = 2$ kip

Fig. 5.5 Deformed shape of pinched cylindrical shell with both end fixed.

5.6. Chapter summary and conclusions

In the present chapter, we have developed a general higher-order theory for one-dimensional analysis of 3-D solids based on a very general approximation of the displacement field of the cross-section in the polar coordinate system. Based on this displacement field, we have derived a one-dimensional governing equation by using the principle of virtual displacement for large deformation. Further, we have developed a weak-form finite element model for the same and applied in the analysis of cylindrical shells under internal pressure and pinching point forces. The numerical results have been validated against the results from a 7-parameter shell theory. Since the present theory results in one-dimensional finite element model, 1-D higher order continuity functions can be used. They proved to be very useful for the gradient dependent theories, which require higher-order continuity. Also, for cases like radial

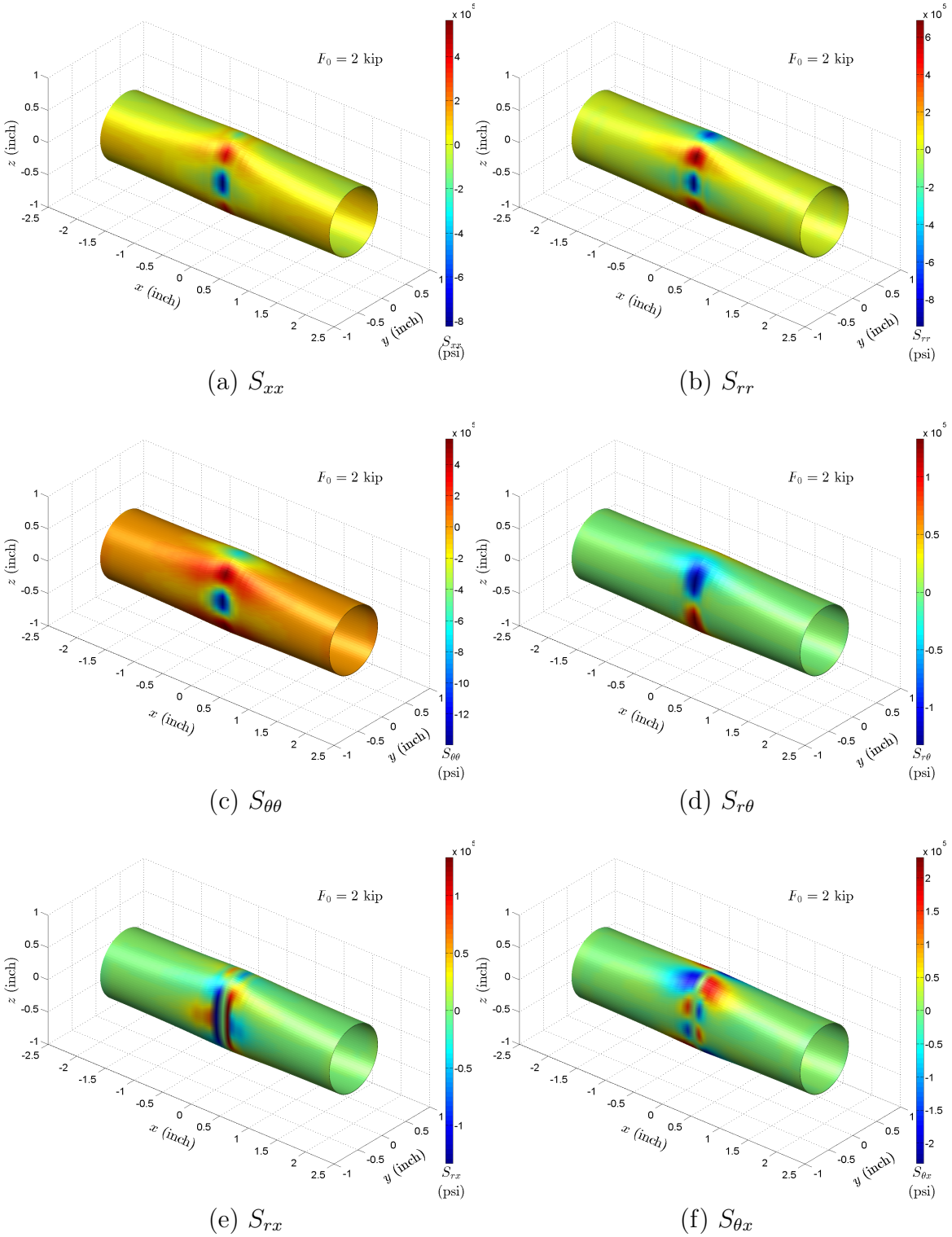

(a) S_{xx} (b) S_{rr}

(c) $S_{\theta\theta}$ (d) $S_{r\theta}$

(e) S_{rx} (f) $S_{\theta x}$

Fig. 5.6 Various components of stress tensor for deformed pinched cylinder.

symmetry, the size of obtained algebraic equations of the finite element formulations is reasonable, as described in the numerical section. However, there is some limitation as far as applying various boundary conditions, which is a limitation of this theory; we can only apply the fixed boundary condition to any cross-section. Any other type of boundary conditions can be applied as constraint condition in the finite element model (something that is yet to be done).

6. A GENERAL HIGHER ORDER ROD THEORY

6.1. Introduction

Rods are structural elements whose centroidal axes can be defined by a space curve and are allowed to move in three-dimensional space. The simulation of rod-like structures in three-dimensional space have many applications, for example, the applications in biophysics like simulation of DNA, surgical simulations or in other areas like, simulation of underwater cables, atomistic simulation of single-wall carbon nanotube (SWCNT), or in computer graphics and robotics, gaming and animation applications in simulating hair or other rod-like objects, to name a few. Historically, the study of bending of elastic rod dates back to 1691 by the work of James Bernoulli. Euler [60] developed the statical theory of rods to analyze bending in its own plane. He also developed a theory of bending of the skewed rod. Then, work of St. Venant introduced the twist and principal torsion about the flexural axis. The exact general equations were given in principle, but obscurely, by Kirchhoff and explicitly by Clebsch, which were capable of modeling both bending and torsion of rods. However, his treatment differs considerably from the modern treatments. In the early years of the 20th century, the Cosserat brothers presented a formulation of Kirchhoffs rod theory using what we now call directors in reference. Truesdell and Ericksens studied the Cosserat brothers work on deformable media [1, 61]. The term "director was introduced by Ericksen and Truesdell in 1958 [62]. The Kirchhoff's rod theory has bending and torsional strains and an inextensible centerline and doesn't exhibit transverse shearing or dilations of the cross section, which can be considered as a special case of Cosserat rod theory. The Cosserat rod theory that accommodates the above additional effects is presented by Green, Naghdi, and Wenner [63, 64]. The continuum formulation of the motion of aforementioned special theory of Cosserat rod or Kirchhoff's rod theory is well established due to the work of Antman[65], Simo[66], and others. In order to obtain a numerical solution, Simo[67] used linearized weak forms of the balance equations and obtained the finite element formulation of three-dimensional finite strain rod model in which, for configuration update, he used an exponential map instead of Euler angle. Goyal, Perkins, and Lee [68] have studied nonlinear behavior of a rod to understand the mechanics of DNA

and underwater cable in three-dimensional space by generalized alpha-method using a finite difference approach to solve the governing differential equations. Goyal, Perkins, and Lee [69] also studied the nonlinear dynamic behavior of intertwining of the rod with self-contact. Kumar, Mukherjee, Fang and co-workers [70, 71, 72, 73] have studied the static deformation of single-walled carbon nanotube using Cosserat rod model by weak form finite element model. Arbind and Reddy [74] have studied the dynamic behavior of Kirchhoff rod using least-square finite element method.

To the best of our knowledge, there has not been any reported research for a general rod theory which can model the deformation of the cross-section of the rod, that is, shearing, dilations, and warping of the cross section of the rod in the existing literature. Most treatments of the rod are based on the rigid motion of the cross-section of the rod during deformation. To fill this gap, we present a general higher order rod theory, which can model a very general deformation of the cross-section of the rod, which is not only specific to thin rod but can also model the deformation of the rod having considerable dimensions as compared to its length (see fig. 6.1). In the present general higher order rod theory, we consider a very general approximation of the displacement field of the cross-section perpendicular to the tangent of the central axis in the curvilinear cylindrical coordinate system. The approximation function could be a general polar Fourier basis functions, which has the attenuating values of the coefficient of higher-order basis functions. Based on this displacement approximation, we develop the governing equation of motion using the principle of virtual displacement for large deformation for the static case. Further, to obtain the solution, we also develop the nonlinear finite element model, followed by some numerical examples of applying the theory discussed herein. This theory can be thought of as an extension of a general higher-order one-dimensional theory in cylindrical coordinates of the previous chapter to a curvilinear cylindrical coordinate system.

6.2. The governing equation of motion

Let us consider a curvilinear- cylindrical coordinate system (r, θ, s) in the reference frame of the rod under investigation, where s is the arc length coordinate measured along the reference curve of the rod and the cross-section of the rod lies in the plane perpendicular to the tangent vector of the reference curve. The coordinate system is shown in fig. 6.2 depicting (r, θ, s) coordinates . And at each point on the curve,

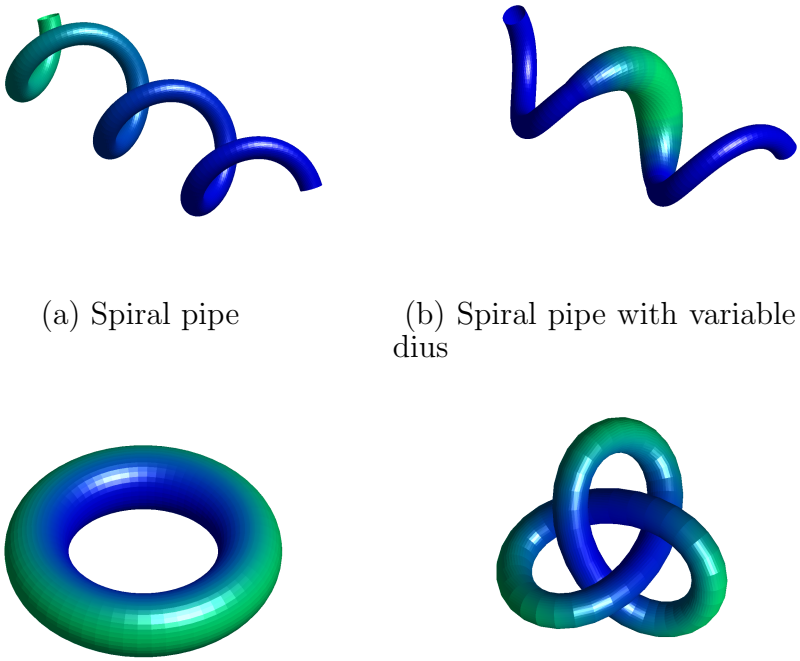

(a) Spiral pipe (b) Spiral pipe with variable radius

(c) Torus (d) Trefoil knot

Fig. 6.1 Various bodies with the central axes defined by space curve.

the tangent $\mathbf{T}$, principal normal $\mathbf{P}$ and binormal $\mathbf{Q}$ (see Appendix E for details) are shown which form the orthonormal basis vectors. The θ coordinate are measured from the principal normal to the binormal vector at any point of the reference curve and r is the radial distance of any point from the reference curve in the normal plane. Now let us consider that $\hat{\mathbf{e}}_s$, $\hat{\mathbf{e}}_r$ and $\hat{\mathbf{e}}_\theta$ are orthonormal basis vectors at any arbitrary point in the curvilinear cylindrical coordinate system. The displacement field in this coordinate system can be written as following:

$$\mathbf{u} = u_s\hat{\mathbf{e}}_s + u_r\hat{\mathbf{e}}_r + u_\theta\hat{\mathbf{e}}_\theta \tag{6.1}$$

In the full generality, we approximate the components of displacement field of the cross-section of the rod as following:

$$u_s = \phi_s^{(0)}(s) + \sum_{j=1}^{n_\theta}\sum_{i=0}^{n_r} f_i(r)(\sin(j\theta)\phi_s^{(k_1)}(s) + \cos(j\theta)\phi_s^{(k_2)}(s)) = \mathbf{A}_s\mathbf{\Phi}_s$$
$$u_r = \phi_r^{(0)}(s) + \sum_{j=1}^{m_\theta}\sum_{i=0}^{m_r} f_i(r)(\sin(j\theta)\phi_r^{(k_1)}(s) + \cos(j\theta)\phi_r^{(k_2)}(s)) = \mathbf{A}_r\mathbf{\Phi}_r$$

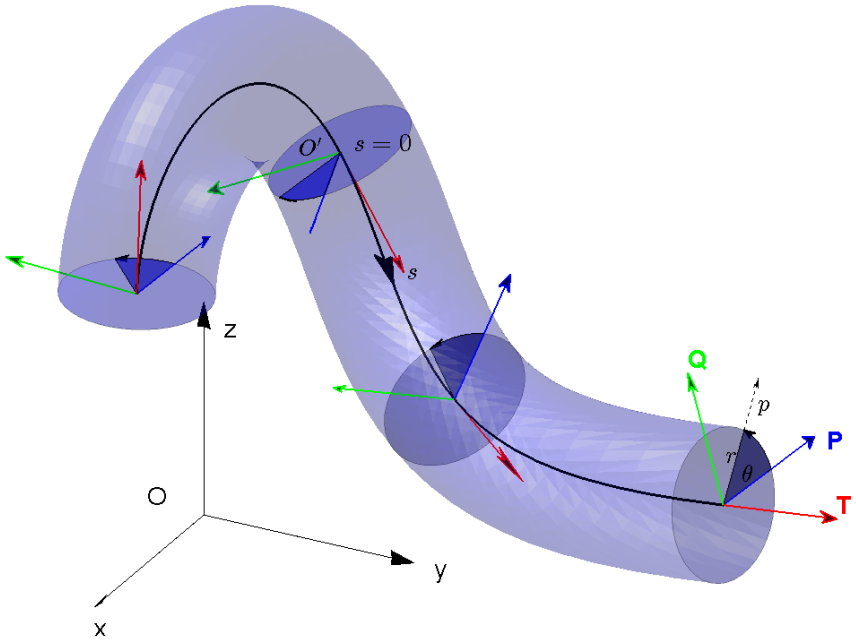

Fig. 6.2 Curvilinear cylindrical coordinate system.

$$u_\theta = \phi_\theta^{(0)}(s) + \sum_{j=1}^{p_\theta} \sum_{i=0}^{p_r} f_i(r)(\sin(j\theta)\phi_\theta^{(k_1)}(s) + \cos(j\theta)\phi_\theta^{(k_2)}(s)) = \mathbf{A}_\theta \mathbf{\Phi}_\theta \quad (6.2)$$

where

$$\begin{aligned}
\mathbf{A}_s &= \begin{bmatrix} \mathbf{a}_s & (\cos\theta)\mathbf{a}_s & (\sin\theta)\mathbf{a}_s & (\cos 2\theta)\mathbf{a}_s & (\sin 2\theta)\mathbf{a}_s & \dots & (\cos n_\theta\theta)\mathbf{a}_s & (\sin n_\theta\theta)\mathbf{a}_s \end{bmatrix} \\
\mathbf{A}_r &= \begin{bmatrix} \mathbf{a}_r & (\cos\theta)\mathbf{a}_r & (\sin\theta)\mathbf{a}_r & (\cos 2\theta)\mathbf{a}_r & (\sin 2\theta)\mathbf{a}_r & \dots & (\cos m_\theta\theta)\mathbf{a}_r & (\sin m_\theta\theta)\mathbf{a}_r \end{bmatrix} \\
\mathbf{A}_\theta &= \begin{bmatrix} \mathbf{a}_\theta & (\cos\theta)\mathbf{a}_\theta & (\sin\theta)\mathbf{a}_\theta & (\cos 2\theta)\mathbf{a}_\theta & (\sin 2\theta)\mathbf{a}_\theta & \dots & (\cos p_\theta\theta)\mathbf{a}_\theta & (\sin p_\theta\theta)\mathbf{a}_\theta \end{bmatrix}
\end{aligned} \quad (6.3)$$

where

$$\begin{aligned}
\mathbf{a}_s &= \begin{bmatrix} 1 & f_1(r) & f_2(r) & \dots & f_{n_r}(r) \end{bmatrix} \\
\mathbf{a}_r &= \begin{bmatrix} 1 & f_1(r) & f_2(r) & \dots & f_{m_r}(r) \end{bmatrix} \\
\mathbf{a}_\theta &= \begin{bmatrix} 1 & f_1(r) & f_2(r) & \dots & f_{p_r}(r) \end{bmatrix}
\end{aligned} \quad (6.4)$$

and

$$\begin{aligned}
\mathbf{\Phi}_s &= \begin{bmatrix} \phi_s^{(0)} & \phi_s^{(1)} & \phi_s^{(2)} & \dots & \phi_s^{(\tilde{n})} \end{bmatrix}^T, \quad \tilde{n} = (1+n_r)(1+2n_\theta) \\
\mathbf{\Phi}_r &= \begin{bmatrix} \phi_r^{(0)} & \phi_r^{(1)} & \phi_r^{(2)} & \dots & \phi_r^{(\tilde{m})} \end{bmatrix}^T, \quad \tilde{m} = (1+m_r)(1+2m_\theta) \\
\mathbf{\Phi}_\theta &= \begin{bmatrix} \phi_\theta^{(0)} & \phi_\theta^{(1)} & \phi_\theta^{(2)} & \dots & \phi_\theta^{(\tilde{p})} \end{bmatrix}^T, \quad \tilde{p} = (1+p_r)(1+2p_\theta)
\end{aligned} \tag{6.5}$$

where $f_i(r)$ are basis functions in variable r which could the polynomial $f_i(r) = r^i$ or linear combination of Bessel function of first and second kind. If we consider Bessel functions for $f_i(r)$, the approximations of displacements components becomes the Fourier series in polar coordinate system. And $\phi_s^{(0)}$, $\phi_r^{(0)}$ and $\phi_\theta^{(0)}$ are the displacement of the centroid of the cross-section along the unit basis vectors of the assumed coordinate system namely along $\hat{\mathbf{e}}_s, \hat{\mathbf{e}}_r$ and $\hat{\mathbf{e}}_\theta$ respectively. Then the displacement vector at a point can also be written as following:

$$\mathbf{u} = \mathbf{A}\mathbf{\Phi}, \quad \text{where } \mathbf{A} = \begin{bmatrix} \mathbf{A}_s & \mathbf{0} & \mathbf{0} \\ \mathbf{0} & \mathbf{A}_r & \mathbf{0} \\ \mathbf{0} & \mathbf{0} & \mathbf{A}_\theta \end{bmatrix}, \quad \mathbf{\Phi} = \begin{Bmatrix} \mathbf{\Phi}_s \\ \mathbf{\Phi}_r \\ \mathbf{\Phi}_\theta \end{Bmatrix}, \quad \mathbf{u} = \begin{Bmatrix} u_s \\ u_r \\ u_\theta \end{Bmatrix} \tag{6.6}$$

The Green-Lagrange strain tensor can be given as following:

$$\mathbf{E} = \frac{1}{2}(\boldsymbol{\nabla}\mathbf{u} + (\boldsymbol{\nabla}\mathbf{u})^T + (\boldsymbol{\nabla}\mathbf{u}) \cdot (\boldsymbol{\nabla}\mathbf{u})^T) \tag{6.7}$$

Based on the displacement field given in Eq. (6.2), the components of Green-Lagrange strain tensor in the assumed cylindrical curvilinear co-ordinate system (see Appendix D for detail derivation) can be given as following:

$$\begin{aligned}
E_{ss} &= (\mathbf{A}_s\mathbf{\Phi}_{s,s} - \kappa\, \cos\theta\, \mathbf{A}_r\mathbf{\Phi}_r + \kappa\, \sin\theta\, \mathbf{A}_\theta\mathbf{\Phi}_\theta) + \frac{1}{2}\left(\mathbf{A}_s\mathbf{\Phi}_{s,s} - \kappa\, \cos\theta\, \mathbf{A}_r\mathbf{\Phi}_r\right. \\
&\quad \left. + \kappa\, \sin\theta\, \mathbf{A}_\theta\mathbf{\Phi}_\theta\right)^2 + \frac{1}{2}\left(\mathbf{A}_r\mathbf{\Phi}_{r,s} + \kappa\, \cos\theta\, \mathbf{A}_s\mathbf{\Phi}_s - \tau\, \mathbf{A}_\theta\mathbf{\Phi}_\theta\right)^2 \\
&\quad + \frac{1}{2}\left(\mathbf{A}_\theta\mathbf{\Phi}_{\theta,s} - \kappa\, \sin\theta\, \mathbf{A}_s\mathbf{\Phi}_s + \tau\mathbf{A}_r\mathbf{\Phi}_r\right)^2 \\
E_{rr} &= \mathbf{A}_{r,r}\mathbf{\Phi}_r + \frac{1}{2}\left(\mathbf{A}_{s,r}\mathbf{\Phi}_s - \kappa\, \cos\theta\, \mathbf{A}_s\mathbf{\Phi}_s\right)^2 + \frac{1}{2}\left(\mathbf{A}_{r,r}\mathbf{\Phi}_r\right)^2 + \frac{1}{2}\left(\mathbf{A}_{\theta,r}\mathbf{\Phi}_\theta + \tau\, \mathbf{A}_s\mathbf{\Phi}_s\right)^2 \\
E_{\theta\theta} &= \frac{1}{r}\left(\mathbf{A}_{\theta,\theta}\mathbf{\Phi}_\theta + \mathbf{A}_r\mathbf{\Phi}_r\right) + \frac{1}{2}\left[\left(\frac{1}{r}\mathbf{A}_{s,\theta}\mathbf{\Phi}_s + \kappa\, \sin\theta\, \mathbf{A}_s\mathbf{\Phi}_s\right)^2\right.
\end{aligned}$$

$$
\begin{aligned}
&+\left(\frac{1}{r}\mathbf{A}_{r,\theta}\mathbf{\Phi}_r-\tau\,\mathbf{A}_s\mathbf{\Phi}_s-\frac{\mathbf{A}_\theta\mathbf{\Phi}_\theta}{r}\right)^2+\left(\frac{1}{r}\mathbf{A}_{\theta,\theta}\mathbf{\Phi}_\theta+\frac{\mathbf{A}_r\mathbf{\Phi}_r}{r}\right)^2\Bigg]\\
2E_{r\theta}=&\frac{1}{r}\mathbf{A}_{r,\theta}\mathbf{\Phi}_r-\frac{\mathbf{A}_\theta\mathbf{\Phi}_\theta}{r}+\mathbf{A}_{\theta,r}\mathbf{\Phi}_\theta+(\mathbf{A}_{s,r}\mathbf{\Phi}_s-\kappa\,\cos\theta\,\mathbf{A}_s\mathbf{\Phi}_s)\left(\frac{1}{r}\mathbf{A}_{s,\theta}\mathbf{\Phi}_s\right.\\
&\left.+\kappa\,\sin\theta\,\mathbf{A}_s\mathbf{\Phi}_s\right)+(\mathbf{A}_{r,r}\mathbf{\Phi}_r)\left(\frac{1}{r}\mathbf{A}_{r,\theta}\mathbf{\Phi}_r-\tau\,\mathbf{A}_s\mathbf{\Phi}_s-\frac{1}{r}\mathbf{A}_\theta\mathbf{\Phi}_\theta\right)\\
&+(\mathbf{A}_{\theta,r}\mathbf{\Phi}_\theta+\tau\,\mathbf{A}_s\mathbf{\Phi}_s)\left(\frac{1}{r}\mathbf{A}_{\theta,\theta}\mathbf{\Phi}_\theta+\frac{1}{r}\mathbf{A}_r\mathbf{\Phi}_r\right)\\
2E_{\theta s}=&\mathbf{A}_\theta\mathbf{\Phi}_{\theta,s}+\frac{1}{r}\mathbf{A}_{s,\theta}\mathbf{\Phi}_s+\tau\mathbf{A}_r\mathbf{\Phi}_r\\
&+\left(\frac{1}{r}\mathbf{A}_{s,\theta}\mathbf{\Phi}_s+\kappa\,\sin\theta\,\mathbf{A}_s\mathbf{\Phi}_s\right)(\mathbf{A}_s\mathbf{\Phi}_{s,s}-\kappa\,\cos\theta\,\mathbf{A}_r\mathbf{\Phi}_r+\kappa\,\sin\theta\,\mathbf{A}_\theta\mathbf{\Phi}_\theta)\\
&+\left(\frac{1}{r}\mathbf{A}_{r,\theta}\mathbf{\Phi}_r-\tau\,\mathbf{A}_s\mathbf{\Phi}_s-\frac{\mathbf{A}_\theta\mathbf{\Phi}_\theta}{r}\right)(\mathbf{A}_r\mathbf{\Phi}_{r,s}+\kappa\,\cos\theta\,\mathbf{A}_s\mathbf{\Phi}_s-\tau\mathbf{A}_\theta\mathbf{\Phi}_\theta)\\
&+\frac{1}{r}(\mathbf{A}_{\theta,\theta}\mathbf{\Phi}_\theta+\mathbf{A}_r\mathbf{\Phi}_r)(\mathbf{A}_\theta\mathbf{\Phi}_{\theta,s}-\kappa\,\sin\theta\,\mathbf{A}_s\mathbf{\Phi}_s+\tau\mathbf{A}_r\mathbf{\Phi}_r)\\
2E_{sr}=&\mathbf{A}_{s,r}\mathbf{\Phi}_s+\mathbf{A}_r\mathbf{\Phi}_{r,s}-\tau\,\mathbf{A}_\theta\mathbf{\Phi}_\theta\\
&+(\mathbf{A}_s\mathbf{\Phi}_{s,s}-\kappa\,\cos\theta\,\mathbf{A}_r\mathbf{\Phi}_r+\kappa\,\sin\theta\,\mathbf{A}_\theta\mathbf{\Phi}_\theta)(\mathbf{A}_{s,r}\mathbf{\Phi}_s-\kappa\,\cos\theta\,\mathbf{A}_s\mathbf{\Phi}_s)\\
&+(\mathbf{A}_{r,r}\mathbf{\Phi}_r)(\mathbf{A}_r\mathbf{\Phi}_{r,s}+\kappa\,\cos\theta\,\mathbf{A}_s\mathbf{\Phi}_s-\tau\mathbf{A}_\theta\mathbf{\Phi}_\theta)\\
&+(\mathbf{A}_\theta\mathbf{\Phi}_{\theta,s}-\kappa\,\sin\theta\,\mathbf{A}_s\mathbf{\Phi}_s+\tau\mathbf{A}_r\mathbf{\Phi}_r)(\mathbf{A}_{\theta,r}\mathbf{\Phi}_\theta+\tau\,\mathbf{A}_s\mathbf{\Phi}_s)
\end{aligned}
\tag{6.8}
$$

where $(\ )_{,s}$ represent the derivative with respect to s and so on. The strain tensor can be rewritten in vector form as follows:

$$
\mathbf{E}\;=\;(\mathbf{A}_1+\frac{1}{2}\mathbf{A}_{nl})\mathbf{\Phi}+(\mathbf{A}_2+\frac{1}{2}\mathbf{A}_{nl_s})\frac{d\mathbf{\Phi}}{ds}
\tag{6.9}
$$

where

$$
\mathbf{E}\;=\;\begin{bmatrix}E_{ss} & E_{rr} & E_{\theta\theta} & 2E_{r\theta} & 2E_{\theta s} & 2E_{sr}\end{bmatrix}^T,\quad \mathbf{\Phi}=\begin{bmatrix}\mathbf{\Phi}_s^T & \mathbf{\Phi}_r^T & \mathbf{\Phi}_\theta^T\end{bmatrix}^T
$$

$$
\mathbf{A}_1\;=\;\begin{bmatrix}\mathbf{0} & -\kappa\,\cos\theta\,\mathbf{A}_r & \kappa\,\sin\theta\,\mathbf{A}_\theta\\ \mathbf{0} & \mathbf{A}_{r,r} & \mathbf{0}\\ \mathbf{0} & (1/r)\mathbf{A}_r & (1/r)\mathbf{A}_{\theta,\theta}\\ \mathbf{0} & (1/r)\mathbf{A}_{r,\theta} & -(1/r)\mathbf{A}_\theta+\mathbf{A}_{\theta,r}\\ (1/r)\mathbf{A}_{s,\theta} & \tau\mathbf{A}_r & \mathbf{0}\\ \mathbf{A}_{s,r} & \mathbf{0} & -\tau\mathbf{A}_\theta\end{bmatrix},\quad \mathbf{A}_2=\begin{bmatrix}\mathbf{A}_s & \mathbf{0} & \mathbf{0}\\ \mathbf{0} & \mathbf{0} & \mathbf{0}\\ \mathbf{0} & \mathbf{0} & \mathbf{0}\\ \mathbf{0} & \mathbf{0} & \mathbf{0}\\ \mathbf{0} & \mathbf{0} & \mathbf{A}_\theta\\ \mathbf{0} & \mathbf{A}_r & \mathbf{0}\end{bmatrix}
$$

$$\mathbf{A}_{nl_s} = \begin{bmatrix} \begin{matrix}(u_{s,s} - \kappa\cos\theta\, u_r \\ +\kappa\sin\theta\, u_\theta)\mathbf{A}_s\end{matrix} & \begin{matrix}(u_{r,s} + \kappa\cos\theta\, u_s \\ -\tau u_\theta)\mathbf{A}_r\end{matrix} & \begin{matrix}(u_{\theta,s} - \kappa\sin\theta\, u_s \\ +\tau u_r)\mathbf{A}_\theta\end{matrix} \\ \mathbf{0} & \mathbf{0} & \mathbf{0} \\ \mathbf{0} & \mathbf{0} & \mathbf{0} \\ \mathbf{0} & \mathbf{0} & \mathbf{0} \\ \left(\frac{1}{r}u_{s,\theta} + \kappa\sin\theta\, u_s\right)\mathbf{A}_s & \left(\frac{1}{r}u_{r,\theta} - \tau u_s - \frac{1}{r}u_\theta\right)\mathbf{A}_r & \left(\frac{1}{r}u_{\theta,\theta} + \frac{1}{r}u_r\right)\mathbf{A}_\theta \\ (u_{s,r} - \kappa\cos\theta\, u_s)\,\mathbf{A}_s & u_{r,r}\mathbf{A}_r & (u_{\theta,r} + \tau u_s)\,\mathbf{A}_\theta \end{bmatrix} \tag{6.10}$$

$$
\mathbf{A}_{nl} \;=\; \begin{bmatrix}
\begin{array}{c}\big\{\kappa\cos\theta\,(u_{r,s}+\kappa\cos\theta\,u_s-\tau u_\theta)\\ -\kappa\sin\theta(u_{\theta,s}-\kappa\sin\theta\,u_s+\tau u_r)\big\}\mathbf{A}_s\end{array} &
\begin{array}{c}\big\{-\kappa\,\cos\theta\,(u_{s,s}-\kappa\cos\theta\,u_r\\ +\kappa\sin\theta\,u_\theta)+\tau(u_{\theta,s}\\ -\kappa\sin\theta\,u_s+\tau u_r)\big\}\mathbf{A}_r\end{array} &
\begin{array}{c}\big\{\kappa\sin\theta\,(u_{s,s}-\kappa\cos\theta\,u_r\\ +\kappa\sin\theta\,u_\theta)-\tau(u_{r,s}\\ +\kappa\,\cos\theta\,u_s-\tau u_\theta)\big\}\mathbf{A}_\theta\end{array} \\
\begin{array}{c}\big\{(u_{s,r}-\kappa\cos\theta\,u_s)(\mathbf{A}_{s,r}-\kappa\cos\theta\mathbf{A}_s)\\ +\tau(u_{\theta,r}+\tau u_s)\mathbf{A}_s\big\}\end{array} &
u_{r,r}\mathbf{A}_{r,r} &
(u_{\theta,r}+\tau u_s)\mathbf{A}_{\theta,r} \\
\begin{array}{c}\big\{\left(\frac{u_{s,\theta}}{r}+\kappa\sin\theta\,u_s\right)\left(\frac{1}{r}\mathbf{A}_{s,\theta}+\kappa\sin\theta\,\mathbf{A}_s\right)\\ -\tau\left(\frac{1}{r}u_{r,\theta}-\tau u_s-\frac{u_\theta}{r}\right)\mathbf{A}_s\big\}\end{array} &
\begin{array}{c}\big\{\frac{1}{r}\left(\frac{1}{r}u_{r,\theta}-\tau u_s-\frac{1}{r}u_\theta\right)\mathbf{A}_{r,\theta}\\ +\frac{1}{r}\left(\frac{1}{r}u_{\theta,\theta}+\frac{u_r}{r}\right)\mathbf{A}_r\big\}\end{array} &
\begin{array}{c}\big\{-\frac{1}{r}\left(\frac{1}{r}u_{r,\theta}-\tau u_s-\frac{1}{r}u_\theta\right)\mathbf{A}_\theta\\ +\frac{1}{r}\left(\frac{1}{r}u_{\theta,\theta}+\frac{u_r}{r}\right)\mathbf{A}_{\theta,\theta}\big\}\end{array} \\
\begin{array}{c}\big\{\left(u_{s,r}-\kappa\cos\theta\,u_s\right)\left(\frac{1}{r}\mathbf{A}_{s,\theta}+\kappa\sin\theta\,\mathbf{A}_s\right)\\ +\left(\frac{1}{r}u_{s,\theta}+\kappa\sin\theta\,u_s\right)\left(\mathbf{A}_{s,r}-\kappa\cos\theta\,\mathbf{A}_s\right)\\ -\tau u_{r,r}\mathbf{A}_s+\tau\left(\frac{1}{r}u_{\theta,\theta}+\frac{u_r}{r}\right)\mathbf{A}_s\big\}\end{array} &
\begin{array}{c}\big\{\frac{1}{r}u_{r,r}\mathbf{A}_{r,\theta}+\left(\frac{1}{r}u_{r,\theta}-\tau u_s\right.\\ \left.-\frac{1}{r}u_\theta\right)\mathbf{A}_{r,r}+\frac{1}{r}\big(u_{\theta,r}\\ +\tau u_s\big)\mathbf{A}_r\big\}\end{array} &
\begin{array}{c}\big\{-\frac{1}{r}u_{r,r}\mathbf{A}_\theta+\frac{1}{r}\big(u_{\theta,r}\\ +\tau u_s\big)\mathbf{A}_{\theta,\theta}+\left(\frac{1}{r}u_{\theta,\theta}\right.\\ \left.+\frac{u_r}{r}\right)\mathbf{A}_{\theta,r}\big\}\end{array} \\
\begin{array}{c}\big\{\left(u_{s,s}-\kappa\cos\theta\,u_r+\kappa\sin\theta\,u_\theta\right)\left(\frac{1}{r}\mathbf{A}_{s,\theta}\right.\\ \left.+\kappa\sin\theta\,\mathbf{A}_s\right)+\kappa\cos\theta\left(\frac{1}{r}u_{r,\theta}-\tau u_s\right.\\ \left.-\frac{1}{r}u_\theta\right)\mathbf{A}_s-\tau\left(u_{r,s}+\kappa\cos\theta\,u_s-\tau u_\theta\right)\mathbf{A}_s\\ -\kappa\sin\theta\,\left(\frac{1}{r}u_{\theta,\theta}+\frac{1}{r}u_r\right)\mathbf{A}_s\big\}\end{array} &
\begin{array}{c}\big\{-\kappa\cos\theta\,\left(\frac{1}{r}u_{s,\theta}+\kappa\sin\theta\,u_s\right)\mathbf{A}_r\\ +\frac{1}{r}\left(u_{r,s}+\kappa\cos\theta\,u_s-\tau u_\theta\right)\mathbf{A}_{r,\theta}\\ +\tau\left(\frac{1}{r}u_{\theta,\theta}+\frac{1}{r}u_r\right)\mathbf{A}_r\\ +\frac{1}{r}\left(u_{\theta,s}-\kappa\sin\theta\,u_s+\tau u_r\right)\mathbf{A}_r\big\}\end{array} &
\begin{array}{c}\big\{\kappa\sin\theta\,\left(\frac{1}{r}u_{s,\theta}+\kappa\sin\theta\,u_s\right)\mathbf{A}_\theta\\ -\tau\left(\frac{1}{r}u_{r,\theta}-\tau u_s-\frac{1}{r}u_\theta\right)\mathbf{A}_\theta\\ -\frac{1}{r}\left(u_{r,s}+\kappa\cos\theta\,u_s-\tau u_\theta\right)\mathbf{A}_\theta\\ +\frac{1}{r}(u_{\theta,s}-\kappa\,\sin\theta\,u_s+\tau u_r)\mathbf{A}_{\theta,\theta}\big\}\end{array} \\
\begin{array}{c}\big\{\left(u_{s,s}-\kappa\cos\theta\,u_r+\kappa\sin\theta\,u_\theta\right)\left(\mathbf{A}_{s,r}\right.\\ \left.-\kappa\cos\theta\,\mathbf{A}_s\right)+\kappa\cos\theta\,u_{r,r}\mathbf{A}_s+\tau\big(u_{\theta,s}\\ -\kappa\sin\theta\,u_s+\tau u_r\big)\mathbf{A}_s\\ -\kappa\sin\theta\,\left(u_{\theta,r}+\tau u_s\right)\mathbf{A}_s\big\}\end{array} &
\begin{array}{c}\big\{-\kappa\cos\theta\,\left(u_{s,r}-\kappa\cos\theta\,u_s\right)\mathbf{A}_r\\ +\left(u_{r,s}+\kappa\cos\theta\,u_s-\tau u_\theta\right)\mathbf{A}_{r,r}\\ +\tau\left(u_{\theta,r}+\tau u_s\right)\mathbf{A}_r\big\}\end{array} &
\begin{array}{c}\big\{\kappa\sin\theta\,\left(u_{s,r}-\kappa\cos\theta\,u_s\right)\mathbf{A}_\theta\\ -\tau u_{r,r}\mathbf{A}_\theta+\big(u_{\theta,s}-\kappa\sin\theta\,u_s\\ +\tau u_r\big)\mathbf{A}_{\theta,r}\big\}\end{array}
\end{bmatrix} \tag{6.11}
$$

The potential energy due to strain can be given as following:

$$\mathcal{U} = \frac{1}{2}\int_0^L \int_A \mathbf{E}\cdot\mathbf{C}_e\cdot\mathbf{E}\, dA\, ds \tag{6.12}$$

Where $\mathbf{C}_e$ is the material constant of elasticity. The component of second Piola-Kirchhoff stress tensor which is the energy conjugate of Green-Lagrange strain tensor, can be given as following:

$$\mathbf{S} = \mathbf{C}_e\cdot\mathbf{E} \tag{6.13}$$

Further the first variation in the potential energy is:

$$\begin{aligned}
\delta\mathcal{U} &= \int_0^L\int_A \delta\mathbf{E}\cdot\mathbf{S}\, dA\, ds \\
&= \int_0^L\int_A \left((\mathbf{A}_1+\mathbf{A}_{nl})\delta\mathbf{\Phi} + (\mathbf{A}_2+\mathbf{A}_{nl_s})\frac{d\delta\mathbf{\Phi}}{ds}\right)\cdot\mathbf{S}\, dA\, ds \\
&= \int_0^L \delta\mathbf{\Phi}\cdot(\mathbf{M}_1+\mathbf{M}_{nl}) + \frac{d\delta\mathbf{\Phi}}{ds}\cdot(\mathbf{M}_{nl_s}+\mathbf{M}_2)\, ds
\end{aligned} \tag{6.14}$$

where

$$\begin{aligned}
&\mathbf{M}_j = \int_A \mathbf{A}_j^T\mathbf{S}\, dA \quad \text{for } j=1,2 \\
&\mathbf{M}_{nl} = \int_A \mathbf{A}_{nl}^T\mathbf{S}\, dA, \quad \mathbf{M}_{nl_s} = \int_A \mathbf{A}_{nl_s}^T\mathbf{S}\, dA
\end{aligned} \tag{6.15}$$

Now let us consider that $\mathbf{f}_b$ is the body force applied on per unit deformed volume and $\mathbf{q}_i$ are traction force applied on the ith boundary surfaces (inner and outer surfaces in case of hollow structures) of the body in the deformed (current) configuration, then the virtual work done by the applied forces in the course of virtual displacement $\delta\mathbf{u}$ in the deformed configuration can be given as following:

$$\delta\mathcal{V} = -\left(\int_v \mathbf{f}_b\cdot\delta\mathbf{u}\, dv + \int_{\bar{\mathcal{S}}_i}\mathbf{q}_i\cdot\delta\mathbf{u}\, d\bar{\mathcal{S}}_i\right) \tag{6.16}$$

where dv and $d\bar{\mathcal{S}}_i$ are the infinitesimal volume and area element in the deformed configuration. The corresponding volume and area element dV and $d\mathcal{S}_i$ in the reference configuration can be given as following:

$$dv = \det(\mathbf{F})\, dV, \quad d\bar{\mathcal{S}}_i\mathbf{n} = \det(\mathbf{F})\,\mathbf{F}^{-T}\cdot(d\mathcal{S}_i\mathbf{N}) \tag{6.17}$$

where $\mathbf{F}$ is the deformation gradient and $\mathbf{n}$ and $\mathbf{N}$ are the outward unit normal vector to the area element in deformed and the reference configuration respectively (see Appendix F for the expression of $\mathbf{N}$ for an arbitrary surface in assumed cylindrical coordinate system in reference configuration). The magnitude of area element and the normal vector can be transformed back to the reference frame as following:

$$d\bar{\mathcal{S}}_i = \det(\mathbf{F})\sqrt{(\mathbf{C}^{-1}\cdot\mathbf{N})\cdot\mathbf{N}}\,d\mathcal{S}_i, \quad \mathbf{n} = \frac{\mathbf{F}^{-T}\cdot\mathbf{N}}{\sqrt{(\mathbf{C}^{-1}\cdot\mathbf{N})\cdot\mathbf{N}}} \tag{6.18}$$

where $\mathbf{C} = \mathbf{F}^T\cdot\mathbf{F}$ is the right Cauchy–Green deformation tensor. Using eqs.(6.16), (6.17) and (6.18), the virtual work done by the external forces can be rewritten in the reference frame as following:

$$\begin{aligned}
\delta\mathcal{V} &= -\int_V (\det(\mathbf{F})\mathbf{f}_b)\cdot\delta\mathbf{u}\,dV - \int_{\mathcal{S}_i}\left(\det(\mathbf{F})\sqrt{(\mathbf{C}^{-1}\cdot\mathbf{N})\cdot\mathbf{N}}\right)\mathbf{q}_i\cdot\delta\mathbf{u}\;d\mathcal{S}_i \\
&= -\int_0^L\Big[\int_A (\det(\mathbf{F})\mathbf{f}_b)\cdot\delta\mathbf{u}\,dA + \int_0^{2\pi}\left(\det(\mathbf{F})\sqrt{(\mathbf{C}^{-1}\cdot\mathbf{N})\cdot\mathbf{N}}\right)\mathbf{q}_i\cdot\delta\mathbf{u}\sqrt{G_i}\,d\theta\Big]\,ds \\
&= -\int_0^L \delta\mathbf{\Phi}\cdot\hat{\mathbf{f}}\,ds
\end{aligned} \tag{6.19}$$

where $\hat{\mathbf{f}}$ is defined (given $\mathbf{f}_b = f_{b_s}\hat{\mathbf{e}}_s + f_{b_r}\hat{\mathbf{e}}_r + f_{b_\theta}\hat{\mathbf{e}}_\theta$ and $\mathbf{q}_i = q_{s_i}\hat{\mathbf{e}}_s + q_{r_i}\hat{\mathbf{e}}_r + q_{\theta_i}\hat{\mathbf{e}}_\theta$) as follows:

$$\begin{aligned}
\hat{\mathbf{f}} &= \begin{bmatrix}\hat{\mathbf{f}}_s & \hat{\mathbf{f}}_r & \hat{\mathbf{f}}_\theta\end{bmatrix}^T, \\
\hat{\mathbf{f}}_s &= \int_A \det(\mathbf{F}) f_{b_s}\mathbf{A}_s^T\,dA + \int_0^{2\pi}\sqrt{G_i}\left(\det(\mathbf{F})\sqrt{(\mathbf{C}^{-1}\cdot\mathbf{N})\cdot\mathbf{N}}\right)q_{s_i}\mathbf{A}_s^T\,d\theta \\
\hat{\mathbf{f}}_r &= \int_A \det(\mathbf{F}) f_{b_r}\mathbf{A}_r^T\,dA + \int_0^{2\pi}\sqrt{G_i}\left(\det(\mathbf{F})\sqrt{(\mathbf{C}^{-1}\cdot\mathbf{N})\cdot\mathbf{N}}\right)q_{r_i}\mathbf{A}_r^T\,d\theta \\
\hat{\mathbf{f}}_\theta &= \int_A \det(\mathbf{F}) f_{b_\theta}\mathbf{A}_\theta^T\,dA + \int_0^{2\pi}\sqrt{G_i}\left(\det(\mathbf{F})\sqrt{(\mathbf{C}^{-1}\cdot\mathbf{N})\cdot\mathbf{N}}\right)q_{\theta_i}\mathbf{A}_\theta^T\,d\theta
\end{aligned} \tag{6.20}$$

here G_i is the determinant of covariant matric tensor of the surface co-ordinate (s,θ) for ith boundary surface in the curvilinear cylindrical coordinate system, (see Appendix F for detail derivation) and can be given as following:

$$G_i = (1-\kappa r_i(s,\theta)\,\cos\theta)^2\left(\left(\frac{\partial r_i(s,\theta)}{\partial\theta}\right)^2 + (r_i(s,\theta))^2\right)$$

$$+\left(r_i(s,\theta)\,\frac{\partial r_i(s,\theta)}{\partial s}-\tau\,r_i(s,\theta)\frac{\partial r_i(s,\theta)}{\partial \theta}\right)^2 \tag{6.21}$$

where $r_i(s,\theta)$ defines the ith boundary surface and κ and τ are the curvature and the torsion of the reference space curve of the rod at arc-length coordinate s (see Appendix E). If the body force is given as force per unit mass then it can be expressed as $\mathbf{f}_b = \rho\mathbf{f}_m = (\rho_0/\det(\mathbf{F}))\mathbf{f}_m$. Here ρ and ρ_0 are the mass density of the body in the deformed and reference configuration respectively. A very common example of distributed traction force at the boundary surface is pressure force which can be given as $\mathbf{q}_i = P_{0_i}\mathbf{n} = (P_{0_i}/\sqrt{(\mathbf{C}^{-1}\cdot\mathbf{N})\cdot\mathbf{N}})\mathbf{F}^{-T}\cdot\mathbf{N}$, where P_{0_i} is the magnitude of the pressure. For the point load at any point, the surface traction force can be given as two dimensional dirac delta function. But it should be noted that constant point force means the area under the dirac-delta function should be taken as constant and it would not depend on the deformation. Similarly, line load can be given by one dimensional dirac delta function. Further, from the principle of virtual displacement (see Reddy [41]), we can write the following:

$$\begin{aligned}
0 &= \delta\mathcal{U}+\delta\mathcal{V} \\
&= \int_0^L \left(\delta\mathbf{\Phi}\cdot(\mathbf{M}_1+\mathbf{M}_{nl}) + \frac{d\delta\mathbf{\Phi}}{ds}\cdot(\mathbf{M}_2+\mathbf{M}_{nl_s}) - \delta\mathbf{\Phi}\cdot\hat{\mathbf{f}}\right) ds \\
&= \int_0^L \delta\mathbf{\Phi}\cdot\left((\mathbf{M}_1+\mathbf{M}_{nl}) - \frac{d}{ds}(\mathbf{M}_2+\mathbf{M}_{nl_s}) - \hat{\mathbf{f}}\right) ds \\
&\quad + [\delta\mathbf{\Phi}\cdot(\mathbf{M}_2+\mathbf{M}_{nl_s})]_0^L
\end{aligned} \tag{6.22}$$

Hence the equation of motion (Euler-Lagrange equation) can be given as:

$$(\mathbf{M}_1+\mathbf{M}_{nl}) - \frac{d}{ds}(\mathbf{M}_2+\mathbf{M}_{nl_s}) - \hat{\mathbf{f}} = 0 \tag{6.23}$$

and the essential and natural boundary variables are

$$\delta\mathbf{\Phi}: \qquad \mathbf{M}_2+\mathbf{M}_{nl_s} \tag{6.24}$$

6.3. Constitutive relation

In this study, we will consider isotropic and homogeneous material with the linear relation between second Piola stress tensor and Green-Lagrange strain tensor:

$$\mathbf{S} = \mathbf{C}_e\cdot\mathbf{E} \tag{6.25}$$

where

$$
\begin{aligned}
\mathbf{C}_e &= \frac{E(1-\nu)}{(1+\nu)(1-2\nu)}
\begin{bmatrix}
1 & \frac{\nu}{1-\nu} & \frac{\nu}{1-\nu} & 0 & 0 & 0 \\
\frac{\nu}{1-\nu} & 1 & \frac{\nu}{1-\nu} & 0 & 0 & 0 \\
\frac{\nu}{1-\nu} & \frac{\nu}{1-\nu} & 1 & 0 & 0 & 0 \\
0 & 0 & 0 & \frac{1-2\nu}{2(1-\nu)} & 0 & 0 \\
0 & 0 & 0 & 0 & \frac{1-2\nu}{2(1-\nu)} & 0 \\
0 & 0 & 0 & 0 & 0 & \frac{1-2\nu}{2(1-\nu)}
\end{bmatrix} \\
\mathbf{E} &= \begin{bmatrix} E_{ss} & E_{rr} & E_{\theta\theta} & 2E_{r\theta} & 2E_{\theta s} & 2E_{sr} \end{bmatrix}^T \\
\mathbf{S} &= \begin{bmatrix} S_{ss} & S_{rr} & S_{\theta\theta} & S_{r\theta} & S_{\theta s} & S_{sr} \end{bmatrix}^T
\end{aligned}
\tag{6.26}
$$

where E and ν are the modulus of elasticity and Poisson's ratio respectively.

6.4. Finite element model

In order to develop a weak form finite element model for the above formulation, we divide the computational domain $[0, L]$ into non-overlapping finite elements, $\Omega^e = [s_1^e, s_2^e]$. Further we write the weak form the governing equation of motion Eq. (6.23) in terms of displacement variables as following:

$$
\begin{aligned}
0 &= \int_{s_1^e}^{s_2^e} \int_A \Big[\left((\mathbf{A}_1 + \mathbf{A}_{nl})\delta\mathbf{\Phi} + (\mathbf{A}_2 + \mathbf{A}_{nl_s})\frac{d\delta\mathbf{\Phi}}{ds} \right) \cdot \mathbf{C}_e \left((\mathbf{A}_1 + \frac{1}{2}\mathbf{A}_{nl})\mathbf{\Phi} \right. \\
&\qquad \left. + (\mathbf{A}_2 + \frac{1}{2}\mathbf{A}_{nl_s})\frac{d\mathbf{\Phi}}{ds} \right) - \delta\mathbf{\Phi} \cdot \hat{\mathbf{f}} \Big] \, dA \, ds
\end{aligned}
\tag{6.27}
$$

We approximate the degrees of freedom vector as:

$$
\mathbf{\Phi}(s) = \mathbf{\Psi}(s)\mathbf{U} \tag{6.28}
$$

where $\mathbf{\Psi}(s)$ is matrix of shape functions which are function of arc-length coordinate s and $\mathbf{U}$ is vector of displacement variables at nodal points which are defined as

following:

$$\boldsymbol{\Psi} = \begin{bmatrix} \psi_1^{(1)} & \dots & \psi_{\tilde{n}_1}^{(1)} & 0 & \dots & 0 & \dots & 0 & \dots & 0 \\ 0 & \dots & 0 & \psi_1^{(2)} & \dots & \psi_{\tilde{n}_2}^{(2)} & \dots & 0 & \dots & 0 \\ \vdots & \ddots & \vdots & \vdots & \ddots & \vdots & \ddots & \vdots & \ddots & \vdots \\ 0 & \dots & 0 & 0 & \dots & 0 & \dots & \psi_1^{(n)} & \dots & \psi_{\tilde{n}_p}^{(n)} \end{bmatrix}^T \tag{6.29}$$

$$\mathbf{U} = \begin{bmatrix} u_{1_1} & \dots & u_{1_{\tilde{n}_1}} & u_{2_1} & \dots & u_{2_{\tilde{n}_2}} & \dots & u_{n_1} & \dots & u_{n_{\tilde{n}_n}} \end{bmatrix}^T \tag{6.30}$$

where $\tilde{n}_1, \tilde{n}_2, \cdots \tilde{n}_n$ are the number of nodal values for $u_1, u_2, \cdots, u_n$ respectively in the considered element. n is the total number of Dofs. And

$$\begin{array}{llllll} u_1 & = \phi_s^{(0)}, & u_2 & = \phi_s^{(1)}, & \cdots & u_{(\tilde{n})} = \phi_s^{(\tilde{n})} \\ u_{\tilde{n}+1} & = \phi_r^{(0)}, & u_{\tilde{n}+2} & = \phi_r^{(1)}, & \cdots & u_{\tilde{n}+\tilde{m}} = \phi_r^{(\tilde{m})} \\ u_{\tilde{n}+\tilde{m}+1} & = \phi_\theta^{(0)}, & u_{\tilde{n}+\tilde{m}+2} & = \phi_\theta^{(1)}, & \cdots & u_{\tilde{n}+\tilde{m}+\tilde{p}} = \phi_\theta^{(\tilde{p})}. \end{array} \tag{6.31}$$

We substitute the approximation of dofs and $\delta\boldsymbol{\Phi} = \boldsymbol{\Psi}\tilde{\mathbf{l}}$ (where $\tilde{\mathbf{l}}$ is the column vector with all element unity and as many elements as the columns of $\boldsymbol{\Psi}$) into the weak form Eq. (6.27) to arrive at the following finite element algebraic equation:

$$\mathbf{KU} - \mathbf{f} = \mathbf{0} \tag{6.32}$$

where $\mathbf{K}$ and $\mathbf{f}$ are the stiffness matrix and force vector respectively, which are given as follows:

$$\begin{aligned} \mathbf{K} &= \int_{s_1^e}^{s_2^e} \boldsymbol{\Psi}^T \left(\mathbf{H}_1 \boldsymbol{\Psi} + \mathbf{H}_2 \frac{d\boldsymbol{\Psi}}{ds} \right) + \frac{d\boldsymbol{\Psi}}{ds}^T \left(\mathbf{H}_3 \boldsymbol{\Psi} + \mathbf{H}_4 \frac{d\boldsymbol{\Psi}}{ds} \right) ds \\ \mathbf{f} &= \int_{s_1^e}^{s_2^e} \boldsymbol{\Psi}^T \hat{\mathbf{f}} \, ds \end{aligned} \tag{6.33}$$

where

$$\begin{aligned} \mathbf{H}_1 &= \int_A (\mathbf{A}_1 + \mathbf{A}_{nl})^T \mathbf{C}_e (\mathbf{A}_1 + \frac{1}{2}\mathbf{A}_{nl}) \, dA, \quad \mathbf{H}_2 = \int_A (\mathbf{A}_1 + \mathbf{A}_{nl})^T \mathbf{C}_e (\mathbf{A}_2 + \frac{1}{2}\mathbf{A}_{nl_s}) \, dA \\ \mathbf{H}_3 &= \int_A (\mathbf{A}_2 + \mathbf{A}_{nl_s})^T \mathbf{C}_e (\mathbf{A}_1 + \frac{1}{2}\mathbf{A}_{nl}) \, dA, \quad \mathbf{H}_4 = \int_A (\mathbf{A}_{nl_s} + \mathbf{A}_2)^T \mathbf{C}_e (\mathbf{A}_2 + \frac{1}{2}\mathbf{A}_{nl_s}) \, dA \end{aligned} \tag{6.34}$$

We note here that matrices $\mathbf{A}_{nl}$ and $\mathbf{A}_{nl_s}$ depends on the displacement variables hence the stiffness matrix is nonlinear and also not symmetric. The nonlinear finite

element equation can be solved by direct (Picard) method or Newton's method (see Reddy [46]). For $(t+1)$th iteration of Newton's method, the solution can be expressed as:

$$\mathbf{T}(\mathbf{U}_t)\delta\mathbf{U}_{t+1} = -(\mathbf{K}(\mathbf{U}_t))\mathbf{U}_t - \mathbf{f}(\mathbf{U}_t), \quad \text{and, } \mathbf{U}_{t+1} = \mathbf{U}_t + \delta\mathbf{U}_{t+1} \tag{6.35}$$

where $\mathbf{T}$ is the tangent matrix given as:

$$\begin{aligned}
\mathbf{T} &= D(\mathbf{KU} - \mathbf{f}) = (D\mathbf{K})\mathbf{U} + \mathbf{K} - D\mathbf{f} \\
&= \mathbf{K} + \int_{s_1^e}^{s_2^e} \mathbf{\Psi}^T \left(\tilde{\mathbf{H}}_1\mathbf{\Psi} + \tilde{\mathbf{H}}_2\frac{d\mathbf{\Psi}}{ds}\right) + \frac{d\mathbf{\Psi}}{ds}^T \left(\tilde{\mathbf{H}}_3\mathbf{\Psi} + \tilde{\mathbf{H}}_4\frac{d\mathbf{\Psi}}{ds}\right) ds \\
&\quad + \int_{s_1^e}^{s_2^e} \mathbf{\Psi}^T \left(\tilde{\mathbf{P}}_1\mathbf{\Psi} + \tilde{\mathbf{P}}_2\frac{d\mathbf{\Psi}}{ds}\right) + \frac{d\mathbf{\Psi}}{ds}^T \left(\tilde{\mathbf{P}}_3\mathbf{\Psi} + \tilde{\mathbf{P}}_4\frac{d\mathbf{\Psi}}{ds}\right) ds - \int_{s_1^e}^{s_2^e} \mathbf{\Psi}^T\tilde{\mathbf{P}}_f\mathbf{\Psi}\, ds
\end{aligned} \tag{6.36}$$

where $D(\mathbf{K})$ represent the derivative of $\mathbf{K}$ with respect to $\mathbf{U}$ and

$$\begin{aligned}
\tilde{\mathbf{H}}_1 &= \frac{1}{2}\int_A (\mathbf{A}_1 + \mathbf{A}_{nl})^T\mathbf{C}_e\mathbf{A}_{nl}\, dA, \quad \tilde{\mathbf{H}}_2 = \frac{1}{2}\int_A (\mathbf{A}_1 + \mathbf{A}_{nl})^T\mathbf{C}_e\mathbf{A}_{nl_s}\, dA \\
\tilde{\mathbf{H}}_3 &= \frac{1}{2}\int_A (\mathbf{A}_2 + \mathbf{A}_{nl_s})^T\mathbf{C}_e\mathbf{A}_{nl}\, dA, \quad \tilde{\mathbf{H}}_4 = \frac{1}{2}\int_A (\mathbf{A}_2 + \mathbf{A}_{nl_s})^T\mathbf{C}_e\mathbf{A}_{nl_s}\, dA
\end{aligned} \tag{6.37}$$

and

$$\begin{aligned}
\tilde{\mathbf{P}}_1 &= \int_A \begin{bmatrix} \mathbf{P}_1^{11} & \mathbf{P}_1^{12} & \mathbf{P}_1^{13} \\ \mathbf{P}_1^{21} & \mathbf{P}_1^{22} & \mathbf{P}_1^{23} \\ \mathbf{P}_1^{31} & \mathbf{P}_1^{32} & \mathbf{P}_1^{33} \end{bmatrix} dA, \quad \tilde{\mathbf{P}}_2 = \int_A \begin{bmatrix} \mathbf{P}_2^{11} & \mathbf{P}_2^{12} & \mathbf{P}_2^{13} \\ \mathbf{P}_2^{21} & \mathbf{P}_2^{22} & \mathbf{P}_2^{23} \\ \mathbf{P}_2^{31} & \mathbf{P}_2^{32} & \mathbf{P}_2^{33} \end{bmatrix} dA \\
\tilde{\mathbf{P}}_3 &= \int_A \begin{bmatrix} \mathbf{P}_3^{11} & \mathbf{P}_3^{12} & \mathbf{P}_3^{13} \\ \mathbf{P}_3^{21} & \mathbf{P}_3^{22} & \mathbf{P}_3^{23} \\ \mathbf{P}_3^{31} & \mathbf{P}_3^{32} & \mathbf{P}_3^{33} \end{bmatrix} dA, \quad \tilde{\mathbf{P}}_4 = \int_A \begin{bmatrix} \mathbf{P}_4^{11} & \mathbf{0} & \mathbf{0} \\ \mathbf{0} & \mathbf{P}_4^{22} & \mathbf{0} \\ \mathbf{0} & \mathbf{0} & \mathbf{P}_4^{33} \end{bmatrix} dA
\end{aligned} \tag{6.38}$$

The block components of the matrix $\tilde{\mathbf{P}}_i$ and $\tilde{\mathbf{P}}_f$ are given in Appendix G. We note that the tangent matrix is not symmetric due to the $D\mathbf{f}$ in the Eq. (6.36) but the part of the tangent matrix coming from the derivative of $\mathbf{KU}$ is symmetric. To keep the symmetry, the tangent matrix can be approximated by dropping $D\mathbf{f}$ from the expression. The convergence might get slower due to this approximation.

6.5. Numerical examples

For the numerical examples, let us consider a spiral duct with the central reference spiral curve given by following parametric equation in rectangular cartesian coordinate system:

$$x = \cos\left(\frac{t}{\sqrt{2}}\right), \qquad y = \frac{t}{\sqrt{2}}, \qquad z = \sin\left(\frac{t}{\sqrt{2}}\right) \tag{6.39}$$

where t is an arbitrary parameter for this space curve and the arc length coordinate s is same as the parameter t for this particular case. Both the curvature (κ) and torsion (τ) of the spiral curve are constant and equal to 0.25 per inch and the -1.125 per inch respectively. The axis of the reference spiral curve lies along the $y-$ axis. The material properties of the all the numerical examples presented in this section are considered as follows:

$$E = 10 \times 10^6 \text{ psi}, \qquad \nu = 0.3, \tag{6.40}$$

Where E and ν are the modulus of elasticity and Poisson's ratio respectively.

6.5.1. Spiral duct under extension or compression point forces

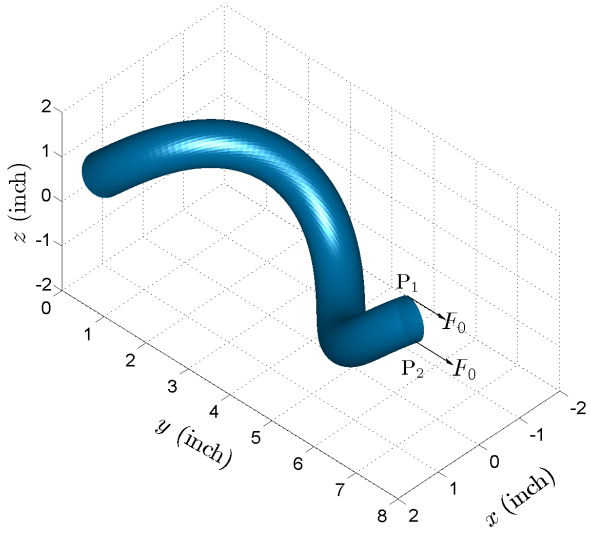

Fig. 6.3 Original spiral duct with applied point forces.

The geometric properties of the spiral pipe are considered as follows:

$$L = 10 \text{ in}, \qquad r_1 = 0.2 \text{ in}, \qquad r_2 = 0.21 \text{ in} \tag{6.41}$$

where L is the length of the spiral pipe measured along the arc-length of central reference spiral curve and r_1 and r_2 are the inner and outer radius of the pipe respectively. One end of the pipe is clamped and point forces are applied at the other end at the points where outer circumference coincide with the binormal direction of the reference spiral curve as shown in the fig. 6.3.

6.5.1.1. Linear analysis

For linear finite element analysis, linear and quadratic elements are considered for approximating all the degrees of freedom. Table 6.1 gives the magnitude of the displacement at point P_1 where one of the point forces is applied (see fig. 6.3), for various order of approximation of different displacement components considering linear and quadratic element in case of two different thickness of the pipe keeping the inner radius of the duct same as given in Eq. (6.41). It can be observed in Table 6.1 that for quadratic elements, the magnitude of the displacement of point P_1 converge faster as we increase the number of elements used in the FE analysis. Also, it is noted that as we increase the order of approximation of u_s, u_r and u_θ that magnitude starts to converge for both thicknesses considered.

6.5.1.2. Nonlinear results

For nonlinear finite element analysis, 24 linear Lagrange elements are used to approximate all the degrees of freedom. Also, the order of approximation of u_s, u_r and u_θ are taken as 3 for both in r and θ basis functions. The Newton's method has been employed to obtained the converged solution for the error tolerance 0.005. Figure 6.4 shows deformed shape under two different extension point loads for 0.01 inch thickness. Here, we note that the cross-section of the pipe get deformed when we increase the extension force, which we cannot get if we model by Kirchhoff rod theory or other rod theories which consider

the cross-section moving as a rigid plane in course of the deformation. Further, fig. 6.5 shows the shape of spiral pipe in case of compressive point loads. Figure 6.6 shows the nonlinear variation of the magnitude of displacement of the point P_1 with respect to the point load applied in the case of extension and compression.

Table 6.1. Linear FEM solutions for displacement of a point, P_1 considering various order of approximation of displacement in case of point extension force, applied at one end with another end fixed.

order of approximation of u_s, u_r and u_θ			Magnitude of displacement of point P_1 in inches.				
			linear element		Quadratic element		
n_r, n_θ	m_r, m_θ	p_r, p_θ	no. of elements	(thickness = 0.02 in.) $F_0 = 22$ lbf displacement	no. of elements	(thickness = 0.02 in.) $F_0 = 22$ lbf displacement	(thickness = 0.01 in.) $F_0 = 21$ lbf displacement
1,1	1,1	1,1	40	0.4866	20	0.5668	1.1778
			60	0.5140	30	0.5697	1.1839
			80	0.5285	40	0.5702	1.1851
			100	0.5381	50	0.5704	1.1855
1,2	1,2	1,2	40	0.5073	20	0.5972	1.3783
			60	0.5371	30	0.6010	1.3911
			80	0.5531	40	0.6018	1.3938
			100	0.5637	50	0.6021	1.3947
1,3	1,3	1,3	40	0.5075	20	0.5975	1.3832
			60	0.5374	30	0.6013	1.3963
			80	0.5534	40	0.6021	1.3990
			100	0.5640	50	0.6024	1.4000
2,2	2,2	2,2	40	0.5231	20	0.6174	1.4241
			60	0.5545	30	0.6214	1.4384
			80	0.5712	40	0.6222	1.4414
			100	0.5823	50	0.6225	1.4424
2,3	2,3	2,3	40	0.5234	20	0.6178	1.4311
			60	0.5548	30	0.6218	1.4458
			80	0.5716	40	0.6226	1.4489
			100	0.5827	50	0.6229	1.4499
3,3	3,3	3,3	40	0.5234	20	0.6178	1.4313
			60	0.5549	30	0.6219	1.4459
			80	0.5716	40	0.6227	1.4490
			100	0.5827	50	0.6230	1.4500
			120	0.5908	60	0.6232	1.4505

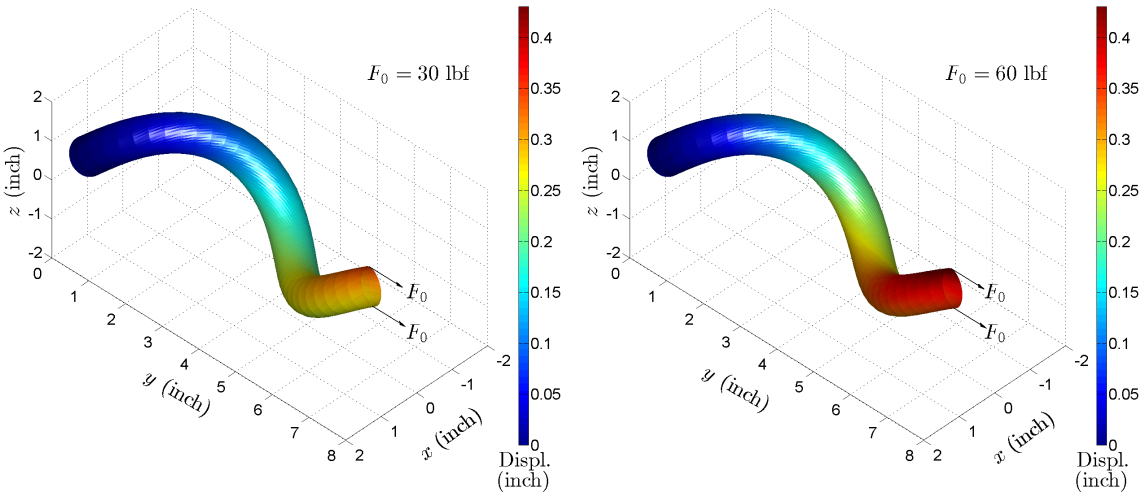

(a) $2F_0 = 60$ lbf (b) $2F_0 = 120$ lbf

Fig. 6.4 Deformed shape of spiral pipe under extension by nonlinear analysis.

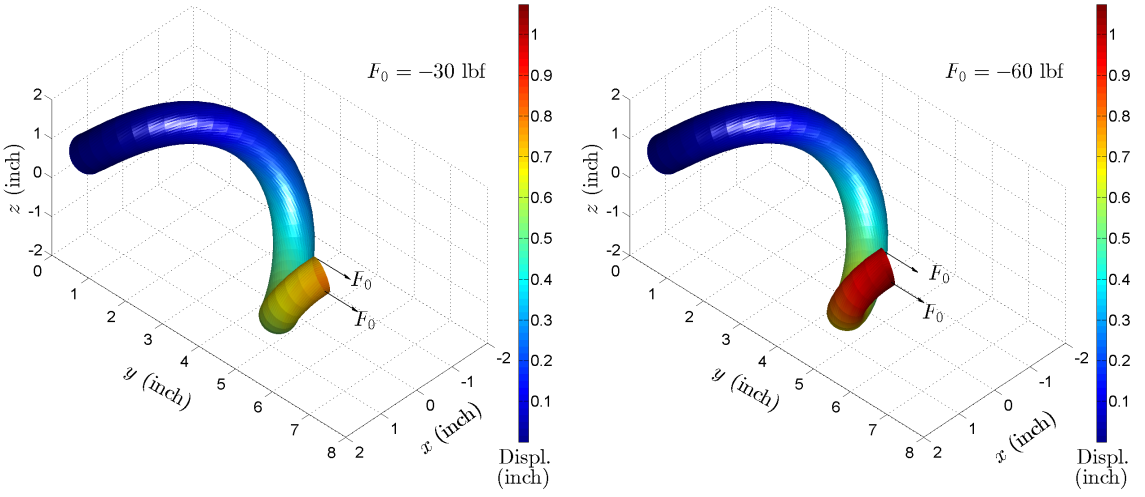

(a) $2F_0 = -60$ lbf (b) $2F_0 = -120$ lbf

Fig. 6.5 Deformed shape of spiral pipe under compression by nonlinear analysis.

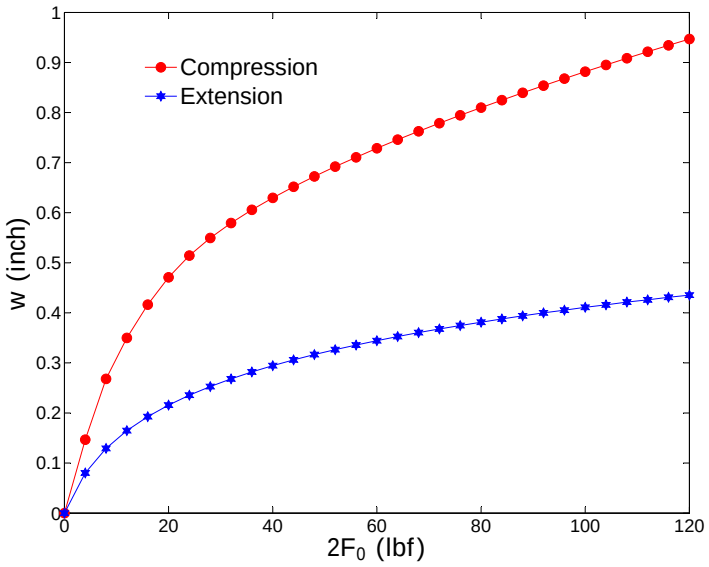

Fig. 6.6 Variation of magnitude of displacement (w) of point P_1 with respect to the total load applied in case of extension and compression.

Further in fig. 6.7, various components of the true stress are depicted in the case of extension point load $2F_0 = 120$ lbf. The second Piola-kirchhoff stress components are calculated at one gauss point in each element and then the Cauchy stress (true stress) has been obtained from the second Piola-kirchhoff stress as following:

$$\boldsymbol{\sigma} = \frac{1}{\det(\mathbf{F})}\mathbf{F}\cdot\mathbf{S}\cdot\mathbf{F}^T \tag{6.42}$$

where $\mathbf{F}$ and $\mathbf{S}$ are the deformation gradient and second Piola-kirchhoff stress tensor respectively. Figure 6.8 shows the distribution of von mises stress in the case of compression and extension.

6.5.2. Spiral duct under internal or external pressure

Let us consider a spiral duct (see fig. 6.9) under uniform internal or external pressure. The geometric specification of the duct are considered as following:

$$L = 15 \text{ inch}, \qquad r_1 = 0.3 \text{ inch}, \qquad r_2 = 0.31 \text{ inch} \tag{6.43}$$

here also the length of the duct, L is measured along the arc-length of the central reference spiral curve and r_1 and r_2 are the inner and outer radius of the duct respectively. The reference central spiral curve of the duct and material properties are given by Eqs. (6.39) and (6.40) respectively. The duct is completely fixed at both

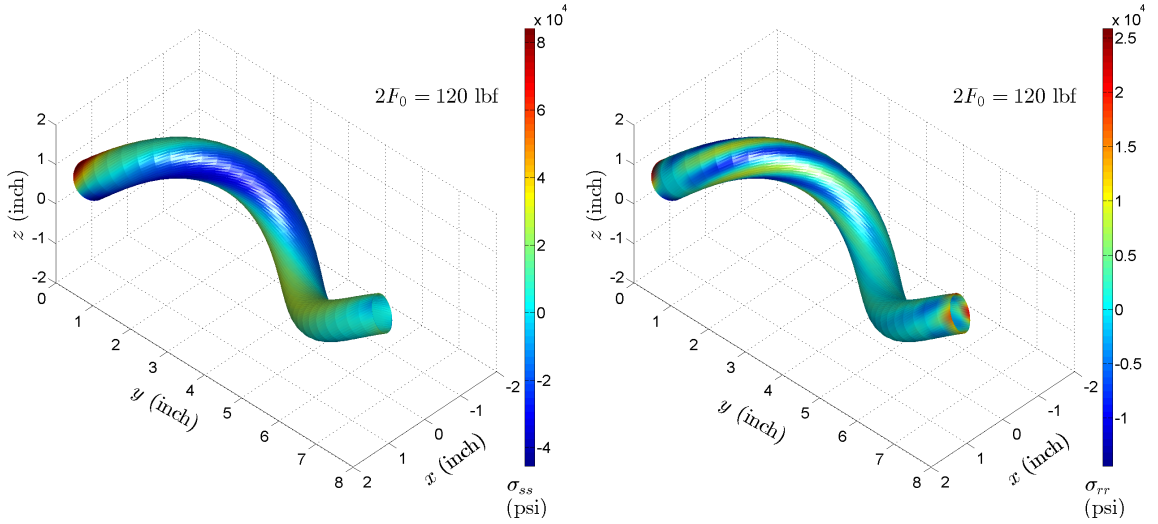

(a) σ_{ss}

(b) σ_{rr}

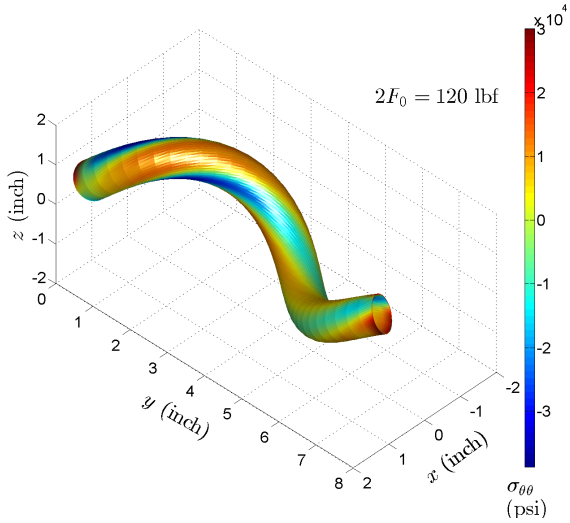

(c) $\sigma_{\theta\theta}$

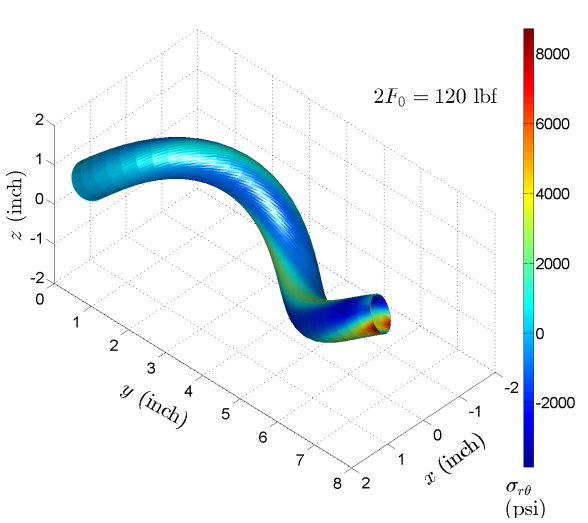

(d) $\sigma_{r\theta}$

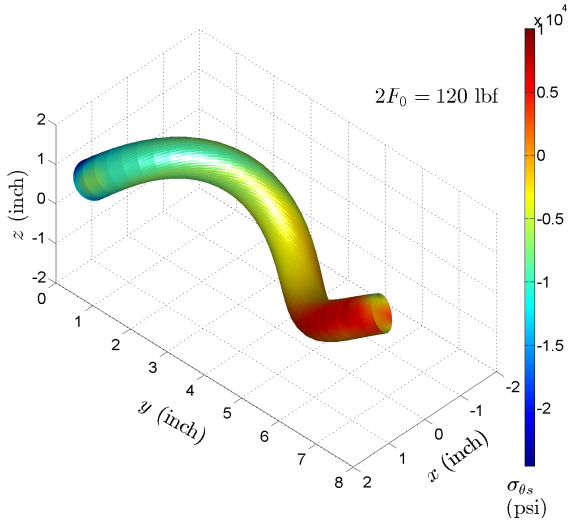

(e) $\sigma_{\theta s}$

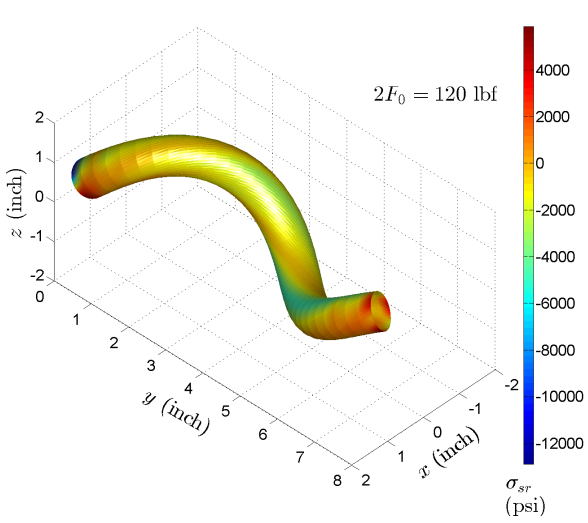

(f) σ_{sr}

Fig. 6.7 Various components of true stress tensor for deformed spiral pipe.

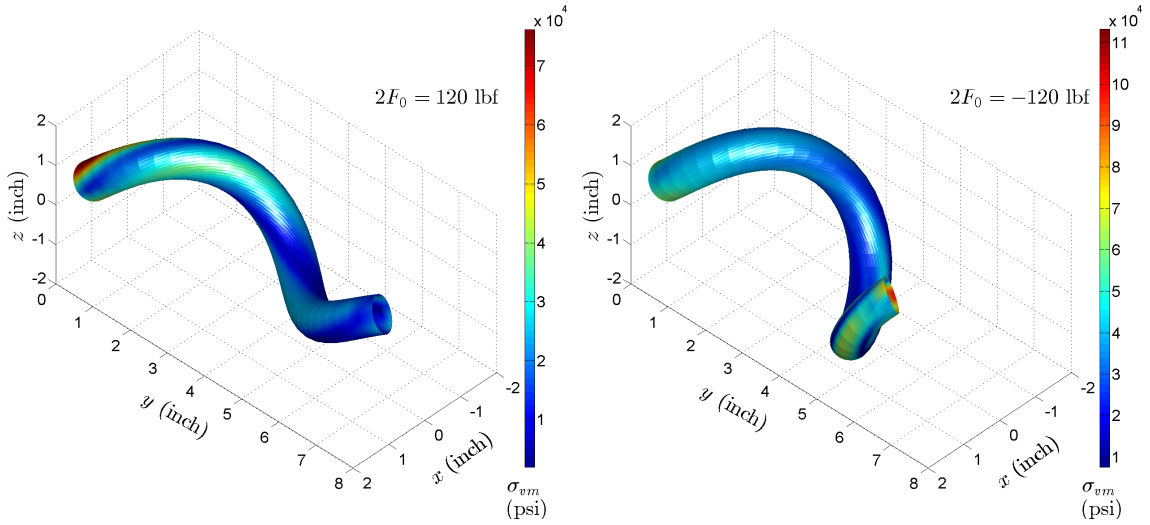

(a) Extension (b) Compression

Fig. 6.8 von-Mises stress in case of extension and compression

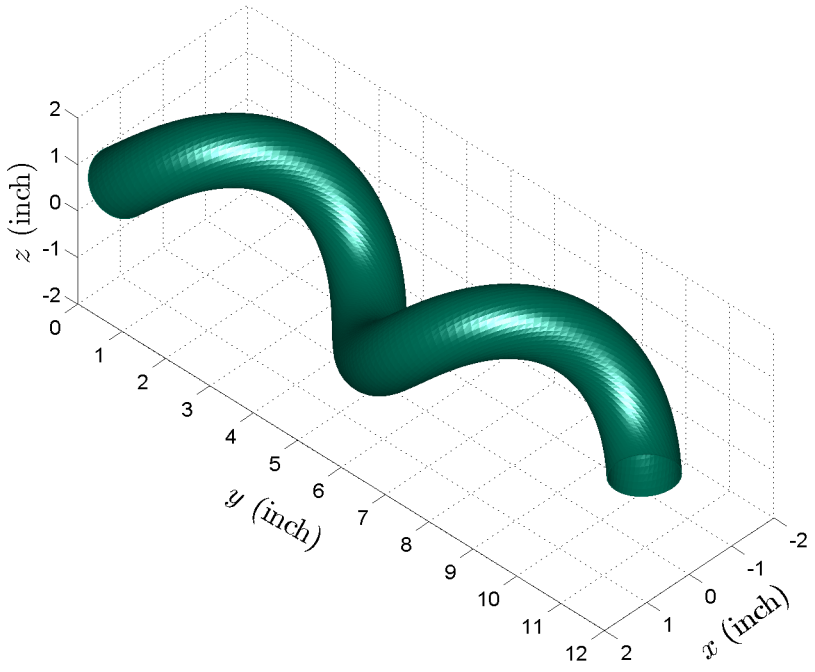

Fig. 6.9 Original shape of spiral duct.

of its ends.

6.5.2.1. Linear analysis

In the linear analysis, the deformation results for the different order of approximation of the displacement components, element type (linear or quadratic Lagrange element), number of elements and duct thickness are tabulated as in the case of previous example. The magnitude of the displacement of the point at $s = 7.5$ inch at the outer surface which coincide with the principal normal direction (*i.e.* $\theta = 0$) are tabulated in Table 6.2 for linear and quadratic Lagrange elements for internal and external pressure applied for the duct with geometric properties described in Eq. (6.43) along with one thicker duct keeping inner radius same, for different order of approximation of u_s, u_r and u_θ. In this case, also, we note the convergence of the magnitude of the point displacement as we increase the order of approximation. And the quadratic elements give faster convergence of the displacement value with respect to the number of elements considered.

6.5.2.2. Nonlinear results

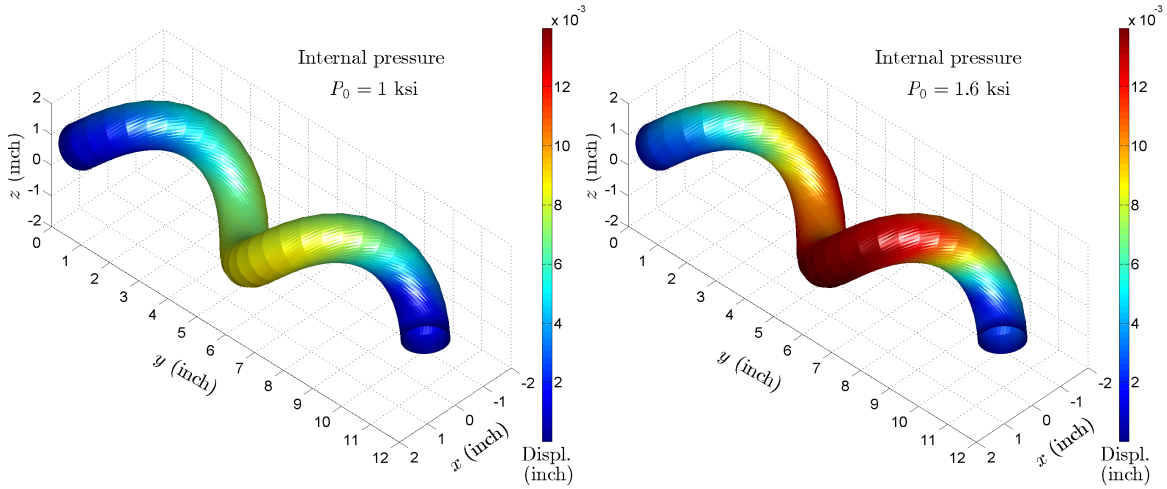

(a) $P_0 = 1$ ksi (b) $P_0 = 1.6$ ksi

Fig. 6.10 Deformed shape of spiral pipe under internal pressure.

For nonlinear finite element analysis, 36 linear Lagrange elements are used to approximate all the degrees of freedom. Also, the order of approximation of u_s, u_r and u_θ are taken as 3 for both in r and θ basis functions as in the example before.

Table 6.2. Linear FEM solutions for displacement of a point on a spiral duct considering various order of approximation of displacement in case of internal and external pressure with fixed end boundary condition.

order of approximation of u_s, u_r and u_θ			Magnitude of displacement (in inch) at $(s, r, \theta) = (7.5 \text{ in}, r_2, 0)$.					
			linear element		Quadratic element			
n_r, n_θ	m_r, m_θ	p_r, p_θ	no. of elements	(thickness = 0.01 in.) $P_0 = 10$ ksi (int. P_0) Disp.	no. of elements	(thickness = 0.01 in.) $P_0 = 10$ ksi (int. P_0) Disp.	(thickness = 0.01 in.) $P_0 = 10$ ksi (ext. P_0) Disp.	(thickness = 0.05 in.) $P_0 = 50$ ksi (int. P_0) Disp.
1,1	1,1	1,1	40	0.06736	20	0.05456	0.05883	0.04997
			60	0.06349	30	0.05356	0.05775	0.04913
			80	0.06082	40	0.05339	0.05757	0.04900
			100	0.05897	50	0.05334	0.05752	0.04896
1,2	1,2	1,2	40	0.09282	20	0.08223	0.08757	0.05401
			60	0.09052	30	0.07959	0.08474	0.05301
			80	0.08850	40	0.07902	0.08413	0.05284
			100	0.08679	50	0.07883	0.08393	0.05279
1,3	1,3	1,3	40	0.09586	20	0.08537	0.09088	0.05404
			60	0.09358	30	0.08246	0.08777	0.05304
			80	0.09157	40	0.08179	0.08704	0.05287
			100	0.08985	50	0.08155	0.08679	0.05282
2,2	2,2	2,2	40	0.09440	20	0.08415	0.08958	0.05486
			60	0.09223	30	0.08136	0.08659	0.05382
			80	0.09029	40	0.08075	0.08594	0.05365
			100	0.08863	50	0.08055	0.08572	0.05359
2,3	2,3	2,3	40	0.09823	20	0.08819	0.09384	0.05490
			60	0.09609	30	0.08506	0.09048	0.05386
			80	0.09419	40	0.08431	0.08968	0.05368
			100	0.09253	50	0.08405	0.08940	0.05363
3,3	3,3	3,3	40	0.09823	20	0.08820	0.09384	0.05492
			60	0.09610	30	0.08507	0.09049	0.05388
			80	0.09420	40	0.08432	0.08968	0.05370
			100	0.09254	50	0.08405	0.08940	0.05365
			120	0.09113	60	0.08392	0.08926	0.05362

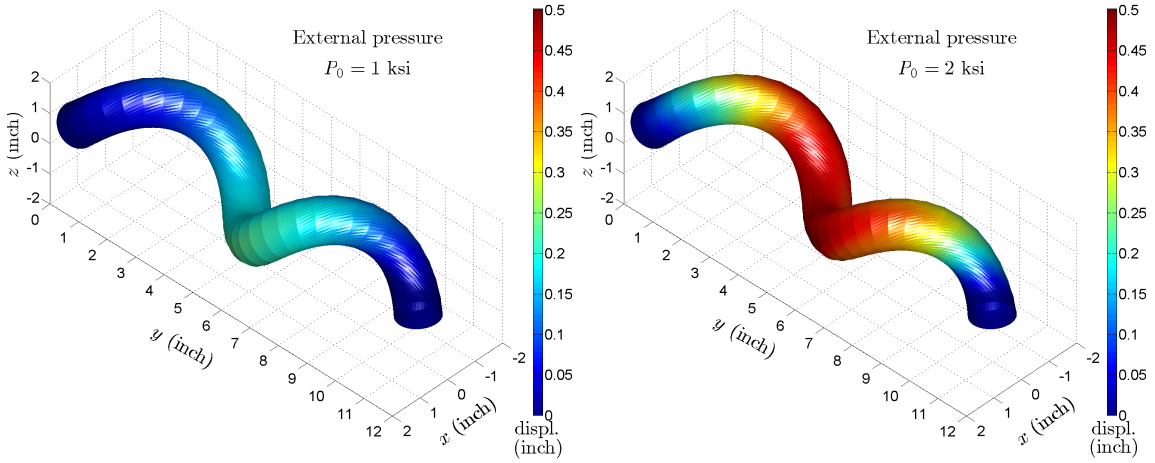

(a) $P_0 = 1$ ksi (b) $P_0 = 2$ ksi

Fig. 6.11 Deformed shape of spiral pipe under external pressure.

The Newton's method has been employed to obtained the converged solution for the error tolerance 0.01. Figures 6.10 and 6.11 show the deformed shape of the duct under uniform internal and external pressure respectively for given pressure P_0. And figs. 6.12 and 6.13 depicts the distribution of von-Mises stress in both internal and external pressure cases and components of Cauchy (true) stress in case of internal pressure respectively.

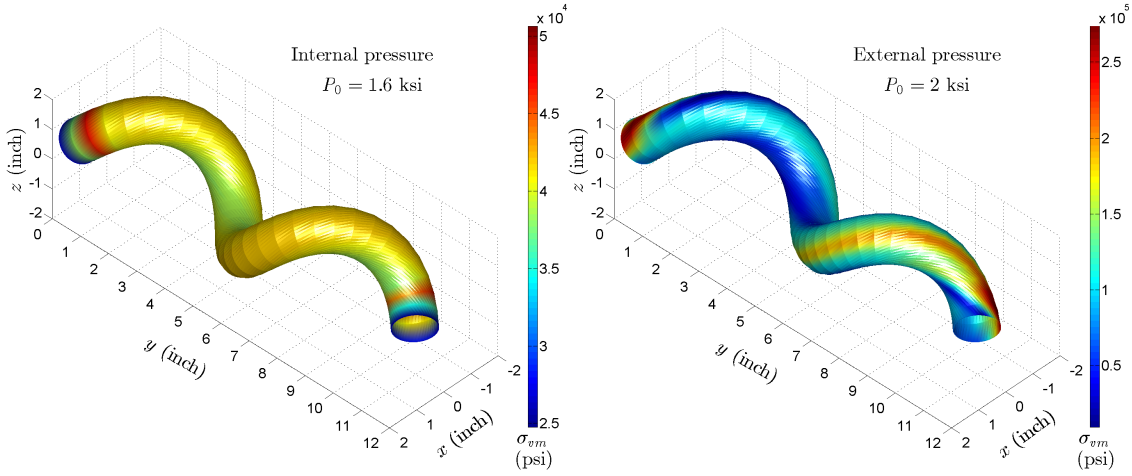

(a) Internal pressure (b) External pressure

Fig. 6.12 von-Mises stress in case of internal and external pressure

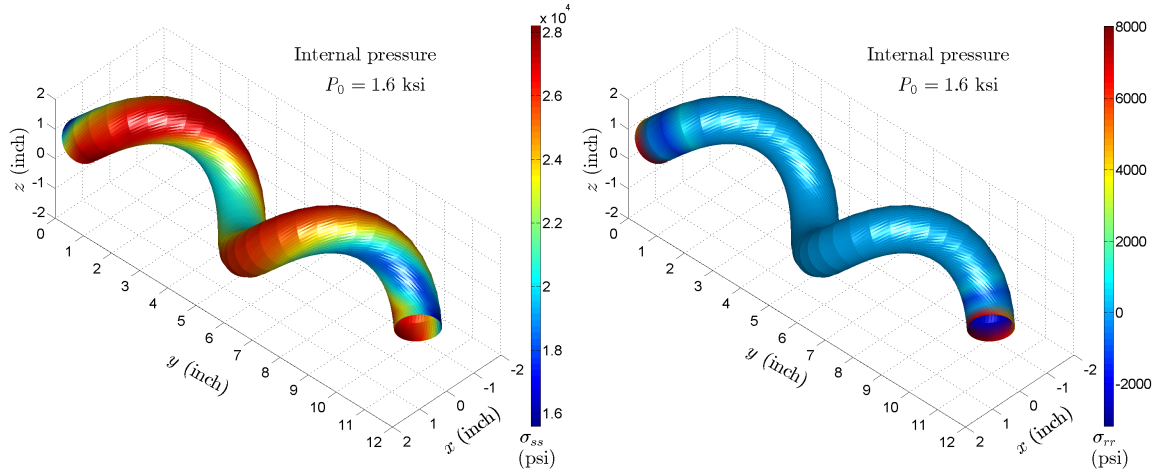

(a) σ_{ss} (b) σ_{rr}

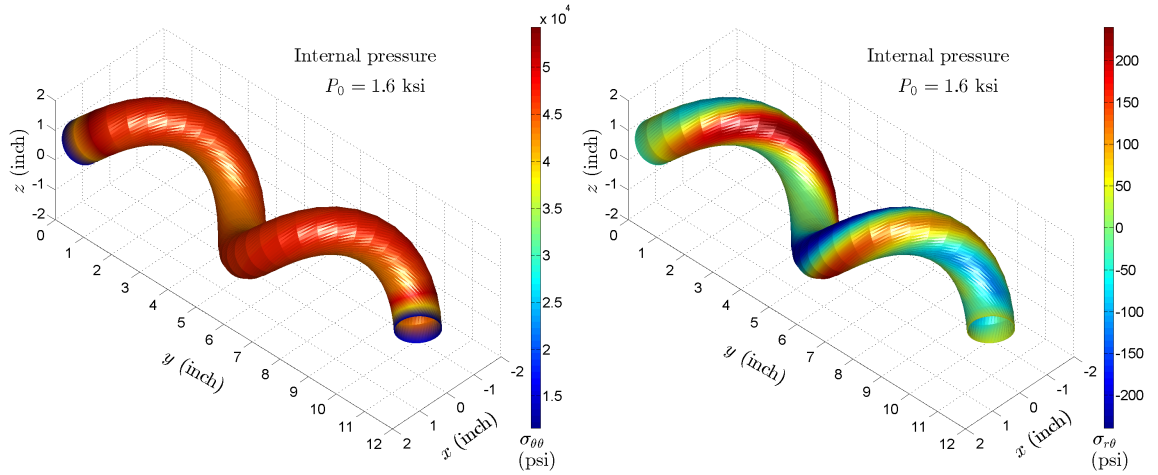

(c) $\sigma_{\theta\theta}$ (d) $\sigma_{r\theta}$

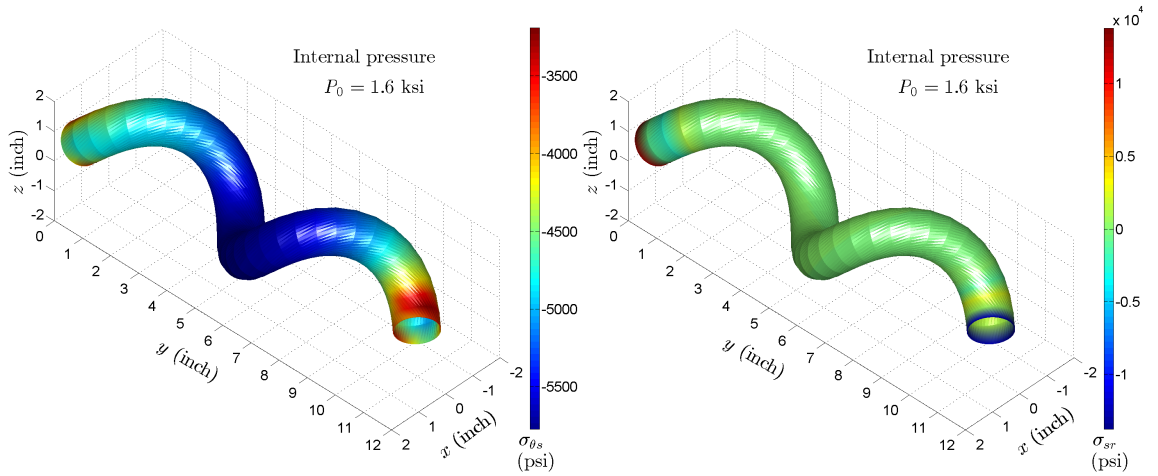

(e) $\sigma_{\theta s}$ (f) σ_{sr}

Fig. 6.13 Various components of stress tensor for deformed spiral pipe subjected to internal pressure.

6.6. Chapter summary and conclusions

In this chapter, a general higher-order theory for the analysis of rods in three-dimensional space has been presented. The displacement field of the cross-section of the rod has been approximated by general basis functions in two-dimensional polar (r, θ) coordinate system. Further, based on the principle of virtual displacements, the governing equations have been obtained in the curvilinear cylindrical coordinate system to model any arbitrarily shaped rod in three dimensions for large deformation. In the numerical examples section the theory has been used to analyze spiral shaped duct under the extensional and compressive point loads and internal and external pressures. Such analysis can not be performed by the existing rod theory because the approximation of the rigid cross-section made in those theories hold good for thin rods only. In the theory discussed herein, we use a very general approximation for the displacement field of the cross-section, and hence can model wide range of phenomenon for thick rod of any arbitrary cross-section (hollow or solid).

7. SUMMARY, CONCLUSIONS AND FUTURE WORKS

In the present study, nonlinear finite element models have been developed for beams and plates in the context of general higher-order beam and plate theories, considering Cosserat continuum for constrained micro-rotation (rotation gradient dependent theory). Chapter 1 presents general introduction and literature review of experimental and theoretical developments for the Cosserat continuum.

In Chapters 2 and 3, the nonlinear finite element model for beams and plates have been developed for the case of rotation gradient dependent strain energy along with the classical strain energy, and studies have been carried to see the effect of material length scale parameters and orientation of small inclusions embedded in the material. We observed stiffening effect due to the inclusion of material length scale parameters and the anisotropic effect due to the ordered orientation of small inclusions in the case of plate bending.

In Chapter 4, the rotation gradient dependent classical plate theory is employed to analyze nanoindentation on CNT-reinforced hard coatings on elastic substrates. The CNT reinforcement is modeled using the material length scale parameter. Since the circular computational domain requires non-rectangular finite elements, for which the C^1 continuity is hard to achieve, which is required for all the gradient dependent theories, a mixed finite element model has been developed to obtained the solution. The contact between coating and substrate is considered to be smooth, which results in higher contact stiffness and hence stiffer response to the indentation as compared to the experimental values in the case of zero length scale. Nevertheless, the stiffening effect of the CNT reinforcement, via the small material length scale parameters in the mathematical model, has been observed. As a future work, the consideration of surface roughness and friction between the contacting surfaces, that is, the coating and the substrate, is suggested while obtaining the contact stiffness. Then the indentation response can be compared to the experimental results to have an idea of the values of material length scale parameter for a given CNT reinforcement.

In chapters 5 and 6, a general higher-order one-dimensional theory has been developed for the classical continuum mechanics in the linear case and curvilinear cylindrical coordinate system for the large deformation case. Based on a very general approximation of the displacement field of the cross-section of the body considered,

the governing equations are obtained. A weak-form nonlinear finite element model has been developed to obtain the solution. These models have been applied to analyze shell structures and beams of hollow cross-sections in 3-D. Such models are very much relevant to the linear or nonlinear finite element analysis of the Cosserat continuum for constrained micro-rotation or other strain gradient-dependent theories; such theories requires C^1 or higher order continuity for the displacement variables in the finite element model, which is very difficult to achieve in two- or three-dimensional domains specially for non-rectangular domains, where the higher-order one-dimensional theories discussed herein allows higher-order continuity element (general Hermite interpolation functions) owing to their one-dimensional nature of analysis. As a future work, these theories can be extended to the rotation gradient dependent theories (Cosserat continuum for constrained micro-rotation) which can be applied in the analysis of shell structure of Cosserat solid by nonlinear finite element model.

The main contributions of the present study are summarized here:

1. The development of nonlinear finite element models of beams and plates for the case of rotation gradient dependent strain energy potential and bring out the effect of material length scale parameter and orientation of small inclusions embedded in the material on the structural response.

2. The rotation gradient dependent classical plate theory is employed to analyze nanoindentation on a CNT-reinforced hard coating on an elastic substrate. A mixed finite element model has been developed to obtain the solution.

3. Developed a general higher-order theory for one-dimensional analysis of 3-D objects based on a very general approximation of the displacement field of the cross-section of the object in the polar coordinate system. Cylindrical shells under internal pressure and pinching point forces, often solved using a shell finite element, is employed to illustrate the usefulness of the developed formulation.

4. A general higher-order theory for the analysis of rods in three-dimensional space is developed, where the displacement field of the cross-section of the rod has been approximated by a very general basis functions in the two-dimensional polar coordinate system. The formulation is used to analyze spiral shaped duct under extension, compressive point loads, and internal and external pressures.

Such analysis can not be performed by the existing rod theory as the approximation of rigid cross-section made in those theories hold good for thin rods only.

REFERENCES

[1] E Cosserat and F Cosserat. Théorie des corps déformables. *Paris*, 1909.

[2] MB Rubin. *Cosserat Theories: Shells, Rods and Points*, volume 79. Springer Science & Business Media, 2013.

[3] GA Maugin. About the cosserats book of 1909. In *Continuum Mechanics Through the Eighteenth and Nineteenth Centuries*, pages 113–136. Springer, 2014.

[4] C Truesdell and R Toupin. *The Classical Field Theories*. Springer, 1960.

[5] RA Toupin. Elastic materials with couple-stresses. *Archive for Rational Mechanics and Analysis*, 11(1):385–414, 1962.

[6] R D Mindlin and H F Tiersten. Effects of couple-stresses in linear elasticity. *Archive for Rational Mechanics and Analysis*, 11(1):415–448, 1962.

[7] RD Mindlin. Micro-structure in linear elasticity. *Archive for Rational Mechanics and Analysis*, 16(1):51–78, 1964.

[8] AC Eringen and ES Suhubi. Nonlinear theory of simple micro-elastic solidsi. *International Journal of Engineering Science*, 2(2):189–203, 1964.

[9] ES Suhubl and AC Eringen. Nonlinear theory of micro-elastic solidsii. *International Journal of Engineering Science*, 2(4):389–404, 1964.

[10] AC Eringen. Linear theory of micropolar elasticity. Technical report, DTIC Document, 1965.

[11] AC Eringen. Linear theory of micropolar viscoelasticity. *International Journal of Engineering Science*, 5(2):191–204, 1967.

[12] RC Dixon and AC Eringen. A dynamical theory of polar elastic dielectricsi. *International Journal of Engineering Science*, 3(3):359–377, 1965.

[13] RC Dixon and AC Eringen. A dynamical theory of polar elastic dielectricsii. *International Journal of Engineering Science*, 3(3):379–398, 1965.

[14] GA Maugin and AC Eringen. Deformable magnetically saturated media. i. field equations. *Journal of Mathematical Physics*, 13(2):143–155, 1972.

[15] GA Maugin and AC Eringen. Deformable magnetically saturated media. ii. constitutive theory. *Journal of Mathematical Physics*, 13(9):1334–1347, 1972.

[16] AC Eringen. *Microcontinuum Field Theories: I. Foundations and Solids*. Springer Science & Business Media, 2012.

[17] F Yang, A Chong, D Lam, and P Tong. Couple stress based strain gradient theory for elasticity. *International Journal of Solids and Structures*, 39(10):2731–2743, 2002.

[18] P Steinmann. A micropolar theory of finite deformation and finite rotation multiplicative elastoplasticity. *International Journal of Solids and Structures*, 31(8):1063–1084, 1994.

[19] AR Srinivasa and JN Reddy. A model for a constrained, finitely deforming, elastic solid with rotation gradient dependent strain energy, and its specialization to von karman plates and beams. *Journal of the Mechanics and Physics of Solids*, 61(3):873–885, 2013.

[20] RD Gauthier and WE Jahsman. A quest for micropolar elastic constants. *Journal of Applied Mechanics*, 42(2):369–374, 1975.

[21] A Askar. Molecular crystals and the polar theories of the continua experimental values of material coefficients for kno 3. *International Journal of Engineering Science*, 10(3):293–300, 1972.

[22] J Pouget and GA Maugin. Nonlinear dynamics of oriented elastic solids. *Journal of Elasticity*, 22(2-3):157–183, 1989.

[23] RS Lakes. Experimental microelasticity of two porous solids. *International Journal of Solids and Structures*, 22(1):55–63, 1986.

[24] R Lakes. Experimental micro mechanics methods for conventional and negative poissons ratio cellular solids as cosserat continua. *Journal of Engineering Materials and Technology*, 113(1):148–155, 1991.

[25] DCC Lam, F Yang, A Chong, J Wang, and P Tong. Experiments and theory in strain gradient elasticity. *Journal of the Mechanics and Physics of Solids*, 51(8):1477–1508, 2003.

[26] SK Park and XL Gao. Bernoulli–euler beam model based on a modified couple stress theory. *Journal of Micromechanics and Microengineering*, 16(11):2355, 2006.

[27] HM Ma, X-L Gao, and JN Reddy. A microstructure-dependent timoshenko beam model based on a modified couple stress theory. *Journal of the Mechanics and Physics of Solids*, 56(12):3379–3391, 2008.

[28] HM Ma, X-L Gao, and JN Reddy. A nonclassical reddy-levinson beam model based on a modified couple stress theory. *International Journal for Multiscale Computational Engineering*, 8(2), 2010.

[29] JV Santos and JN Reddy. Vibration of timoshenko beams using non-classical elasticity theories. *Shock and Vibration*, 19(3):251–256, 2012.

[30] JN Reddy. Microstructure-dependent couple stress theories of functionally graded beams. *Journal of the Mechanics and Physics of Solids*, 59(11):2382–2399, 2011.

[31] A Arbind and JN Reddy. Nonlinear analysis of functionally graded microstructure-dependent beams. *Composite Structures*, 98:272–281, 2013.

[32] A Arbind, JN Reddy, and AR Srinivasa. Modified couple stress-based third-order theory for nonlinear analysis of functionally graded beams. *Latin American Journal of Solids and Structures*, 11(3):459–487, 2014.

[33] X-L Gao, JX Huang, and JN Reddy. A non-classical third-order shear deformation plate model based on a modified couple stress theory. *Acta Mechanica*, 224(11):2699–2718, 2013.

[34] JN Reddy. A simple higher-order theory for laminated plates. *Journal of Applied Mechanics*, 51:745–752, 1984.

[35] JN Reddy. *Mechanics of Laminated Composite Plates and Shells: Theory and Analysis,*. CRC Press, Boca Raton, FL, 2nd edition, 2004.

[36] J Kim and JN Reddy. Analytical solutions for bending, vibration, and buckling of fgm plates using a couple stress-based third-order theory. *Composite Structures*, 103:86–98, 2013.

[37] J Kim and JN Reddy. A general third-order theory of functionally graded plates with modified couple stress effect and the von kármán nonlinearity: theory and finite element analysis. *Acta Mechanica*, pages 1–26, 2015.

[38] JN Reddy and AR Srinivasa. Non-linear theories of beams and plates accounting for moderate rotations and material length scales. *International Journal of Non-Linear Mechanics*, 66:43–53, 2014.

[39] L Brand. *Vector and Tensor Analysis*. New York, 1947.

[40] JN Reddy and J Kim. A nonlinear modified couple stress-based third-order theory of functionally graded plates. *Composite Structures*, 94(3):1128–1143, 2012.

[41] JN Reddy. *Energy Principles and Variational Methods in Applied Mechanics*. John Wiley & Sons, 3rd edition, 2017.

[42] JN Reddy. *An Introduction to Continuum Mechanics*. Cambridge University Press, 2nd edition, 2013.

[43] RD Mindlin. Influence of couple-stresses on stress concentrations. *Experimental Mechanics*, 3(1):1–7, 1963.

[44] GN Praveen and JN Reddy. Nonlinear transient thermoelastic analysis of functionally graded ceramic-metal plates. *International Journal of Solids and Structures*, 35(33):4457–4476, 1998.

[45] JN Reddy. Analysis of functionally graded plates. *International Journal for Numerical Methods in Engineering*, 47(1-3):663–684, 2000.

[46] JN Reddy. *An Introduction to Nonlinear Finite Element Analysis: with applications to heat transfer, fluid mechanics, and solid mechanics*. OUP Oxford, 2nd edition, 2015.

[47] SR Bakshi, V Singh, K Balani, DG McCartney, S Seal, and A Agarwal. Carbon nanotube reinforced aluminum composite coating via cold spraying. *Surface and Coatings Technology*, 202(21):5162–5169, 2008.

[48] ET Thostenson and T-W Chou. Aligned multi-walled carbon nanotube-reinforced composites: processing and mechanical characterization. *Journal of physics D: Applied physics*, 35(16):L77, 2002.

[49] M Warner and EM Terentjev. *Liquid Crystal Elastomers*, volume 120. OUP Oxford, 2003.

[50] M Warner, CD Modes, and D Corbett. Curvature in nematic elastica responding to light and heat. In *Proceedings of the Royal Society of London A: Mathematical, Physical and Engineering Sciences*, volume 466, pages 2975–2989. The Royal Society, 2010.

[51] M Warner, CD Modes, and D Corbett. Suppression of curvature in nematic elastica. In *Proceedings of the Royal Society of London A: Mathematical, Physical and Engineering Sciences*, volume 466, pages 3561–3578. The Royal Society, 2010.

[52] A Arbind, JN Reddy, and AR Srinivasa. Nonlinear analysis of beams with rotation gradient dependent potential energy for constrained micro-rotation. *European Journal of Mechanics - A/Solids*, 65:178–194, 2017.

[53] Y Miyamoto, WA Kaysser, BH Rabin, A Kawasaki, and RG Ford. *Functionally Graded Materials: Design, Processing and Applications*, volume 5. Springer Science & Business Media, 2013.

[54] V Popov. *Contact Mechanics and Friction: Physical Principles and Applications*. Springer Science & Business Media, 2010.

[55] AA Polycarpou. Measurement and modeling of normal contact stiffness and contact damping at the meso scale. *Journal of Vibration and Acoustics*, 127(1):52–60, 2005.

[56] JN Reddy. *Theory and Analysis of Elastic Plates and Shells*. CRC press, 2nd edition, 2007.

[57] A Arbind, JN Reddy, and AR Srinivasa. Nonlinear analysis of plates with rotation gradient dependent potential energy for constrained micro-rotation. *Journal of Engineering Mechanics*, to appear, 2017.

[58] P Khodabakhshi and JN Reddy. A unified beam theory with strain gradient effect and the von kármán nonlinearity. *ZAMM-Journal of Applied Mathematics and Mechanics/Zeitschrift für Angewandte Mathematik und Mechanik*, 97(1):70–91, 2017.

[59] MG Rivera and JN Reddy. Stress analysis of functionally graded shells using a 7-parameter shell element. *Mechanics Research Communications*, 78:60–70, 2016.

[60] L Euler. Genuina principia doctrinae de statu aequilibrii et motu corporum tam perfecte flexibilium quam elasticorum. *Novi Commentarii Academiae Scientiarum Imperialis Petropolitanae*, 15(1770):381–413, 1771.

[61] E Cosserat and F Cosserat. Sur la statique de la ligne deformable. *CR Acad. Sci. Paris*, 145:1409–1412, 1907.

[62] JL Ericksen and C Truesdell. Exact theory of stress and strain in rods and shells. *Archive for Rational Mechanics and Analysis*, 1(1):295–323, 1957.

[63] AE Green, PM Naghdi, and ML Wenner. On the theory of rods. i. derivations from the three-dimensional equations. *Proceedings of the Royal Society of London. A. Mathematical and Physical Sciences*, 337(1611):451–483, 1974.

[64] AE Green, PM Naghdi, and ML Wenner. On the theory of rods. ii. developments by direct approach. *Proceedings of the Royal Society of London. A. Mathematical and Physical Sciences*, 337(1611):485–507, 1974.

[65] SS Antman. Nonlinear problems of elasticity, volume 107 of applied mathematical sciences, 2005.

[66] JC Simo. A finite strain beam formulation. the three-dimensional dynamic problem. part i. *Computer Methods in Applied Mechanics and Engineering*, 49(1):55–70, 1985.

[67] JC Simo and L Vu-Quoc. A three-dimensional finite-strain rod model. part ii: Computational aspects. *Computer Methods in Applied Mechanics and Engineering*, 58(1):79–116, 1986.

[68] S Goyal, NC Perkins, and CL Lee. Nonlinear dynamics and loop formation in kirchhoff rods with implications to the mechanics of dna and cables. *Journal of Computational Physics*, 209(1):371–389, 2005.

[69] S Goyal, NC Perkins, and CL Lee. Non-linear dynamic intertwining of rods with self-contact. *International Journal of Non-Linear Mechanics*, 43(1):65–73, 2008.

[70] A Kumar and S Mukherjee. A geometrically exact rod model including in-plane cross-sectional deformation. *Journal of Applied Mechanics*, 78(1):011010, 2011.

[71] C Fang, A Kumar, and S Mukherjee. A finite element analysis of single-walled carbon nanotube deformation. *Journal of Applied Mechanics*, 78(3):034502, 2011.

[72] A Kumar, S Mukherjee, JT Paci, K Chandraseker, and GC Schatz. A rod model for three dimensional deformations of single-walled carbon nanotubes. *International Journal of Solids and Structures*, 48(20):2849–2858, 2011.

[73] A Kumar and TJ Healey. A generalized computational approach to stability of static equilibria of nonlinearly elastic rods in the presence of constraints. *Computer Methods in Applied Mechanics and Engineering*, 199(25):1805–1815, 2010.

[74] A Arbind and JN Reddy. Transient analysis of cosserat rod with inextensibility and unshearability constraints using the least-squares finite element model. *International Journal of Non-Linear Mechanics*, 79:38–47, 2016.

[75] A Hoger and DE Carlson. On the derivative of the square root of a tensor and guo's rate theorems. *Journal of Elasticity*, 14(3):329–336, 1984.

APPENDIX A

THE DERIVATION OF THE GOVERNING EQUATIONS AND BOUNDARY CONDITIONS FOR COSSERAT CONTINUA (THREE-DIMENSIONAL) FOR CONSTRAINED MICRO-ROTATION

In this appendix, we present a detailed derivation of the governing equations and the boundary conditions for the three-dimensional hyperelastic Cosserat continuum with constrained micro-rotation for finite deformation (and finite rotation) from a Lagrangian mechanics point of view. The idea was put forth by Srinivasa and Reddy [19]. Let us consider a body $\mathcal{B}$ of fixed material. Let a particle X occupy position $\mathbf{X}$ in the reference frame at time $t = 0$ and it occupies position $\mathbf{x}$ at any subsequent time t. Let $\mathbf{f}$ be the body forces acting on the body and $\mathbf{u}$ be the displacement field caused by the forces. To obtain the governing equations of motion, we set the first variation of the following Lagrangian to zero:

$$\mathbb{L} = \int_{\mathcal{B}} \{\psi(U_{AB}, R_{iA}R_{iB,C}) - P_{iA}G_{iA} - f_i u_i\}\, dV \tag{A.1}$$

where $\mathbf{P}$ is the Lagrange multiplier, ψ is the potential energy stored in the body due to deformation, $\mathbf{U}$ is the symmetric positive-definite right stretch tensor, and $\mathbf{R}$ is orthogonal rotation tensor. The upper and lower case subscript index of tensors or vectors represent components of the tensor in reference and current configurations, respectively. In the case of stable equilibrium, the above condition also minimise the potential energy with respect to the displacement field for given constrained condition, whereas in the case of unstable or neutral equilibrium it would not minimise the potential energy but still gives the equations of equilibrium. Let us define the following quantities:

$$\theta_{ABC} = R_{iA}R_{iB,C} \tag{A.2}$$

and the constraint condition

$$G_{iB} = R_{iA}U_{AB} - x_{i,B}, \text{ where } \quad x_{i,B} = F_{iB}, \text{ and } \quad \mathbf{F} = \mathbf{RU} \tag{A.3}$$

where $\mathbf{F}$ is the deformation gradient. We also have the following conditions from the symmetric and orthogonal properties of $\mathbf{U}$ and $\mathbf{R}$ respectively:

$$\delta U_{AB} = \delta U_{BA}, \quad \delta R_{iA} = \delta\Omega_{ij}R_{jA}, \quad \delta\Omega_{ij} = -\delta\Omega_{ji} \tag{A.4}$$

For minimizing (in the case of stable equilibrium) the Lagrangian considered in Eq. (A.1), with the above given conditions, we put $\delta\mathbb{L} = 0$ and obtain the following equation:

$$\begin{aligned} 0 &= \int_{\mathcal{B}} \Big[\frac{\partial \psi}{\partial U_{AB}} \delta U_{AB} + \frac{\partial \psi}{\partial \theta_{ABC}} (\delta R_{iA} R_{iB,C} + R_{iA} \delta R_{iB,C}) \\ &\quad - \delta P_{iA} G_{iA} - P_{iA} \delta G_{iA} - f_i \delta u_i \big] \, dV \\ &= \int_{\mathcal{B}} \Big[\delta U_{AB} \left(\frac{\partial \psi}{\partial U_{AB}} - P_{iB} R_{iA} \right) + \delta R_{iA} \left(\frac{\partial \psi}{\partial \theta_{ABC}} R_{iB,C} - P_{iB} U_{AB} \right) \\ &\quad + \delta R_{iB,C} \frac{\partial \psi}{\partial \theta_{ABC}} - \delta P_{iA} G_{iA} + P_{iA} \delta x_{i,A} - f_i \delta x_i \Big] \, dV \end{aligned} \tag{A.5}$$

Integrating by parts and using $\delta R_{iA} = \delta \Omega_{ij} R_{jA}$, we obtain the following equation:

$$\begin{aligned} 0 = \int_{\mathcal{B}} \Big[& \delta U_{AB} \left(\frac{\partial \psi}{\partial U_{AB}} - P_{iB} R_{iA} \right) + \delta \Omega_{ij} R_{jA} \left(\frac{\partial \psi}{\partial \theta_{ABC}} R_{iB,C} - P_{iB} U_{AB} - \left(\frac{\partial \psi}{\partial \theta_{ABC}} \right)_{,C} \right) \\ & - \delta P_{iA} G_{iA} - (P_{iA,A} + f_i) \delta x_i \Big] \, dV + \underbrace{\oint_{\partial \mathcal{B}} \left[\delta R_{iB} \frac{\partial \psi}{\partial \theta_{ABC}} R_{iA} N_C + \delta x_i P_{iA} N_A \right] dS}_{\text{Boundary terms}} \end{aligned} \tag{A.6}$$

where $\mathbf{N}$ is the unit normal at the boundary surface in the reference frame. Using the fact that $\mathbf{U}$ and $\mathbf{\Omega}$ are symmetric and skew symmetric tensors, respectively, we obtain the following Euler–Lagrange equations:

$$\begin{aligned} \delta U_{AB} : &\quad \left(\frac{\partial \psi}{\partial U_{AB}} - P_{iB} R_{iA} \right)_{sym} = 0 \implies \frac{\partial \psi}{\partial \mathbf{U}} = \frac{1}{2} (\mathbf{P}^t \mathbf{R} + \mathbf{R}^t \mathbf{P}) \\ \delta \Omega_{ij} : &\quad \left[R_{jA} \left(\frac{\partial \psi}{\partial \theta_{ABC}} R_{iB,C} - P_{iB} U_{AB} - \left(\frac{\partial \psi}{\partial \theta_{ABC}} \right)_{,C} \right) \right]_{skewsym} = 0 \\ \implies & \operatorname{Div}(\mathbf{M}) = \mathbf{P}\mathbf{F}^t + \mathbf{F}\mathbf{P}^t, \text{ where } M_{ijC} = -M_{jiC} = \frac{\partial \psi}{\partial \theta_{ABC}} (R_{iA} R_{jB} - R_{jA} R_{iB}) \\ \delta x_i : &\quad P_{iA,A} = f_i \implies \operatorname{Div}(\mathbf{P}) = \mathbf{f} \\ \delta P_{iA} : &\quad G_{iA} = 0 \implies \mathbf{G} = 0 \end{aligned} \tag{A.7}$$

Here the "Div" means the divergence in the coordinate frame of the reference configuration. The boundary condition is

$$\oint_{\partial \mathcal{B}} \left[\delta R_{iB} \frac{\partial \psi}{\partial \theta_{ABC}} R_{iA} N_C + \delta x_i P_{iA} N_A \right] dS = 0 \tag{A.8}$$

Let us write the boundary condition as, without the loss of generality,

$$\oint_{\partial\mathcal{B}} \left[\frac{\partial R_{iB}}{\partial F_{jK}}\frac{\partial \psi}{\partial \theta_{ABC}} R_{iA}N_C\delta F_{jK} + \delta x_i P_{iA}N_A\right] dS = 0 \tag{A.9}$$

Let us define $\mathbf{M}^n$, a second order "surface tension" like tensor for the solid, components of which can be given as

$$M^n_{jK} \;=\; \frac{\partial R_{iB}}{\partial F_{jK}}\frac{\partial \psi}{\partial \theta_{ABC}} R_{iA}N_C \tag{A.10}$$

Then the boundary condition becomes

$$\oint_{\partial\mathcal{B}} \left[M^n_{jK}\delta F_{jK} + \delta x_i P_{iA}N_A\right] dS = 0 \implies \oint_{\partial\mathcal{B}} \mathbf{M}^n : \delta\nabla\mathbf{x} + \delta\mathbf{x}\cdot(\mathbf{P}\cdot\mathbf{N})\, dS = 0 \tag{A.11}$$

The boundary condition can be further simplified for a smooth boundary surface as

$$\oint_{\partial\mathcal{B}} (\mathbf{M}^n\cdot\mathbf{N})\cdot\frac{\partial\delta\mathbf{x}}{\partial n} - \mathrm{Div}_s\mathbf{M}^n\cdot\delta\mathbf{x} + (\mathrm{Div}_s\mathbf{N})\mathbf{N}\cdot(\mathbf{M}^n\cdot\delta\mathbf{x}) + \delta\mathbf{x}\cdot(\mathbf{P}\cdot\mathbf{N})\, dS = 0 \tag{A.12}$$

where n is the coordinate along the normal direction ($\mathbf{N}$) to the surface and Div_s is the surface divergence operator. Hence, the primary and corresponding secondary boundary variables are

$$\begin{aligned} \delta\mathbf{x}: &\quad \mathbf{P}\cdot\mathbf{N} + (\nabla_s\cdot\mathbf{N})\mathbf{N}\cdot\mathbf{M}^n - \mathrm{div}_s(\mathbf{M}^n) \\ \frac{\partial\delta\mathbf{x}}{\partial n}: &\quad \mathbf{M}^n\cdot\mathbf{N} \end{aligned} \tag{A.13}$$

The boundary conditions are

$$\begin{aligned} \mathbf{x} &= \text{ constant} = \mathbf{X} \text{ or } \mathbf{P}\cdot\mathbf{N} + (\nabla_s\cdot\mathbf{N})\mathbf{N}\cdot\mathbf{M}^n - \mathrm{div}_s(\mathbf{M}^n) = \mathbf{0} \\ \frac{\partial\mathbf{x}}{\partial n} &= \text{ constant or } \mathbf{M}^n\cdot\mathbf{N} = \mathbf{0} \end{aligned} \tag{A.14}$$

APPENDIX B

COMPUTATION OF SKEW-SYMMETRIC PART OF STRESS TENSOR FOR MICROSTRUCTURE DEPENDENT PLATE

The skew-symmetric part of the second Piola–Kirchhoff stress tensor ($\mathbf{S}$) can be obtained by means of balance of angular momentum (see [19, **?**]) as follows:

$$\mathbf{S}^a = \frac{1}{2}(\mathbf{S} - \mathbf{S}^T) = \frac{1}{2}\mathbf{F}^{-1}(\mathrm{div}(\mathbf{M}))\mathbf{F}^{-T} \tag{B.1}$$

In the indicial notation, we can write

$$S^a_{kp} = \frac{1}{2}F^{-1}_{ki}\left(\mathrm{div}(\mathbf{M})\right)_{ij}F^{-T}_{jp} \tag{B.2}$$

where $\mathbf{F}$ is the deformation gradient and $\mathbf{M}$ is the third-order couple stress tensor defined in the case of finite rotation (see [19]). The divergence of $\mathbf{M}$ is taken with respect to the reference configuration and can be given as follows:

$$\begin{aligned}\left(\mathrm{div}(\mathbf{M})\right)_{ij} &= \left(\frac{\partial\psi}{\partial\Omega_{CAB}}\right)_{,C}(R_{iA}R_{jB} - R_{jA}R_{iB}) \\ &\quad + \frac{\partial\psi}{\partial\Omega_{CAB}}(R_{iA,C}R_{jB} - R_{jA,C}R_{iB} + R_{iA}R_{jB,C} - R_{jA}R_{iB,C})\end{aligned} \tag{B.3}$$

where ψ is the potential energy density function, $\mathbf{R}$ is the rotation tensor at any point, and $\boldsymbol{\Omega}$ is defined in Eq. (3.3). From Eq. (3.13), we have

$$\begin{aligned}\boldsymbol{\chi} &= \begin{bmatrix}2\omega_{x,x} & 2\omega_{x,y} & 2\omega_{x,z} & 2\omega_{y,x} & 2\omega_{y,y} & 2\omega_{y,z} & 2\omega_{z,x} & 2\omega_{z,y} & 2\omega_{z,z}\end{bmatrix}^T \\ &= 2\begin{bmatrix}-\Omega_{123} & -\Omega_{223} & \Omega_{323} & \Omega_{113} & \Omega_{213} & \Omega_{313} & -\Omega_{112} & -\Omega_{212} & -\Omega_{312}\end{bmatrix}^T \\ &= 2\hat{\boldsymbol{\chi}}\end{aligned} \tag{B.4}$$

We also have

$$\Omega_{CAB} = -\Omega_{CBA} \tag{B.5}$$

Let us consider the case $A = 1,\ B = 2$ and $A = 2,\ B = 1$ in the following divergence definition,

$$\left(\mathrm{div}(\mathbf{M})\right)_{ij} = \left(\frac{\partial\psi}{\partial\Omega_{CAB}}(R_{iA}R_{jB} - R_{jA}R_{iB})\right)_{,C} \tag{B.6}$$

and use eq. (B.5) to obtain the following expression:

$$\begin{aligned}
&\left(\frac{\partial\psi}{\partial\Omega_{C12}}(R_{i1}R_{j2}-R_{j1}R_{i2})\right)_{,C}+\left(\frac{\partial\psi}{\partial\Omega_{C21}}(R_{i2}R_{j1}-R_{j2}R_{i1})\right)_{,C}\\
=&\left(\frac{\partial\psi}{\partial\Omega_{C12}}(R_{i1}R_{j2}-R_{j1}R_{i2})\right)_{,C}+\left(\left(-\frac{\partial\psi}{\partial\Omega_{C12}}\right)(-(R_{j2}R_{i1}-R_{i2}R_{j1}))\right)_{,C}\\
=&\left(2\frac{\partial\psi}{\partial\Omega_{C12}}(R_{i1}R_{j2}-R_{j1}R_{i2})\right)_{,C} \qquad \text{(B.7)}
\end{aligned}$$

When we treat $\Omega_{C12}=-\Omega_{C21}=\hat{\chi}_C$ (say) in the energy density function as one variable, then Eq. (B.7) becomes,

$$\left(2\frac{\partial\psi}{\partial\Omega_{C12}}(R_{i1}R_{j2}-R_{j1}R_{i2})\right)_{,C}=\left(\frac{\partial\psi}{\partial\hat{\chi}_C}(R_{i1}R_{j2}-R_{j1}R_{i2})\right)_{,C} \qquad \text{(B.8)}$$

From Eq. (3.16), we have

$$\mathbf{m}=\mathbf{C}_l\boldsymbol{\chi}=\frac{\partial\psi}{\partial\boldsymbol{\chi}}=\frac{1}{2}\frac{\partial\psi}{\partial\hat{\boldsymbol{\chi}}} \qquad \text{(B.9)}$$

Then the divergence of the third-order couple stress tensor, $\mathbf{M}$, can be obtained by summing over all the nine terms of m_i with their corresponding rotation terms:

$$\begin{aligned}
(\mathrm{div}(\mathbf{M}))_{ij} =\;& 2[(m_1(R_{i2}R_{j3}-R_{j2}R_{i3}))_{,x}+(m_2(R_{i2}R_{j3}-R_{j2}R_{i3}))_{,y}\\
&+(m_3(R_{i2}R_{j3}-R_{j2}R_{i3}))_{,z}+(m_4(R_{i1}R_{j3}-R_{j1}R_{i3}))_{,x}\\
&+(m_5(R_{i1}R_{j3}-R_{j1}R_{i3}))_{,y}+(m_6(R_{i1}R_{j3}-R_{j1}R_{i3}))_{,z}\\
&+(m_7(R_{i1}R_{j2}-R_{j1}R_{i2}))_{,x}+(m_8(R_{i1}R_{j2}-R_{j1}R_{i2}))_{,y}\\
&+(m_9(R_{i1}R_{j2}-R_{j1}R_{i2}))_{,z}] \qquad \text{(B.10)}
\end{aligned}$$

where $()_{,x}$, for example, represents the derivative with respect to x. The above expression requires the computation of derivative of the rotation tensor, which is given as follows:

$$\mathbf{R}_{,i}=(\mathbf{F}_{,i}-\mathbf{R}\mathbf{U}_{,i})\mathbf{U}^{-1}, \quad \text{for } i=x,y,z \qquad \text{(B.11)}$$

where $\mathbf{U}$ is the right stretch tensor, and it's derivative (see Hoger and Carlson [75]) can be given as

$$\begin{aligned}
\mathbf{U}_{,i} =\;& a_1\mathbf{U}^2(\mathbf{C}_{,i})\mathbf{U}^2+a_2\{\mathbf{U}^2(\mathbf{C}_{,i})\mathbf{U}+\mathbf{U}(\mathbf{C}_{,i})\mathbf{U}^2\}\\
&+a_3\{\mathbf{U}^2(\mathbf{C}_{,i})+(\mathbf{C}_{,i})\mathbf{U}^2\}+a_4\mathbf{U}(\mathbf{C}_{,i})\mathbf{U}\}\\
&+a_5\{\mathbf{U}\mathbf{C}_{,i}+\mathbf{C}_{,i}\mathbf{U}\}+a_6\delta\mathbf{C} \qquad \text{(B.12)}
\end{aligned}$$

where

$$
\begin{aligned}
a_1 &= \frac{4}{\Delta_s} I_1 & a_4 &= \frac{4}{\Delta_s}(I_1^3 + I_3) \\
a_2 &= -\frac{4}{\Delta_s} I_1^2 & a_5 &= -\frac{4}{\Delta_s} I_1^2 I_2 \\
a_3 &= \frac{4}{\Delta_s}(I_1 I_2 - I_3) & a_6 &= \frac{4}{\Delta_s}[I_1^2 I_3 + (I_1 I_2 - I_3) I_2] \\
\Delta_s &= 8(I_1 I_2 - I_3) I_3
\end{aligned}
\tag{B.13}
$$

Here I_1, I_2, and I_3 are principal invariants of $\mathbf{U}$, $\mathbf{C}$ is the right Cauchy–Green deformation tensor, and it's derivative can be obtained as follows:

$$
\mathbf{C} = \mathbf{F}^T \mathbf{F}, \quad \mathbf{C}_{,i} = \mathbf{F}_{,i}^T \mathbf{F} + \mathbf{F}^T \mathbf{F}_{,i} \text{ for } i = x, y, z \tag{B.14}
$$

where the deformation gradient in terms of the variables in displacement field considered (see Eq. (3.5)) in the general higher-order plate theory is given as follows:

$$
\mathbf{F} = \nabla \mathbf{u} + \mathbf{I} \tag{B.15}
$$

Here $\mathbf{I}$ is third-order identity tensor and $\nabla \mathbf{u}$ is the displacement gradient tensor:

$$
\nabla \mathbf{u} = \begin{bmatrix} \frac{\partial u_1}{\partial x} & \frac{\partial u_1}{\partial y} & \frac{\partial u_1}{\partial z} \\ \frac{\partial u_2}{\partial x} & \frac{\partial u_2}{\partial y} & \frac{\partial u_2}{\partial z} \\ \frac{\partial u_3}{\partial x} & \frac{\partial u_3}{\partial y} & \frac{\partial u_3}{\partial z} \end{bmatrix} = \begin{bmatrix} \mathbf{A}_x \boldsymbol{\phi}_{x,x} & \mathbf{A}_x \boldsymbol{\phi}_{x,y} & \mathbf{A}_{x,z} \boldsymbol{\phi}_x \\ \mathbf{A}_y \boldsymbol{\phi}_{y,x} & \mathbf{A}_y \boldsymbol{\phi}_{y,y} & \mathbf{A}_{y,z} \boldsymbol{\phi}_y \\ \mathbf{A}_z \boldsymbol{\phi}_{z,x} & \mathbf{A}_z \boldsymbol{\phi}_{z,y} & \mathbf{A}_{z,z} \boldsymbol{\phi}_z \end{bmatrix} \tag{B.16}
$$

The derivative of the deformation gradient can be obtained as follows:

$$
\mathbf{F}_{,x} = \begin{bmatrix} \mathbf{A}_x \boldsymbol{\phi}_{x,xx} & \mathbf{A}_x \boldsymbol{\phi}_{x,xy} & \mathbf{A}_{x,z} \boldsymbol{\phi}_{x,x} \\ \mathbf{A}_y \boldsymbol{\phi}_{y,xx} & \mathbf{A}_y \boldsymbol{\phi}_{y,xy} & \mathbf{A}_{y,z} \boldsymbol{\phi}_{y,x} \\ \mathbf{A}_z \boldsymbol{\phi}_{z,xx} & \mathbf{A}_z \boldsymbol{\phi}_{z,xy} & \mathbf{A}_{z,z} \boldsymbol{\phi}_{z,x} \end{bmatrix}
$$

$$
\mathbf{F}_{,y} = \begin{bmatrix} \mathbf{A}_x \boldsymbol{\phi}_{x,xy} & \mathbf{A}_x \boldsymbol{\phi}_{x,yy} & \mathbf{A}_{x,z} \boldsymbol{\phi}_{x,y} \\ \mathbf{A}_y \boldsymbol{\phi}_{y,xy} & \mathbf{A}_y \boldsymbol{\phi}_{y,yy} & \mathbf{A}_{y,z} \boldsymbol{\phi}_{y,y} \\ \mathbf{A}_z \boldsymbol{\phi}_{z,xy} & \mathbf{A}_z \boldsymbol{\phi}_{z,yy} & \mathbf{A}_{z,z} \boldsymbol{\phi}_{z,y} \end{bmatrix}
$$

$$\mathbf{F}_{,z} = \begin{bmatrix} \mathbf{A}_{x,z}\boldsymbol{\phi}_{x,x} & \mathbf{A}_{x,z}\boldsymbol{\phi}_{x,y} & \mathbf{A}_{x,zz}\boldsymbol{\phi}_{x} \\ \mathbf{A}_{y,z}\boldsymbol{\phi}_{y,x} & \mathbf{A}_{y,z}\boldsymbol{\phi}_{y,y} & \mathbf{A}_{y,zz}\boldsymbol{\phi}_{y} \\ \mathbf{A}_{z,z}\boldsymbol{\phi}_{z,x} & \mathbf{A}_{z,z}\boldsymbol{\phi}_{z,y} & \mathbf{A}_{z,zz}\boldsymbol{\phi}_{z} \end{bmatrix}. \tag{B.17}$$

APPENDIX C

AREA ELEMENT AND NORMAL VECTOR FOR ARBITRARY SURFACE IN A CYLINDRICAL COORDINATE SYSTEM

Consider an arbitrary surface embedded in three-dimensional Euclidean space, $\mathbb{R}^3$, as shown in fig. C.1. We consider the x-axis as the axis of the surface, reference to which we will consider a cylindrical coordinate system with surface coordinates, $z^1 = x$ and $z^2 = \theta$, as shown in fig. C.1. The radius r of the cross-section (see fig. C.1) measured from the x-axis defines the geometry of the surface and hence given as $r(x, \theta)$ at each point c on the x-axis. Consider an arbitrary point p on the

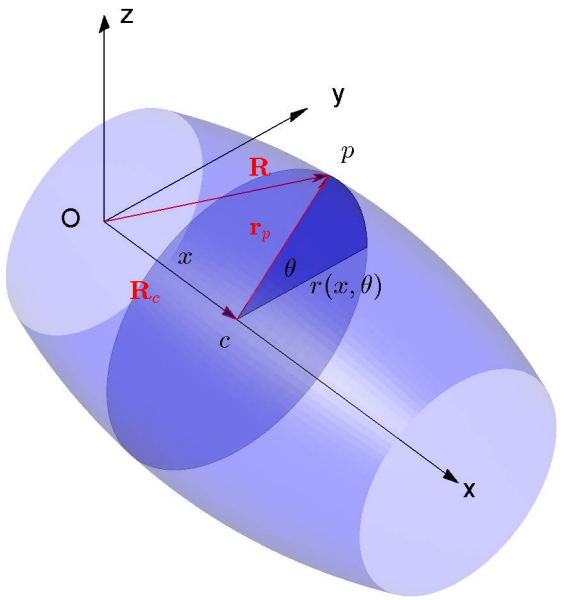

Fig. C.1 Arbitrary surface in cylindrical coordinate system.

surface and its corresponding point c on the x-axis. Then the position vector of point p with respect to the origin is given by

$$\mathbf{R} \;=\; \mathbf{R}_c + \mathbf{r}_p = \mathbf{R}_c + r(x,\theta)\,\cos\theta\,\mathbf{e}_y + r(x,\theta)\,\sin\theta\,\mathbf{e}_z \qquad \text{(C.1)}$$

where $\mathbf{R}_c$ is the position vector of point c and $\mathbf{r}_p$ is the position vector of point p with respect to point c; $\mathbf{e}_x,\ \mathbf{e}_y$ and $\mathbf{e}_z$ are the unit vectors along the $x,\ y$ and z axis. Further, the covariant basis for the surface coordinate (x, θ) can be given as follows:

$$\begin{aligned} \mathbf{z}_x &= \frac{\partial \mathbf{R}}{\partial x} = \mathbf{e}_x + \frac{\partial r}{\partial x}\,\cos\theta\,\mathbf{e}_y + \frac{\partial r}{\partial x}\,\sin\theta\,\mathbf{e}_z \\ \mathbf{z}_\theta &= \frac{\partial \mathbf{R}}{\partial \theta} = \left(\frac{\partial r}{\partial \theta}\,\cos\theta - r\,\sin\theta\right)\mathbf{e}_y + \left(\frac{\partial r}{\partial \theta}\,\sin\theta + r\,\cos\theta\right)\mathbf{e}_z \end{aligned} \tag{C.2}$$

If $\mathbf{G}$ be the covariant matric tensor then its components are given by

$$\begin{aligned} G_{xx} &= 1 + \left(\frac{\partial r}{\partial x}\right)^2 \\ G_{\theta\theta} &= \left(\frac{\partial r}{\partial \theta}\right)^2 + r^2 \\ G_{x\theta} &= G_{\theta x} = \frac{\partial r}{\partial x}\frac{\partial r}{\partial \theta} \end{aligned} \tag{C.3}$$

The determinant, G, of the covariant matric tensor is defined by

$$G = r^2 + \left(\frac{\partial r}{\partial \theta}\right)^2 + \left(r\,\frac{\partial r}{\partial x}\right)^2 \tag{C.4}$$

Hence, the area element on the surface can be written as

$$d\mathcal{S} = \sqrt{G}\,d\theta\,dx = \sqrt{r^2 + \left(\frac{\partial r}{\partial \theta}\right)^2 + \left(r\,\frac{\partial r}{\partial x}\right)^2}\,d\theta\,dx \tag{C.5}$$

If the radius r is function of x only (as in the case of surface of revolution), the area element reduces to:

$$d\mathcal{S} = \sqrt{1 + \left(\frac{\partial r}{\partial x}\right)^2}\,r\,d\theta\,dx \tag{C.6}$$

and for constant radius (r), the area element reduce to $r\,d\theta\,dx$ as expected. The covariant basis vectors span the tangent plane and hence the outward normal vector of the surface can be given by the normalized cross product of the covariant basis vectors as followins:

$$\mathbf{N} = \frac{\mathbf{z}_\theta \times \mathbf{z}_x}{|\mathbf{z}_\theta \times \mathbf{z}_x|} = \frac{1}{|\mathbf{z}_\theta \times \mathbf{z}_x|}\left[-r\frac{\partial r}{\partial x}\,\mathbf{e}_x + \left(\frac{\partial r}{\partial \theta}\,\sin\theta + r\,\cos\theta\right)\mathbf{e}_y\right.$$

$$- \left(\frac{\partial r}{\partial \theta} \cos\theta - r \sin\theta \right) \mathbf{e}_z \Bigg] \tag{C.7}$$

where

$$|\mathbf{z}_\theta \times \mathbf{z}_x| = \sqrt{r^2 + r^2 \left(\frac{\partial r}{\partial x} \right)^2 + \left(\frac{\partial r}{\partial \theta} \right)^2} \tag{C.8}$$

We also have

$$\mathbf{e}_y = \cos\theta \mathbf{e}_r - \sin\theta \mathbf{e}_\theta, \quad \mathbf{e}_z = \sin\theta \mathbf{e}_r + \cos\theta \mathbf{e}_\theta \tag{C.9}$$

where $\mathbf{e}_x$, $\mathbf{e}_r$ and $\mathbf{e}_\theta$ is an orthonormal basis in the (x, r, θ) (cylindrical) coordinate system. In the cylindrical coordinate system, the outward unit normal vector to the surface at any arbitrary surface point can be given as

$$\mathbf{N} = \frac{1}{|\mathbf{z}_\theta \times \mathbf{z}_x|} \left[- r \frac{\partial r}{\partial x} \mathbf{e}_x + r \, \mathbf{e}_r - \frac{\partial r}{\partial \theta} \mathbf{e}_\theta \right] \tag{C.10}$$

In the case of surface of revolution (i.e., for $r(x)$), we put $\frac{\partial r}{\partial \theta} = 0$ in the above expression, and for constant radius (r), we have the following result:

$$|\mathbf{z}_\theta \times \mathbf{z}_s| = r, \quad \mathbf{N} = \mathbf{e}_r \tag{C.11}$$

APPENDIX D

GREEN–LAGRANGE STRAIN TENSOR IN A CYLINDRICAL CURVILINEAR COORDINATE SYSTEM

Let us consider a curve $\mathcal{C}$ in a three-dimensional Euclidean space. Let s be the curvilinear coordinate along the the curve. Let us associate a right-handed orthogonal unit vector triplet $\mathbf{T}, \mathbf{P}$, and $\mathbf{Q}$ at each point of the space curve, $\mathcal{C}$, and $\mathbf{T}$ be the unit tangent vector along the curve; $\mathbf{P}$ and $\mathbf{Q}$ be the principal normal and binormal vectors, respectively (see Appendix E). Now, let us also consider a polar coordinate system (r, θ) in the normal plane at each point of the curve $\mathcal{C}$. The angle, θ, is measured from the principal normal $\mathbf{P}$ towards the binormal $\mathbf{Q}$. Then r, θ along with the coordinate s constitutes a curvilinear cylindrical coordinate system (see fig. 6.2). Let us define the coordinates $z^1 = s$, $z^2 = r$, and $z^3 = \theta$ in the indicial notation convention. Now, if $\mathbf{R}$ is the position vector of any arbitrary point $\mathcal{P}$ from the origin $\mathcal{O}$, then the covariant basis vectors can be defined as

$$\mathbf{e}_s = \frac{\partial \mathbf{R}}{\partial s} = \mathbf{T}, \quad \mathbf{e}_r = \frac{\partial \mathbf{R}}{\partial r}, \quad \mathbf{e}_\theta = \frac{\partial \mathbf{R}}{\partial \theta} \tag{D.1}$$

We note that the basis vectors are not necessarily unit vectors. Now the nonzero component of covariant matric tensor and, consequently, the contravariant matric tensor can be given as follows:

$$\begin{aligned} g_{ss} = 1, \quad g_{rr} = 1, \quad g_{\theta\theta} = r^2 \\ g^{ss} = 1, \quad g^{rr} = 1, \quad g^{\theta\theta} = \frac{1}{r^2} \end{aligned} \tag{D.2}$$

The contravariant basis vectors can be obtained by raising the indices of covariant basis vectors as

$$\mathbf{e}^s = g^{sk}\mathbf{e}_k = \mathbf{e}_s = \mathbf{T}, \quad \mathbf{e}^r = \mathbf{e}_r, \quad \mathbf{e}^\theta = \frac{1}{r^2}\mathbf{e}_\theta \tag{D.3}$$

where the repeated indices imply summation. In terms of the vectors $\mathbf{P}$ and $\mathbf{Q}$, the basis vectors can be given as follows:

$$\mathbf{e}_s = \mathbf{T}, \quad \mathbf{e}_r = \cos\theta\,\mathbf{P} + \sin\theta\,\mathbf{Q}, \quad \mathbf{e}_\theta = -r\sin\theta\,\mathbf{P} + r\cos\theta\,\mathbf{Q} \tag{D.4}$$

and also

$$\mathbf{P} = \cos\theta\,\mathbf{e}_r - \frac{\sin\theta}{r}\,\mathbf{e}_\theta, \quad \mathbf{Q} = \sin\theta\,\mathbf{e}_r + \frac{\cos\theta}{r}\,\mathbf{e}_\theta \tag{D.5}$$

For the given displacement field $\mathbf{u} = u^s\mathbf{e}_s + u^r\mathbf{e}_r + u^\theta\mathbf{e}_\theta = u^i\mathbf{e}_i$, the gradient $\boldsymbol{\nabla}\mathbf{u}$ can be obtained as,

$$\boldsymbol{\nabla}\mathbf{u} = (\nabla_i u^j)\mathbf{e}^i\mathbf{e}_j = \left(\frac{\partial u^j}{\partial z^i} + \Gamma^j_{ik}u^k\right)\mathbf{e}^i\mathbf{e}_j \tag{D.6}$$

where ∇_i denotes the covariant derivative operator for $i = s, r, \theta$ and Γ^j_{ik} are the Christoffel symbols, which are defined as

$$\Gamma^j_{ik} = \mathbf{e}^j \cdot \frac{\partial \mathbf{e}_i}{\partial z^k} \tag{D.7}$$

There are 27 various Christoffel symbols for the cylindrical curvilinear coordinate system adopted. In order to calculate various Christoffel symbols, we first consider the following Frenet formula for a spatial curve:

$$\frac{\partial \mathbf{T}}{\partial s} = \kappa\mathbf{P}, \quad \frac{\partial \mathbf{P}}{\partial s} = -\kappa\mathbf{T} + \tau\mathbf{Q}, \quad \frac{\partial \mathbf{Q}}{\partial s} = -\tau\mathbf{P} \tag{D.8}$$

where κ and τ are the curvature and the twist of the spatial curve and can be function of the curvilinear coordinate s of the space curve: Using Eqs. (D.4), (D.5), and (D.8) we have the following derivatives:

$$\begin{aligned}
&\frac{\partial \mathbf{e}_s}{\partial s} = \kappa\cos\theta\,\mathbf{e}_r - \frac{\kappa}{r}\sin\theta\,\mathbf{e}_\theta, \quad \frac{\partial \mathbf{e}_r}{\partial s} = -\kappa\cos\theta\,\mathbf{e}_s + \frac{\tau}{r}\,\mathbf{e}_\theta, \quad \frac{\partial \mathbf{e}_\theta}{\partial s} = \kappa r\sin\theta\,\mathbf{e}_s - \tau r\,\mathbf{e}_r \\
&\frac{\partial \mathbf{e}_r}{\partial r} = \mathbf{0}, \quad \frac{\partial \mathbf{e}_r}{\partial \theta} = \frac{1}{r}\,\mathbf{e}_\theta, \quad \frac{\partial \mathbf{e}_\theta}{\partial \theta} = -r\,\mathbf{e}_r
\end{aligned} \tag{D.9}$$

Now using Eqs. (D.7) and (D.9), various Christoffel symbols can be computed as:

$$\begin{aligned}
&\Gamma^s_{ss} = 0, \quad \Gamma^r_{ss} = \kappa\,\cos\theta, \quad \Gamma^\theta_{ss} = -\frac{\kappa}{r}\,\sin\theta \\
&\Gamma^s_{rs} = \Gamma^s_{sr} = -\kappa\,\cos\theta, \quad \Gamma^r_{rs} = \Gamma^r_{sr} = 0, \quad \Gamma^\theta_{rs} = \Gamma^\theta_{sr} = \frac{\tau}{r} \\
&\Gamma^s_{\theta s} = \Gamma^s_{s\theta} = \kappa r\,\sin\theta, \quad \Gamma^r_{\theta s} = \Gamma^r_{s\theta} = -\tau r, \quad \Gamma^\theta_{\theta s} = \Gamma^\theta_{s\theta} = 0 \\
&\Gamma^\theta_{\theta r} = \Gamma^\theta_{r\theta} = \frac{1}{r}, \quad \Gamma^r_{\theta\theta} = -r, \quad \Gamma^s_{rr} = \Gamma^r_{rr} = \Gamma^\theta_{rr} = 0 \\
&\Gamma^s_{r\theta} = \Gamma^s_{\theta r} = \Gamma^r_{r\theta} = \Gamma^r_{\theta r} = \Gamma^s_{\theta\theta} = \Gamma^\theta_{\theta\theta} = 0
\end{aligned} \tag{D.10}$$

Further, using Eqs. (D.6), (D.10), and (D.3), the gradient of the displacement field

can be given as following:

$$
\begin{aligned}
\boldsymbol{\nabla}\mathbf{u} &= \left(\frac{\partial u^j}{\partial z^i} + \Gamma^j_{ik} u^k\right)\mathbf{e}^i\mathbf{e}_j = \left(\frac{\partial u^s}{\partial s} - \kappa\,\cos\theta\,u^r + \kappa r\,\sin\theta\,u^\theta\right)\mathbf{e}^s\mathbf{e}_s \\
&+ \left(\frac{\partial u^r}{\partial s} + \kappa\,\cos\theta\,u^s - \tau\,r\,u^\theta\right)\mathbf{e}^s\mathbf{e}_r + \left(\frac{\partial u^\theta}{\partial s} - \frac{\kappa}{r}\,\sin\theta\,u^s + \frac{\tau}{r}u^r\right)\mathbf{e}^s\mathbf{e}_\theta \\
&+ \left(\frac{\partial u^s}{\partial r} - \kappa\,\cos\theta\,u^s\right)\mathbf{e}^r\mathbf{e}_s + \frac{\partial u^r}{\partial r}\mathbf{e}^r\mathbf{e}_r + \left(\frac{\partial u^\theta}{\partial r} + \frac{\tau\,u^s}{r} + \frac{u^\theta}{r}\right)\mathbf{e}^r\mathbf{e}_\theta \\
&+ \left(\frac{\partial u^s}{\partial \theta} + \kappa\,r\,\sin\theta\,u^s\right)\mathbf{e}^\theta\mathbf{e}_s + \left(\frac{\partial u^r}{\partial \theta} - \tau\,r\,u^s - r\,u^\theta\right)\mathbf{e}^\theta\mathbf{e}_r \\
&+ \left(\frac{\partial u^\theta}{\partial \theta} + \frac{u^r}{r}\right)\mathbf{e}^\theta\mathbf{e}_\theta \\
&= \left(\frac{\partial u^s}{\partial s} - \kappa\,\cos\theta\,u^r + \kappa r\,\sin\theta\,u^\theta\right)\mathbf{e}_s\mathbf{e}_s \\
&+ \left(\frac{\partial u^r}{\partial s} + \kappa\,\cos\theta\,u^s - \tau\,r\,u^\theta\right)\mathbf{e}_s\mathbf{e}_r + \left(\frac{\partial u^\theta}{\partial s} - \frac{\kappa}{r}\,\sin\theta\,u^s + \frac{\tau}{r}u^r\right)\mathbf{e}_s\mathbf{e}_\theta \\
&+ \left(\frac{\partial u^s}{\partial r} - \kappa\,\cos\theta\,u^s\right)\mathbf{e}_r\mathbf{e}_s + \frac{\partial u^r}{\partial r}\mathbf{e}_r\mathbf{e}_r + \left(\frac{\partial u^\theta}{\partial r} + \frac{\tau\,u^s}{r} + \frac{u^\theta}{r}\right)\mathbf{e}_r\mathbf{e}_\theta \\
&+ \frac{1}{r^2}\left(\frac{\partial u^s}{\partial \theta} + \kappa\,r\,\sin\theta\,u^s\right)\mathbf{e}_\theta\mathbf{e}_s + \frac{1}{r^2}\left(\frac{\partial u^r}{\partial \theta} - \tau\,r\,u^s - r\,u^\theta\right)\mathbf{e}_\theta\mathbf{e}_r \\
&+ \frac{1}{r^2}\left(\frac{\partial u^\theta}{\partial \theta} + \frac{u^r}{r}\right)\mathbf{e}_\theta\mathbf{e}_\theta
\end{aligned}
\tag{D.11}
$$

Let us introduced the unit covariant basis vectors as

$$
\hat{\mathbf{e}}_s = \mathbf{e}_s, \quad \hat{\mathbf{e}}_r = \mathbf{e}_r, \quad \hat{\mathbf{e}}_\theta = \frac{1}{r}\,\mathbf{e}_\theta \tag{D.12}
$$

Then the displacement field can be expressed in terms of the unit basis as follows:

$$
\mathbf{u} = \hat{u}^s\hat{\mathbf{e}}_s + \hat{u}^r\hat{\mathbf{e}}_r + \hat{u}^\theta\hat{\mathbf{e}}_\theta \implies \hat{u}^s = u^s, \quad \hat{u}^r = u^r, \quad \hat{u}^\theta = r\,u^\theta \tag{D.13}
$$

Then the gradient of the displacement field takes the form:

$$
\begin{aligned}
\boldsymbol{\nabla}\mathbf{u} &= \left(\frac{\partial \hat{u}^s}{\partial s} - \kappa\,\cos\theta\,\hat{u}^r + \kappa\,\sin\theta\,\hat{u}^\theta\right)\hat{\mathbf{e}}_s\hat{\mathbf{e}}_s \\
&+ \left(\frac{\partial \hat{u}^r}{\partial s} + \kappa\,\cos\theta\,\hat{u}^s - \tau\,\hat{u}^\theta\right)\hat{\mathbf{e}}_s\hat{\mathbf{e}}_r + \left(\frac{\partial \hat{u}^\theta}{\partial s} - \kappa\,\sin\theta\,\hat{u}^s + \tau\hat{u}^r\right)\hat{\mathbf{e}}_s\hat{\mathbf{e}}_\theta \\
&+ \left(\frac{\partial \hat{u}^s}{\partial r} - \kappa\,\cos\theta\,\hat{u}^s\right)\hat{\mathbf{e}}_r\hat{\mathbf{e}}_s + \frac{\partial \hat{u}^r}{\partial r}\hat{\mathbf{e}}_r\hat{\mathbf{e}}_r + \left(\frac{\partial \hat{u}^\theta}{\partial r} + \tau\,\hat{u}^s\right)\hat{\mathbf{e}}_r\hat{\mathbf{e}}_\theta \\
&+ \left(\frac{1}{r}\frac{\partial \hat{u}^s}{\partial \theta} + \kappa\,\sin\theta\,\hat{u}^s\right)\hat{\mathbf{e}}_\theta\hat{\mathbf{e}}_s + \left(\frac{1}{r}\frac{\partial \hat{u}^r}{\partial \theta} - \tau\,\hat{u}^s - \frac{\hat{u}^\theta}{r}\right)\hat{\mathbf{e}}_\theta\hat{\mathbf{e}}_r
\end{aligned}
$$

$$+\frac{1}{r}\left(\frac{\partial \hat{u}^{\theta}}{\partial \theta}+\hat{u}^{r}\right)\hat{\mathbf{e}}_{\theta}\hat{\mathbf{e}}_{\theta} \tag{D.14}$$

The transpose of the displacement gradient is

$$\begin{aligned}
\boldsymbol{\nabla}\mathbf{u}^{T} &= \left(\frac{\partial \hat{u}^{s}}{\partial s}-\kappa\,\cos\theta\,\hat{u}^{r}+\kappa\,\sin\theta\,\hat{u}^{\theta}\right)\hat{\mathbf{e}}_{s}\hat{\mathbf{e}}_{s} \\
&+\left(\frac{\partial \hat{u}^{s}}{\partial r}-\kappa\,\cos\theta\,\hat{u}^{s}\right)\hat{\mathbf{e}}_{s}\hat{\mathbf{e}}_{r}+\left(\frac{1}{r}\frac{\partial \hat{u}^{s}}{\partial \theta}+\kappa\,\sin\theta\,\hat{u}^{s}\right)\hat{\mathbf{e}}_{s}\hat{\mathbf{e}}_{\theta} \\
&+\left(\frac{\partial \hat{u}^{r}}{\partial s}+\kappa\,\cos\theta\,\hat{u}^{s}-\tau\,\hat{u}^{\theta}\right)\hat{\mathbf{e}}_{r}\hat{\mathbf{e}}_{s}+\frac{\partial \hat{u}^{r}}{\partial r}\hat{\mathbf{e}}_{r}\hat{\mathbf{e}}_{r}+\left(\frac{1}{r}\frac{\partial \hat{u}^{r}}{\partial \theta}-\tau\,\hat{u}^{s}-\frac{\hat{u}^{\theta}}{r}\right)\hat{\mathbf{e}}_{r}\hat{\mathbf{e}}_{\theta} \\
&+\left(\frac{\partial \hat{u}^{\theta}}{\partial s}-\kappa\,\sin\theta\,\hat{u}^{s}+\tau\hat{u}^{r}\right)\hat{\mathbf{e}}_{\theta}\hat{\mathbf{e}}_{s}+\left(\frac{\partial \hat{u}^{\theta}}{\partial r}+\tau\,\hat{u}^{s}\right)\hat{\mathbf{e}}_{\theta}\hat{\mathbf{e}}_{r} \\
&+\frac{1}{r}\left(\frac{\partial \hat{u}^{\theta}}{\partial \theta}+\hat{u}^{r}\right)\hat{\mathbf{e}}_{\theta}\hat{\mathbf{e}}_{\theta}
\end{aligned} \tag{D.15}$$

For the given displacement field $\mathbf{u}$, the Green–Lagrange strain tensor takes the form

$$\mathbf{E}=E_{ij}\hat{\mathbf{e}}_{i}\hat{\mathbf{e}}_{j}=\frac{1}{2}(\boldsymbol{\nabla}\mathbf{u}+(\boldsymbol{\nabla}\mathbf{u})^{T}+(\boldsymbol{\nabla}\mathbf{u})\cdot(\boldsymbol{\nabla}\mathbf{u})^{T}) \tag{D.16}$$

The Green–Lagrange strain tensor components in terms of the components of displacement vector can be given as

$$\begin{aligned}
E_{ss} &= \left(\frac{\partial \hat{u}^{s}}{\partial s}-\kappa\,\cos\theta\,\hat{u}^{r}+\kappa\,\sin\theta\,\hat{u}^{\theta}\right)+\frac{1}{2}\left(\frac{\partial \hat{u}^{s}}{\partial s}-\kappa\,\cos\theta\,\hat{u}^{r}+\kappa\,\sin\theta\,\hat{u}^{\theta}\right)^{2} \\
&+\frac{1}{2}\left(\frac{\partial \hat{u}^{r}}{\partial s}+\kappa\,\cos\theta\,\hat{u}^{s}-\tau\,\hat{u}^{\theta}\right)^{2}+\frac{1}{2}\left(\frac{\partial \hat{u}^{\theta}}{\partial s}-\kappa\,\sin\theta\,\hat{u}^{s}+\tau\hat{u}^{r}\right)^{2} \\
E_{rr} &= \frac{\partial \hat{u}^{r}}{\partial r}+\frac{1}{2}\left(\frac{\partial \hat{u}^{s}}{\partial r}-\kappa\,\cos\theta\,\hat{u}^{s}\right)^{2}+\frac{1}{2}\left(\frac{\partial \hat{u}^{r}}{\partial r}\right)^{2}+\frac{1}{2}\left(\frac{\partial \hat{u}^{\theta}}{\partial r}+\tau\,\hat{u}^{s}\right)^{2} \\
E_{\theta\theta} &= \frac{1}{r}\left(\frac{\partial \hat{u}^{\theta}}{\partial \theta}+\hat{u}^{r}\right)+\frac{1}{2}\Bigg[\left(\frac{1}{r}\frac{\partial \hat{u}^{s}}{\partial \theta}+\kappa\,\sin\theta\,\hat{u}^{s}\right)^{2}+\left(\frac{1}{r}\frac{\partial \hat{u}^{r}}{\partial \theta}-\tau\,\hat{u}^{s}-\frac{\hat{u}^{\theta}}{r}\right)^{2} \\
&+\left(\frac{1}{r}\frac{\partial \hat{u}^{\theta}}{\partial \theta}+\frac{\hat{u}^{r}}{r}\right)^{2}\Bigg] \\
2E_{r\theta} &= \frac{1}{r}\frac{\partial \hat{u}^{r}}{\partial \theta}-\frac{\hat{u}^{\theta}}{r}+\frac{\partial \hat{u}^{\theta}}{\partial r}+\left(\frac{\partial \hat{u}^{s}}{\partial r}-\kappa\,\cos\theta\,\hat{u}^{s}\right)\left(\frac{1}{r}\frac{\partial \hat{u}^{s}}{\partial \theta}+\kappa\,\sin\theta\,\hat{u}^{s}\right) \\
&+\frac{\partial \hat{u}^{r}}{\partial r}\left(\frac{1}{r}\frac{\partial \hat{u}^{r}}{\partial \theta}-\tau\,\hat{u}^{s}-\frac{\hat{u}^{\theta}}{r}\right)+\left(\frac{\partial \hat{u}^{\theta}}{\partial r}+\tau\,\hat{u}^{s}\right)\left(\frac{1}{r}\frac{\partial \hat{u}^{\theta}}{\partial \theta}+\frac{\hat{u}^{r}}{r}\right) \\
2E_{\theta s} &= \frac{\partial \hat{u}^{\theta}}{\partial s}+\frac{1}{r}\frac{\partial \hat{u}^{s}}{\partial \theta}+\tau\hat{u}^{r}+\left(\frac{1}{r}\frac{\partial \hat{u}^{s}}{\partial \theta}+\kappa\,\sin\theta\,\hat{u}^{s}\right)\left(\frac{\partial \hat{u}^{s}}{\partial s}-\kappa\,\cos\theta\,\hat{u}^{r}+\kappa\,\sin\theta\,\hat{u}^{\theta}\right)
\end{aligned}$$

$$
\begin{aligned}
& + \left(\frac{1}{r}\frac{\partial \hat{u}^r}{\partial \theta} - \tau\,\hat{u}^s - \frac{\hat{u}_\theta}{r}\right)\left(\frac{\partial \hat{u}^r}{\partial s} + \kappa\,\cos\theta\,\hat{u}^s - \tau\hat{u}^\theta\right) \\
& + \frac{1}{r}\left(\frac{\partial \hat{u}^\theta}{\partial \theta} + \hat{u}^r\right)\left(\frac{\partial \hat{u}^\theta}{\partial s} - \kappa\,\sin\theta\,\hat{u}^s + \tau\hat{u}^r\right) \\
2E_{sr} \;=\; & \frac{\partial \hat{u}^s}{\partial r} + \frac{\partial \hat{u}^r}{\partial s} - \tau\,\hat{u}^\theta + \left(\frac{\partial \hat{u}^s}{\partial s} - \kappa\,\cos\theta\,\hat{u}^r + \kappa\,\sin\theta\,\hat{u}^\theta\right)\left(\frac{\partial \hat{u}^s}{\partial r} - \kappa\,\cos\theta\,\hat{u}^s\right) \\
& + \frac{\partial \hat{u}^r}{\partial r}\left(\frac{\partial \hat{u}^r}{\partial s} + \kappa\,\cos\theta\,\hat{u}^s - \tau\hat{u}^\theta\right) + \left(\frac{\partial \hat{u}^\theta}{\partial s} - \kappa\,\sin\theta\,\hat{u}^s + \tau\hat{u}^r\right)\left(\frac{\partial \hat{u}^\theta}{\partial r} + \tau\,\hat{u}^s\right)
\end{aligned}
\tag{D.17}
$$

For zero curvature κ and twist τ the curve becomes straight line, and the above strain components would reduced to the strain in cylindrical-coordinate system. Also the deformation gradient, $\mathbf{F}$, can be obtained as $\mathbf{F} = \nabla\mathbf{u} + \mathbf{I}$.

APPENDIX E

PRINCIPAL NORMAL, BINORMAL, TANGENT VECTOR, CURVATURE AND TORSION OF SPACE CURVE

Let us consider a curve $\mathcal{C}$ embedded in three-dimensional Euclidean space, $\mathbb{R}^3$. Further, we consider a rectangular cartesian system for the ambient space and the curve is parameterized by the arbitrary coordinate, t. Let us also associate a coordinate s with the curve $\mathcal{C}$. The position vector of any arbitrary point P on the curve $\mathcal{C}$ with respect to the origin O is given as

$$\mathbf{R} = x(t)\hat{\mathbf{e}}_x + y(t)\hat{\mathbf{e}}_y + z(t)\hat{\mathbf{e}}_z \tag{E.1}$$

Then the unit tangent vector can be given as

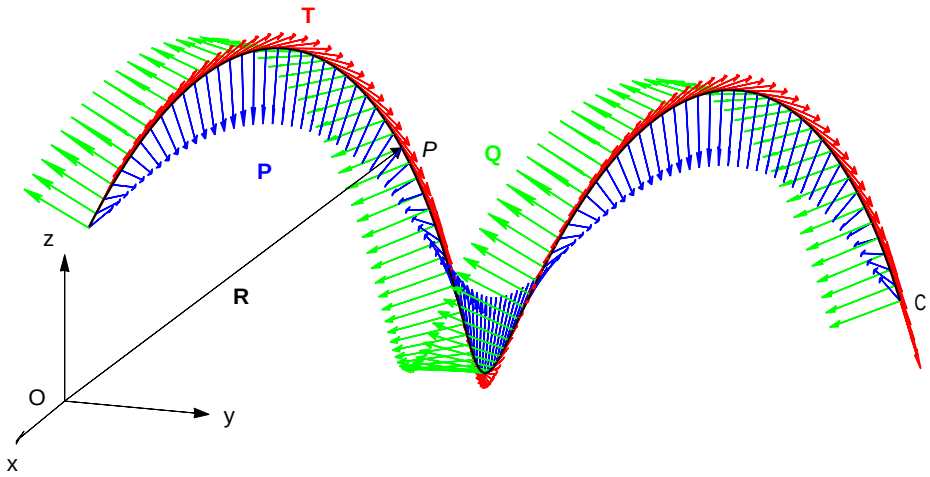

Fig. E.1 Space curve with its tangent, principal normal and binormal vector.

$$\mathbf{T} = \frac{d\mathbf{R}}{ds} = \frac{1}{\sqrt{U}}\frac{d\mathbf{R}}{dt}, \quad \text{where} \quad U = \frac{d\mathbf{R}}{dt}\cdot\frac{d\mathbf{R}}{dt} \tag{E.2}$$

The Frenet formula for a spatial curve is

$$\frac{d\mathbf{T}}{ds} = \kappa\mathbf{P}, \quad \frac{d\mathbf{P}}{ds} = -\kappa\mathbf{T} + \tau\mathbf{Q}, \quad \frac{d\mathbf{Q}}{ds} = -\tau\mathbf{P} \tag{E.3}$$

where $\mathbf{P}$ and $\mathbf{Q}$ are the principal normal and binormal vector, respectively; κ and τ are curvature and torsion of space curve, respectively. The curvature can be obtained as follows:

$$\kappa = \left|\frac{d\mathbf{T}}{ds}\right| = \sqrt{\frac{1}{U}\left(\frac{d\mathbf{T}}{dt}\cdot\frac{d\mathbf{T}}{dt}\right)} \tag{E.4}$$

The principal normal and binormal are

$$\mathbf{P} = \frac{1}{\kappa}\frac{d\mathbf{T}}{ds} = \frac{1}{\kappa\sqrt{U}}\frac{d\mathbf{T}}{dt}, \qquad \mathbf{Q} = \mathbf{T}\times\mathbf{P} \tag{E.5}$$

and we can obtain the torsion by the following Frenet formula:

$$\tau\mathbf{Q} = \frac{d\mathbf{P}}{ds} - \kappa\mathbf{T} = \frac{1}{\sqrt{U}}\frac{d\mathbf{P}}{dt} - \kappa\mathbf{T} \tag{E.6}$$

Also, the curvilinear coordinate can be given in terms of arbitrary parametrization as follows:

$$s = \int_{t_1}^{t_2} \sqrt{U}\, dt \tag{E.7}$$

In the case of a planar curve, the tangent $\mathbf{T}$ and principle normal $\mathbf{P}$ at all points of the curve lie in the same plane; hence, the binormal vector $\mathbf{Q}$ is constant along the curve which lies out of curve plane as shown in the fig. E.2 and the torsion (τ) for the planer curve is zero.

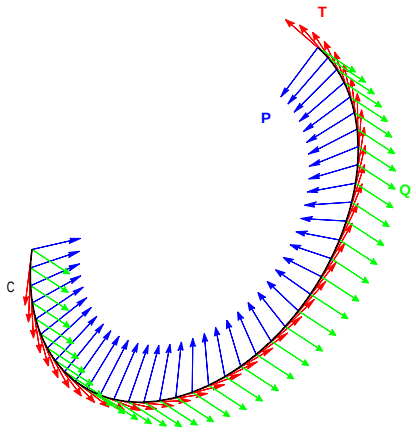

Fig. E.2 Plane curve with its tangent, principal normal and binormal vector.

APPENDIX F

AREA ELEMENT AND NORMAL VECTOR FOR ARBITRARY SURFACE IN CURVILINEAR CYLINDRICAL COORDINATE SYSTEM

Consider an arbitrary surface embedded in three-dimensional Euclidean space, $\mathbb{R}^3$, as shown in fig. F.1. We consider a space curve, $\mathcal{C}$, as the axis of the surface, reference

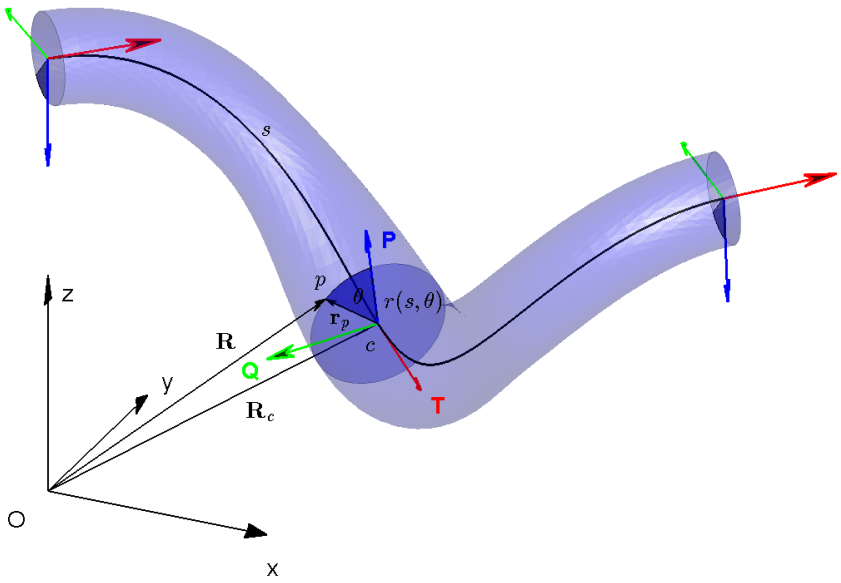

Fig. F.1 Arbitrary surface in curvilinear cylindrical coordinate system.

Consider a arbitrary point p on the surface and its corresponding point c on the reference curve. Then the position vector of point p with respect to the ambient coordinate system can be given as

$$\mathbf{R} \;=\; \mathbf{R}_c + \mathbf{r}_p = \mathbf{R}_c + r(s,\theta)\,\cos\theta\,\mathbf{P} + r(s,\theta)\,\sin\theta\,\mathbf{Q} \tag{F.1}$$

where $\mathbf{R}_c$ is the position vector of point c and $\mathbf{r}_p$ is the position vector of point p with respect to point c. The vectors $\mathbf{P}$, $\mathbf{Q}$, and $\mathbf{T}$ are the unit principal normal,

binormal, and the tangent vector, respectively, of the reference curve $\mathcal{C}$ at point c. Further, the covariant basis for the surface coordinate (s, θ) can be given as follows:

$$\begin{aligned}
\mathbf{z}_s &= \frac{\partial \mathbf{R}}{\partial s} = (1 - \kappa r \cos\theta)\mathbf{T} + \left(\frac{\partial r}{\partial s}\cos\theta - \tau\, r \sin\theta\right)\mathbf{P} + \left(\frac{\partial r}{\partial s}\sin\theta + \tau\, r \cos\theta\right)\mathbf{Q} \\
\mathbf{z}_\theta &= \frac{\partial \mathbf{R}}{\partial \theta} = \left(\frac{\partial r}{\partial \theta}\cos\theta - r \sin\theta\right)\mathbf{P} + \left(\frac{\partial r}{\partial \theta}\sin\theta + r \cos\theta\right)\mathbf{Q}
\end{aligned} \tag{F.2}$$

If $\mathbf{G}$ is the covariant matric tensor, then its components can be obtained as follows:

$$\begin{aligned}
G_{ss} &= (1 - \kappa r \cos\theta)^2 + \left(\frac{\partial r}{\partial s}\cos\theta - \tau\, r \sin\theta\right)^2 + \left(\frac{\partial r}{\partial s}\sin\theta + \tau\, r \cos\theta\right)^2 \\
&= (1 - \kappa r \cos\theta)^2 + \left(\frac{\partial r}{\partial s}\right)^2 + \tau^2 r^2 \\
G_{\theta\theta} &= \left(\frac{\partial r}{\partial \theta}\right)^2 + r^2 \\
G_{s\theta} &= G_{\theta s} = \frac{\partial r}{\partial s}\frac{\partial r}{\partial \theta} + \tau r^2
\end{aligned} \tag{F.3}$$

Further, the determinant G of the covariant matric tensor can be given as

$$G = (1 - \kappa r \cos\theta)^2 \left(\left(\frac{\partial r}{\partial \theta}\right)^2 + r^2\right) + \left(r\frac{\partial r}{\partial s} - \tau\, r\frac{\partial r}{\partial \theta}\right)^2 \tag{F.4}$$

Hence, the area element on the surface can be obtained as follows:

$$d\mathcal{S} = \sqrt{G}\, d\theta\, ds = \sqrt{(1 - \kappa r \cos\theta)^2 \left(\left(\frac{\partial r}{\partial \theta}\right)^2 + r^2\right) + \left(r\frac{\partial r}{\partial s} - \tau\, r\frac{\partial r}{\partial \theta}\right)^2}\, d\theta\, ds \tag{F.5}$$

In the case of a pipe of constant radius (r), the area element reduce to

$$d\mathcal{S} = r(1 - \kappa r \cos\theta)\, d\theta\, ds \tag{F.6}$$

The covariant basis vector spans the tangent plane, and the outward normal vector can be obtained by the normalized cross product of the covariant basis vectors as follows:

$$\mathbf{N} = \frac{\mathbf{z}_\theta \times \mathbf{z}_s}{|\mathbf{z}_\theta \times \mathbf{z}_s|} = \frac{1}{|\mathbf{z}_\theta \times \mathbf{z}_s|}\left[r\left(\tau\frac{\partial r}{\partial \theta} - \frac{\partial r}{\partial s}\right)\mathbf{T} + (1 - \kappa r \cos\theta)\left(\frac{\partial r}{\partial \theta}\sin\theta + r \cos\theta\right)\mathbf{P}\right.$$

$$-(1-\kappa r\,\cos\theta)\left(\frac{\partial r}{\partial\theta}\,\cos\theta - r\,\sin\theta\right)\mathbf{Q}\Bigg] \tag{F.7}$$

where

$$|\mathbf{z}_\theta \times \mathbf{z}_s| \;=\; \sqrt{r^2\left(\tau\frac{\partial r}{\partial\theta}-\frac{\partial r}{\partial s}\right)^2 + (1-\kappa r\,\cos\theta)^2\left(\left(\frac{\partial r}{\partial\theta}\right)^2 + r^2\right)} \tag{F.8}$$

Now from Eqs. (D.4),(D.5), and (D.12), we obtain

$$\mathbf{P} = \cos\theta\hat{\mathbf{e}}_r - \sin\theta\hat{\mathbf{e}}_\theta, \quad \mathbf{Q} = \sin\theta\hat{\mathbf{e}}_r + \cos\theta\hat{\mathbf{e}}_\theta, \quad \mathbf{T} = \hat{\mathbf{e}}_s \tag{F.9}$$

where $\hat{\mathbf{e}}_s$, $\hat{\mathbf{e}}_r$ and $\hat{\mathbf{e}}_\theta$ form orthonormal basis vectors in the (s, r, θ) coordinate system. Then, in this coordinate system, the outward unit normal vector to the surface can be given as

$$\mathbf{N} \;=\; \frac{1}{|\mathbf{z}_\theta \times \mathbf{z}_s|}\left[r\left(\tau\frac{\partial r}{\partial\theta}-\frac{\partial r}{\partial s}\right)\hat{\mathbf{e}}_s + (1-\kappa r\,\cos\theta)\left(r\,\hat{\mathbf{e}}_r - \frac{\partial r}{\partial\theta}\hat{\mathbf{e}}_\theta\right)\right] \tag{F.10}$$

In the case of a pipe of constant radius (r) we have

$$|\mathbf{z}_\theta \times \mathbf{z}_s| = r\,(1-\kappa r\,\cos\theta), \quad \mathbf{N} = \hat{\mathbf{e}}_r \tag{F.11}$$

If the radius of the surface is a function of s only, then the unit normal vector to the surface can be obtained by substituting $\frac{\partial r}{\partial\theta} = 0$ in the expression (F.10).

APPENDIX G

COMPONENTS OF $\tilde{\mathbf{P}}_i$ AND $\tilde{\mathbf{P}}_f$ USED IN TANGENT MATRIX FOR THE HIGHER-ORDER ROD THEORY

The block components of $\tilde{\mathbf{P}}_i$ for $i = 1, 2, 3, 4$ in Eq. (6.38) are given as follows:

$$
\begin{aligned}
\mathbf{P}_1^{11} &= \kappa^2 S_{ss}\mathbf{A}_s^T\mathbf{A}_s + S_{rr}\big\{(\mathbf{A}_{s,r}^T - \kappa\cos\theta\mathbf{A}_s^T)(\mathbf{A}_{s,r} - \kappa\cos\theta\,\mathbf{A}_s) + \tau^2\mathbf{A}_s^T\mathbf{A}_s\big\} \\
&\quad + S_{\theta\theta}\Big\{\left(\frac{1}{r}\mathbf{A}_{s,\theta}^T + \kappa\sin\theta\,\mathbf{A}_s^T\right)\left(\frac{1}{r}\mathbf{A}_{s,\theta} + \kappa\sin\theta\,\mathbf{A}_s\right) + \tau^2\mathbf{A}_s^T\mathbf{A}_s\Big\} \\
&\quad + S_{r\theta}\Big\{\left(\frac{1}{r}\mathbf{A}_{s,\theta}^T + \kappa\sin\theta\,\mathbf{A}_s^T\right)(\mathbf{A}_{s,r} - \kappa\cos\theta\,\mathbf{A}_s) \\
&\quad + \big(\mathbf{A}_{s,r}^T - \kappa\cos\theta\,\mathbf{A}_s^T\big)\left(\frac{1}{r}\mathbf{A}_{s,\theta} + \kappa\sin\theta\,\mathbf{A}_s\right)\Big\} - 2\tau\kappa\cos\theta\,S_{\theta s}\mathbf{A}_s^T\mathbf{A}_s \\
&\quad - 2\tau\kappa\sin\theta\,S_{sr}\mathbf{A}_s^T\mathbf{A}_s \\
\mathbf{P}_1^{12} &= -\kappa\tau\sin\theta S_{ss}\mathbf{A}_s^T\mathbf{A}_r - \frac{\tau}{r}S_{\theta\theta}\mathbf{A}_s^T\mathbf{A}_{r,\theta} + S_{r\theta}\Big\{-\tau\mathbf{A}_s^T\mathbf{A}_{r,r} + \frac{\tau}{r}\mathbf{A}_s^T\mathbf{A}_r\Big\} \\
&\quad + S_{\theta s}\Big\{-\kappa\cos\theta\,\big(\frac{1}{r}\mathbf{A}_{s,\theta}^T + \kappa\sin\theta\,\mathbf{A}_s^T\big)\mathbf{A}_r + \frac{1}{r}\kappa\cos\theta\,\mathbf{A}_s^T\mathbf{A}_{r,\theta} - \frac{1}{r}\kappa\sin\theta\,\mathbf{A}_s^T\mathbf{A}_r\Big\} \\
&\quad + S_{sr}\Big\{-\kappa\cos\theta\,\big(\mathbf{A}_{s,r}^T - \kappa\cos\theta\,\mathbf{A}_s^T\big)\mathbf{A}_r + \kappa\cos\theta\,\mathbf{A}_s^T\mathbf{A}_{r,r} + \tau^2\mathbf{A}_s^T\mathbf{A}_r\Big\} \\
\mathbf{P}_1^{13} &= -\kappa\tau\cos\theta\,S_{ss}\mathbf{A}_s^T\mathbf{A}_\theta + \tau S_{rr}\mathbf{A}_s^T\mathbf{A}_{\theta,r} + \frac{\tau}{r}S_{\theta\theta}\mathbf{A}_s^T\mathbf{A}_\theta + \frac{\tau}{r}S_{r\theta}\mathbf{A}_s^T\mathbf{A}_{\theta,\theta} \\
&\quad + S_{\theta s}\Big\{\frac{\kappa\sin\theta}{r}\mathbf{A}_{s,\theta}^T\mathbf{A}_\theta + (\kappa^2\sin^2\theta - \frac{1}{r}\kappa\cos\theta + \tau^2)\mathbf{A}_s^T\mathbf{A}_\theta - \frac{1}{r}\kappa\sin\theta\,\mathbf{A}_s^T\mathbf{A}_{\theta,\theta}\Big\} \\
&\quad + S_{sr}\big\{\kappa\sin\theta\,\big(\mathbf{A}_{s,r}^T - \kappa\cos\theta\,\mathbf{A}_s^T\big)\mathbf{A}_\theta - \kappa\sin\theta\,\mathbf{A}_s^T\mathbf{A}_{\theta,r}\big\} \\
\mathbf{P}_1^{21} &= -\kappa\tau\sin\theta\,S_{ss}\mathbf{A}_r^T\mathbf{A}_s - \frac{\tau}{r}S_{\theta\theta}\mathbf{A}_{r,\theta}^T\mathbf{A}_s + \tau S_{r\theta}\Big(\frac{1}{r}\mathbf{A}_r^T\mathbf{A}_s - \mathbf{A}_{r,r}^T\mathbf{A}_s\Big) \\
&\quad + S_{\theta s}\Big(-\kappa\cos\theta\,\mathbf{A}_r^T\left(\frac{1}{r}\mathbf{A}_{s,\theta} + \kappa\sin\theta\,\mathbf{A}_s\right) + \frac{\kappa\cos\theta}{r}\mathbf{A}_{r,\theta}^T\mathbf{A}_s - \frac{\kappa\sin\theta}{r}\mathbf{A}_r^T\mathbf{A}_s\Big) \\
&\quad + S_{sr}\Big(-\kappa\cos\theta\,\mathbf{A}_r^T\,(\mathbf{A}_{s,r} - \kappa\cos\theta\,\mathbf{A}_s) + \kappa\cos\theta\,\mathbf{A}_{r,r}^T\mathbf{A}_s + \tau^2\mathbf{A}_r^T\mathbf{A}_s\Big) \\
\mathbf{P}_1^{22} &= \big((\kappa^2\cos^2\theta + \tau^2)S_{ss} + \frac{1}{r^2}S_{\theta\theta} + \frac{2\tau}{r}S_{\theta s}\big)\mathbf{A}_r^T\mathbf{A}_r + S_{rr}\mathbf{A}_{r,r}^T\mathbf{A}_{r,r} + \frac{1}{r^2}S_{\theta\theta}\mathbf{A}_{r,\theta}^T\mathbf{A}_{r,\theta} \\
&\quad + \frac{1}{r}S_{r\theta}\big\{\mathbf{A}_{r,\theta}^T\mathbf{A}_{r,r} + \mathbf{A}_{r,r}^T\mathbf{A}_{r,\theta}\big\} \\
\mathbf{P}_1^{23} &= -\kappa^2\cos\theta\,\sin\theta\,S_{ss}\mathbf{A}_r^T\mathbf{A}_\theta + \frac{1}{r^2}S_{\theta\theta}\big(\mathbf{A}_r^T\mathbf{A}_{\theta,\theta} - \mathbf{A}_{r,\theta}^T\mathbf{A}_\theta\big) \\
&\quad + \frac{1}{r}S_{r\theta}\big(-\mathbf{A}_{r,r}^T\mathbf{A}_\theta + \mathbf{A}_r^T\mathbf{A}_{\theta,r}\big) + \frac{\tau}{r}S_{\theta s}\big(\mathbf{A}_r^T\mathbf{A}_{\theta,\theta} - \mathbf{A}_{r,\theta}^T\mathbf{A}_\theta\big) \\
&\quad + \tau S_{sr}\big(\mathbf{A}_r^T\mathbf{A}_{\theta,r} - \mathbf{A}_{r,r}^T\mathbf{A}_\theta\big) \\
\mathbf{P}_1^{31} &= (\frac{\tau}{r}S_{\theta\theta} - \kappa\tau\cos\theta\,S_{ss})\mathbf{A}_\theta^T\mathbf{A}_s + \tau S_{rr}\mathbf{A}_{\theta,r}^T\mathbf{A}_s + \frac{\tau}{r}S_{r\theta}\mathbf{A}_{\theta,\theta}^T\mathbf{A}_s \\
&\quad + S_{\theta s}\mathbf{A}_\theta^T\left(\kappa\sin\theta\,\mathbf{A}_\theta^T\left(\frac{1}{r}\mathbf{A}_{s,\theta} + \kappa\sin\theta\,\mathbf{A}_s\right) + \tau^2\mathbf{A}_\theta^T\mathbf{A}_s\right.
\end{aligned}
$$

$$
\begin{aligned}
&\quad -\frac{\kappa\cos\theta}{r}\mathbf{A}_\theta^T\mathbf{A}_s - \frac{1}{r}\kappa\,\sin\theta\mathbf{A}_{\theta,\theta}^T\mathbf{A}_s\Big)\\
&\quad +S_{sr}\big(\kappa\sin\theta\,\mathbf{A}_\theta^T\,(\mathbf{A}_{s,r}-\kappa\cos\theta\,\mathbf{A}_s) - \kappa\sin\theta\,\mathbf{A}_{\theta,r}^T\mathbf{A}_s\big)\\
\mathbf{P}_1^{32} &= -\kappa^2\sin\theta\,\cos\theta\,S_{ss}\mathbf{A}_\theta^T\mathbf{A}_r + \frac{1}{r^2}S_{\theta\theta}\big(\mathbf{A}_{\theta,\theta}^T\mathbf{A}_r - \mathbf{A}_\theta^T\mathbf{A}_{r,\theta}\big)\\
&\quad +\frac{1}{r}S_{r\theta}\big(-\mathbf{A}_\theta^T\mathbf{A}_{r,r} + \mathbf{A}_{\theta,r}^T\mathbf{A}_r\big) + \frac{\tau}{r}S_{\theta s}\,\big(\mathbf{A}_{\theta,\theta}^T\mathbf{A}_r - \mathbf{A}_\theta^T\mathbf{A}_{r,\theta}\big)\\
&\quad +\tau S_{sr}\big(\mathbf{A}_{\theta,r}^T\mathbf{A}_r - \mathbf{A}_\theta^T\mathbf{A}_{r,r}\big)\\
\mathbf{P}_1^{33} &= (\kappa^2\sin^2\theta+\tau^2)S_{ss}\mathbf{A}_\theta^T\mathbf{A}_\theta + S_{rr}\mathbf{A}_{\theta,r}^T\mathbf{A}_{\theta,r} + \frac{1}{r^2}S_{\theta\theta}\big(\mathbf{A}_\theta^T\mathbf{A}_\theta + \mathbf{A}_{\theta,\theta}^T\mathbf{A}_{\theta,\theta}\big)\\
&\quad +\frac{1}{r}S_{r\theta}\big(\mathbf{A}_{\theta,\theta}^T\mathbf{A}_{\theta,r} + \mathbf{A}_{\theta,r}^T\mathbf{A}_{\theta,\theta}\big) + \frac{2\tau}{r}S_{\theta s}\mathbf{A}_\theta^T\mathbf{A}_\theta\\
\mathbf{P}_2^{11} &= S_{\theta s}\Big(\frac{1}{r}\mathbf{A}_{s,\theta}^T\mathbf{A}_s + \kappa\sin\theta\,\mathbf{A}_s^T\mathbf{A}_s\Big) + S_{sr}\big(\mathbf{A}_{s,r}^T - \kappa\cos\theta\,\mathbf{A}_s^T\big)\mathbf{A}_s\\
\mathbf{P}_2^{12} &= (\kappa\cos\theta\,S_{ss} - \tau S_{\theta s})\mathbf{A}_s^T\mathbf{A}_r\\
\mathbf{P}_2^{13} &= (-\kappa\sin\theta\,S_{ss} + \tau S_{sr})\mathbf{A}_s^T\mathbf{A}_\theta\\
\mathbf{P}_2^{21} &= -\kappa\cos\theta\,S_{ss}\mathbf{A}_r^T\mathbf{A}_s\\
\mathbf{P}_2^{22} &= \frac{1}{r}S_{\theta s}\mathbf{A}_{r,\theta}^T\mathbf{A}_r + S_{sr}\mathbf{A}_{r,r}^T\mathbf{A}_r\\
\mathbf{P}_2^{23} &= \tau S_{ss}\mathbf{A}_r^T\mathbf{A}_\theta + \frac{1}{r}S_{\theta s}\mathbf{A}_r^T\mathbf{A}_\theta\\
\mathbf{P}_2^{31} &= \kappa\sin\theta\,S_{ss}\mathbf{A}_\theta^T\mathbf{A}_s\\
\mathbf{P}_2^{32} &= -(\tau S_{ss} + \frac{1}{r}S_{\theta s})\mathbf{A}_\theta^T\mathbf{A}_r\\
\mathbf{P}_2^{33} &= S_{sr}\mathbf{A}_{\theta,r}^T\mathbf{A}_\theta + \frac{1}{r}S_{\theta s}\mathbf{A}_{\theta,\theta}^T\mathbf{A}_\theta\\
\mathbf{P}_3^{11} &= S_{\theta s}\mathbf{A}_s^T\left(\frac{1}{r}\mathbf{A}_{s,\theta} + \kappa\sin\theta\,\mathbf{A}_s\right) + S_{sr}\mathbf{A}_s^T\,(\mathbf{A}_{s,r} - \kappa\cos\theta\,\mathbf{A}_s)\\
\mathbf{P}_3^{12} &= -\kappa\cos\theta\,S_{ss}\mathbf{A}_s^T\mathbf{A}_r\\
\mathbf{P}_3^{13} &= \kappa\sin\theta\,S_{ss}\mathbf{A}_s^T\mathbf{A}_\theta\\
\mathbf{P}_3^{21} &= (\kappa\cos\theta\,S_{ss} - \tau S_{\theta s})\mathbf{A}_r^T\mathbf{A}_s\\
\mathbf{P}_3^{22} &= \frac{1}{r}S_{\theta s}\mathbf{A}_r^T\mathbf{A}_{r,\theta} + S_{sr}\mathbf{A}_r^T\mathbf{A}_{r,r}\\
\mathbf{P}_3^{23} &= -(\tau S_{ss} + \frac{1}{r}S_{\theta s})\mathbf{A}_r^T\mathbf{A}_\theta\\
\mathbf{P}_3^{31} &= (-\kappa\sin\theta\,S_{ss} + \tau S_{sr})\mathbf{A}_\theta^T\mathbf{A}_s\\
\mathbf{P}_3^{32} &= (\tau S_{ss} + \frac{1}{r}S_{\theta s})\mathbf{A}_\theta^T\mathbf{A}_r\\
\mathbf{P}_3^{33} &= \frac{1}{r}S_{\theta s}\mathbf{A}_\theta^T\mathbf{A}_{\theta,\theta} + S_{sr}\mathbf{A}_\theta^T\mathbf{A}_{\theta,r}\\
\mathbf{P}_4^{11} &= S_{ss}\mathbf{A}_s^T\mathbf{A}_s\\
\mathbf{P}_4^{22} &= S_{ss}\mathbf{A}_r^T\mathbf{A}_r\\
\mathbf{P}_4^{33} &= S_{ss}\mathbf{A}_\theta^T\mathbf{A}_\theta
\end{aligned}
\tag{G.1}
$$

If the body force is defined as force per unit mass, then we have $\mathbf{f}_b = \rho \mathbf{f}_m = (\rho_0/\det(\mathbf{F}))\mathbf{f}_m$, where ρ and ρ_0 are the mass densities of the body in the deformed and reference configurations, respectively. Then the force vector in Eq. (6.20) can be expressed as:

$$\begin{aligned}
\hat{\mathbf{f}} &= \begin{bmatrix} \hat{\mathbf{f}}_s & \hat{\mathbf{f}}_r & \hat{\mathbf{f}}_\theta \end{bmatrix}^T, \\
\hat{\mathbf{f}}_s &= \int_A \rho_0 f_{m_s} \mathbf{A}_s^T \, dA + \int_0^{2\pi} \sqrt{G_i}\, q_{s_i}\, \zeta \mathbf{A}_s^T \, d\theta \\
\hat{\mathbf{f}}_r &= \int_A \rho_0 f_{m_r} \mathbf{A}_r^T \, dA + \int_0^{2\pi} \sqrt{G_i}\, q_{r_i}\, \zeta \mathbf{A}_r^T \, d\theta \\
\hat{\mathbf{f}}_\theta &= \int_A \rho_0 f_{m_\theta} \mathbf{A}_\theta^T \, dA + \int_0^{2\pi} \sqrt{G_i}\, q_{\theta_i}\, \zeta \mathbf{A}_\theta^T \, d\theta
\end{aligned} \tag{G.2}$$

where $\zeta = \left(\det(\mathbf{F})\sqrt{(\mathbf{C}^{-1}\cdot\mathbf{N})\cdot\mathbf{N}}\right)$. If the force (per unit area) vector $\mathbf{q}_i$ does not depend on the deformed configuration, then the matrix $\tilde{\mathbf{P}}_f$ used in tangent matrix is given as follows:

$$\tilde{\mathbf{P}}_f = \int_0^{2\pi} \sqrt{G_i} \begin{bmatrix} q_{s_i}\frac{\partial\zeta}{\partial u_s}\mathbf{A}_s^T\mathbf{A}_s & q_{s_i}\frac{\partial\zeta}{\partial u_r}\mathbf{A}_s^T\mathbf{A}_r & q_{s_i}\frac{\partial\zeta}{\partial u_\theta}\mathbf{A}_s^T\mathbf{A}_\theta \\ q_{r_i}\frac{\partial\zeta}{\partial u_s}\mathbf{A}_r^T\mathbf{A}_s & q_{r_i}\frac{\partial\zeta}{\partial u_r}\mathbf{A}_r^T\mathbf{A}_r & q_{r_i}\frac{\partial\zeta}{\partial u_\theta}\mathbf{A}_r^T\mathbf{A}_\theta \\ q_{\theta_i}\frac{\partial\zeta}{\partial u_s}\mathbf{A}_\theta^T\mathbf{A}_s & q_{\theta_i}\frac{\partial\zeta}{\partial u_r}\mathbf{A}_\theta^T\mathbf{A}_r & q_{\theta_i}\frac{\partial\zeta}{\partial u_\theta}\mathbf{A}_\theta^T\mathbf{A}_\theta \end{bmatrix} d\theta \tag{G.3}$$

where the derivative $\frac{\partial\zeta}{\partial\alpha}$ for $\alpha = u_s, u_r, u_\theta$ can be given as following:

$$\frac{\partial\zeta}{\partial\alpha} = \frac{\partial\det(\mathbf{F})}{\partial\alpha}\sqrt{(\mathbf{C}^{-1}\cdot\mathbf{N})\cdot\mathbf{N}}) - \frac{\det(\mathbf{F})}{2\sqrt{(\mathbf{C}^{-1}\cdot\mathbf{N})\cdot\mathbf{N})}}\left((\mathbf{C}^{-1}\cdot\frac{\partial\mathbf{C}}{\partial\alpha}\cdot\mathbf{C}^{-1})\cdot\mathbf{N}\right)\cdot\mathbf{N} \tag{G.4}$$

where

$$\frac{\partial\det(\mathbf{F})}{\partial\alpha} = \text{cofactor}(F_{ij})\frac{\partial F_{ij}}{\partial\alpha}, \quad \frac{\partial\mathbf{C}}{\partial\alpha} = \frac{\partial\mathbf{F}^T}{\partial\alpha}\cdot\mathbf{F} + \mathbf{F}^T\cdot\frac{\partial\mathbf{F}}{\partial\alpha} \tag{G.5}$$

where F_{ij} are the components of $\mathbf{F}$ in the assumed coordinate system, and summation convention ion the repeated indices is implied. Also, the constant point force with fixed direction, $\mathbf{q}_i$, can be expressed in terms of the Dirac delta function in two dimensions. In this case, we note that constant point force means the volume under the two-dimensional Dirac delta function should be taken as a constant, and it would

not depend on the deformation, giving $\tilde{\mathbf{P}}_f = \mathbf{0}$.

Another common example of distributed traction force at the boundary surface is the pressure force, which is as $\mathbf{q}_i = P_{0_i}\mathbf{n} = (P_{0_i}/\sqrt{(\mathbf{C}^{-1}\cdot\mathbf{N})\cdot\mathbf{N}})\mathbf{F}^{-T}\cdot\mathbf{N}$, where P_{0_i} is the magnitude of the pressure. If we use the Dirac delta function for P_0 with constant magnitude, we obtain a constant follower point force always acting along the normal direction to the surface at the point of application. In such cases, we have,

$$\hat{\mathbf{f}}_s = \int_0^{2\pi} \sqrt{G_i}\, P_{0_i}\, \zeta_s \mathbf{A}_s^T\, d\theta,\ \hat{\mathbf{f}}_r = \int_0^{2\pi} \sqrt{G_i}\, P_{0_i}\, \zeta_r \mathbf{A}_r^T\, d\theta,\ \hat{\mathbf{f}}_\theta = \int_0^{2\pi} \sqrt{G_i}\, P_{0_i}\, \zeta_\theta \mathbf{A}_\theta^T\, d\theta \tag{G.6}$$

where $\boldsymbol{\zeta} = \det(\mathbf{F})\,\mathbf{F}^{-T}\cdot\mathbf{N} = \zeta_s\hat{\mathbf{e}}_s + \zeta_r\hat{\mathbf{e}}_r + \zeta_\theta\hat{\mathbf{e}}_\theta$. Then the the matrix $\tilde{\mathbf{P}}_f$ can be given as following:

$$\tilde{\mathbf{P}}_f = \int_0^{2\pi} \sqrt{G_i}\, P_{0_i} \begin{bmatrix} \frac{\partial\zeta_s}{\partial u_s}\mathbf{A}_s^T\mathbf{A}_s & \frac{\partial\zeta_s}{\partial u_r}\mathbf{A}_s^T\mathbf{A}_r & \frac{\partial\zeta_s}{\partial u_\theta}\mathbf{A}_s^T\mathbf{A}_\theta \\ \frac{\partial\zeta_r}{\partial u_s}\mathbf{A}_r^T\mathbf{A}_s & \frac{\partial\zeta_r}{\partial u_r}\mathbf{A}_r^T\mathbf{A}_r & \frac{\partial\zeta_r}{\partial u_\theta}\mathbf{A}_r^T\mathbf{A}_\theta \\ \frac{\partial\zeta_\theta}{\partial u_s}\mathbf{A}_\theta^T\mathbf{A}_s & \frac{\partial\zeta_\theta}{\partial u_r}\mathbf{A}_\theta^T\mathbf{A}_r & \frac{\partial\zeta_\theta}{\partial u_\theta}\mathbf{A}_\theta^T\mathbf{A}_\theta \end{bmatrix} d\theta \tag{G.7}$$

where the derivative $\frac{\partial\boldsymbol{\zeta}}{\partial\alpha}$ for $\alpha = u_s, u_r, u_\theta$ is given as

$$\begin{aligned} \frac{\partial\boldsymbol{\zeta}}{\partial\alpha} &= \frac{\partial\zeta_s}{\partial\alpha}\hat{\mathbf{e}}_s + \frac{\partial\zeta_r}{\partial\alpha}\hat{\mathbf{e}}_r + \frac{\partial\zeta_\theta}{\partial\alpha}\hat{\mathbf{e}}_\theta \\ &= \frac{\partial\det(\mathbf{F})}{\partial\alpha}\mathbf{F}^{-T}\cdot\mathbf{N} - \det(\mathbf{F})\left(\mathbf{F}^{-T}\cdot\frac{\partial\mathbf{F}^T}{\partial\alpha}\cdot\mathbf{F}^{-T}\right)\cdot\mathbf{N} \end{aligned} \tag{G.8}$$

and

$$\begin{aligned} \frac{\partial\mathbf{F}}{\partial u_s} &= \begin{bmatrix} \beta_{s_1} & \beta_{s_2} - \kappa\,\cos\theta & \frac{1}{r}\beta_{s_3} + \kappa\,\sin\theta \\ -\kappa\,\cos\theta & 0 & -\tau \\ -\kappa\,\sin\theta & \tau & 0 \end{bmatrix}, \\ \frac{\partial\mathbf{F}}{\partial u_r} &= \begin{bmatrix} -\kappa\,\cos\theta & 0 & 0 \\ \beta_{r_1} & \beta_{r_2} & \frac{1}{r}\beta_{r_3} \\ \tau & 0 & \frac{1}{r} \end{bmatrix}, \quad \frac{\partial\mathbf{F}}{\partial u_\theta} = \begin{bmatrix} \kappa\sin\theta & 0 & 0 \\ -\tau & 0 & -\frac{1}{r} \\ \beta_{\theta_1} & \beta_{\theta_2} & \frac{1}{r}\beta_{\theta_3} \end{bmatrix} \end{aligned} \tag{G.9}$$

with

$$
\begin{aligned}
\beta_{s_1} &= \frac{u_{s,ss}}{u_{s,s}} + \frac{u_{s,sr}}{u_{s,r}} + \frac{u_{s,s\theta}}{u_{s,\theta}} & \beta_{r_3} &= \frac{u_{r,\theta s}}{u_{r,s}} + \frac{u_{r,\theta r}}{u_{r,r}} + \frac{u_{r,\theta\theta}}{u_{r,\theta}} \\
\beta_{s_2} &= \frac{u_{s,rs}}{u_{s,s}} + \frac{u_{s,rr}}{u_{s,r}} + \frac{u_{s,r\theta}}{u_{s,\theta}} & \beta_{\theta_1} &= \frac{u_{\theta,ss}}{u_{\theta,s}} + \frac{u_{\theta,sr}}{u_{\theta,r}} + \frac{u_{\theta,s\theta}}{u_{\theta,\theta}} \\
\beta_{s_3} &= \frac{u_{s,\theta s}}{u_{s,s}} + \frac{u_{s,\theta r}}{u_{s,r}} + \frac{u_{s,\theta\theta}}{u_{s,\theta}} & \beta_{\theta_2} &= \frac{u_{\theta,rs}}{u_{\theta,s}} + \frac{u_{\theta,rr}}{u_{\theta,r}} + \frac{u_{\theta,r\theta}}{u_{\theta,\theta}} \\
\beta_{r_1} &= \frac{u_{r,ss}}{u_{r,s}} + \frac{u_{r,sr}}{u_{r,r}} + \frac{u_{r,s\theta}}{u_{r,\theta}} & \beta_{\theta_3} &= \frac{u_{\theta,\theta s}}{u_{\theta,s}} + \frac{u_{\theta,\theta r}}{u_{\theta,r}} + \frac{u_{\theta,\theta\theta}}{u_{\theta,\theta}} \\
\beta_{r_2} &= \frac{u_{r,rs}}{u_{r,s}} + \frac{u_{r,rr}}{u_{r,r}} + \frac{u_{r,r\theta}}{u_{r,\theta}}
\end{aligned}
\tag{G.10}
$$